# BULLETIN

## OF THE KARAGANDA UNIVERSITY

# CHEMISTRY
## Series

# CONTENTS

## ORGANIC CHEMISTRY

## PHYSICAL AND ANALYTICAL CHEMISTRY

## INORGANIC CHEMISTRY

## CHEMICAL TECHNOLOGY

## METHODS OF TEACHING CHEMISTRY

# ORGANIC CHEMISTRY

A.N. Klivenko, B.Kh. Mussabayeva[*], B.S. Gaisina, A.N. Sabitova

*Shakarim University of Semey, Kazakhstan*
*(\*Corresponding author′s e-mail: binur.mussabayeva@mail.ru)*

## Biocompatible cryogels: preparation and application

Polymer cryogels are very promising for producing functional materials. Their porous structure makes them indispensable for some areas of medicine, catalysis, and biotechnology. In this review we focused on methods for producing cryogels based on biopolymers, interpolyelectrolyte complexes of biopolymers, and composite cryogels based on them. First, the properties of cryogels and brief theoretical information about the production of cryogels based on biopolymers were considered. The second section summarizes the latest advances in the production of cryogels based on complexes of biopolymers and composite cryogels. The features of the synthesis and the factors affecting the final properties of materials were considered. In the final part the fields of application of cryogels of the considered types in biotechnology, catalysis and medicine were studied in detail. In biotechnology cryogels are used to immobilize molecules and cells, as a basis for cell growth, and as chromatographic materials for cell separation. In catalysis cryogels are used as a matrix for the immobilization of metal nanoparticles, as well as for the immobilization of enzymes. Biocompatible cryogels and their composites are widely used in medicine for bone and cartilage tissue regeneration, drug delivery, providing a long-term profile of drug release in the body.

*Keywords:* cryogel, biocompatible, biopolymer, macroporosity, immobilization, biotechnology, catalysis, drug delivery, tissue engineering.

### *Introduction*

Cryogels are porous polymer materials with the system of communicating pores. The term cryogel was first used by V.I. Lozinsky to refer to gels prepared in a frozen solvent medium [1]. Cryogels are synthesized by cryogelation (cryogenic gelation), based on the use of the effect of lowering the temperature below the freezing point of a pure solvent [2]. Visually, the mixture is a solid. The uncured zones of frozen multicomponent systems are called non-frozen liquid microphase (NFLMP). The polymer framework of the cryogel is formed in such unfrozen micro-regions [1]. When the frozen preparation is thawed, a macroporous cryogel is formed, the pore-forming agents are polycrystals of the frozen solvent.

The primary condition for the synthesis of cryogels is the content in the initial systems of structural elements that allow, as a result of forces of different nature (chemical bonds, Van der Waals forces, electrostatic interactions), to form three-dimensional agglomerates. The following groups of initial systems are distinguished [1, 3]: 1) colloidal sols; 2) solutions of monomers; 3) solutions of polymers with a crosslinking agent; 4) solutions of polymers capable of self-stacking; 5) solutions of polyelectrolytes, including low-molecular or polymer counterions.

The main difference between cryogels and other types of polymer materials is their morphology. The porous structure of the cryogel in combination with swelling, collapse, thermal and pH sensitivity opens up broad prospects for the use of these objects in various fields.

Porous materials are divided into 2 groups by origin [4]: addition systems (corpuscular) and subtraction systems (spongy). According to their structural and geometric characteristics, they are also divided into 2 types: regular porous structures with the same size of pores, channels, and walls, and stochastic bodies, in which the pore sizes, their location, wall thickness, and other parameters are random. According to this

classification, cryogels belong to stochastic subtraction systems, in which pores of random sizes are cavities, channels, or slits in a continuous matrix.

The review presents the data from the sources of recent 15 years on the preparation of cryogels based on biopolymers, mainly polysaccharides, and their application in different fields. During the making of this review article we focused on cryogels, which are prepared on the basis of complexes of polymers and biopolymers. We paid special attention to cryogels prepared on the basis of only natural polymers. Together, the review summarizes the methods for producing composite cryogels. In the subsequent sections of review the methods of applications of these cryogels are highlighted, especially in the field of biotechnology, catalysis and medicine.

*Biopolymers based cryogels*

Biopolymers usually contain a significant number of charged functional groups. This increases their bioavailability, biodegradability, and ensures their involvement in chemical processes occurring in a living organism. Thus, biopolymers are often polyelectrolytes. If a polyelectrolyte solution is used as the initial system, the formation of cryogels occurs as a result of the formation of sufficiently stable ion bridges between the polyelectrolyte units [1, 3].

An example of the formation of cross-linked systems by such a mechanism are gels based on gellan and guar gum [5]. However, the implementation of this mechanism for the production of cryogels is a difficult task. Since the rate of gelation is very high, when the critical concentration of gelation is reached, gelation in such systems usually occurs earlier than the freezing of initial monomer mixture. This leads to the fact that there is no cryoconcentration effect in the system and the resulting gels cannot be attributed to cryogels [1]. In [6] cryogels based on chitosan and calcium alginate were obtained by freezing the initial solution at –20 °C, followed by immersion of the frozen mixtures in alcohol solutions containing components that initiate the gelation process. In the case of chitosan it is NaOH, in the case of alginate it is $Ca^{2+}$ ions. The researchers [7] obtained an alginate-based cryogel by sublimation of the initial mixture containing sodium alginate and gelatin, and then they kept the sublimate in a solution containing $Ca^{2+}$ ions for 3 days. The obtained cryogels [6, 7] were used for cell growth.

Cryogels of cationic polyelectrolyte chitosan were prepared by crosslinking at subzero temperature. Glutaraldehyde (HA) [8], diglycidyl ethers of glycols [9] were used as crosslinking agents; the authors [10] used non-toxic biodegradable crosslinking agents-oxidized dextran and 1,1,3,3-tetramethoxypropane.

A new cryogel was prepared by cryopolymerization of salecan and acryloyloxyethyltrimethylammonium chloride using triallyl cyanurate (TAC) as a crosslinking agent [11]. The structure of cryogels was confirmed by IR spectroscopy and X-ray analysis. Adding more hydrophilic salecan inside of cryogels has significantly increased the water absorption. In vitro cytotoxicity analysis the non-cytotoxic nature of cryogels has been confirmed. They were biocompatible and maintained the adhesion, proliferation, and viability of L929 and 3 T3-L1 cells, as shown by cell proliferation and live/dead cell analysis. Overall, this work opens the door to the design and development of a mechanically robust salecan-based cryogel for cell adhesion and proliferation, as well as further applications in soft tissue engineering.

For the preparation of new biocompatible macroporous cryogels based on dextran and hyaluronan derivatives, the electron-beam reaction of free-radical crosslinking was used [12]. This approach ensures the production of high-purity materials with high porosity without the use of additional crosslinkers or initiators. It was found that the applied radiation dose and chemical composition strongly affect the properties of the resulting cryogel materials. Preliminary cytotoxicity tests illustrate the excellent in vitro cytocompatibility of the obtained cryogels, which makes them attractive as matrices for tissue regeneration procedures.

The use of non-toxic crosslinking agents in the production of biocompatible cryogels is also important. In [13] a single-stage method for producing chitosan or gelatin cryogels is proposed. For this purpose, non-toxic and biodegradable crosslinking agents such as oxidized dextran and 1,1,3,3-tetramethoxypropane are used. The chitosan cryogels prepared in this way had a degree of degradation ~2 times higher than the cryogels prepared by the two-stage method, i.e., reduced with borohydride. In addition, these cryogels showed significantly higher viability (~80 %) of fibroblast cells in vitro compared to cryogels crosslinked with glutaraldehyde (~40 %). Thus, cryogels prepared without the use of harmful crosslinking agents can be used as biocompatible and biodegradable scaffolds for cell culture and other biomedical applications.

A natural derivative of dialdehyde carboxymethylcellulose (DCMC) was used as a crosslinking agent for the production of spongy collagen cryogels by freezing-thawing [14]. Studies have shown that the crosslinking reaction and cryogenic treatment do not destroy the triple helix of collagen, but increase the thermal stability

of collagen; cryogels have a heterophase structure with interconnected macropores, and swell quickly. The swelling coefficient depends on the content of DCMC and on the medium pH. Tests for compatibility with blood in vitro showed that the introduction of DCMC does not cause a decrease in hemolysis and blood clotting compared to pure collagen. Thus, the resulting cryogels have great potential in tissue engineering and other biomedical applications.

Macroporous cryogels of hyaluronic acid (HA) with a tunable porous structure, viscoelasticity, and high mechanical strength were synthesized from methacrylated HA in aqueous solutions at a temperature of –18 °C by a free radical mechanism [15]. Poly(N,N-dimethylacrylamide) (PDMAA) was used as a filler. The porosity and average pore diameter decrease with increasing PDMAA content in cryogels due to a decrease in the amount of ice template during cryogeling. In addition, there is a reversible gel-sol transition due to the outflow and inflow of water through the pores. This flow-dependent viscoelasticity is of great interest, since it protects the cryogel network from damage during deformations, and therefore acts as a self-defense mechanism.

The review [16] considered the formation of various physically cross-linked cryogels from polysaccharides, such as hyaluronan, carboxymethylated cottage cheese, carboxymethylated cellulose, xanthan, β-glucan, locust bean gum, starch, maltodextrins, and agarose. Cryogels have tunable structural, mechanical, and biological properties, and therefore can have numerous applications.

*Complex and composite cryogels of biopolymers*

The synthesis of complex, composite, hybrid cryogels allows researchers to solve issues related to the improving the mechanical characteristics of materials, chemical properties of substances, as well as to give cryogels the ability to respond to changes in external conditions such as temperature, pH, and ionic strength. Therefore, cryogels based on pure polymers have a much smaller scope of application, and therefore are much less often used.

In [17] the features of the formation of cryogels of interpolyelectrolyte complexes (IPEC) based on chitosan and sodium alginate were studied. Complexation occurs by the mechanism of electrostatic interaction between oppositely charged carboxyl groups of pyranose cycles of L-guluronic acid of neighboring alginate polymer chains and chitosan amino groups, as well as due to numerous hydrogen bonds. It is shown that the conformational state of the lyophilizing component, which is in excess in the system, has a decisive influence on the mechanism of IPEC formation. It was found that changes in the degree of binding of chitosan and alginate significantly affect the formation of the inner surface of cryogels based on them. It is shown that the most developed mesoporous structure is obtained when a denser gel is formed in the system.

Cryogels based on pectin and chitosan were prepared by cryotropic gelation. A 1 % solution of pectin was layered on a frozen solution of chitosan and $CaCl_2$, the mass ratio of pectin and chitosan was 3:1. The cryogel was formed for 4-6 hours at a temperature of 15-22 °C with slow thawing of the chitosan and $CaCl_2$ solution. According to SEM data, cryogels have a macroporous leaf-like structure [18]. It was found that cryogels based on *Heracleum* pectin are more resistant to degradation *in vitro* compared to cryogels from apple pectin. The inclusion of chitosans with a high degree of deacetylation in the composition of cryogels increases the time of their degradation [19].

pH-Sensitive cryogels based on two biodegradable polyelectrolytes (chitosan and 2-hydroxyethylcellulose (HEC)) were prepared by cryogenic treatment of semi-diluted aqueous solutions and UV-induced crosslinking in the frozen state. $H_2O_2$ and N,N'-methylene bisacrylamide, were used as the photoinitiator and crosslinking agent respectively. The resulting cryogels were opalescent spongy materials that rapidly release/absorb water due to their open porous structure [20].

New porous films based on xanthan and polyvinyl alcohol (PVA) were obtained by a universal and nondestructive freezing/thawing method. The stability of the films depends on the crystal zones created by the PVA during the freeze/thaw treatment. Cryogels with increased mechanical strength were synthesized by increasing the number of freeze/thaw cycles from three to seven, and pore stability was improved by applying grape pomace. The resulting film showed excellent antioxidant and antimicrobial activity, which indicates the possibility of using these systems in food packaging [21].

A new cryogels consisting of various compositions of chitosan and hyaluronic acid (0, 10, 20, 30 and 50 wt. % hyaluronic acid) were prepared. Morphological studies have shown that the porosity of cryogels is 90–95 %. It is noted that the mechanical properties of the cryogels are better than those of pure chitosan cryogels. The new cryogels do not have a significant cytotoxic effect and can be used in tissue engineering [22].

*Applications of biocompatible cryogels*

The physical and chemical properties of cryogels, such as macroporosity, elasticity, water permeability, and ease of chemical modification, are of great practical interest in various fields, such as biotechnology, catalysis, regenerative medicine, bioremediation, and water purification.

*Application in biotechnology*

The use of cryogels in biotechnology as chromatographic materials, templates for the immobilization of molecules and cells and the basis for cell growth is associated with high biocompatibility, non-toxicity, and excellent mechanical characteristics [23].

The separation of protein mixtures on cryogels was carried out in [24–26]. It should be noted that cryogels have a relatively low sorption capacity relative to proteins (less than 100 mg/g), which limits their wide use in protein separation processes compared to classical chromatographic methods [26].

Cryogels are used for the production of chromatographic columns, for this purpose, the starting materials must have the following properties [27]:

– high porosity;
– high capacity for the retained substance;
– low cost of manufacture and ease of filling the column.

Cell separation on chromatographic columns is a common application of cryogels [28]. When cells come into contact with the column material, multiple interactions of different nature occur, as a result of which the cells can become so firmly fixed in the column volume that their removal is impossible [23]. The use of macroporous cryogels as the column material reduces the multiplicity of bonds formed between the material and the cell. This is achieved by selecting a cryogel material that has a small supply of functional groups that bind cells. Reducing the activity of cell binding by functional groups of cryogel can be achieved by changing the external parameters or by preliminary functionalization of the cell surface [26]. The advantage of cryogel chromatographic columns in comparison with classical ones is their elasticity. This property allows the removal of bound cells by mechanical action on the column (Fig. 1) [29, 30].
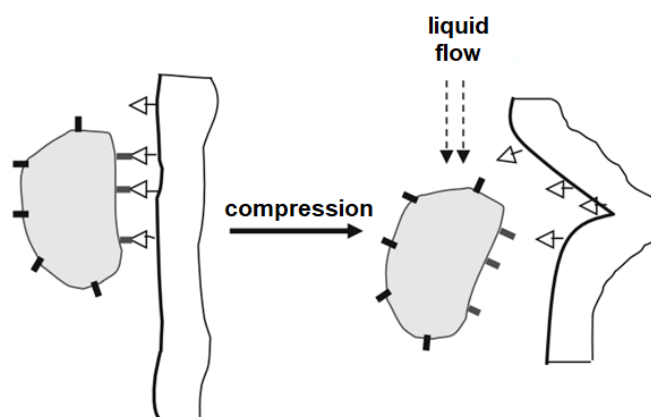


Figure 1. Mechanism of removal of bound cells from the cryogel column under mechanical action [30]

Mechanical actions break the bonds between the cryogel and the substrate and allow removing most of the bound particles.

Cell immobilization in PVA-based cryogels is widely used for cleaning environmental objects from pollutants in analytical practice [26]. When immobilizing cells in cryogels, they do not use direct cell culture on the cryogel, but add spores of microorganisms to the initial mixture. After immobilization of the spores in the resulting cryogel, cell growth is initiated [31].

The authors [32] showed that immobilized cells don't lose the ability to secrete various hydrolytic enzymes — amylases, proteases, and lipases. Cryogel-immobilized cells are used in the waste water treatment processes of the food industry. Fats and oils inhibit the metabolism of the active biomass used to treat such wastewater by forming a hydrophobic film on its surface. Preliminary treatment of wastewater using the proposed biocatalysts reduces the level of oxygen consumption required for oxidation by 2.7–3 times and increases the efficiency of wastewater treatment.

*Application in catalysis*

Catalysis is one of the most promising applications of cryogels. This fact is due to the large surface area per unit volume of the cryogel material. The elasticity, the possibility of varying the pore size, the ease of functionalization-all this opens up wide prospects for the use of cryogel materials in catalysis. One of the most promising developments related to the use of cryogels in catalysis is the so-called flow-through catalytic reactor (Fig. 2) [33, 34]. A special feature of this development is that the reaction mixture is pumped through the volume of the cryogel, while the reaction occurs on the surface of the cryogel pores, which are saturated with catalytically active groups (nanoparticles, enzyme molecules, etc.). This approach allows to get the finished product in one stage without further cleaning it from the catalyst particles.
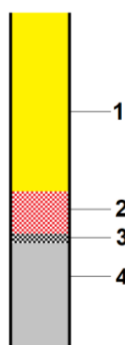


*1* — initial mixture; *2* — cryogel-catalyst; *3* — Schott filter; *4* — mixture of reaction products

Figure 2. Schematic structure of a flow-through catalytic reactor

In [34, 35] the results of the use of a macroporous amphoteric cryogel based on methacrylic acid (MAA) and dimethylaminoethyl methacrylate (DMAEM) crosslinked with methylene bisacrylamide (MBAA) for the immobilization of gold nanoparticles (GNP) are presented. The resulting DMAEM-MAA/GNP composite was used as a flow-type catalytic reactor for the reduction of 4-nitrophenol. The high stability of the prepared catalysts, which withstood at least 100 catalytic cycles, is shown.

Cryogels based on poly-1-vinylimidazole (p-VI) were synthesized by cryopolymerization [36]. After modification with dihaloidalkyl, the synthesized cryogels were used as templates for in situ production of cobalt and nickel metal nanoparticles (Fig. 3A). Poly(1-vinyl imidazole) (p-VI)/metal composites are also used as a catalyst for the hydrolysis of $NaBH_4$ to produce hydrogen. The cryogel matrix based on p-VI showed good operational properties even after 5 catalytic cycles, and the catalyst based on the p-VI/Co composite provided 100 % substrate conversion with a slight loss of catalytic activity. In addition, the proportion of nanoparticles in the cryogel matrix compared to hydrogel and microgel matrices was significantly higher (Fig. 3B).
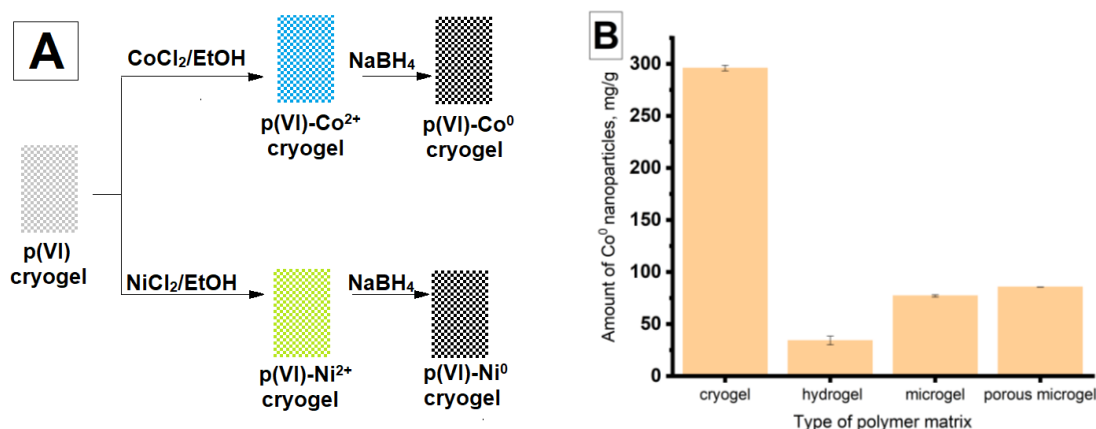


Figure 3. (A) Scheme for the production of cobalt and nickel nanoparticles in a matrix of cryogels based on poly-1-vinylimidazole. (B) The dependence of amount of $Co^0$ nanoparticles on the type of polymer matrix [36]

A cationic cryogel based on poly(3-acrylamidoproply)trimethylammonium chloride (p-APTMACl) was used to stabilize Co and Ni nanoparticles [37].

A series of papers are devoted to the immobilization of enzymes in the cryogel matrix [35, 38–40]. Enzyme immobilization is a promising method for a variety of applications, including biotechnology, medicine, biochemistry, and environmental protection. Enzymes have a very high sensitivity to external conditions and are quickly deactivated when optimal conditions are violated, which, in turn, leads to the impossibility of their repeated usage [38, 41]. However, the immobilization of enzymes in cryogel matrix significantly expands the possibilities of their application.

The resulting composite poly(methyl methacrylate-glycidyl methacrylate (p-MMA-GMA)/amylase is used for the catalytic hydrolysis of starch to produce glucose. It was found that the rate of starch hydrolysis by amylase immobilized in the cryogel matrix is 4 times less than in the case of free amylase, but the stability of the catalyst exceeds the stability of free amylase.

The authors [38, 41] note the prospects of the developed catalysts in comparison with the available analogues, since cryogel-immobilized enzymes allow to prepare the finished product, avoiding the stage of purification and separation of the substrate and the enzyme (Figure 4).

An interesting method of amylase immobilization in a PVA-based cryogel is described in [42]. An aqueous solution of PVA and amylase was frozen and then lyophilized. It is known [1] that cryogenic treatment of aqueous PVA solutions leads to the formation of PVA cryogels. It was found [42] that such treatment of PVA-amylase solutions also leads to the formation of cryogels, and the amylase is automatically integrated into the PVA cryogel matrix. The resulting cryogels were tested in the starch hydrolysis reaction. The substrate conversion rate averaged 70-90 %. Based on the obtained PVA-amylase cryogels, microreactors were constructed by freezing the initial mixture in the capillary. It is shown that the conversion of the substrate in the case of using a microreactor, with rare exceptions, did not exceed 30 %.
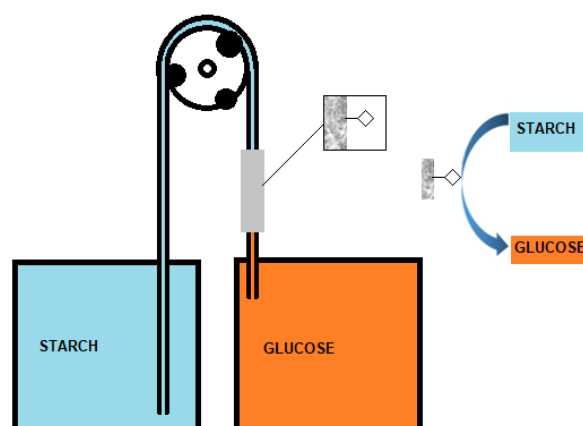


Figure 4. Scheme for the production of glucose from starch on the p-MMA-GMA/amylase catalyst [41]

The laccase enzyme (broad-spectrum oxidase) was immobilized in a cryogel based on polyethylene glycol methacrylate (PEGMA) and tetraethylene glycol diacrylate (TEGDA) [43]. Redox mediators were introduced into the initial mixture: lilac aldehyde or 2,2'-azino-bis-3-ethylbenzothiazoline-6-sulfonic acid. The polymerization reaction was initiated by electron beam irradiation. The resulting cryogels were used as a bioreactor in the oxidation reaction of bisphenol A, as a model wastewater pollutant. It was found that the cryogel-laccase biocatalytic reactor is effective in disinfection of wastewater and completely decomposes the pollutant bisphenol A in the model wastewater within 24 hours.

Cryogels based on functionalized polyacrylamides and alginate were also used to immobilize laccase [44]. It has been shown that the immobilized laccase enzyme successfully removes 70 % of phenolic compounds, more than 55 % of dyes from wastewater and provides 93-99 % of the discoloration of some dyes in solution.

PAA-based cryogel was used to produce a series of modified cryogels that exhibit the properties of cationic (allylamine), anionic (acrylic acid), and amphoteric (allylamine-acrylic acid) cryogels for use as catalysts in the production of biofuels. For this purpose, cryogels of various compositions were mixed with a mixture of methanol and oleate. It is shown that the activity of the cationic catalyst is significantly higher than that of the anionic and amphoteric ones. The relatively high stability of the catalyst over 5 cycles was established [44].

Thus, catalysts based on cryogels and nanoparticles, enzymes, and microorganisms immobilized in their matrix can be successfully used as wide-spectrum catalytic systems.

*Application in medicine*

Biocompatible cryogels and their composites are used in medicine for drug delivery, wound healing, and as materials for bone and cartilage tissue regeneration [45, 46]. The frames made by cryogelization are spongy, highly porous, mechanically stable, elastic, and can be easily cut into any desired shape. Therefore, cryogel materials are of great interest in tissue engineering.

*Restoration of bone and cartilage tissue*

Bone and cartilage are relatively rigid structures compared to other types of tissue. Therefore, materials for the restoration of such tissues must have appropriate mechanical characteristics, as well as be suitable for the germination of osteocytes (bone tissue cells) and chondrocytes (cartilage tissue cells). Cryogels are very promising materials for use in cartilage and bone engineering due to their porosity and functionality. The necessary mechanical strength is achieved by introducing inorganic fillers. For example, in [47], the authors used a polyelectrolyte chitosan/chondroitin sulfate complex modified with nanobio-glass based on silicon, calcium, and phosphorus oxides. An increase in the mass content of nano bio-glass in the composite leads to an increase in the mechanical strength of the composite and a decrease in the pore size. *In vivo* studies have shown excellent bioactivity: increased bioapatite formation, suitable pore size, porosity, and suitable mechanical strength in biological conditions.

Also cryogel chitosan/gelatin crosslinked with glutaraldehyde or genipine was used for bone tissue regeneration by the authors of [48]. For the synthesis the cryogels used covalent crosslinking of macromolecules of chitosan with glutaraldehyde and genipin. The formation of a porous structure is provided by the method of lyophilic drying. The use of genipin provides high biocompatibility of cryogels, however, when studying cell infiltration, it was found that cryogels crosslinked with genipin do not reach the desired level of infiltration and do not provide conditions for cell proliferation.

A composite cryogel based on the chitosan/gelatin-hydroxylapatite system crosslinked with glutaraldehyde was also prepared by freezing and thawing [49]. The cryogel was saturated with hydroxyapatite at a temperature of 37 °C, pH 7.4 in a synthetic body fluid medium (Figure 5). With an increase in the gelatin content in the cryogel, it leads to an increase in the content of hydroxyapatite. The cryogels do not have cytotoxicity against fibroblasts, which was proved in the experiment on rats.
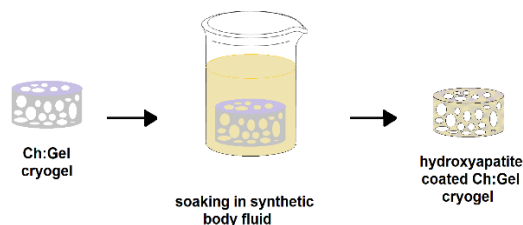


Figure 5. Scheme of preparation a composite cryogel chitosan/gelatin-hydroxylapatite [50]

Modification of hydroxylapatite with cerium and zinc was carried out in [50]. Modified cryogel chitosan/gelatin-Ce-Zn-hydroxylapatite has higher protein adsorption rates, lower biodegradation and cell germination compared to cryogel chitosan/gelatin-hydroxylapatite.

*Restoration of cartilage tissue*

Physical cryogels have an advantage over synthetic ones in the processes of cartilage tissue repair, since they do not require the use of toxic crosslinking agents and do not harm cells [51]. In addition, the lack of blood vessels in the cartilage tissue is a serious limitation of the creation of cartilage substitutes [46]. Elastic macroporous cryogel framework gelatin/chondroitin-6-sulfate/hyaluronan (GCH) is used for the restoration of cartilage tissue.

By replacing 20 % of gelatin by chitosan a new GCH-chitosan cryogel has been synthesized with larger pores, higher ultimate strain (stress) and elastic modulus, and a lower stress relaxation percentage comparing to GCH cryogel. Chondrocytes proliferate and differentiate in cryogels. Implantation of a cryogenic chondrocyte/GCH-chitosan structure into a full-thickness articular cartilage defect regenerates cartilage with a modulus of elasticity similar to native cartilage [52].

Cryogels of the composition gelatin/hyaluronic acid, gelatin/chondroitin sulfate modified with methacrylate were prepared in [53]. It was found that cryogel gelatin/chondroitin sulfate *in vitro* showed significant stimulation of cartilage tissue. In addition, when placed in the subcutaneous tissue of the mouse for 6 weeks, the cryogels showed a uniform distribution of cells with the preservation of the normal phenotype. And when implanted in the osteochondral defect of the New Zealand white rabbit, complete integration with the host tissue and cell germination were observed.

Cryogel based on chitosan and gluconic acid was synthesized by freezing-thawing without the use of crosslinking agents [54]. To prepare materials of cartilage tissue substitutes an average pore diameter of 100 to 300 microns is a prerequisite. The authors established the optimal synthesis temperature and the initial ratio of the components to achieve the desired pore diameter. In experiments on the stability of cryogels in the cellular environment and the proliferation of DNA and glucosaminoglycans, the superiority of a cryogel without a crosslinking agent over a chemically crosslinked cryogel of a similar structure was shown.

The authors of [55] used platelet lysate and oxidized dextran to produce cryogel as a material for cartilage tissue. The complete biodegradability of the synthesized materials under *in vivo* conditions was demonstrated in experiments with rats.

*Cryogels in drug delivery systems*

Cryogel-based drug and biomolecule delivery systems are the subject of intensive research. Biopolymers are widely used for the construction of such materials by combining them with synthetic polymers [56, 57], forming polymer complexes [58] and individually [59]. It is important to note that for drug delivery systems, an important condition is not only and not so much the porosity of the gel material, but the binding of the drug with the polymer matrix as well. Often, hydrolytically cleavable bonds such as simple and ester bonds are used to conjugate the drug with the matrix. These types of bonds provide a long-term drug release profile and increase the half-life of drugs in the body [60].

Three-dimensional (3D) biocomposites based on chitosan and clinoptilolite were obtained by cryogelation. Biocomposites were studied as carriers of the medicinal substances sodium diclofenac and indomethacin. It has been shown that drug delivery preferably occurs at pH 7.4 (intestinal environment), and at pH 1.2 (stomach environment) there is a decrease in drug release [59].

Chitosan cryogel scaffolds including Hypericum perforatum (HP) vegetable oil have been developed, which exhibit unique antimicrobial and antioxidant properties [61]. The composition showed the greatest antimicrobial activity against *E. coli* and *L. pneumophila*. The resulting cryogel scaffolds are promising materials as wound dressings for exudative and long-term healing wounds.

Collagen cryogels with polysaccharide functional components (dextran and carboxymethylcellulose) showed good bio- and hemocompatibility. These cryogels can be used as potential scaffolds for use in tissue engineering and regenerative medicine [62].

Cryogels based on apple pectin and chitosan are used as anti-adhesive barrier materials [63]. The anti-adhesive effect is provided due to the short time of biodegradation of cryogels based on apple pectin, non-degradable cryogels based on hogweed pectin do not have an anti-adhesive effect.

A series of cryogels based on glycol chitosan and ε-polylysine significantly reduce bleeding. The inclusion of ε-polylysine significantly increases the ability to kill a multidrug-resistant bacterial infection (MDR). The effectiveness of wound healing, treated with cryogel, was significantly higher compared to the control. Polysaccharide-peptide cryogels can become competitive multifunctional wound dressings for the control of bleeding and healing of MDR-infected wounds [64].

Examples of medical application and initial polymers for the synthesis of cryogels are shown in Table.

T a b l e

**Composition of cryogels and areas of their application for medical purposes**

| Chemical composition of cryogel | Application area | Reference |
|---|---|---|
| 1 | 2 | 3 |
| Chitosan/Chondroitin sulfate | | 46 |
| Chitosan/Gelatin crosslinked with Glutaraldehyde or Genipine | | 47 |
| Chitosan/Gelatin-Hydroxylapatite crosslinked with Glutaraldehyde | Prosthetics and bone regeneration | 48 |
| Chitosan/Gelatin-Ce-Zn-Hydroxylapatite | | 49 |
| Collagen/Hydroxylapatite | | 65, 66 |
| Gelatin/Hydroxylapatite | | 67 |

| 1 | 2 | 3 |
|---|---|---|
| Gelatin/Nanohydroxylapatite | Prosthetics and bone regeneration | 68 |
| Hyaluronic acid/Gelatin | | 69 |
| Alginate | | 70, 71 |
| Chitosan-Agarose-Gelatin | Restoration of cartilage tissue | 72 |
| PVA/Chitosan | | 73 |
| Polyhydroxyethylmethacrylate-Gelatin | | 74 |
| Hyaluronic acid/Polyethylenimine | | 75 |
| Hyaluronic acid | | 76 |
| Gelatin /Hyaluronic acid | | 77 |
| Carrageenan/Alginate | | 78 |
| Sodium Alginate/ acetylated Dextran | Drug delivery | 79 |
| Nanocellulose/Gelatin | | 80 |

## Conclusions

Thus, based on the literature data, it can be concluded that cryogels based on biopolymers, especially polysaccharides, due to their unique properties, namely, macroporosity, elasticity, biodegradability, biocompatibility, and biological activity are promising materials for application in biotechnology, catalysis, and medicine.

In the field of cryogel synthesis, it is necessary to develop technologies that make it possible to prepare a biocompatible material without the use of harmful and toxic substances. In this regard, cryogels based on interpolyelectrolyte complexes of natural polymers seem promising.

According to the authors, the most promising areas of development of cryogel technologies are the development of biocatalytic systems and tissue engineering. The most important task of researchers for a breakthrough in these areas in the near future will be to develop a method for producing biocompatible cryogels of the desired strength. This approach will make it possible to obtain cryogels that are comparable in mechanical strength to bone and cartilage tissues. Despite the complexity of the task, the authors believe that in the foreseeable future the technology of 3D-printing cryogels will be developed in order to produce catalysts, as well as joint prostheses based on biocompatible durable cryogels.

## References

1   Lozinsky V.I. Cryogels on the basis of natural and synthetic polymers: preparation, properties and application / V.I. Lozinsky // Russian Chemical Reviews. — 2002. — Vol. 71(6). — P. 489–511. https://doi.org/10.1070/RC2002v071n06ABEH000720

2   Klivenko A.N. Synthesis and phisico-chemical properties of macroporous cryogels / A.N. Klivenko, G.S. Tatykhanova, G.A. Mun, S.E. Kudaibergenov // International Journal of Biology and Chemistry. — 2015. — Vol. 8(1). — P. 52–60. https://doi.org/10.26577/2218-7979-2015-8-1-52-60

3   Lozinsky V.I. A Brief History of Polymeric Cryogels / V.I. Lozinsky // Advanced polymer science. — 2014. — Vol. 263. — P. 1–48. https://doi:10.1007/978-3-319-05846-7_1

4   Плаченов Т.Г. Порометрия / Т.Г. Плаченов, С.Д. Колосенцев. — Л.: Химия, 1988. — 176 с.

5   Kudaibergenov S.E. Physico-chemical and rheological properties of gellan in aqueous-salt solutions and oilfield saline water / S.E. Kudaibergenov, G.S. Tatykhanova, V.B. Sigitov, Z.A. Nurakhmetova, E.V. Blagikh, I.S. Gussenov, T.M. Seilkhanov // Macromolecular Symposia. — 2016. — Vol. 363(1). — P. 20–35. https://doi.org/10.1002/masy.201500139

6   Ho M.H. Preparation of porous scaffolds by using freeze-extraction and freeze-gelation methods / M.H. Ho, P.Y. Kuo, H.J. Hsieh, T.Y. Hsien, L.T. Hou, J.Y. Lai, D.M. Wang // Biomaterials. — 2004. — Vol. 25(1). — P. 129–138. https://doi.org/10.1016/S0142-9612(03)00483-6

7   Petrenko Y.A. Coupling of gelatin to inner surfaces of pore walls in spongy alginate-based scaffolds facilitates the adhesion, growth and differentiation of human bone marrow mesenchymal stromal cells / Y.A. Petrenko, R.V. Ivanov, A.Y. Petrenko, V.I. Lozinsky // Journal of Materials Science-Materials in Medicine. — 2011. — V. 22 (6). — P. 1529–1540. https://doi.org/10.1007/s10856-011-4323-6

8   Nikanorov V.V. Synthesis and characteristics of cryogels of chitosan crosslinked by glutaric aldehyde / V.V. Nikanorov, R.V. Ivanov, N.R. Kil'deeva, L.N. Bulatnikova, V.I. Lozinsky // Polymer Science. Series A. — 2010. — Vol. 52(8). — P. 828–834. DOI: 10.1134/s0965545x10080092

9 Патент РФ 0002699562. Способ получения пористых материалов на основе хитозана / Братская С.Ю., Привар Ю.О., Нестеров Д.В., Пестов А.В. — № 219.017.c933; опубл. 08.09.2019.

10 Berillo D. Oxidized dextran as crosslinker for chitosan cryogel scaffolds and formation of polyelectrolyte complexes between chitosan and gelatin / D. Berillo, L. Elowsson, H. Kirsebom // Macromolecular Bioscience. — 2012. — Vol. 12(8). — P. 1090–1099. DOI: 10.1002/mabi.201200023

11 Hu X. Design of a novel polysaccharide-based cryogel using triallyl cyanurate as crosslinker for cell adhesion and proliferation / X. Hu, Y. Wang, L. Zhang, M. Xu // International Journal of Biological Macromolules. — 2019. — Vol. 126. — P. 221–228. https://doi.org/10.1016/j.ijbiomac.2018.12.226

12 Reichelt S. Biocompatible polysaccharide-based cryogels / S. Reichelt, J. Becher, J. Weisser, A. Prager, U. Decker, S. Möller, A. Berg, M. Schnabelrauch // Materials Science & Engineering: C. — 2014. — Vol. 35. — P. 164–170. https://doi.org/10.1016/j.msec.2013.10.034

13 Akilbekova D. Biocompatible scaffolds based on natural polymers for regenerative medicine / D. Akilbekova, M. Shaimerdenova, S. Adilov, D. Berillo // International Journal of Biological Macromolecules. — 2018. — Vol. 114. — P. 324–333. https://doi.org/10.1016/j.ijbiomac.2018.03.116

14 Tan H. Collagen cryogel cross-linked by naturally derived dialdehyde carboxymethyl cellulose / H. Tan, H. Wu, C. Li, C. Mu, H. Li, W. Lin // Carbohydrate Polymers. — 2015. — Vol. 129. — P. 17–24. https://doi.org/10.1016/j.carbpol.2015.04.029

15 Tavsani B. Macroporous methacrylated hyaluronic acid cryogels of high mechanical strength and flow-dependent viscoelasticity / B. Tavsani, O. Okay // Carbohydrate Polymers. — 2020. — Vol. 229:115458. https://doi.org/10.1016/j.carbpol.2019.115458

16 Zhang H. Physically crosslinked hydrogels from polysaccharides prepared by freeze–thaw technique / H. Zhang, F. Zhang, J. Wu // Reactive and Functional Polymers. — 2013. — Vol. 73(7). — P. 923–928. https://doi.org/10.1016/j.reactfunctpolym.2012.12.014

17 Brovko O.S. Gels of sodium alginate–chitosan interpolyelectrolyte complexes / O.S. Brovko, I.A. Palamarchuk, N.A. Val'chuk, D.G. Chukhchin, K.G. Bogolitsyn, T.A. Boitsova // Russian Journal of Physical Chemistry A. — 2017. — Vol. 91(8). — P. 1580–1585. https://doi.org/10.1134/S0036024417160014

18 Konovalova M.V. Preparation and characterization of cryogels based on pectin and chitosan / M.V. Konovalova, D.V. Kurek, S.G. Litvinets, E.A. Martinson, V.P. Varlamov // Progress on Chemistry and Application of Chitin and its Derivative. — 2016. — Vol. 21. — P. 114–121. DOI: 10.15259/PCACD.21.12

19 Коновалова М.В. Деградация in vitro пектин-хитозановых криогелей / М.В. Коновалова, Д.В. Курек, Е.А. Дурнев, С.Г. Литвинец, В.П. Варламов // Изв. Уфим. науч. центра РАН. — 2016. — № 3–1. — С. 42–45.

20 Stoyneva V. Stimuli sensitive super-macroporous cryogels based on photo-crosslinked 2-hydroxyethylcellulose and chitosan / V. Stoyneva, D. Momekova, B. Kostovs, P. Petrov // Carbohydrate Polymers. — 2014. — Vol. 99. — P. 825–830. https://doi.org/10.1016/j.carbpol.2013.08.095

21 Raschip I.E. Development of antioxidant and antimicrobial xanthan-based cryogels with tuned porous morphology and controlled swelling features / I.E. Raschip, N. Fifere, C-D. Varganici, M.V. Dnu // International Journal of Biological Macromolecules. — 2020. — Vol. 156. — P. 608–620. https://doi.org/10.1016/j.ijbiomac.2020.04.086

22 Kutlusoy T. Chitosan-co-Hyaluronic acid porous cryogels and their application in tissue engineering / T. Kutlusoy, B. Oktay, N.K. Apohan, M. Süleymanoğlu, S.E. Kuruca // International Journal of Biological Macromolecules. — 2017. — Vol. 103. — P. 366–378. https://doi.org/10.1016/j.ijbiomac.2017.05.067

23 Lozinsky V.I. Polymeric cryogels as promising materials of biotechnological interest / V.I. Lozinsky, I.Y. Galaev, F.M. Plieva, I.N. Savinal, H. Jungvid, B. Mattiasson // Trends in biotechnology. — 2003. — Vol. 21(10). — P. 445–451. https://doi.org/10.1016/j.tibtech.2003.08.002

24 Alkan H. Antibody purification with protein A attached supermacroporous poly(hydroxyethyl methacrylate) cryogel / H. Alkan, N. Bereli, Z. Baysal, A. Denizli // Biochemical engineering journal. — 2009. — Vol. 45(3). — P. 201–208. https://doi.org/10.1016/j.bej.2009.03.013

25 Akduman B. Purification of yeast alcohol dehydrogenase by using immobilized metal affinity cryogels / B. Akduman, M. Uygun, D.A. Uygun, S. Akgol, A. Denizli // Materials Science & Engineering C-Materials for biological applications. — 2013. — Vol. 33(8). — P. 4842–4848. https://doi.org/10.1016/j.msec.2013.08.007

26 Mattiasson B. Cryogels for biotechnological applications / B. Mattiasson // Advanced Polymer Science. — 2014. — Vol. 263. — P. 245–281. https://doi.org/10.1007/978-3-319-05846-7_7

27 Krajnc N. Monolithic macroporous polymers as chromatographic matrices / N. Krajnc, F. Smrekar, V. Frankovic, A. Trancar, A. Podgornik // Macroporous polymers: production properties and bitechnological/biomedical applications / Mattiasson B. et al. – Boca Raton: CRC Press, 2010. — P. 291–334. DOI: 10.1201/9781420084627-c12

28 Dainiak M. Cryogels as matrices for cell separation and cell cultivation / M. Dainiak, A. Kumar, I. Galaev, B. Mattiasson // Macroporous polymers: production properties and bitechnological/biomedical applications / Mattiasson B. et al. — Boca Raton: CRC Press, 2010. — P. 363–404. DOI: 10.1201/9781420084627-c14

29 Galaev I.Y. Effect of matrix elasticity on affinity binding and release of bioparticles. Elution of bound cells by temperature-induced shrinkage of the smart macroporous hydrogel / I.Y. Galaev, M.B. Dainiak, F. Plieva, B. Mattiasson // Langmuir. — 2007. — Vol. 23(1). — P. 35–40. https://doi.org/10.1021/la061462e

30 Dainiak M.B. Detachment of affinity-captured bioparticles by elastic deformation of a macroporous hydrogel / M.B. Dainiak, A. Kumar, I.Y. Galaev, B. Mattiasson // Proceedings of the National academy of sciences of the United States of America. — 2006. — Vol. 103(4). — P. 849-854. https://doi.org/10.1073/pnas.0508432103

31 Efremenko E.N. L(+)-lactic acid production using poly(vinyl alcohol)-cryogel-entrapped Rhizopus oryzae fungal cells / E.N. Efremenko, O.V. Spiricheva, D.V. Veremeenko, A.V. Baibak, V.I. Lozinsky // Journal of Chemical technology and Biotechnology. — 2006. — Vol. 81(4). — P. 519–522. DOI: 10.1002/jctb.1524

32 Efremenko E. New biocatalyst with multiple enzymatic activities for treatment of complex food wastewaters / E. Efremenko, O. Senko, D. Zubaerova, E. Podorozhko, V. Lozinsky // Food technology and biotechnology. — 2008. — Vol. 46(2). — P. 208–212.

33  Klivenko A. Gold nanoparticles stabilized by amphoteric cryogel-perspective flow-through catalytic reactor for oxidation and reduction processes / A. Klivenko, A. Yergaziyeva, S. Kudaibergenov // Nanomaterials: Application & Properties (NAP-2016): Proceedings of International Conference (September 9-14, 2016). — Lviv, Ukraine. — P. 02NSA03-1-02NSA03-5. DOI: 10.1109/NAP.2016.7757304

34  Tatykhanova G.S. Flow-through catalytic reactor based on macroporous amphoteric cryogels and gold nanoparticles / G.S. Tatykhanova, A.N. Klivenko, G.M. Kudaibergenova, S.E. Kudaibergenov // Macromolecular Symposia. — 2016. — Vol. 363 (1). — P. 49–56. https://doi.org/10.1002/masy.201500137

35  Kudaibergenov S.E. Macroporous amphoteric hydrogels (Cryogels): design of flow-through catalytic reactor / Kudaibergenov S.E., Tatykhanova G.S., Klivenko A.N. // EMN meeting on hydrogel materials: Book of abstracts (May 9-13, 2016). — Singapore. — P. 50–51.

36  Sahiner N. Super-fast hydrogen generation via super porous Q-P(VI)-M cryogel catalyst systems from hydrolysis of $NaBH_4$ / N. Sahiner, F. Seven, H. Al-Lohedan // International Journal of Hydrogen Energy. — 2015. — Vol. 40(13). — P. 4605–4616. https://doi.org/10.1016/j.ijhydene.2015.02.049

37  Sahiner N. A facile synthesis route to improve the catalytic activity of inherently cationic and magnetic catalyst systems for hydrogen generation from sodium borohydride hydrolysis / N. Sahiner, F. Seven // Fuel processing technology. — 2015. — Vol. 132. — P. 1–8. https://doi.org/10.1016/j.fuproc.2014.12.008

38  Uygun D.A. Immobilization of alcohol dehydrogenase onto metal-chelated cryogels / D.A. Uygun, B. Akduman, M. Uygun, S. Akgol, A. Denizli // Journal of Biomaterials Science. Polymer edition. — 2015. — Vol. 26(7). — P. 446–457. DOI: 10.1080/09205063.2015.1023241

39  Demiryas N. Poly(acrylamide-allyl glycidyl ether) cryogel as a novel stationary phase in dye-affinity chromatography / N. Demiryas, N. Tuzmen, I.Y. Galaev, E. Piskin, A. Denizli // Journal of Applied Polymer Science. — 2007. — Vol. 105(4). — P. 1808–1816. https://doi.org/10.1002/app.26187

40  Jahangiri E. Electron Beam-Induced immobilization of laccase on porous supports for waste water treatment applications / E. Jahangiri, S. Reichelt, I. Thomas, K. Hausmann, D. Schlosser, A. Schulze // Molecules. — 2014. — Vol. 19(8). — P. 11860–11882. DOI: 10.3390/molecules190811860

41  Uygun M. Immobilization of amyloglucosidase onto macroporous cryogels for continuous glucose production from starch / M. Uygun, B. Akduman, B. Ergonul, D.A. Uygun, S. Akgol, A. Denizli // Journal of Biomaterials Science. Polymer edition. — 2015. — Vol. 26(16). — P. 1112–1125. https://doi.org/10.1080/09205063.2015.1078928

42  Nakagawa K. Preparation of alpha-amylase-immobilized freeze-dried poly(vinyl alcohol) foam and its application to microfluidic enzymatic reactor / K. Nakagawa, Y. Goto // Chemical Engineering and Processing. — 2015. — Vol. 91. — P. 35–42. https://doi.org/10.1016/j.cep.2015.03.010

43  Yavaser R. Laccase immobilized polyacrylamide-alginate cryogel: A candidate for treatment of effluents / R. Yavaser, A.A. Karagozler // Prosess Biochemistry. — 2021. — Vol. 101. — P. 137–146. https://doi.org/10.1016/j.procbio.2020.11.021

44  Yang C. Polyacrylamide based cryogels as catalysts for biodiesel / C. Yang, G.-F. Liu, X.-L. Zhou, Y.-R. Liu, J. Wang, L.-L. Tian, X.-Y. Hu, Y.-Y. Wang // Catalysis letters. — 2015. — Vol. 145(9). — P. 1778-1783. https://doi.org/10.1007/s10562-015-1580-x

45  Auriemma G. Technologies and Formulation Design of Polysaccharide-Based Hydrogels for Drug Delivery / G. Auriemma, P. Russo, P. Del Gaudio, C.A. García-González, M. Landín, R.P. Aquino // Molecules. — 2020. — Vol. 25(14). — P. 3156–3191. https://doi.org/10.3390/molecules25143156

46  Sultankulov B. Progress in the Development of Chitosan-Based Biomaterials for Tissue Engineering and Regenerative Medicine / B. Sultankulov, D. Berillo, K. Sultankulova, T. Tokay, A. Saparov // Biomolecules. — 2019. — Vol. 9(9). — P. 1–16. doi: 10.3390/biom9090470

47  Singh B.N. Design and evaluation of chitosan/chondroitin sulfate/nano-bioglass based composite scaffold for bone tissue engineering / B.N. Singh, V. Veeresh, S.P. Mallick, Y. Jain, S. Sinha, A. Rastogi, P. Srivastava // International Journal of Biological Macromolecules. — 2019. — Vol. 133. — P. 817–830. https://doi.org/10.1016/j.ijbiomac.2019.04.107

48  Georgopoulou A. Chitosan/gelatin scaffolds support bone regeneration / A. Georgopoulou, F. Papadogiannis, A. Batsali, J. Marakis, K. Alpantaki, A.G. Eliopoulos, C. Pontikoglou, M. Chatzinikolaidou // Journal of Materials Science-Materials in Medicine. — 2018. — Vol. 29(5). — P. 1–13. https://doi.org/10.1007/s10856-018-6064-2

49  Ofkeli F. Biomimetic mineralization of chitosan/gelatin cryogels and in vivo biocompatibility assessments for bone tissue engineering / F. Ofkeli, D. Demir, N. Bolgen // Journal of Applied Polymer Science. — 2021. — Vol. 138(14). — P. 1–12. https://doi.org/10.1002/app.50337

50  Wu S.Q. Cryogel biocomposite containing chitosan-gelatin/cerium-zinc doped hydroxyapatite for bone tissue engineering / S.Q. Wu, S.Z. Ma, C. Zhang, G.Q. Cao, D.J. Wu, C.Z. Gao, S. Lakshmanan // Saudi Journal of Biological Sciences. — 2020. — Vol. 27(10). — P. 2638–2644. https://doi.org/10.1016/j.sjbs.2020.05.045

51  Offeddu G.S. Cartilage-like electrostatic stiffening of responsive cryogel scaffolds / G.S. Offeddu, I. Mela, P. Jeggle, R.M. Henderson, S.K. Smoukov, M.L. Oyen // Scientific Reports. — 2017. — Vol. 7. — P. 1–10. https://doi.org/10.1038/srep42948

52  Kuo C.-Y. Incorporation of chitosan in biomimetic gelatin/chondroitin-6-sulfate/hyaluronan cryogel for cartilage tissue engineering / C.-Y. Kuo, C.-H. Chen, C.-Y. Hsiao, J.-P. Chen // Carbohydrate Polymers. — 2015. — Vol. 117. — P. 722–730. https://doi.org/10.1016/j.carbpol.2014.10.056

53  Han M.E. Gelatin-based extracellular matrix cryogels for cartilage tissue engineering / M.E. Han, B.J. Kang, S.H. Kim, H.D. Kim, N.S. Hwang // Journal of Industrial and Engineering Chemistry. — 2017. — Vol. 45. — P. 421–429. https://doi.org/10.1016/j.jiec.2016.10.011

54  Takei T. Toxic Chemical Cross-linker-free Cryosponges Made from Chitosan-Gluconic Acid Conjugate for Chondrocyte Culture / T. Takei, H. Yoshitomi, K. Fukumoto, S. Danjo, T. Yoshinaga, H. Nishimata, M. Yoshida // Journal of Chemical Engineering of Japan. — 2017. — Vol. 50(2). — P. 142–148. https://doi.org/10.1252/jcej.16we145

55  Seker S. Macroporous elastic cryogels based on platelet lysate and oxidized dextran as tissue engineering scaffold: In vitro and in vivo evaluations / S. Seker, A.E. Elcin, Y.M. Elcin // Materials Science & Engineering C-Materials for Biological Applications. — 2020. — Vol. 110. — P. 1–11. https://doi.org/10.1016/j.msec.2020.110703

56 Pacelli S. Dextran-polyethylene glycol cryogels as spongy scaffolds for drug delivery / S. Pacelli, L. Di Muzio, P. Paolicelli, V. Fortunati, S. Petralito, J. Trilli, M.A. Casadei // International Journal of Biological Macromolecules. — 2021. — Vol. 166. — P. 1292–1300. https://doi.org/10.1016/j.ijbiomac.2020.10.273

57 Georgiev G.L. Super-macroporous composite cryogels based on biodegradable dextran and temperature-responsive poly(N-isopropylacrylamide) / G.L. Georgiev, D. Borisova, P.D. Petrov // Journal of Applied Polymer Science. — 2020. — Vol. 137(42). — P. 1–8. https://doi.org/10.1002/app.49301

58 Chaux-Gutierrez A.M. Cryogels from albumin and low methoxyl amidated pectin as a matrix for betalain encapsulation / A.M. Chaux-Gutierrez, E.J. Perez-Monterroza, D.M. Granda-Restrepo, M.A. Mauro // Journal of Food Processing and Preservation. — 2020. — Vol. 44(11). — P. 1–10. https://doi.org/10.1111/jfpp.14843

59 Dinu M.V. Synthesis, characterization and drug release properties of 3D chitosan/clinoptilolite biocomposite cryogels / M.V. Dinu, A.I. Cocarta, E.S. Dragan // Carbohydrate Polymers. — 2016. — Vol. 153. — P. 203–211. https://doi.org/10.1016/j.carbpol.2016.07.111

60 Ari B. Biodegradable super porous inulin cryogels as potential drug carrier / B. Ari, N. Sahiner // Polymers for Advanced Technologies. — 2020. — Vol. 31(11). — P. 2863–2873. https://doi.org/10.1002/pat.5014

61 Bölgen N. Development of Hypericum perforatum oil incorporated antimicrobial and antioxidant chitosan cryogel as a wound dressing material / N. Bölgen, D. Demir, S. Yalçın, S. Özdemir // International Journal of Biological Macromolecules. — 2020. — Vol. 161. — P. 1581–1590. https://doi.org/10.1016/j.ijbiomac.2020.08.056

62 Odabas S. Functional Polysaccharides Blended Collagen Cryogels / S. Odabas // Hacettepe Journal of Biology and Chemistry. — 2018. — Vol. 46(1). — P. 113–120. DOI: 10.15671/HJBC.2018.219

63 Konovalova M.V. Preparation and biocompatibility evaluation of pectin and chitosan cryogels for biomedical application / M.V. Konovalova, P.A. Markov, E.A. Durnev, D.V. Kurek, S.V. Popov, V.P. Varlamov // Journal of Biomedical Materials Research. A. — 2017. — Vol. 105(2). — P. 547–556. DOI: 10.1002/jbm.a.35936

64 Hou Y. Polysaccharide-Peptide Cryogels for Multidrug-Resistant-Bacteria Infected Wound Healing and Hemostasis / Y. Hou, F. Feng, J. Zhou, X. Feng, Y. Fan // Advanced Helthcare Matarials. — 2020. — Vol. 9(3):1901041. https://doi.org/10.1002/adhm.201901041

65 Salgado C.L. Clarifying the Tooth-Derived Stem Cells Behavior in a 3D Biomimetic Scaffold for Bone Tissue Engineering Applications / C.L. Salgado, C.C. Barrias, F.J.M. Monteiro // Frontiers in Bioengineering and Biotechnology. — 2020. — Vol. 8. — P. 1–15. https://doi.org/10.3389/fbioe.2020.00724

66 Rodrigues S.C. Preparation and characterization of collagen-nanohydroxyapatite biocomposite scaffolds by cryogelation method for bone tissue engineering applications / S.C. Rodrigues, C.L. Salgado, A. Sahu, M.P. Garcia, M.H. Fernandes, F.J. Monteiro // Journal of Biomedical Materials Research. A. — 2013. — Vol. 101(4). — P. 1080–1094. https://doi.org/10.1002/jbm.a.34394

67 Gu L.H. Comparative study of gelatin cryogels reinforced with hydroxyapatites with different morphologies and interfacial bonding / L.H. Gu, Y.F. Zhang, L.W. Zhang, Y.Q. Huang, D.W. Zuo, Q. Cai, X.P. Yang // Biomedical Materials. — 2020. — Vol. 15(3). — P. 1–14. https://doi.org/10.1088/1748-605X/ab7388

68 Shalumon K.T. Rational design of gelatin/nanohydroxyapatite cryogel scaffolds for bone regeneration by introducing chemical and physical cues to enhance osteogenesis of bone marrow mesenchymal stem cells / K.T. Shalumon, H.T. Liao, C.Y. Kuo, C.B. Wong, C.J. Li, P.A. Mini, J.P. Chen // Materials Science & Engineering C-Materials for Biological Applications. — 2019. — Vol. 104. — P. 1-19. https://doi.org/10.1016/j.msec.2019.109855

69 Rezaeeyazdi M. Injectable Hyaluronic Acid-co-Gelatin Cryogels for Tissue-Engineering Applications / M. Rezaeeyazdi, T. Colombani, A. Memic, S.A. Bencherif // Materials. — 2018. — Vol. 11(8). — P. 1–18. doi: 10.3390/ma11081374

70 Petrenko Y.A. Comparison of the Methods for Seeding Human Bone Marrow Mesenchymal Stem Cells to Macroporous Alginate Cryogel Carriers / Y.A. Petrenko, R.V. Ivanov, V.I. Lozinsky, A.Y. Petrenko // Bulletin of Experimental Biology and Medicine. — 2011. — Vol. 150(4). — P. 543–546. https://doi.org/10.1007/s10517-011-1185-3

71 Petrenko Y.A. Growth and Adipogenic Differentiation of Mesenchymal Stromal Bone Marrow Cells during Culturing in 3D Macroporous Agarose Cryogel Sponges / Y.A. Petrenko, A.Y. Petrenko, L.G. Damshkaln, N.A. Volkova, V.I. Lozinsky // Bulletin of Experimental Biology and Medicine. — 2008. — Vol. 146(1). — P. 129–132. https://doi.org/10.1007/s10517-008-0236-x

72 Bhat S. Cell proliferation on three-dimensional chitosan-agarose-gelatin cryogel scaffolds for tissue engineering applications / S. Bhat, A. Kumar // Journal of Bioscience and Bioengineering. — 2012. — Vol. 114(6). — P. 663–670. DOI: 10.1016/j.jbiosc.2012.07.005

73 Mathews D.T. Vascular cell viability on polyvinyl alcohol hydrogels modified with water-soluble and -insoluble chitosan / D.T. Mathews, Y.A. Birney, P.A. Cahill, G.B. McGuinness // Journal of Biomedical Materials Research Part B-Applied Biomaterials. — 2008. — Vol. 84B (2). — P. 531–540. doi: 10.1002/jbm.b.30901

74 Singh D. Proliferation of Chondrocytes on a 3-D Modelled Macroporous Poly(Hydroxyethyl Methacrylate)-Gelatin Cryogel / D. Singh, A. Tripathi, V. Nayak, A. Kumar // Journal of Biomaterials Science-Polymer Edition. — 2011. — Vol. 22(13). — P. 1733–1751. DOI: 10.1163/092050610X522486

75 Demirci S. Superporous hyaluronic acid cryogel composites embedding synthetic polyethyleneimine microgels and Halloysite Nanotubes as natural clay / S. Demirci, S.S. Suner, M. Sahiner, N. Sahiner // European Polymer Journal. — 2017. — Vol. 93. — P. 775–784. https://doi.org/10.1016/j.eurpolymj.2017.04.022

76 He T. Hyaluronic acid-based shape memory cryogel scaffolds for focal cartilage defect repair / T. He, B. Li, T. Colombani, K.J. Navare, S.A. Bencherif, A.G. Bajpayee // Osteoarthritis and Cartilage. — 2020. — Vol. 28. — P. 504–504. DOI: 10.1089/ten.TEA.2020.0264

77 Chen C.H. Dual Function of Glucosamine in Gelatin/Hyaluronic Acid Cryogel to Modulate Scaffold Mechanical Properties and to Maintain Chondrogenic Phenotype for Cartilage Tissue Engineering / C.H. Chen, C.Y. Kuo, Y.J. Wang, J.P. Chen // International Journal of Molecular Sciences. — 2016. — Vol. 17(11). — P. 1957–1978. DOI: 10.3390/ijms17111957

78 Ki S.B. Effect of cross-linkers in fabrication of carrageenan-alginate matrices for tissue engineering application / S.B. Ki, D. Singh, S.C. Kim, T.W. Son, S.S. Han // Biotechnology and Applied Biochemistry. — 2013. — Vol. 60(6). — P. 589–595. DOI: 10.1002/bab.1123

79  Bauleth-Ramos T. Acetalated Dextran Nanoparticles Loaded into an Injectable Alginate Cryogel for Combined Chemotherapy and Cancer Vaccination / T. Bauleth-Ramos, T.Y. Shih, M.A. Shahbazi, A.J. Najibi, A.S. Mao, D.F. Liu, P. Granja, H.A. Santos, B. Sarmento, D.J. Mooney // Advanced Functional Materials. — 2019. — Vol. 29(35):1903686. https://doi.org/10.1002/adfm.201903686

80  Li J. Nanocellulose/Gelatin Composite Cryogels for Controlled Drug Release / J. Li, Y.J. Wang, L. Zhang, Z.Y. Xu, H.Q. Dai, W.B. Wu // Acs Sustainable Chemistry & Engineering. — 2019. — Vol. 7(6). — P. 6381–6389. https://doi.org/10.1021/acssuschemeng.9b00161

А.Н. Кливенко, Б.Х. Мұсабаева, Б.С. Гайсина, А.Н. Сабитова

## Биоүйлесімді криогельдер: алынуы және қолданылуы

Полимерлі криогельдер пайдалы функционалды материалдарды алу үшін өте перспективалы заттар болып табылады. Криогельдердің кеуекті құрылымы оларды медицинаның, катализдің және биотехнологияның кейбір салаларында баға жетпес материал етеді. Осы шолуда биополимерлерден және де биополимерлердің интерполиэлектролитті комплекстерінен алынатын криогельдерге және оларға негізделген композиттік криогельдер алу әдістеріне ерекше назар аударылған. Алдымен, криогельдердің ерекше қасиеттері туралы және биополимерлер негізінде криогельді материалдарды өндіру туралы қысқаша теориялық мәліметтер берілген. Шолудың екінші бөлімінде биополимерлер мен олардың комплекстеріне негізделген композиттік криогельдер өндірудегі әлемдегі соңғы жетістіктер жинақталған. Криогельдерді синтездеу ерекшеліктері және де синтезделетін криогельді материалдардың қажетті болатын қасиеттеріне әсер ететін факторлар қарастырылды. Шолудың қорытынды бөлімінде қарастырылатын типтегі полимерлі криогельдерді биотехнологияда, катализде және медицинада қолдану салалары егжей-тегжейлі зерттелген. Биотехнология саласында криогельді материалдар молекулаларды және де биологиялық жасушаларды иммобилизациялау үшін, жасуша өсуінің негізі ретінде, сонымен қоса жасушаларды өзара бөлу үшін хроматографиялық материалдар ретінде пайдаланылады. Катализ саласында полимерлі криогельдер металл нанобөлшектерін иммобилизациялау үшін, сондай-ақ ферменттерді иммобилизациялау үшін матрица ретінде қолданылады. Биологиялық үйлесімді криогельдер мен олардың композиттері медицина саласында сүйек және шеміршек ұлпаларын қалпына келтіру үшін, сондай-ақ дәрі-дәрмектерді адрестік жеткізу үшін кеңінен қолданылады, бұл организмде дәрі-дәрмектерді бөліп шығарудың ұзақ мерзімді профилін қамтамасыз етеді.

*Кілт сөздер:* криогель, биоүйлесімді, биополимер, макрокеуектілік, иммобильдеу, биотехнология, катализ, дәрі-дәрмекті жеткізу, ұлпалық инженерия.

А.Н. Кливенко, Б.Х. Мусабаева, Б.С. Гайсина, А.Н. Сабитова

## Биосовместимые криогели: получение и применение

Полимерные криогели являются весьма перспективными веществами для получения функциональных материалов. Пористая структура делает криогели незаменимыми материалами в некоторых областях медицины, катализа и биотехнологии. В данном обзоре авторы сосредоточились на методах получения криогелей на основе биополимеров, интерполиэлектролитных комплексов биополимеров и композитных криогелей на их основе. Сначала рассмотрены свойства криогелей и краткие теоретические сведения о способах получения криогелей на основе биополимеров. Во втором разделе обзора обобщены последние достижения в производстве криогелей на основе комплексов биополимеров и композитных криогелей. Рассмотрены особенности синтеза криогелей и факторы, влияющие на требуемые конечные свойства криогелевых материалов. В заключительной части обзора подробно изучены области применения криогелей рассматриваемых типов в биотехнологии, катализе и медицине. В биотехнологии криогелевые материалы используются для иммобилизации молекул и биологических клеток, в качестве основы для роста клеток, а также хроматографических материалов для разделения клеток. В катализе криогелевые материалы применяются как матрицы для иммобилизации наночастиц металлов и ферментов. Биосовместимые криогели и композиты на их основе находят широкое применение в медицине для регенерации костной и хрящевой ткани, а также для адресной доставки лекарственных средств, обеспечивая долгосрочный профиль высвобождения лекарственных средств в организме.

*Ключевые слова:* криогель, биосовместимый, биополимер, макропористость, иммобилизация, биотехнология, катализ, доставка лекарств, тканевая инженерия.

# References

1    Lozinsky, V.I. (2002). Cryogels on the basis of natural and synthetic polymers: preparation, properties and application. *Russian Chemical Reviews, 71,* 489–511. https://doi.org/10.1070/RC2002v071n06ABEH000720

2    Klivenko, A.N., Tatykhanova, G.S., Mun, G.A., & Kudaibergenov, S.E. (2015). Synthesis and phisico-chemical properties of macroporous cryogels. *International Journal of Biology and Chemistry, 8,* 52–60. https://doi.org/10.26577/2218-7979-2015-8-1-52-60

3    Lozinsky, V. I. (2014). A Brief History of Polymeric Cryogels. Advanced Polymer Science, 263, 1–48. https://doi:10.1007/978-3-319-05846-7_1

4    Plachenov, T.G., & Kolosentsev, S.D. (1988) *Porometriia [Porometry].* Leningrad: Khimiia [in Russian].

5    Kudaibergenov, S.E., Tatykhanova, G.S., Sigitov, V.B., Nurakhmetova, Z.A., Blagikh, E.V., Gussenov, I.S., & et al. (2016). Physico-chemical and rheological properties of gellan in aqueous-salt solutions and oilfield saline water. *Macromolecular symposia, 363,* 20-35. https://doi.org/10.1002/masy.201500139

6    Ho, M.H., Kuo, P.Y., Hsieh, H.J., Hsien, T.Y., Hou, L.T., Lai, J.Y., & et al. (2004). Preparation of porous scaffolds by using freeze-extraction and freeze-gelation methods. *Biomaterials, 25,* 129-138. https://doi.org/10.1016/S0142-9612(03)00483-6

7    Petrenko, Y.A., Ivanov, R.V., Petrenko, A.Y., & Lozinsky, V.I. (2011). Coupling of gelatin to inner surfaces of pore walls in spongy alginate-based scaffolds facilitates the adhesion, growth and differentiation of human bone marrow mesenchymal stromal cells. *Journal of Materials Science-Materials in Medicine, 22,* 1529-1540. https://doi.org/10.1007/s10856-011-4323-6

8    Nikanorov, V.V., Ivanov, R.V., Kil'deeva, N.R., Bulatnikova, L.N., & Lozinsky, V.I. (2010). Synthesis and characteristics of cryogels of chitosan crosslinked by glutaric aldehyde. *Polymer Science. Series A, 52*, 828-834. DOI: 10.1134/s0965545x10080092

9    Patent RF 0002699562. Sposob polucheniia poristykh materialov na osnove khitozana [Method for producing porous materials based on chitosan] / Bratskaya S.Yu., Privar Yu.O., Nesterov D.V., Pestov A.V. — № 219.017.c933; publ. 08.09.2019 [in Russian].

10   Berillo, D., Elowsson, L., & Kirsebom, H. (2012). Oxidized dextran as crosslinker for chitosan cryogel scaffolds and formation of polyelectrolyte complexes between chitosan and gelatin. *Macromolecular bioscience, 12,* 1090-1099. DOI: 10.1002/mabi.201200023

11   Hu, X., Wang, Y., Zhang, L., & Xu, M. (2019). Design of a novel polysaccharide-based cryogel using triallyl cyanurate as crosslinker for cell adhesion and proliferation. *International Journal of Biological Macromolecules, 126,* 221-228. https://doi.org/10.1016/j.ijbiomac.2018.12.226

12   Reichelt, S., Becher, J., Weisser, J., Prager, A., Decker, U., Möller, S., & et al. (2014). Biocompatible polysaccharide-based cryogels. *Materials Science & Engineering: C, 35,* 164-170. https://doi.org/10.1016/j.msec.2013.10.034

13   Akilbekova, D., Shaimerdenova, M., Adilov, S., & Berillo, D. (2018). Biocompatible scaffolds based on natural polymers for regenerative medicine. *International Journal of Biological Macromolecules, 114,* 324-333. https://doi.org/10.1016/j.ijbiomac.2018.03.116

14   Tan, H., Wu, B., Li, C., Mu, C., Li, H., & Lin, W. (2015). Collagen cryogel cross-linked by naturally derived dialdehyde carboxymethyl cellulose. *Carbohydrate Polymers, 129,* 17-24. https://doi.org/10.1016/j.carbpol.2015.04.029

15   Tavsani, B., & Okay, O. (2020). Macroporous methacrylated hyaluronic acid cryogels of high mechanical strength and flow-dependent viscoelasticity. *Carbohydrate Polymers, 229*:115458. https://doi.org/10.1016/j.carbpol.2019.115458

16   Zhang, H., Zhang, F., & Wu, J. (2013). Physically crosslinked hydrogels from polysaccharides prepared by freeze–thaw technique. *Reactive and Functional Polymers, 73*, 923–928. https://doi.org/10.1016/j.reactfunctpolym.2012.12.014

17   Brovko, O.S., Palamarchuk, I.A., Val'chuk, N.A., Chukhchin D.G., Bogolitsyn K.G., & Boitsova, T.A. (2017). Gels of sodium alginate–chitosan interpolyelectrolyte complexes. *Russian Journal of Physical Chemistry A, 91, 1580*–1585. https://doi.org/10.1134/S0036024417160014

18   Konovalova, M.V., Kurek, D.V., Litvinets, S.G., Martinson, E.A., & Varlamov, V.P. (2016). Preparation and characterization of cryogels based on pectin and chitosan. *Progress on Chemistry and Application of Chitin and its Derivative, 21,* 114-121. DOI: 10.15259/PCACD.21.12

19   Konovalova, M.V., Kurek, D.V., Durnev, E.A., Litvinec, S.G., & Varlamov, V.P. (2016). Degradatsiia *in vitro* pektin-khitozanovykh kriogelei [*In vitro* degradation of pectin-chitosan cryogels]. *Izvestiia Ufimskogo nauchnogo tsentra RAN — Proceedings of the Ufa Scientific Center of the Russian Academy of Sciences, 3-1,* 42–45 [in Russian].

20   Stoyneva, V., Momekova, D., Kostovs, B., & Petrov, P. (2014). Stimuli sensitive super-macroporous cryogels based on photo-crosslinked 2-hydroxyethylcellulose and chitosan. *Carbohydrate Polymers, 99,* 825-830. https://doi.org/10.1016/j.carbpol.2013.08.095

21   Raschip, I.E., Fifere, N., Varganici, C-D., & Dnu, M.V. (2020). Development of antioxidant and antimicrobial xanthan-based cryogels with tuned porous morphology and controlled swelling features. *International Journal of Biological Macromolecules, 156,* 608-620. https://doi.org/10.1016/j.ijbiomac.2020.04.086

22   Kutlusoy, T., Oktay, B., Apohan, N.K., Süleymanoğlu, M., & Kuruca, S.E. (2017). Chitosan-co-Hyaluronic acid porous cryogels and their application in tissue engineering. *International Journal of Biological Macromolecules, 103,* 366-378. https://doi.org/10.1016/j.ijbiomac.2017.05.067

23   Lozinsky, V.I., Galaev, I.Y., Plieva, F.M., Savinal, I.N., Jungvid, H., & Mattiasson, B. (2003). Polymeric cryogels as promising materials of biotechnological interest. *Trends in biotechnology, 21,* 445-451. https://doi.org/10.1016/j.tibtech.2003.08.002

24   Alkan, H., Bereli, N., Baysal, Z., & Denizli, A. (2009). Antibody purification with protein A attached supermacroporous poly(hydroxyethyl methacrylate) cryogel. *Biochemical engineering journal, 45,* 201-208. https://doi.org/10.1016/j.bej.2009.03.013

25   Akduman, B., Uygun, M., Uygun, D. A., Akgol, S., & Denizli, A. (2013). Purification of yeast alcohol dehydrogenase by using immobilized metal affinity cryogels. *Materials Science & Engineering C-Materials for Biological Applications, 33,* 4842-4848. https://doi.org/10.1016/j.msec.2013.08.007

26   Mattiasson, B. (2014). Cryogels for biotechnological applications. *Advanced Polymer Science, 263*, 245-281. https://doi.org/10.1007/978-3-319-05846-7_7

27  Krajnc, N., Smrekar, F., Frankovic, V., Trancar, A., & Podgornik, A. (2010). Monolithic macroporous polymers as chromatographic matrices. *Macroporous polymers: production properties and bitechnological/biomedical applications.* Mattiasson B. et al. (Ed.); (P. 291-334). Boca Raton: CRC Press. DOI: 10.1201/9781420084627-c12

28  Dainiak, M., Kumar, A., Galaev, I., & Mattiasson, B. (2010). Cryogels as matrices for cell separation and cell cultivation. *Macroporous polymers: production properties and bitechnological/biomedical applications.* Mattiasson B. et al. (Ed.); (P. 363-404). Boca Raton: CRC Press. DOI: 10.1201/9781420084627-c14

29  Galaev, I. Y., Dainiak, M. B., Plieva, F., & Mattiasson, B. (2007). Effect of matrix elasticity on affinity binding and release of bioparticles. Elution of bound cells by temperature-induced shrinkage of the smart macroporous hydrogel. *Langmuir, 23,* 35-40. https://doi.org/10.1021/la061462e

30  Dainiak, M. B., Kumar, A., Galaev, I. Y., & Mattiasson, B. (2006). Detachment of affinity-captured bioparticles by elastic deformation of a macroporous hydrogel. *Proceedings of the National academy of sciences of the United States of America, 103*, 849-854. https://doi.org/10.1073/pnas.0508432103

31  Efremenko, E.N., Spiricheva, O.V., Veremeenko, D.V., Baibak, A.V., & Lozinsky, V.I. (2006). L(+)-lactic acid production using poly(vinyl alcohol)-cryogel-entrapped Rhizopus oryzae fungal cells. *Journal of Chemical Technology and Biotechnology, 81,* 519-522. DOI: 10.1002/jctb.1524

32  Efremenko, E., Senko, O., Zubaerova, D., Podorozhko, E., & Lozinsky, V. (2008). New biocatalyst with multiple enzymatic activities for treatment of complex food wastewaters. *Food technology and biotechnology, 46,* 208-212.

33  Klivenko, A., Yergaziyeva, A., & Kudaibergenov, S. Gold nanoparticles stabilized by amphoteric cryogel-perspective flow-through catalytic reactor for oxidation and reduction processes. Proceedings from International Conference on Nanomaterials: Application & Properties (NAP-2016. September 9-14, 2016). (P. 02NSA03-1-02NSA03-5). Lviv, Ukraine. DOI: 10.1109/NAP.2016.7757304

34  Tatykhanova, G.S., Klivenko, A.N., Kudaibergenova, G.M., & Kudaibergenov, S.E. (2016). Flow-through catalytic reactor based on macroporous amphoteric cryogels and gold nanoparticles. *Macromolecular Symposia, 363*, 49-56. https://doi.org/10.1002/masy.201500137

35  Kudaibergenov, S.E., Tatykhanova, G.S., & Klivenko, A.N. Macroporous amphoteric hydrogels(Cryogels): design of flow-through catalytic reactor. Proceedings from EMN meeting on hydrogel materials. (May 9-13, 2016). (P. 50-51). Singapore.

36  Sahiner, N., Seven, F., & Al-Lohedan, H. (2015). Super-fast hydrogen generation via super porous Q-P(VI)-M cryogel catalyst systems from hydrolysis of $NaBH_4$. *International Journal of Hydrogen Energy, 40*, 4605-4616. https://doi.org/10.1016/j.ijhydene.2015.02.049

37  Sahiner, N., & Seven, F. (2015). A facile synthesis route to improve the catalytic activity of inherently cationic and magnetic catalyst systems for hydrogen generation from sodium borohydride hydrolysis. *Fuel Processing Technology, 132,* 1-8. https://doi.org/10.1016/j.fuproc.2014.12.008

38  Uygun, D. A., Akduman, B., Uygun, M., Akgol S., & Denizli, A. (2015). Immobilization of alcohol dehydrogenase onto metal-chelated cryogels. *Journal of Biomaterials Science. Polymer edition, 26,* 446-457. DOI: 10.1080/09205063.2015.1023241

39  Demiryas N., Tuzmen N., Galaev I. Y., Piskin E., & Denizli A. (2007). Poly(acrylamide-allyl glycidyl ether) cryogel as a novel stationary phase in dye-affinity chromatography. *Journal of Applied Polymer Science, 105*, 1808-1816. https://doi.org/10.1002/app.26187

40  Jahangiri E., Reichelt S., Thomas I., Hausmann K., Schlosser D., & Schulze A. (2014). Electron Beam-Induced immobilization of laccase on porous supports for waste water treatment applications. *Molecules, 19*, 11860-11882. DOI: 10.3390/molecules190811860

41  Uygun M., Akduman B., Ergonul B., Uygun D. A., Akgol S., & Denizli A. (2015). Immobilization of amyloglucosidase onto macroporous cryogels for continuous glucose production from starch. *Journal of Biomaterials Science. Polymer edition,* 26, 1112-1125. https://doi.org/10.1080/09205063.2015.1078928

42  Nakagawa, K., & Goto, Y. (2015). Preparation of alpha-amylase-immobilized freeze-dried poly(vinyl alcohol) foam and its application to microfluidic enzymatic reactor. *Chemical Engineering and Processing, 91*, 35-42. https://doi.org/10.1016/j.cep.2015.03.010

43  Yavaser, R., & Karagozler, A.A. (2021). Laccase immobilized polyacrylamide-alginate cryogel: A candidate for treatment of effluents. *Prosess Biochemistry, 101*, 137-146. https://doi.org/10.1016/j.procbio.2020.11.021

44  Yang, C., Liu, G.-F., Zhou, X.-L., Liu, Y.-R., Wang, J., Tian, L.-L., & et al. Polyacrylamide based cryogels as catalysts for biodiesel. *Catalysis letters, 145,* 1778-1783. https://doi.org/10.1007/s10562-015-1580-x

45  Auriemma, G., Russo, P., Del Gaudio, P., García-González, C.A., Landín, M., & Aquino, R.P. (2020). Technologies and Formulation Design of Polysaccharide-Based Hydrogels for Drug Delivery. *Molecules, 25,* 3156-3191. https://doi.org/10.3390/molecules25143156

46  Sultankulov, B., Berillo, D., Sultankulova, K., Tokay, T., & Saparov, A. (2019). Progress in the Development of Chitosan-Based Biomaterials for Tissue Engineering and Regenerative Medicine. *Biomolecules, 9*, 1-16. doi: 10.3390/biom9090470

47  Singh, B.N., Veeresh, V., Mallick, S.P., Jain, Y., Sinha, S., Rastogi, A., & et al. (2019). Design and evaluation of chitosan/chondroitin sulfate/nano-bioglass based composite scaffold for bone tissue engineering. *International Journal of Biological Macromolecules, 133,* 817-830. https://doi.org/10.1016/j.ijbiomac.2019.04.107

48  Georgopoulou, A., Papadogiannis, F., Batsali, A., Marakis, J., Alpantaki, K., Eliopoulos, A. G., & et al. (2018). Chitosan/gelatin scaffolds support bone regeneration. *Journal of Materials Science-Materials in Medicine, 29*, 1-13. https://doi.org/10.1007/s10856-018-6064-2

49  Ofkeli, F., Demir, D., & Bolgen, N. (2021). Biomimetic mineralization of chitosan/gelatin cryogels and in vivo biocompatibility assessments for bone tissue engineering. *Journal of Applied Polymer Science, 138*, 1-12. https://doi.org/10.1002/app.50337

50  Wu, S.Q., Ma, S.Z., Zhang, C., Cao, G.Q., Wu, D.J., Gao, C.Z., & et al. (2020). Cryogel biocomposite containing chitosan-gelatin/cerium-zinc doped hydroxyapatite for bone tissue engineering. *Saudi Journal of Biological Sciences, 27,* 2638-2644. https://doi.org/10.1016/j.sjbs.2020.05.045

51  Offeddu, G.S., Mela, I., Jeggle, P., Henderson, R.M., Smoukov, S.K., & Oyen, M.L. (2017). Cartilage-like electrostatic stiffening of responsive cryogel scaffolds. *Scientific Reports, 7*, 1-10. https://doi.org/10.1038/srep42948

52  Kuo, C.-Y., Chen, C.-H., Hsiao, C.-Y., & Chen, J.-P. (2015). Incorporation of chitosan in biomimetic gelatin/chondroitin-6-sulfate/hyaluronan cryogel for cartilage tissue engineering. *Carbohydrate Polymers, 117*, 722–730. https://doi.org/10.1016/j.carbpol.2014.10.056

53  Han, M.E., Kang, B.J., Kim, S.H., Kim, H.D., & Hwang, N.S. (2017). Gelatin-based extracellular matrix cryogels for cartilage tissue engineering. *Journal of Industrial and Engineering Chemistry, 45,* 421-429. https://doi.org/10.1016/j.jiec.2016.10.011

54  Takei, T., Yoshitomi, H., Fukumoto, K., Danjo, S., Yoshinaga, T., Nishimata, H., & et al. (2017). Toxic Chemical Cross-linker-free Cryosponges Made from Chitosan-Gluconic Acid Conjugate for Chondrocyte Culture. *Journal of Chemical Engineering of Japan, 50,* 142-148. https://doi.org/10.1252/jcej.16we145

55  Seker, S., Elcin, A E., & Elcin, Y.M. (2020). Macroporous elastic cryogels based on platelet lysate and oxidized dextran as tissue engineering scaffold: In vitro and in vivo evaluations. *Materials Science & Engineering C-Materials for Biological Applications, 110,* 1-11. https://doi.org/10.1016/j.msec.2020.110703

56  Pacelli, S., Di Muzio, L., Paolicelli, P., Fortunati, V., Petralito, S., Trilli, J., & et al. (2021). Dextran-polyethylene glycol cryogels as spongy scaffolds for drug delivery. *International Journal of Biological Macromolecules, 166*, 1292-1300. https://doi.org/10.1016/j.ijbiomac.2020.10.273

57  Georgiev, G.L., Borisova, D., & Petrov, P.D. (2020). Super-macroporous composite cryogels based on biodegradable dextran and temperature-responsive poly(N-isopropylacrylamide). *Journal of Applied Polymer Science, 137*, 1-8. https://doi.org/10.1002/app.49301

58  Chaux-Gutierrez, A.M., Perez-Monterroza, E.J., Granda-Restrepo, D.M., & Mauro, M.A. (2020). Cryogels from albumin and low methoxyl amidated pectin as a matrix for betalain encapsulation. *Journal of Food Processing and Preservation, 44*, 1-10. https://doi.org/10.1111/jfpp.14843

59  Dinu, M.V., Cocarta, A.I., & Dragan, E.S. (2016). Synthesis, characterization and drug release properties of 3D chitosan/clinoptilolite biocomposite cryogels. *Carbohydrate Polymers, 153,* 203–211. https://doi.org/10.1016/j.carbpol.2016.07.111

60  Ari, B., & Sahiner, N. (2020). Biodegradable super porous inulin cryogels as potential drug carrier. *Polymers for Advanced Technologies, 31*, 2863-2873. https://doi.org/10.1002/pat.5014

61  Bölgen, N., Demir, D., Yalçın, S., & Özdemir, S. (2020). Development of Hypericum perforatum oil incorporated antimicrobial and antioxidant chitosan cryogel as a wound dressing material. *International Journal of Biological Macromolecules, 161,* 1581-1590. https://doi.org/10.1016/j.ijbiomac.2020.08.056

62  Odabas, S. (2018). Functional Polysaccharides Blended Collagen Cryogels. *Hacettepe Journal of Biology and Chemistry, 46,* 113-120. DOI: 10.15671/HJBC.2018.219

63  Konovalova, M.V., Markov, P.A., Durnev, E.A., Kurek, D.V., Popov, S.V. & Varlamov, V.P. (2017). Preparation and biocompatibility evaluation of pectin and chitosan cryogels for biomedical application. *Journal of Biomedical Materials Research. PartA, 105,* 547-556. DOI: 10.1002/jbm.a.35936

64  Hou, Y., Feng, F., Zhou, J., Feng, X., & Fan, Y. (2020). Polysaccharide-Peptide Cryogels for Multidrug-Resistant-Bacteria Infected Wound Healing and Hemostasis. *Advanced Helthcare Matarials, 9*, 1901041. https://doi.org/10.1002/adhm.201901041

65  Salgado, C.L., Barrias, C.C., & Monteiro, F.J.M. (2020). Clarifying the Tooth-Derived Stem Cells Behavior in a 3D Biomimetic Scaffold for Bone Tissue Engineering Applications. *Frontiers in Bioengineering and Biotechnology, 8*, 1-15. https://doi.org/10.3389/fbioe.2020.00724

66  Rodrigues, S.C., Salgado, C.L., Sahu, A., Garcia, M.P., Fernandes, M.H., & Monteiro, F.J. (2013). Preparation and characterization of collagen-nanohydroxyapatite biocomposite scaffolds by cryogelation method for bone tissue engineering applications. *Journal of Biomedical Materials Research. Part A, 101,* 1080-1094. https://doi.org/10.1002/jbm.a.34394

67  Gu, L.H., Zhang, Y.F., Zhang, L.W., Huang, Y.Q., Zuo, D.W., Cai, Q., & et al. (2020). Comparative study of gelatin cryogels reinforced with hydroxyapatites with different morphologies and interfacial bonding. *Biomedical Materials, 15,* 1-14. https://doi.org/10.1088/1748-605X/ab7388

68  Shalumon, K.T., Liao, H.T., Kuo, C.Y., Wong, C.B., Li, C.J., Mini, P.A., & et al. (2019). Rational design of gelatin/nanohydroxyapatite cryogel scaffolds for bone regeneration by introducing chemical and physical cues to enhance osteogenesis of bone marrow mesenchymal stem cells. *Materials Science & Engineering C-Materials for Biological Applications, 104*, 1-19. https://doi.org/10.1016/j.msec.2019.109855

69  Rezaeeyazdi, M., Colombani, T., Memic, A., & Bencherif, S.A. (2018). Injectable Hyaluronic Acid-co-Gelatin Cryogels for Tissue-Engineering Applications. *Materials, 11,* 1-18. doi: 10.3390/ma11081374

70  Petrenko, Y.A., Ivanov, R.V., Lozinsky, V.I., & Petrenko, A.Y. (2011). Comparison of the Methods for Seeding Human Bone Marrow Mesenchymal Stem Cells to Macroporous Alginate Cryogel Carriers. *Bulletin of Experimental Biology and Medicine, 150,* 543-546. https://doi.org/10.1007/s10517-011-1185-3

71  Petrenko, Y.A., Petrenko, A.Y., Damshkaln, L.G., Volkova, N.A., & Lozinsky, V.I. (2008). Growth and Adipogenic Differentiation of Mesenchymal Stromal Bone Marrow Cells during Culturing in 3D Macroporous Agarose Cryogel Sponges. *Bulletin of Experimental Biology and Medicine, 146,* 129-132. https://doi.org/10.1007/s10517-008-0236-x

72  Bhat, S., & Kumar, A. (2012). Cell proliferation on three-dimensional chitosan-agarose-gelatin cryogel scaffolds for tissue engineering applications. *Journal of Bioscience and Bioengineering, 114,* 663-670. DOI: 10.1016/j.jbiosc.2012.07.005

73  Mathews, D.T., Birney, Y.A., Cahill, P.A., & McGuinness, G.B. (2008). Vascular cell viability on polyvinyl alcohol hydrogels modified with water-soluble and -insoluble chitosan. *Journal of Biomedical Materials Research. Part B-Applied Biomaterials, 84B,* 531-540. doi:10.1002/jbm.b.30901

74  Singh, D., Tripathi, A., Nayak, V., & Kumar, A. (2011). Proliferation of Chondrocytes on a 3-D Modelled Macroporous Poly(Hydroxyethyl Methacrylate)-Gelatin Cryogel. *Journal of Biomaterials Science. Polymer Edition, 22*, 1733-1751. DOI: 10.1163/092050610X522486

75  Demirci, S., Suner, S.S., Sahiner, M., & Sahiner, N. (2017). Superporous hyaluronic acid cryogel composites embedding synthetic polyethyleneimine microgels and Halloysite Nanotubes as natural clay. *European Polymer Journal, 93*, 775-784. https://doi.org/10.1016/j.eurpolymj.2017.04.022

76  He, T., Li, B., Colombani, T., Navare, K.J., Bencherif, S.A., & Bajpayee, A.G. (2020). Hyaluronic acid-based shape memory cryogel scaffolds for focal cartilage defect repair. *Osteoarthritis and Cartilage, 28,* 504-504. DOI: 10.1089/ten.TEA.2020.0264

77  Chen, C.H., Kuo, C.Y., Wang, Y.J., & Chen, J.P. (2016). Dual Function of Glucosamine in Gelatin/Hyaluronic Acid Cryogel to Modulate Scaffold Mechanical Properties and to Maintain Chondrogenic Phenotype for Cartilage Tissue Engineering. *International Journal of Molecular Sciences, 17*, 1957-1978. DOI: 10.3390/ijms17111957

78  Ki, S.B., Singh, D., Kim, S. C., Son, T.W., & Han, S.S. (2013). Effect of cross-linkers in fabrication of carrageenan-alginate matrices for tissue engineering application. *Biotechnology and Applied Biochemistry, 60*, 589-595. DOI: 10.1002/bab.1123

79  Bauleth-Ramos, T., Shih, T.Y., Shahbazi, M.A., Najibi, A.J., Mao, A.S., Liu, D.F., & et al. (2019). Acetalated Dextran Nanoparticles Loaded into an Injectable Alginate Cryogel for Combined Chemotherapy and Cancer Vaccination. *Advanced Functional Materials, 29*, 1903686. https://doi.org/10.1002/adfm.201903686

80  Li, J., Wang, Y.J., Zhang, L., Xu, Z.Y., Dai, H.Q., & Wu, W.B. (2019). Nanocellulose/Gelatin Composite Cryogels for Controlled Drug Release. *Acs Sustainable Chemistry & Engineering, 7,* 6381-6389. https://doi.org/10.1021/acssuschemeng.9b00161

## Information about authors:

*Klivenko Alexey Nikolayevich* — PhD of Chemistry, acting associate professor of Chemical technologies and Ecology department, Chemical technologies and Ecology department, Shakarim University of Semey, Semey, Tanirbergenov street, 1, Kazakhstan; e-mail: alexeyklivenko@mail.ru; https://orcid.org/0000-0002-8971-686X;

*Mussabayeva Binur Khabasovna* (*corresponding author*) — Candidate of chemical sciences, Professor of Chemical technologies and Ecology department, Shakarim University of Semey, Semey, Tanirbergenov street, 1, Kazakhstan; e-mail: binur.mussabayeva@mail.ru; https://orcid.org/0000-0003-2209-1209;

*Gaisina Balzhan Sailauovna* — PhD student of Chemical technologies and Ecology department, Shakarim University of Semey, Semey, Tanirbergenov street, 1, Kazakhstan; e-mail: balzhan-1982@mail.ru; https://orcid.org/0000-0002-8468-2744

*Sabitova Alfira Nurzhanovna* — PhD of Petrochemistry, Head of Chemical technologies and Ecology department, Shakarim University of Semey, Semey, Tanirbergenov street, 1, Kazakhstan; e-mail: alfa-1983@mail.ru; https://orcid.org/0000-0002-3360-7998.

# R.P. Bhole[1*], S. Jadhav[1], R. Chikhale[2], Y. Shinde[1], C.G. Bonde[3]

[1]*Department of Pharmaceutical Chemistry, Dr. D.Y. Patil Institute of Pharmaceutical Sciences and Research, Pimpri, Pune, India;*
[2]*Department of Pharmacy, UCL School of Pharmacy, London, United Kingdom;*
[3]*SPTM School of Pharmacy, Shirpur, Dist: Dhule, India*
*(\*Corresponding author's e-mail: ritesh.bhole@dypvp.edu.in)*

## Synthesis and evaluation of vitamin-drug conjugate for its anticancer activity

Cancer is the uncontrolled growth of cells in the human body that has the ability to spread. The purpose of the study is to explore that vitamins can be used as a targeting moiety for new anticancer drugs to address issues like non-selectivity, systemic toxicity. 5-Fluorouracil acetic acid–Vitamin D3 (5FUAC-Vit.D3) conjugate has been synthesized, characterized, and evaluated for its anticancer activity. 5-FUAC-Vit.D3 conjugate was synthesized via esterification mechanism in the presence of N-Hydroxy succinimide (NHS) and 1-(3-Dimethyla-minopropyl)-3-ethylcarbodiimide (EDC) by using HCL as coupling agent. Formation of 5-FUAC-Vit.D3 conjugate via esteric bond and the structure of the compounds were confirmed by spectroscopic data, i.e., IR, NMR, and mass spectra. The docking studies showed that 5-FUAC-Vit.D3 conjugate interacted at Arg-215 and Lys-47 of the human thymidylate synthase proteins, through hydrogen bonding and ionic bonds respectively with a binding score of -8.614 which is higher than only 5-FU (-3.475). So, it was proved that forming 5-FUAC-Vit.D3 conjugate shows greater binding to the target protein.

*Keywords:* synthesis, molecular modeling, molecular docking, vitamin-drug conjugate, 5-fluorouracil acetic acid, vitamin D3.

## *Introduction*

Following cardiovascular diseases, cancer is the world's second leading cause of death [1]. Cancer is described as the uncontrolled growth of cells in the human body that are able to spread to other parts of the body [2]. If this spread is not controlled, cancer may lead to severe death [3]. There are several strategies for treating cancer but chemotherapy is the most widely used method for treating cancer, however it has the drawback of being non-selective. Since cytotoxic chemotherapy does not discriminate between tumor and non-tumor cells, it causes serious, frequently life-threatening side effects in susceptible healthy cells [4]. The most difficult step in conventional chemotherapy is the delivery of a cytotoxic agent that kills proliferating tumor cells [5–6]. Since anticancer therapy should last longer, and that longer therapy may be the cause of its side-effect profile. The other side of the coin, i.e., side effect minimization, also has to focus to get effective drug. Although the side effect profile is widespread, it has generally been shown to inhibit the rapid growth required to maintain normal cells such as hair follicles, bone marrow and gastrointestinal tract cells. This leads to the potential undesirable side effects observed in cancer treatment. Low aqueous solubility, short biological half-life, multidrug tolerance, and non-specificity or dose-limiting cellular toxicity are other limitations of free chemotherapeutic agents in cancer treatment [7]. Consequently, it is still difficult to achieve selectivity of anti-cancer drugs for cancer cells and to reach breakthrough in cancer research, which may spare healthy tissue and help to overcome the intrinsic limitations of conventional anticancer drugs.

To achieve successful tumor-targeting drug delivery it should include a tumor-recognizing moiety and a chemotherapeutic agent that is linked directly by a linker. As a result, a conjugate acting 'prodrug' is produced, which, once integrated into a cancer cell, readily splits and regenerates the cytotoxic agent's activity. In these conditions the so-called vitamin-mediated drug targeting has recently emerged as a new concept for carrying anticancer drugs particular to tumors [8–10]. Since cancerous cells grow quickly, they demand more vitamins as well as other nutrients than healthy cells, and the receptors involved in the cellular internalization of vitamins are abundantly expressed on the surface of growing cancer cells. As a result, it is thought to be worthwhile to develop "Vitamin-Drug Conjugate" that could be able to target tumor cells [11–13]. Vitamin drug conjugates will be nontoxic, it will specifically be internalized into cancerous cells and release the anticancer drugs without loss of potency, it will minimize the systemic toxicity by being stable in blood circulation, and provide a target-specific activity by sparing the normal cell that will minimize the side effects [14–15].

Recently, cancer being widely increasing, there has been a greater need for formulating targeted drug delivery with minimum side effects. These needs can be fulfilled by "Vitamin-Drug Conjugate" (targeted)

formation. In this study 5-Fluorouracil and cholecalciferol are used as raw materials to synthesize vitamin drug conjugates. 5-Fluorouracil is an anticancer drug belonging to the antimetabolite class. It is used in the treatment of the large number of malignant tumors, some of which include breast, colon, rectal, ovarian, and bladder cancer. 5-Fluorouracil is acted as an antitumor agent by converting intracellularly into some active metabolites. These active metabolites interfere with RNA production and thymidylate synthase action, resulting in anti-cancer activity. Recently, the ability of vitamin D3 to enhance the anti-tumor activity of chemotherapeutic drugs by activating apoptosis was reported. Vitamin D3 is selected as targeting moiety to cancerous cells as cancerous cells have an unquenchable appetite for vitamins. When Vitamin D3 is combined with 5-Fluoroura-cil, the anticancer activity of 5-Fluorouracil is increased compared to 5-Fluorouracil administered alone. 5-Fluorouracil shows various undesirable effects during cancer treatment if 5-Fluorouracil is given alone. So, by conjugating vitamin D3 with 5-Fluorouracil via an acid liable spacer, this conjugate acts as a prodrug, which has the potential to overcome the non-specificity and toxicity issue of 5-Fluorouracil. This approach not only overcomes associated toxic effects but also improved the desired bioavailability with a reduction in dose and dosage frequency. This combination shows a synergistic effect with targeted drug delivery of 5-Fluorouracil in the tumor tissues. Here we present high yield synthetic procedures for conjugate preparation as well as complete characterization results. Molecular modeling studies were also performed for the given synthetic conjugate for comparing the binding affinity of conjugate with 5-Fluorouracil.

## Experimental

$^1$H NMR spectra of the compounds were recorded on Bruker Avance III HD NMR 500 MHZ spectro-photometer using CDCl$_3$ as a solvent and operating at 500 MHz at room temperature with tetramethyl silane (TMS) as the internal reference. FTIR analysis was carried out to get the FTIR spectra on the FTIR spectro-photometer, Shimadzu FT-IR 8400S. Mass spectra were recorded on the mass spectrometer, Shimadzu LC-MS 8040. TLC was used to monitor the reaction progress and to check the purity of the compound, using Silica Gel plates F254 on Aluminum sheets. Docking studies were carried out using MOE-Dock, Chemical Computing Group Inc. on a machine having Pentium 1.6 GHz workstation, 512 MB memory using the Windows operating system.

## Methodology

### Synthesis of 5-Fluorouracil — Vitamin D3 conjugates

*1. Synthesis of 5- Fluorouracil-acetic Acid (5-FUAC)*

5-FUAC was synthesized according to the previously described method [16-17] with some modifications. 5 FU (24g) dissolved completely in 152 ml KOH (0.3 g, 5.3 mmol) aqueous solution (9.12 g) then stir the reaction mixture at 100 °C for 70 mins. After that prepare 40 ml of chloroacetic acid solution in aqueous KOH and add it to the above mixture slowly and stir using a magnetic stirrer under 60 °C for 6 hours. Then acidified the product to pH 2 with concentrated hydrochloric acid, followed by cooling at 4 °C for 12 hours. Then extract the mixture using a separating funnel as, take 50 ml of the above reaction mixture in separating funnel, add 30ml of ethyl acetate to it and shake for 10 mins. Collect the supernatant (i.e., ethyl acetate layer/organic layer) in a beaker separately, and pour the aqueous layer again in the separating funnel and add fresh ethyl acetate 30 ml to it and shake it for 10 min. Repeat the procedure for 3 times for each of the 50 ml of solution. Repeat the same procedure for the whole of the above reaction mixture. Then take the collected supernatant layer (120 ml) and add 1–2 spoons of sodium sulphate to it and keep it for 30 mins. Then filter the solution, evaporate the filtrate using Rota evaporator at 60 °C. Dry the product, and record the yield and Rf value of the synthesized product. The product yield was found to be 62 % and the Rf value of the conjugate was found to be 0.35 using mobile phase (Chloroform:Methanol:Triethylamine = 7:1:2 in proportion) and silica plate as stationary phase.

*Physical and spectral data for 5-FUAC (Intermediate product)*: IR (KBr, 4500–500 cm$^{-1}$) $\gamma$ = 1690 (C=O acid), 3194 (N–H), 2835 (C–H), 1211 (C–N), 1404 (C–F), 1479 (C–C);1H NMR (CDCl$_3$, 500 MHz): $\delta$ = 4.60 (2H, s), 8.65 (1H, s). 11.46 (1H, s) ppm; Ms: m/z (%) = 189.4 (M$^+$)

*2. Synthesis of 5- Fluorouracil-acetic Acid- Vitamin D3 conjugate*

First, a solution of 5-FUAC (0.496 g) in 1 ml of dimethylformamide was prepared, then a solution of Vitamin D3 (0.5 g) in 20 ml of dimethylformamide and 2–3 drops of dichloromethane were added dropwise. Thereafter, 0.196 g (1.7 mmol) of N-Hydroxy succinimide (NHS) and 0.4 g (2.09 mmol) of 1-(3-Dimethyl-aminopropyl)-3-ethylcarbodiimide HCl (EDC·HCl) were added subsequently. The above solution was incu-bated for 16 hrs away from light. Then the reaction mixture was precipitated with 150 ml of isopropanol,

filtered and dried. The yield and Rf value of the conjugate were recorded. The product yield was found to be 48 % and Rf value of the conjugate was found to be 0.5 using mobile phase (Chloroform:Methanol:Triethylamine = 7:1:2 in proportion) and silica plate as stationary phase.

*Physical and Spectral data for 5 FUAC-Vitamin-D3 Conjugate*: M.P. — 74–76 °C; IR (KBr, 4500–500 cm$^{-1}$) 1726 C=O (ester), 1200 C–O (ester), 1618 (C=O stretch in pyrimidine ring), 3337 (N–H stretch), 2932 (C–H stretch), 1199, 1101 (C–N), 1377 (C–F), 1431 (C–C), 3067, 3050 (C=CH$_2$), 1618 (C=C) cm$^{-1}$; $^1$H NMR (CDCl$_3$, 500 MHz): δ (ppm) = 0.60–0.72 (q, 2H), 0.78–0.84 (8H, d), 0.94 (3H, s), 1.04 (3H, d), 1.16–1.32 (2H, 1.24 quint), 1.35–1.76 (12H, 1.65 m), 1.95 (1H, m), 2.18–2.52 (6H, 2.23, m), 2.59 (1H, dd, J = 14.2, 3.1 Hz), 4.58–4.59 (2H, s), 4.78 (1H, d), 4.94–5.09 (2H, m), 6.06 (1H, d), 6.32 (1H, d), 8.60 (1H, s) ppm; Ms: m/z (%) = 554.3 (M$^+$).

*Molecular* Docking

5-FU and 5-FUAC-Vitamin D3 conjugate were docked in thymidylate synthase active site using MOE-Dock, Chemical Computing Group Inc.

*Procedure*: Protein (Code — 1HVY) was retrieved from PDB data resources with a resolution of 1.90 Å. The structure of 5-FU and Vitamin-D3 were retrieved from PubChem and conjugated. All the structures were energy minimized and their lower energy conformations were generated considering *pK$_a$* of ionizable groups and pH of the medium. The protein crystal structures of human thymidylate synthase were prepared and the missing residues were modeled. The parameters during protein preparation were set with ionization and tautomerization using the Epic module for a pH range of 7 to 9. The molecular docking program was run to evaluate ligand-protein binding energy and interactions.

### Result and Discussion

5-FUAC-Vitamin D3 conjugate was synthesized, and the synthetic route is shown in Figure 1. The melting point and TLC were performed for the synthetic conjugate to confirm its purity and homogeneity. The structures of 5-FUAC and 5-FUAC-Vitamin D3 Conjugate were characterized by IR, NMR, and mass spectrometry. The data of IR, NMR, and Mass spectrometry was listed in the experimental section. Molecular modeling studies were performed for comparing the binding affinity of conjugate with 5-FU. Molecular docking studies of 5-FU and 5-FU- Vitamin-D3 Conjugate also were studied and results were shown in Table 1.

*FTIR*

The main peaks observed in the IR spectra of 5-fluorouracil acetic acid are 1690 cm$^{-1}$ for C=O of carboxylic acid, 3194 cm$^{-1}$ for N–H stretching, 1400 cm$^{-1}$ for C–F, and 1211 cm$^{-1}$ for C–N. The IR spectra of 5-fluorouracil acetic-acid — vitamin D3 conjugate are observed at 1726 cm$^{-1}$ for C=O (ester), 1199 cm$^{-1}$ for C–O (ester), and 1618 cm$^{-1}$ for C=O stretch in pyrimidine ring. The peaks observed at 1726 cm$^{-1}$ which is of C=O of ester and at 1199 cm$^{-1}$ which is for C–O of ester. These peaks show the formation of 5-FUAC Vitamin D3 conjugate via formation of an esteric linkage. They are seen in the IR spectra of 5-FUAC-Vitamin D3 conjugate and absent in the IR spectra of other compounds.

Step-I

Step-II
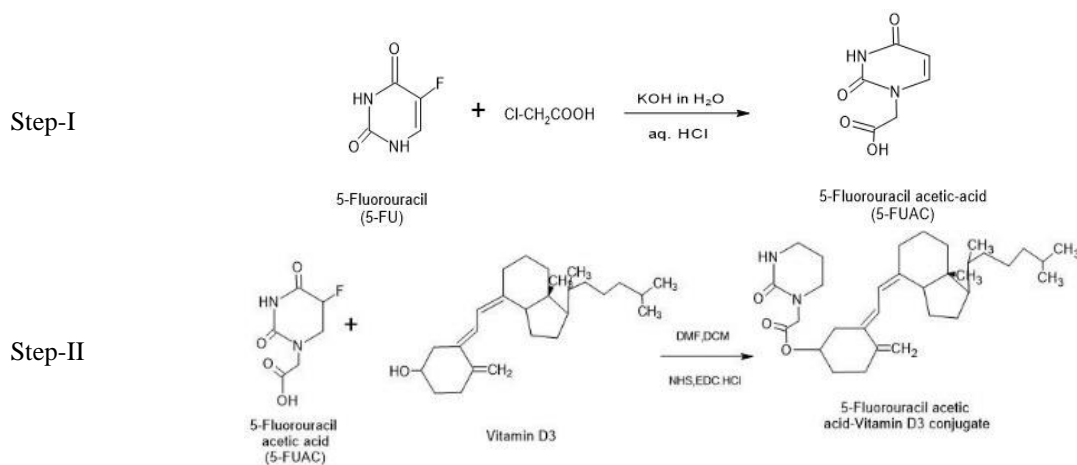


Figure 1. Synthetic scheme of 5- FUAC-Vitamin D3 conjugate

**Docking Scores of 5-FU and 5-FUAC-Vit.D3 conjugate**

| Sr. No. | Molecule code/ structure | Docking score | Interactions with target protein |
|---|---|---|---|
| 1 | 5-FU | –3.47 | 5-FU-C=O — ASN 226 (Hydrogen Bond) |
| 2 | 5-FU-Vit D3 conjugate | –8.614 | 5-FU-Vit-D C=O — Arg-215(Hydrogen Bond)<br>5-FU-Vit-D C-O — Lys-47 (Ionic Bond) |

*NMR*

The ^{1}H NMR spectra of 5-FUAC-Vitamin D3 are at δ value of 4.58–4.59 (2H, s), 4.78 (1H, d), 4.94–5.09 (2H, m). The NMR spectra of 5-FUAC-vitamin D3 showed the peaks at the above mentioned δ values, which confirm the structure of 5-FUAC-vitamin D3 conjugate. The peaks observed in the range of 3–5 ppm show the formation of esteric bond in the conjugate.

*Mass Spectroscopy*

Mass spectra of 5-FUAC-Vitamin D3 conjugate were recorded for its structural confirmation. The mass spectra of 5-FUAC-vitamin D3 conjugate showed the molecular ion peak at 554.3 m/z, which confirms the conjugation of 5-FUAC with Vitamin D3 by forming an esteric linkage and formation of the final product, i.e., 5-FUAC-Vitamin D3 conjugate.

*Molecular Docking*

The 5-FUAC-Vitamin D3 conjugate was evaluated by molecular modelling studies. The conjugate was docked on the thymidylate synthase (PDB Code — 1HVY) active site as shown in Figure 2.

The docking studies showed that 5-FUAC-Vitamin-D3 conjugate interacted at Arg-215 and Lys-47 of the human thymidylate synthase proteins, through hydrogen bonding and ionic bonds respectively with a binding score of –8.614 which is higher than 5-FU i.e., –3.475 as shown in Table 1. So, it was proved that forming 5-FUAC-Vitamin D3 conjugate shows greater binding to the target protein. The greater binding will also reveals that this conjugate will aid in the anticancer activity of the compound.
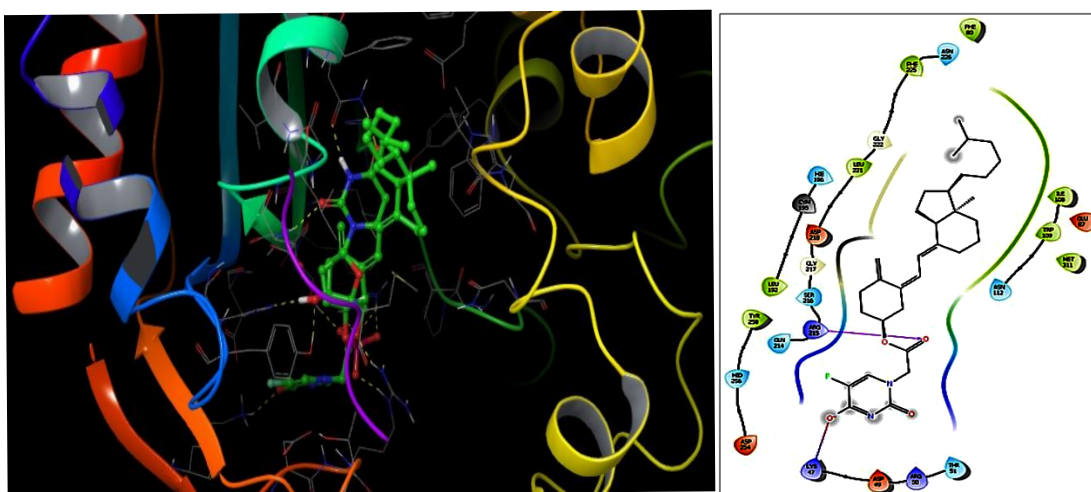


Figure 2. Binding interaction of 5-FU-Vit-D conjugate in the active site of human thymidylate synthase enzyme (Target of 5-FU, PDB Code — 1HVY)

*Conclusion*

5-Fluorouracil-Vitamin D conjugate was successfully synthesized, characterized, and evaluated. The characterization was carried out by performing IR, NMR, and Mass spectroscopy which suggested the formation of 5-FUAC-Vitamin D3 conjugate through an esteric linkage.

5FUAC-Vitamin D3 conjugate was designed and may be proven as a novel prodrug approach, that will have the potential to overcome non-specificity and toxicity issues of 5-FU. The present prodrug approach will also have the potential to improve the potency and bioavailability of the anticancer drug. Molecular docking analysis of 5-Fluorouracilacetic acid-Vitamin D3 conjugate with the human thymidylate synthase revealed excellent binding affinity compared to 5-FU. Moreover, this will also help in the accumulation of the drug in

more extend than the conventional therapies. The present study may be extended further for other anticancer drugs by forming conjugates with other vitamins.

## References

1 Padma, V.V. (2015). An overview of targeted cancer therapy. *BioMedicine, 5(4)*. https://doi.org/10.7603/s40681-015-0019-4

2 Definition of Cancer. (n.d.). Retrieved January 18, 2021, from https://www.medicinenet.com/cancer/definition.htm

3 Luo, S., Wang, Z., Patel, M., Khurana, V., Zhu, X., Pal, D., & Mitra, Ashim. K. (2011). Targeting SVCT for enhanced drug absorption: Synthesis and in vitro evaluation of a novel vitamin C conjugated prodrug of saquinavir. *International Journal of Pharmaceutics, 414(1)*, 77–85. https://doi.org/10.1016/j.ijpharm.2011.05.001

4 Allen, T.M. (2002). Ligand-targeted therapeutics in anticancer therapy. *Nature Reviews Cancer, 2(10)*, 750–763. https://doi.org/10.1038/nrc903

5 Chari, R.V.J. (1998). Targeted delivery of chemotherapeutics: Tumor-activated prodrug therapy. *Advanced Drug Delivery Reviews, 31(1)*, 89–104. https://doi.org/10.1016/S0169-409X(97)00095-1

6 Ojima, I., Geng, X., Wu, X., Qu, C., Borella, C. P., Xie, H., Wilhelm, S. D., Leece, B. A., Bartle, L. M., Goldmacher, V. S., & Chari, R.V.J. (2002). Tumor-Specific Novel Taxoid−Monoclonal Antibody Conjugates. *Journal of Medicinal Chemistry, 45(26)*, 5620–5623. https://doi.org/10.1021/jm025540g

7 Seifu, M. F., & Nath, L.K. (2019). Polymer-drug conjugates: Novel carriers for cancer chemotherapy. *Polymer-Plastics Technology and Materials, 58(2)*, 158–171. https://doi.org/10.1080/03602559.2018.1466172

8 Fortin, S., & Bérubé, G. (2013). Advances in the development of hybrid anticancer drugs. *Expert Opinion on Drug Discovery, 8(8)*, 1029–1047. https://doi.org/10.1517/17460441.2013.798296

9 Mahato, R., Tai, W., & Cheng, K. (2011). Prodrugs for improving tumor targetability and efficiency. *Advanced Drug Delivery Reviews, 63(8)*, 659–670. https://doi.org/10.1016/j.addr.2011.02.002

10 Bildstein, L., Dubernet, C., & Couvreur, P. (2011). Prodrug-based intracellular delivery of anticancer agents. *Advanced Drug Delivery Reviews, 63(1–2)*, 3–23. https://doi.org/10.1016/j.addr.2010.12.005

11 Bhole, R.P., Jadhav, S., Zambare, Y.B., Chikhale, R. V., & Bonde, C.G. (n.d.). Vitamin-anticancer drug conjugates: A new era for cancer therapy. *İstanbul Journal of Pharmacy, 50(3)*, 312–322.

12 Chen, S., Zhao, X., Chen, J., Chen, J., Kuznetsova, L., Wong, S.S., & Ojima, I. (2010). Mechanism-Based Tumor-Targeting Drug Delivery System. Validation of Efficient Vitamin Receptor-Mediated Endocytosis and Drug Release. *Bioconjugate Chemistry, 21(5)*, 979–987. https://doi.org/10.1021/bc9005656

13 Russell-Jones, G., McTavish, K., & McEwan, J. (2011). Preliminary studies on the selective accumulation of vitamin-targeted polymers within tumors. *Journal of Drug Targeting, 19(2)*, 133–139. https://doi.org/10.3109/10611861003734027

14 Ojima, I., Zuniga, E.S., Berger, W.T., & Seitz, J.D. (2011). Tumor-targeting drug delivery of new-generation taxoids. *Future Medicinal Chemistry, 4(1)*, 33–50. https://doi.org/10.4155/fmc.11.167

15 Jaracz, S., Chen, J., Kuznetsova, L. V., & Ojima, I. (2005). Recent advances in tumor-targeting anticancer drug conjugates. *Bioorganic & Medicinal Chemistry, 13(17)*, 5043–5054. https://doi.org/10.1016/j.bmc.2005.04.084

16 Kumar, S. U., Gopinath, P., & Negi, Y.S. (2017). Synthesis and bio-evaluation of xylan-5-fluorouracil-1-acetic acid conjugates as prodrugs for colon cancer treatment. *Carbohydrate Polymers, 157*, 1442–1450. https://doi.org/10.1016/j.carbpol.2016.09.096

17 Udo, K., Hokonohara, K., Motoyama, K., Arima, H., Hirayama, F., & Uekama, K. (2010). 5-Fluorouracil acetic acid/β-cyclodextrin conjugates: Drug release behavior in enzymatic and rat cecal media. *International Journal of Pharmaceutics, 388(1–2)*, 95–100. https://doi.org/10.1016/j.ijpharm.2009.12.039

Р.П. Бхоле, Ш. Джадхав, Р.Чикхале, Й. Шинде, К.Г. Бонде

## Витамин-дәрілік конъюгаттың қатерлі ісікке қарсы белсенділігін синтездеу және бағалау

Қатерлі ісік — адам ағзасында таралу қабілеті бар жасушалардың бақылаусыз өсуі. Зерттеудің мақсаты витаминдерді селективтілік пен жүйелік уыттылық сияқты мәселелерді шешу үшін ісікке қарсы жаңа препараттардың негізгі компоненті ретінде қолдануға болатынын көрсету. 5-фторурацил сірке қышқылы-D3 витамині (5FUAC-Vit.D3) синтезделді, сипатталды және оның ісікке қарсы белсенділігі бағаланды. 5-FUAC-Vit.D3 конъюгациясы HCl байланыстырушы ретінде N-гидроксисукцинимид (NHS) және 1-(3-диметиламинопропил)-3-этилкарбодиимид (EDC) қатысуымен этерификация механизмімен синтезделді. Эфир байланысы арқылы 5-FUAC-Vit.D3 конъюгатының түзілуі, сонымен қатар қосылыстардың құрылымы IR, NMR және масс-спектрометрия мәліметтерімен расталды. Докингтік зерттеулер 5-FUAC-Vit.D3 конъюгациясы сәйкесінше –8.614 байланыс индексі бар сутек пен иондық байланыстар арқылы адам тимидилатсинтазасы ақуыздарының Arg-215 және Lys-47-мен өзара әрекеттесетінін көрсетті, бұл басындағы 5-ФУ (-3.475) препаратымен салыстырғанда жоғары болатыны байқалды. Сонымен, түзілетін 5-FUAC-Vit.D3 конъюгаты мақсатты ақуызбен көбірек әрекеттесетіні байқалды.

*Кілт сөздер*: синтез, молекулалық модельдеу, молекулалық қондыру, дәрілік конъюгат, 5-фторурацилсірке қышқылы, D3 витамині.

Р.П. Бхоле, Ш. Джадхав, Р.Чикхале, Й. Шинде, К.Г. Бонде

## Синтез и оценка конъюгата «витамин – лекарственный препарат» на предмет его противораковой активности

Рак — это неконтролируемый рост клеток человеческого тела, который имеет способность распространяться. Цель исследования — показать, что витамины могут применяться в качестве целевого компонента для новых противоопухолевых препаратов с целью решения таких проблем, как неселективность и системная токсичность. Конъюгат «5-фторурацил уксусная кислота – витамин D3» (5FUAC-Vit.D3) был синтезирован, охарактеризован и оценен на предмет его противораковой активности. Конъюгат 5-FUAC-Vit.D3 был синтезирован по механизму этерификации в присутствии N-гидроксисукцинимида (NHS) и 1-(3-диметиламинопропил)-3-этилкарбодиимида (EDC) с использованием HCl в качестве связующего агента. Образование конъюгата 5-FUAC-Vit.D3 через сложно-эфирную связь, а также структура соединений были подтверждены данными ИК, ЯМР и масс-спектрометрии. Докинговые исследования показали, что конъюгат 5-FUAC-Vit.D3 взаимодействует с Arg-215 и Lys-47 белков тимидилат-синтазы человека посредством водородных и ионных связей с показателем связывания соответственно –8,614, что выше, чем для исходного 5-FU (–3,475). В целом, было отмечено, что образующийся конъюгат 5-FUAC-Vit.D3 показывает большее связывание с целевым белком.

*Ключевые слова:* синтез, молекулярное моделирование, молекулярный докинг, конъюгат «витамин–лекарство», 5-фторурацилуксусная кислота, витамин D3.

## Information about authors:

**Bhole Ritesh Prakash** — PhD, Associate Professor, Dr. D.Y. Patil Institute of Pharmaceutical Sciences and Research, Sant Tukaram Nagar, Pimpri, Pune-411018, India; e-mail: ritesh.bhole@dypvp.edu.in; https://orcid.org/0000-0003-4088-7470;

**Chikhale Rupesh V.** — PhD, Research Associate, UCL School of Pharmacy, London, United Kingdom; https://orcid.org/0000-0001-5622-3981;

**Shinde Yogita** — M. Pharm, Research Scholar, Dr. D.Y. Patil Institute of Pharmaceutical Sciences and Research, Sant Tukaram Nagar, Pimpri, Pune-411018, India; e-mail: shindeyogita48@gmail.com;

**Jadhav Shradha** — M. Pharm Research Schloar, Dr. D.Y. Patil Institute of Pharmaceutical Sciences and Research, Sant Tukaram Nagar, Pimpri, Pune-411018, India; e-mail: Jadhavshradha@gmail.com, https://orcid.org/0000-0002-6443-5009;

**Bonde Chandrakant Ghansham** — PhD, Professor, SPTM, NMIMS, School of Pharmacy, Shirpur, Dist: Dhule, India; e-mail: chandrakant.bonde@nmims.edu; https://orcid.org/0000–0001–5712–1119.

A. Iskineyeva[1], A. Mustafaeva[1], G. Zamaratskaya[2], S. Fazylov[3*], I.A. Pustolaikina[3],
O.A. Nurkenov[3], A. Sarsenbekova[3], T. Seilkhanov[4], R. Bakirova[5]

[1]*S. Seifullin Kazakh Agrotechnical University, Nur-Sultan, Kazakhstan;*
[2]*Department of Molecular Sciences, BioCenter, Swedish University of Agricultural Sciences, Upsala, Sweden;*
[3]*Karagandy University of the name of academician E.A. Buketov, Kazakhstan;*
[4]*Sh. Ualikhanov Kokshetau University, Kokshetau, Kazakhstan;*
[5]*Karaganda Medical University, Kazakhstan*
*(\*Corresponding author's e-mail: iosu8990@mail.ru)*

# Preparation of encapsulated α-tocopherol acetate and study of its physico-chemical and biological properties

The article discusses the results of research for obtaining encapsulated vitamin E using a water-soluble oligosaccharide (cyclodextrin). The inclusion complexes of β-CD with α-tocopherol were obtained in an aqueous-alcoholic medium by coprecipitation and microwave activation. The highest yields of target clathrate inclusion complexes of vitamin E with cyclodextrin were obtained under microwave synthesis conditions. Molecular modeling of inclusion complexes of α-tocopherol acetate with β-cyclodextrin in the ratios of 1:1, 1:2, 1:3, and 1:4 was performed using the MM+ method. Based on semi-empirical PM3 calculations, without taking into account the influence of the environment, the total energy of the systems under study was estimated. Data on the study of the structure of the clathrate complex of α-tocopherol acetate with β-cyclodextrin was presented. The surface morphology of the resulting "guest-host" clathrate complex was described using a scanning electron microscope. The spectral properties of the inclusion complex were characterized by FT-IR and $^1$H and $^{13}$C NMR spectroscopy data. The study of the $^1$H NMR and $^{13}$C NMR spectra of β-CD in the free and bound state in the form of the β-CD: VE clathrate made it possible to reveal the displacements of the signals of the nuclei $(\pm \Delta\delta)$ $^1$H and $^{13}$C of the host molecule both in the region of weak and strong fields. The experimental results confirmed the possibility of the formation of inclusion complexes of α-tocopherol acetate with β-cyclodextrin at various ratios. The data on the study of the effect of encapsulated α-tocopherol acetate on the safety of food meat products was presented.

*Keywords*: α-tocopherol acetate, cyclodextrin, oligosaccharides, vitamin E, starch, inclusion complexes, NMR spectroscopy, clathrate.

*Introduction*

α-Tocopherol (vitamin E) is a fat-soluble vitamin that is necessary for the normal functioning of the human body. It inhibits antioxidant properties and is involved in many metabolic processes. The daily requirement of α-tocopherol is 10–15 IU/day. At present, α-tocopherol acetate (VE) is widely used as an ingredient in food production (Fig. 1). Under production conditions α-tocopherol acetate is easily destroyed under oxygen and ultraviolet rays [1, 2]. Thus, there is a need to obtain its encapsulated water-soluble forms with improved biofunctional properties.

Currently, water-soluble cyclodextrins derived from starch are widely used for encapsulating vitamins and pharmaceuticals. This innovative direction in food and pharmaceutical industry is of high practical importance [5]. Biologically active compounds encapsulated by oligasaccharides make up almost 50 % of all manufactured pharmaceutical and food products in Japan and about 25–30 % in Europe, the USA and Russia [6].

Cyclodextrins (CDs) are enzyme-modified starch derivatives. They are able to form "guest-host" inclusion complexes with molecules of low hydrophilicity due to the hydrophobic inner surface of these ring-shaped molecules. The variants of these cyclic oligosaccharides consist of 6, 7, or 8 glucopyranose units (α-, β -, and γ-CDs, respectively) with different sizes (0.5-0.9 nm in diameter), which determines the geometric arrangement of the guest molecules in the cavity (Fig. 1). VE can be better preserved in the cyclodextrin shell from the actions of oxidizing agents and have improved digestibility.

The process of complexation of VE with β-cyclodextrin (β-CD) has been previously studied [3–7]. The results indicated a possibility to use the β-CD inclusion complexes with VE in the manufacturing confectionery products. The optimal stoichiometric ratio of the components in the "β-CD:VE" complex was shown to be 1:3 mol/mol [3]. The VE inclusion complexes were obtained by grinding in the paste and co-precipitation [3–7].

However, the use of these methods cannot provide the complete formation of a nanostructured complex (clathrates) of the native form of β-CD with VE.
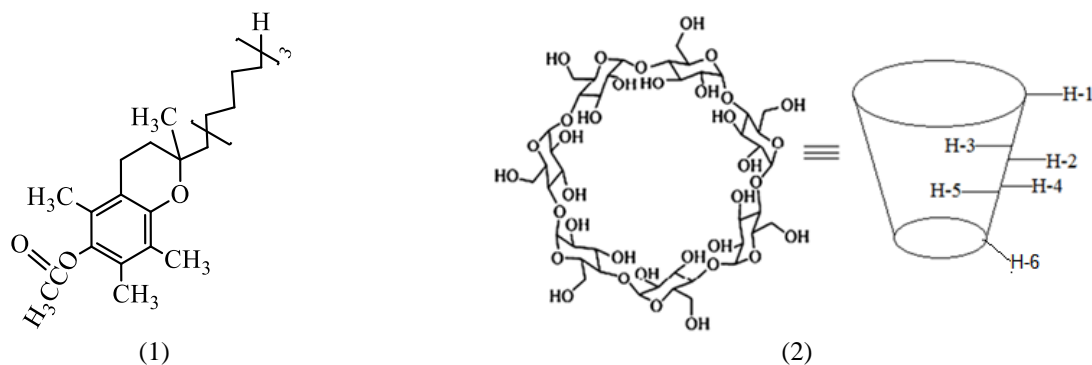


Figure 1. Structural formulas of α-tocopherol acetate (1) and β-CD (2)

Other research groups used methods of ultrasonic (UV) and microwave irradiation (MW) of a solution of a mixture of VE and β-CD in a ratio of 1:1 to obtain clathrate complexes V, but there are no descriptions of methods for carrying out UV and MW syntheses of inclusion complexes [8–10].

The aim of our work was to develop technological methods for obtaining encapsulated complexes of VE inclusion and to study their physical and chemical properties, as well as its safety in food products. The physicochemical properties and structural features of the obtained "β-CD:VE" complexes were studied using modern physicochemical methods, namely SEM, DSC, IR, NMR$^1$H and $^{13}$C spectroscopy.

*Experimental*

The following reagents were used in the experiments:
– vitamin E (α-tocopherol acetate, VE) $C_{31}H_{52}O_3$, transparent viscous oil of light-yellow color (1 IU of vitamin E = 1 mg). Molar mass of α-tocopherol acetate is 472.76 g/mol, $d^{20}_4 = 0.9545–0.9665$; $n^{20}_4 = 1.4958–1.4972$; maximum absorption E = 42.5 at 285.5 nm;
– β-cyclodextrin (99.5 %), (company "Fluka"), white crystalline substance, m.p. 280–299 °C, soluble in water when heated, well soluble in dimethylsulfoxide and pyridine.

The preparation of β-CD inclusion complexes with VE was carried out in an aqueous-alcohol medium. A mixture of calculated amounts of β-CD (mmol) and VE (mmol) in different ratios (1:1, 2:1, 3:1, 4:1) was dissolved in a mixture of solvents water:ethanol (1:1) and heated in a microwave oven for 160–180 seconds in increments of 2 minutes at 80 °C. The microwave activation of the reaction medium was carried out at a power of 850 W using the Anton PaarMonowave 300 device. Under these conditions the highest yield of "β-CD:VE" clathrates was observed at the 2:1 ratio. The resulting products were white powders that are dissolved in water to form colloidal solutions of milky white color. The solubility of the "β-CD:VE" (2:1) complex in water (with a slight heating) was $21–22 \pm 0.05$ mg/100 ml.

The IR spectra of the "β-CD:VE" inclusion complexes were taken on a Cary 600 Series IR Fourier spectrometer manufactured by Agilent Technologies (USA). The $^1$H and $^{13}$C NMR spectra of the obtained clathrates were recorded on a JNM-ECA Jeol 400 spectrometer (frequency 399.78 MHz, DMSO-d$_6$). The surface morphology of the samples of the inclusion complexes was studied using a scanning electron microscope (SEM) from Tescon Mira3 LMN (Czech Republic). The results of thermal analysis of samples of the inclusion complexes "β-CD:VE" (2:1 and 4:1) (weight 12 mg) were studied using a differential scanning calorimeter Setaram DTA/DSC and they were described by us in [11].

Molecular modeling of inclusion complexes of VE with β-cyclodextrin was performed by molecular mechanics MM+ using the HyperChem 8.0 software. The initial structure of β-cyclodextrin was taken from the PubcChem database (PubChem SID24892722). First, the structure of the complex was built and its geometry was optimized by the MM+ method. Then the assessment of the geometric and energy parameters of the model was carried out by semiempirical PM3 method using Single Point calculations. All calculations were performed without taking into account the effect of the solvent (gas phase, vacuum).

Obtaining meat sausage samples and analysis of quality and safety indicators of VE encapsulated by β-CD as part of a food product were carried out on the basis of the Kazakh Agrotechnical University (Nur-Sultan).

*Results and Discussion*

*Molecular modeling of complexes of "β-CD:VE" using the HyperChem program. PM3 Calculation method*

Assessment of the geometric parameters of the VE and β-cyclodextrin molecules showed the possibility of the inclusion complexes formation between them. The spatial "elongation" of the VE molecule does not exclude the possibility of the formation of β-CD: VE complexes with stoichiometry as 1:1, 1:2, 1:3 and 1:4.

Molecular modeling of "β-CD:VE" inclusion complexes in various ratios was performed. Structures of optimized complexes are shown in Figures 2–4.



$E_{total} = -500093$ kcal/mol
a) Type I

$E_{total} = -500142$ kcal/mol
b) Type II
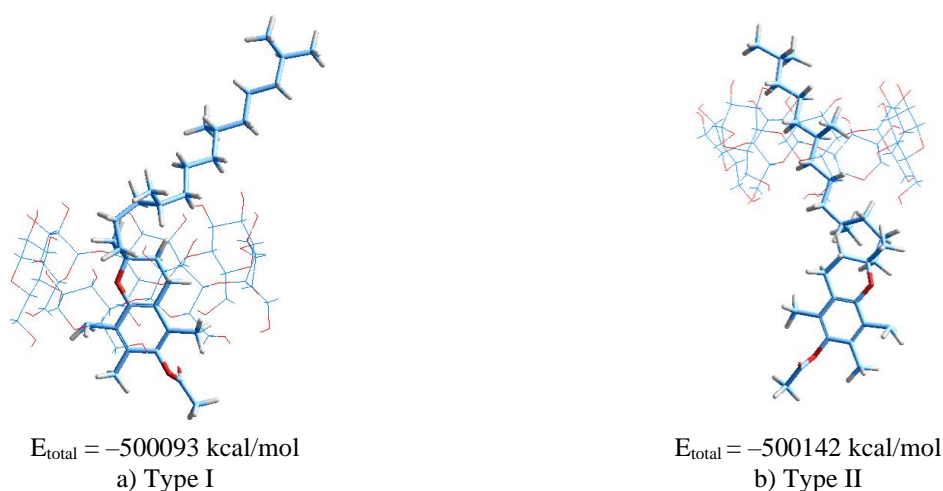
Figure 2. Molecular models of the VE complex with β-CD

It can be seen from the data presented in Figure 2 that the formation of two types of inclusion complex is possible as a result of the 1:1 interaction of VE with β-cyclodextrin (Fig. 2):

– Type I — due to the penetration of the chroman ring VE into the cavity of the cyclodextrin;

– Type II — due to the penetration of the isoprenoid side chain VE into the cavity of the cyclodextrin.

Comparison of the total energies of these complexes of two types in Figure 2 showed that the formation of the inclusion complex of α-tocopherol acetate with β-cyclodextrin by Type II at $\Delta E = 49$ kcal/mol is thermodynamically more favorable.

The next step was molecular modeling of the "β-CD:VE" inclusion complexes in the ratios of 1:2 and 1:3. Molecular models of "β-CD:VE" complexes obtained as a result of geometry optimization by molecular mechanics in ratios 1:2 and 1:3 are shown in Figure 3.



$E_{total} = -876579$ kcal/mol
a) complex ratio 1: 2

$E_{total} = -1253252$ kcal/mol
b) complex ratio 1:3
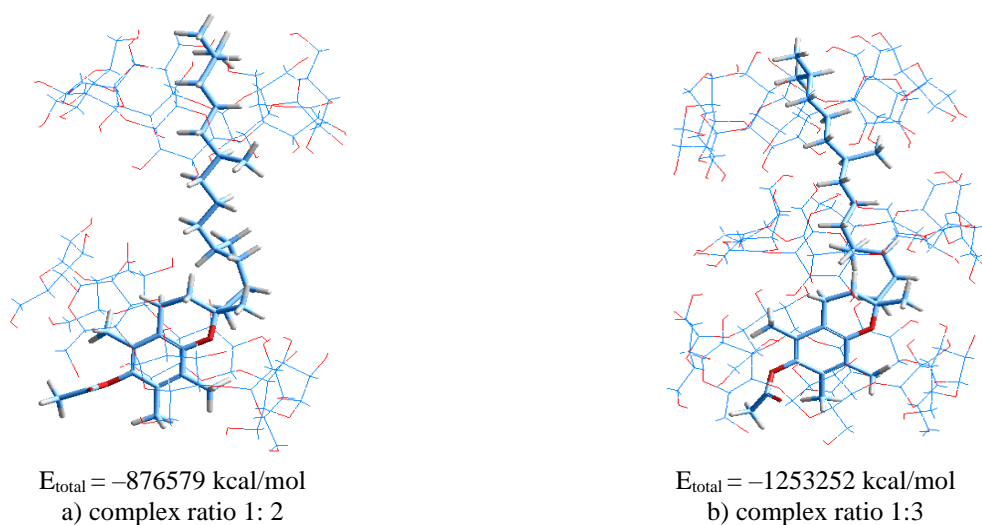
Figure 3. Molecular model of the "β-CD:VE" complex in the ratios of 1:2 (a) and 1:3 (b)

It can be seen from the molecular models shown in Figure 3 that complexation with two molecules of cyclodextrin does not cause noticeable deformation of the cyclodextrin ring, while complexation with three molecules of cyclodextrin leads to the reversal of some glucoside rings and flattening of the walls of the toroidal cavity, i.e. to conformational deformation.

It was interesting to simulate the inclusion complex of VE acetate with four β-cyclodextrin molecules. As a result of geometry optimization by the MM+ method, a molecular model of the "β-CD:VE" complex in a ratio of 1:4 was obtained (Fig. 4).
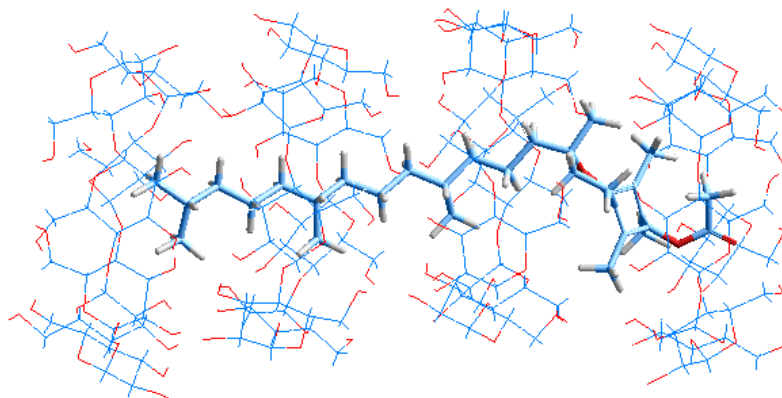


Figure 4. Molecular model of the "β-CD:VE" complex in a ratio of 1:4 ($E_{total} = -1629877$ kcal/mol)

The analysis of the geometry showed that the bounds between VE and fourth cyclodextrin ring were weakly. Thus it can be concluded that the complexes of the 1:4 composition are quite unstable compared to the complexes with the ratios of 1:1, 1:2 and 1:3.

*Study of the morphology of "β-CD:VE" clathrate inclusion complexes*

The morphology of the β-CD particles and the "β-CD:VE" inclusion complexes were analyzed using a scanning electron microscope (SEM). Figure 5 shows scanned electronic micrographs of the "β-CD:VE" inclusion complex (2:1). The studied samples of clathrates were sprayed with a conductive layer of carbon. The images were obtained at accelerating voltages of 3 and 7 kV. The magnification in the panels (*a–d*) is from 931 to 7560×.

The images of the samples (a, b) show the layered structure of β-cyclodextrin, and the samples (c, d) "β-CD:E" (2:1) show a change in the morphology and shape of the crystals (there is a state of crystallization of the raw material, the layered structure is not visible, the shape of the crystals is different, the crystal forms are covered with a film [12–14].

*IR and $^1H$ NMR spectroscopic investigation of the "β-CD:VE" complex*

Figure 6 shows the IR spectra of β-CD (a, b) in the free state and in the form of clathrate. The peaks of the carbonyl C=O and aromatic CH groups are clearly visible at 1763 and 2947 cm$^{-1}$, respectively, in the VE Fourier-IR spectrum. There are fluctuations in the carbon skeleton (C-C bonds) in the region of 1211 cm$^{-1}$. A comparison of the IR spectra of free β-CD (Fig. 6*a*, *b*) and the "β-CD: VE" clathrate (Fig. 6*c*, *d*) shows a slight blurring in the appearance of the characteristic absorption bands of the functional groups of the β-CD molecule, which indicates the absence of covalent interactions between VE and the internal functional groups of the β-CD torus.

However, some characteristic absorption peaks of the C-H, NH, and C-O bonds of the β-CD molecule in the complex have offsets, namely from 3387, 2924, 1651, and 1423 cm$^{-1}$ to 3410, 2929, 1655, and 1469 cm$^{-1}$, respectively. It should also be noted that a characteristic peak of the carbonyl C=O-group in VE appears in the IR spectrum of the clathrate complex (Fig. 6*c*) at 1759 cm$^{-1}$. This may mean that VE molecules enter the inner torus of β-CD with their side alicyclic chain. These data indicate a change in the structural framework of the internal torus of the "host" (β-CD) in favor of the formation of the "β-CD:VE" inclusion complex (Fig. 7) [8–10].
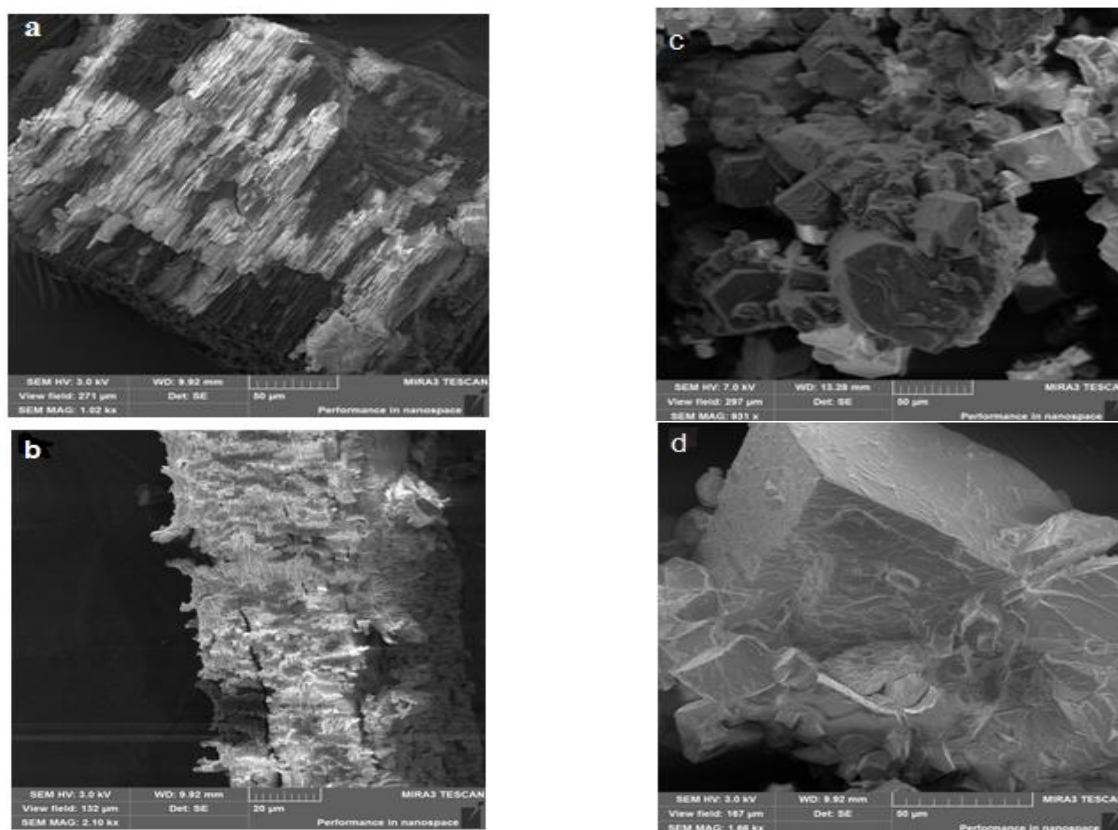
Figure 5. Scanned electron micrographs of β-CD (a, b) and the "β-CD:VE" inclusion complex (2:1) (c, d) at various magnifications
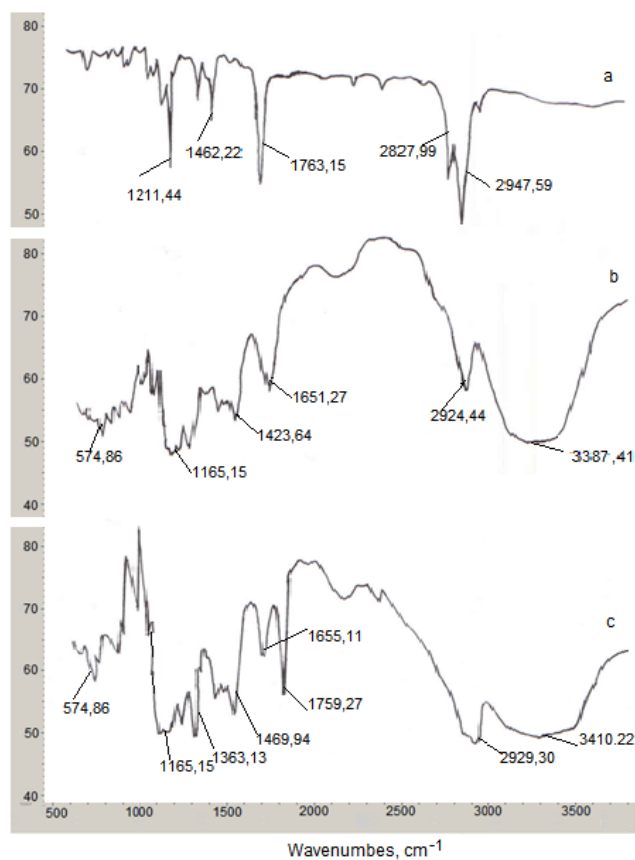


Figure 6. IR-Fourier spectra of VE (a), β-CD (b) and the "β-CD:VE" clathrate complex (KBr) (c)
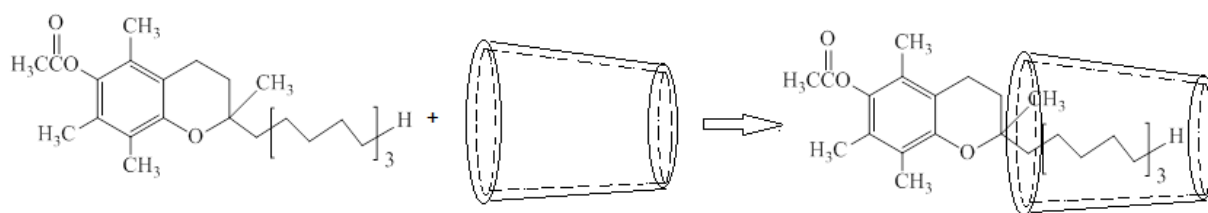
Figure 7. Scheme of the "β-CD:VE" complex formation

The formation of internal and external protons can be distinguished using the NMR spectra of CD and its clathrate complexes. Formation of a substrate complex with CD displaces the proton signals of the initial CD in the NMR spectrum [14]. During the formation of the inner complex shifts of the third and fifth protons are observed, and during the formation of the outer complex shifts of the second and fours protons are observed. One can judge about the formation of internal or external complexes, respectively, according to the magnitude of the chemical shifts of internal or external protons of β-CD.

The shift of the $^1H$ and $^{13}C$ nuclei ($\pm\Delta\delta$) signals both in the region of weak and strong fields (Table 1) have been observed in the "β-CD:VE" complexes [14, 15].

The study of the $^1H$ (a) and $^{13}C$ (b) β-CD NMR spectra in the free and bound state in the form of the "β-CD:VE" clathrate (Table 1) revealed the biases of all the signals of the $^1H$ and $^{13}C$ nuclei of the "host" molecule ($\pm\Delta\delta$) both in the area of weak and strong fields (Table 1). This fact confirms the non-valent binding to the "guest" molecule. In the "β-CD:VE" $^1H$ NMR spectrum, the greatest difference in the values of the chemical shift is characteristic for the intra-atmospheric H-3 protons ($\Delta\delta = -0.05$ ppm), on the basis of which it can be concluded that an internal (inclusive) complex is formed in the clathrate [9, 15, 16]. In the case of the carbon spectrum there is a less significant difference in the change in chemical shifts, which ranges from –0.01 to 0.01 ppm.

T a b l e   1

**Chemical shifts of $^1H$ and $^{13}C$ NMR of β-cyclodextrin in the free state and in the "β-CD:VE" inclusion complex**

| Atom no. | The value of $\delta_0$ in the free state, ppm | | Value of $\delta$ as part of the complex, ppm | | Changing the chemical shift, $\Delta\delta = \delta - \delta_0$, ppm | |
|---|---|---|---|---|---|---|
| | $\delta_0(^1H)$ | $\delta_0(^{13}C)$ | $\delta(^1H)$ | $\delta(^{13}C)$ | $\delta(^1H)$ | $\Delta(^{13}C)$ |
| H-1 | 4,77 | 102,43 | 4,78 | 102,44 | 0,01 | 0,01 |
| H-2 | 3,59 | 73,54 | 3,57 | 73,55 | -0,02 | 0,01 |
| H-3 | 3,55 | 72,52 | 3,50 | 72,53 | -0,05 | 0,01 |
| H-4 | 3,45 | 82,00 | 3,44 | 82,00 | -0,01 | 0,00 |
| H-5 | 3,32 | 72,87 | 3,30 | 72,88 | -0,02 | 0,01 |
| H-6 | 3,60 | 60,40 | 3,58 | 60,39 | -0,02 | -0,01 |

*Study of the effect of the "β-CD:VE" clathrate complex on some biological properties of a food product*

Testing of the proposed solutions with an assessment of the quality and safety indicators of VE encapsulated with *β*-cyclodextrin in the food product was performed. Sausages made from lamb (70 %) and turkey (20 %) were selected as a food model. The basic product for the development of recipes was the Lamb sausage produced according to the GOST 16351-86 (production date 20.09.2020). Organoleptic evaluation of semi-smoked sausages with the "β-CD: VE" clathrate complex was carried out on a 9-point scale according to the GOST 9959-91 "Meat products".

General conditions for organoleptic evaluation. The moisture content was determined according to the GOST 9793-74 by drying the suspension to a constant mass (at 105±3 °C). Physico-chemical and microbiological characteristics of meat product samples with encapsulated vitamin complex "β-CD:VE" were determined in the testing laboratory of "Nuritest" LLP (Almaty, certificate of accreditation KZ.N.02.0043 dated February 08, 2020).

Organoleptic evaluation of the meat sausages demonstrated that the products with the vitamin complex "β-CD:VE" have been characterized by a delicate meat smell, a juicy and tender consistency, and a light brown color. The microbiological parameters of the semi-finished product prototypes meet the requirements of the regulatory documentation according to the results presented in Table 2.

T a b l e  2

**Physico-chemical and microbiological characteristics of meat sausage products
with encapsulated vitamin complex "β-CD:VE"**

| Name of indicators | Permissible norms for regulatory documents | Actually received | Designation of regulatory documentation for test methods |
|---|---|---|---|
| **Microbiological studies**: | | | |
| Pathogenic microorganisms, including Salmonella, in 25 g | Not allowed | Not detected | GOST 31659-2012 |
| L. monocytogenes, в 25 г | Not allowed | Not detected | GOST 32031-2012 |
| BGKP (coliforms), in 25 g | Not allowed | Not detected | GOST 9958-81 |
| Staphylococcus aureus, в 1 г. | Not allowed | Not detected | GOST 9958-81 |
| Sulfite-reducing clostridium, in 0.1 g | Not allowed | Not detected | GOST 9958-81 |
| **Physical and chemical properties:** | | | |
| Peroxidenumber, mmol (1/2) / kg | – | 3.48±0.35 | State Standard (GOST) R 51487-99 |
| **Nutritional value, g/100 g:** | | | |
| Proteins | – | 21.64±0.02 | 25011-81 |
| Fats | – | 25.95±0.03 | GOST 23042-86 |
| Carbohydrates | – | 0.98±0.05 | I.M. Skurichin, No.1, 1987 |
| Moisture content | – | 49.18±0.24 | GOST 9793-74 |
| Ash | – | 2.25±0.02 | GOST 15113-8-77 |
| **Energy value, kcal/kJ/100g** | – | 324/1355 | I.M. Skurichin, No.1, 1987 |
| **Vitamins, mg/100g:** | | | |
| Vitamin E | – | 11.28±1.13 | I.M. Skurichin, No.1, 1987 |

*Conclusion*

The present study proposed the most optimal method for obtaining inclusion complexes of β-CD with VE. The highest yields of target clathrate inclusion complexes of VE with cyclodextrin were obtained under microwave synthesis conditions. Molecular modeling of inclusion complexes of VE with β-CD in ratios of 1:1, 1:2, 1:3, and 1:4 was performed using the MM+ method. The total energy of the systems under study was estimated based on semiempirical PM3 calculations. The study of $^1$H and $^{13}$C NMR spectra of β-CD in a free and bound state in the form of a clathrate "β-CD:VE" made it possible to establish the structural features of supramolecular clathrate complexes of VE. Results of the safety of encapsulated vitamin complex "β-CD:VE" was confirmed by microbiological analysis of a meat product with an encapsulated vitamin complex "β-CD:VE". The microbiological indicators of the meat products correspond to the regulatory documents. The developed scientific approach is of interest for the use of encapsulated vitamins in the production of functional food products.

References

1    Виташевская В.Ю. Краткий обзор российского рынка функциональных (обогащенных) продуктов / В.Ю. Виташевская // Russian Foods & Drinks Market Magazin. — 2014. — № 2. — С. 61–65.

2    Шехирева Д.А. Функциональное питание. Функциональные ингредиенты и пищевые продукты / Д.А. Шехирева // Интернет ресурс. URL: https://www.bibliofond.ru/view.aspx? id=802656.

3    Шагина С.А. Создание комплексов включений циклодекстринов на основе бета-специфичной циклодекстринглюканотрансферазы: Автореф. дис. … канд. техн. наук / С.А. Шагина. — М., 2008. — 27 с.

4    Иванова Л.А. Получение комплексов циклодекстринов с биологически активными веществами / Л.А. Иванова, Д.Г. Шипарева, С.А. Скрылева, И.С. Тихонова // Пищевая промышленность. — 2011. — № 10. — С. 67–69.

5    Loftsson T. Self-association of cyclodextrins and cyclodextrin complexes / T. Loftsson, M. Masson, M. Brewster // J. Pharmaceut. Sci. — 2004. — Vol. 93. — P. 1091–1099.

6 Novosyolova N. Formation of inclusion complexes of cyclodextrins with oil-soluble vitamins / N. Novosyolova // Materials of XII International Conference "Surface forces". June 29 — July 5, 2002. — Zvenigorod, 2002. — P. 127.

7 Новосёлова Н.В. Циклодекстрины и их комплексы включения с маслорастворимыми витаминами / Н.В. Новосёлова, В.Н. Матвеенко // Наука и образование – 2004: Материалы Междунар. науч.-техн. конф. — Мурманск, 2004. — Ч. 4. — С. 144–148.

8 Xi Y. pH-Responsive Emulsions with β-Cyclodextrin/VE Assembled Shells for Controlled Delivery of Polyunsaturated Fatty Acids / Y. Xi, Y. Zou, Z.Luo, L. Qi, X. Lu // J. Agric. Food Chem. — 2019. — Vol. 67. — P. 11931–11941. https://doi.org/10.1021/acs.jafc.9b04168

9 Bao D.C. Preparation of VE microcapsules and its controlled release chracteristics / D.C. Bao, Q.G. Zhang, X.D. Liu, Ma X.J., Q. Yuan. //Acta Physiol. Chim. Sin. — 2004. — Vol. 20(2). — P. 178–181.

10 JIao F.P. Preparation and spectra properties of inclusion complexes of vitamin E with b-cyclodextrin / F.P.JIao, X.Q. Chen, H.Z. Yu, L. Yang // Journal of Food Processing and Preservation. — 2010. — Vol. 34. — P. 114–124. https://doi.org/10.1111/j.1745-4549.2008.00327.x

11 Burkeyev M. Thermal decomposition of b-cyclodextrin and its inclusion complex with vitamin E / M. Burkeyev, S. Fazylov, R. Bakirova, A.Iskineyeva, A. Sarsenbekova, E. Tazhbaev, S. Davrenbekov // Mendeleev communication. — 2021. — Vol. 31. — P. 76–78. https://doi.org/10.1016/j.mencom.2021.01.023

12 Szejtli J. Past, present and future of cyclodextrin research / J. Szejtli // Pure and Applied Chemistry. — 2004. — Vol. 76, No. 10. — P. 1825–1845.

13 Aree T. Crystal structure of β-cyclodextrindimethyl-sulfoxide inclusion complex / T. Aree, N. Chaichit // Carbohydrate Research. — 2002. — Vol. 337. — P. 2487–2494. https://doi.org/10.1016/s0008-6215(02)00485-8

14 JIao F.P. Preparation and spectra properties of inclusion complexes of vitamin E with b-cyclodextrin / F.P.JIao, X.Q. Chen, H.Z.Yu, L. Yang // Journal of Food Processing and Preservation. — 2010. — Vol. 34. — P. 114–124. https://doi.org/10.1111/j.1745-4549.2008.00327.x

15 Demarco P.V., Thakkar A.L. Cyclohepta-Amylose Inclusion Complexes. A Proton Magnetic Resonance Study / P.V. Demarco, A.L. Thakkar // Journal of the Chemical Society D: Chemical Communications. — 1970. — P. 2–4. http://dx.doi.org/10.1039/c29700000002.

16 Bakirova R. Obtaining and Investigation of the beta-CyclodextrinInclution Complex with Vitamin D-3 Oil Solution / R. Bakirova, A. Nukhuly, A. Iskineyeva, S. Fazylov, M. Burkeev, A.Mustafaeva, E. Minaeva, A. Sarsenbekova // Scientifica. — 2020. — Vol. 2020. — P. 1–8. — ID6148939. https://doi.org/10.1155/2020/6148939

А. Искинеева, А. Мұстафаева, Г. Замаратская, С. Фазылов, И.А. Пустолайкина,
О.А. Нүркенов, А. Сарсенбекова, Т. Сейлханов, Р. Бәкірова

## Қапталған α-токоферол ацетатының алынуы және оның физикалық-химиялық пен биологиялық қасиеттерін зерттеу

Мақалада суда еритін олигосахаридті (циклодекстринді) қолдана отырып, сырты қапталған Е дәруменін алу бойынша зерттеу нәтижелері талқыланған. α-Токоферол ацетатын β-циклодекстринмен қапталған кешенін алу сулы-спиртті ортада тұнбаға бірге түсіру және микротолқынды өңдеу технологиясын қолдана отырып алынған. Е витамині циклодекстринмен кешенді қосылысының ең жоғары шығымы микротолқынды өңдеу жағдайында алынды. ММ+ әдістемесімен α-токоферол ацетатының β-цикло-декстринмен 1:1, 1:2, 1:3 және 1:4 қатынастағы комплексті кешендерінің молекулярлы үлгіленулері орындалды. РМ полуэмперикалық РМ3 есептеулері арқылы зерттелуші жүйелердің толық энергиясы реакциялық сұйық ортаның әсерінсіз бағаланды. Олигосахаридпен α-токоферол ацетатының клаттаттық кешенінің құрылымын зерттеу бойынша деректер келтірілген. Алынған клатрат кешенінің беткі морфологиясы сканерлеуші электронды микроскоптың көмегімен сипатталған. Қосылу кешенінің құрылыстары ИҚ-Фурье және ЯМР ¹H және ¹³C спектроскопия деректерімен сипатталады. β-Цикло-декстриннің жекелік және клатартты комплекс түріндегі ЯМР ¹H и ЯМР ¹³C спектрлерін талдау молекулаларлардағы ¹H және¹³C ядроларының әлсіз және күшті өріс жақтарға жылжуларын (±Δδ) анықтауға мүмкіншілік жасады. Тәжірибелердің нәтижелері α-токоферол ацетатын β-циклодекстрин-мен әртүрлі арақатынаста қосу кешенінің қалыптасуын растады. Инкапсуланған α-токоферол ацетатының тағамдық ет өнімдерінің қауіпсіздігіне әсерін зерттеу бойынша деректер келтірілген.

*Кілт сөздер*: α-токоферола ацетат, циклодекстрин, олигосахаридтер, Е витамині, крахмал, қосылу кешені, ЯМР спектроскопиясы, клатрат.

А. Искинеева, А. Мустафаева, Г. Замаратская, С. Фазылов, И.А. Пустолайкина,
О.А. Нуркенов, А. Сарсенбекова, Т. Сейлханов, Р. Бакирова

# Получение инкапсулированного ацетата α-токоферола и исследование его физико-химических и биологических свойств

В статье обсуждены результаты исследования по получению инкапсулированного витамина Е с использованием водорастворимого олигосахарида (циклодекстрина). Получение комплексов включения β-ЦД с α-токоферолом осуществлено в водно-спиртовой среде методами соосаждения и микроволновой активации. Наиболее высокие выходы целевых клатратных комплексов включения витамина Е с циклодекстрином были получены в условиях микроволнового синтеза. Выполнено молекулярное моделирование комплексов включения α-токоферола ацетата с β-циклодекстринами в соотношениях 1:1, 1:2, 1:3 и 1:4 с помощью метода ММ+. На основании полуэмпирических PM3 расчетов без учета влияния среды выполнена оценка полной энергии исследуемых систем. Приведены данные по изучению структуры клатратного комплекса ацетата α-токоферола с β-циклодекстрином. Морфология поверхности полученного клатратного комплекса «гость–хозяин» описана с помощью сканирующего электронного микроскопа. Спектральные свойства комплекса включения охарактеризованы данными ИК-Фурье и ЯМР $^1$H и $^{13}$C спектроскопии. Изучение спектров ЯМР $^1$H и ЯМР $^{13}$C β-CD в свободном состоянии и связанном в форме клатрата «β-CD:VE» позволило выявить смещения сигналов ядер (±Δδ) $^1$H и $^{13}$C молекулы «хозяина» как в область слабых, так и сильных полей. Результаты экспериментов подтвердили возможность образования комплексов включения ацетата α-токоферола с β-циклодекстрином при различных соотношениях. Приведены данные по изучению влияния инкапсулированного α-токоферола ацетата на безопасность пищевых мясных продуктов.

*Ключевые слова*: α-токоферола ацетат, циклодекстрин, олигосахариды, витамин Е, крахмал, комплексы включения, ЯМР-спектроскопия, клатрат.

## References

1    Vitashevskaya, B.U. (2014). Kratkii obzor rossiiskogo rynka (obogashennykh) produktov [Brief overview of the Russian market of functional (enriched) products]. *Russian Foods & Drinks Market Magazin*, *2*, 61–65 [in Russian].

2    Shekhirova, D.A. Funktsionalnoe pitanie. Funktsionalnye ingredienty i pishchevye produkty [Functional nutrition. Functional ingredients and food products]. Retrieved from: https://www.bibliofond.ru/view.aspx? id=802656 [in Russian].

3    Shagina, S.A. (2008). Sozdanie kompleksov vklucheniia tsiklodekstrinov na osnove beta-spetsifichnoi tsiklodekstrintransferazy [Creation of complexes of cyclodextrin inclusions based on beta-specific cyclodextringlucanotransferase]. *Candidate's thesis.* Moscow [in Russian].

4    Ivanova, L.A. (2011). Polushenie kompleksov s biologicheski aktivnymi veshchestvami [Preparation of complexes of cyclodextrins with biologically active substances]. *Pishchevaia promyshlennost — Food industry, 10*, 67–69 [in Russian].

5    Loftsson T., Masson M., & Brewster, M. (2004). Self-association of cyclodextrins and cyclodextrin complexes. *J. Pharmaceut. Sci.*, *93,* 1091–1099.

6    Novosyolova, N. (2002). Formation of inclusion complexes of cyclodextrins with oil-soluble vitamins. Proceedings from Surface forces: *XII International Conference* (June 29 — July 5). Zvenigorod.

7    Novosyolova, N., & Matveenko, V.N. (2004). Tsiklodekstriny i ikh kompleksy vkliucheniia s maslorastvorimymi vitaminami [Cyclodextrins and their inclusion complexes with oil-soluble vitamins]. Proceedings from Science and Education – 2004: *International Scientific and Technical Conference*. (Pt. 4, p. 144–148). Murmansk [in Russian].

8    Xi, Y., Zou, Y., Luo, Z., Qi, L., & Lu, X. (2019). pH-Responsive Emulsions with β-Cyclodextrin/VE Assembled Shells for Controlled Delivery of Polyunsaturated Fatty Acids. *J. Agric. Food Chem.*, *67,* 11931–11941. https://doi.org/10.1021/acs.jafc.9b04168.

9    Bao, D.C., Zhang, Q.G., Liu, X.D., Ma, X.J., & Yuan, Q. (2004). Preparation of VE microcapsules and its controlled release chracteristics. *Acta Physiol. Chim. Sin.*, *20(2)*, 178–181.

10    JIao, F.P., Chen, X.Q., Yu, H.Z., & Yang, L. (2010). Preparation and spectra properties of inclusion complexes of vitamin E with b-cyclodextrin. *Journal of Food Processing and Preservation, 34,* 114–124. https://doi.org/10.1111/j.1745-4549.2008.00327.x.

11    Burkeyev, M., Fazylov, S., Bakirova, R., Iskineyeva, A., Sarsenbekova, A., Tazhbaev, E., & Davrenbekov, S. (2021). Thermal decomposition of b-cyclodextrin and its inclusion complex with vitamin E. *Mendeleev communication, 31,* 76–78. https://doi.org/10.1016/j.mencom.2021.01.023.

12    Szejtli, J. (2004). Past, present and future of cyclodextrin research. *Pure and Applied Chemistry, 76, 10*, 1825–1845.

13    Aree, T., & Chaichit, N. (2002). Crystal structure of β-cyclodextrindimethyl-sulfoxide inclusion complex. *Carbohydrate Research, 337*, 2487–2494. https://doi.org/10.1016/s0008-6215(02)00485-8.

14    JIao, F.P., Chen, X.Q., Yu, H.Z., & Yang, L. (2010). Preparation and spectra properties of inclusion complexes of vitamin E with b-cyclodextrin. *Journal of Food Processing and Preservation, 34*, 114–124. https://doi.org/10.1111/j.1745-4549.2008.00327.x.

15    Demarco, P.V., Thakkar, A.L. (1970). Cyclohepta-Amylose Inclusion Complexes. A Proton Magnetic Resonance Study. *Journal of the Chemical Society D: Chemical Communications,* 2-4. https://doi.org/10.1039/c29700000002.

16  Bakirova, R.A., Nukhuly, A., Iskineyeva, A., Fazylov, S., Burkeev, M., Mustafaeva, A., Minaeva, E., & Sarsenbekova, A. (2020). Obtaining and Investigation of the beta-CyclodextrinInclution Complex with Vitamin D-3 Oil Solution.*Scientifica*.*1-8*. ID 6148939. https://doi.org/10.1155/2020/6148939.

## Information about authors

**Mustafayeva Ayaulim** — Candidate of Thechnical Sciences, SakenSeifullin Kazakh Agrotechnical University, Nur-Sultan, Kazakhstan, e-mail: ayaulym.mustafa@mail.ru, https://orcid.org/0000-0003-0693-6427.

**Iskineyeva Ainara** — PhD student of SakenSeifullin Kazakh Agrotechnical University, Nur-Sultan, Kazakhstan, e-mail: iskeneeva_aynara@mail.ru, https://orcid.org/0000-0002-1705-6372.

**Zamaratskaya Galia** — Ph-Doctor, Associate Professor ofSwedish University of Agricultural Sciences, Uppsala, Sweden, e-mail: galia.zamaratskaia@slu.se, https://orcid.org/0000-0003-0926-4849;

**Fazylov Serik** (corresponding author) — Academician of the National Academy of Sciences of the Republic of Kazakhstan, Doctor of Chemical Sciences, Professor, Karagandy University of the name of academician E.A. Buketov, Kazakhstan, e-mail: iosu8990@mail.ru, https://orcid.org/0000-0002-4240-6450.

**Pustolaikina Irina** — Candidate of chemical sciences, Assoc. Professor, Karagandy University of the name of academician E.A. Buketov, Universitetskaya street, 28, 100028, Karaganda, Kazakhstan; e-mail: ipustolaikina@gmail.com, https://orcid.org/0000-0001-6319-666X;

**Nurkenov Oralgazy** — Doctor of Chemical Sciences, Professor, Institute of Organic Synthesis and Coal Chemistry of the Republic of Kazakhstan, Karaganda, Kazakhstan; e-mail: nurkenov_oral@mail.ru, https://orcid.org/0000-0002-2771-0411.

**Sarsenbekova Akmaral** — Ph-Doctor of Karaganda university, Karaganda, Kazakhstan, chem_akmaral@mail.ru, https://orcid.org/0000-0002-8951-3616.

**Seilkhanov Tolegen** — Candidate of Chemical Sciences, Sh. Ualikhanov Kokshetau State University, e-mail: tseilkhanov@mail.ru, https://orcid.org/0000-0003-0079-4755;

**Bakirova Ryszhan** — Doctor of medical sciences, Professor of «Karaganda Medical University» non-commercial joint-stock company, Kazakhstan; e-mail: bakir15@mail.ru, https://orcid.org/0000-0002-1592-8579.

# PHYSICAL AND ANALYTICAL CHEMISTRY

## S.S. Bhujbal*, M. Kale, B. Chawale

*Dr. D.Y. Patil Institute of Pharmaceutical Sciences and Research, Pimpri, Pune – 411018, Maharashtra, India*
*(\*Corresponding author′s e-mail: santosh.bhujbal@dypvp.edu.in)*

# Molecular docking identification of plant-derived inhibitors of the COVID-19 main protease

COVID-19 cases increase at a high rate and become dangerous in recent months. As a consequence, some healthcare and research organizations are attempting to find an effective cure for the COVID-19 outbreak. Many natural products have been reported to have powerful activity against COVID-19 in recent research studies. The primary aim of this article is to establish natural bioactive compounds with suitable antiviral properties. Lui et al. have reported in their study that SARS-Cov-2 main protease is present in a crystalline structure known as a novel therapeutic drug target. It is important to inhibit SARS-Cov-2 main protease to stop the replication of viral proteins. In this study natural compounds were screened using molecular modeling techniques to investigate probable bioactive compounds that block SARS-Cov-2. From these studies many natural compounds were found to have the potential to interact with viral proteins and show inhibitory activity against COVID-19 main protease (Mpro) and these natural compounds were also compared to known antiviral drugs such as Saquinavir and Remdesivir. Besides that, additional research is needed before these potential leads can be developed into natural therapeutic agents against COVID-19 to fight the epidemic.

*Keywords*: Natural compounds, SARS-Cov-2, Efficacy, Drug target, Molecular modeling, Viral proteins, Mpro, Binding affinity.

*List of Abbreviations*

**Mpro**: Main Protease (Covid-19)
**SARS-Cov-2**: Severe Acute Respiratory Syndrome Coronavirus-2
**WHO**: World Health Organization
**PDB:** Protein Data Bank
**SDF:** Spatial Data File
**3CLPro:** 3-Chromotrypsin Like Protease
**CASTp:** Computed Atlas of Surface Topography of Proteins

*Introduction*

World Health Organization (WHO) declared that the novel coronavirus infection is pandemic, and this infection going high day by day in all regions of the world [1]. This pandemic caused by novel coronavirus, SARS-Cov-2 (Severe Acute Respiratory Syndrome Coronavirus-2) was firstly reported in Wuhan, (China) in December 2019 [2]. As world's population is growing high it leads to the occurrence of many chronic diseases as well as lifestyle-related diseases. So this problem can be overcome by focusing on traditional herbal medicines to enhance as well as improve quality of life [3]. Herbal medications are commonly used by most people because they have long-term safety, good efficacy, and low toxicity, and they have shown remarkable results in the treatment of a variety of viral infections. Still, there is no specific treatment against COVID-19 infection. So to control the spread of COVID-19 infection, many research works are carried out to find effective as well as preventive therapy against COVID-19 infection [4]. So that many researchers taking an effort to design new treatments to avoid COVID-19 infection for examining secondary metabolites obtained from plants by using

molecular docking to study inhibition of enzyme-like main protease (Mpro) as well chymotrypsin-like protease (3CL pro), which is responsible for viral infection [1, 5].

Molecular docking is one of the best approaches to design, develop, and evaluate new treatment. There are various new therapeutic techniques developed to find new entities, but protease enzyme inhibitor is one of the novel therapeutic strategies, which are selected from natural bioactive compounds to find out effective medicine with minimum side effects. In the present study we analyze ten ligands for their binding affinity [5]. Most of the selected ligands are essential parts of many edibles from India and other regions. They show efficacy against the COVID-19 6LU protease. The main motive of the present study is to find out the ability of these ligands to inhibit COVID-19 main protease and to design natural products that can be effective in the treatment of COVID-19 infection. Ligands selected for docking analysis are present in spices and show tolerable binding affinity with COVID-19 6LUT protease. Further, these ligands are compared with synthetic drugs having remarkable antiviral properties, such as Remdesivir and Saquinavir [6].

Molecular docking studies are generally used for the analysis of complex structures obtained by the interaction through ligand and target molecules. Three-dimensional structure and probable binding sites are determined by molecular docking methods. The molecular docking approach is commonly used to identify several binding interactions such as enzyme-substrate interaction, lipid-protein interaction, drug-enzyme interaction, etc [7, 8]. The molecular modeling technique is widely used in various structure-based drug designs (SBDD), because of its characteristic to determine actual binding conformation in ligand and target site. Because of its ability to generate accurate conformation between ligand and target, it is rapidly used to identify binding conformation in target and drug, and therefore it is an important tool in rational drug designing [9].

In the 1980s, the molecular docking technique constituted a crucial mechanism because of the development of 1st algorithm. Molecular modeling analysis particularly analyzes the binding affinity of the target molecule with ligand and based on this; it may help to suggest a potential treatment against a specific disease. In these cases in-silico approach of molecular docking become a faster technique. In silico approach helps to reduce the time and cost of the process for the identification of complex structures and binding techniques. So in drug discovery molecular docking with in silico approach becomes a very quick and common easy to apply method [10, 11]. In general molecular docking process is shown in Figure 1.
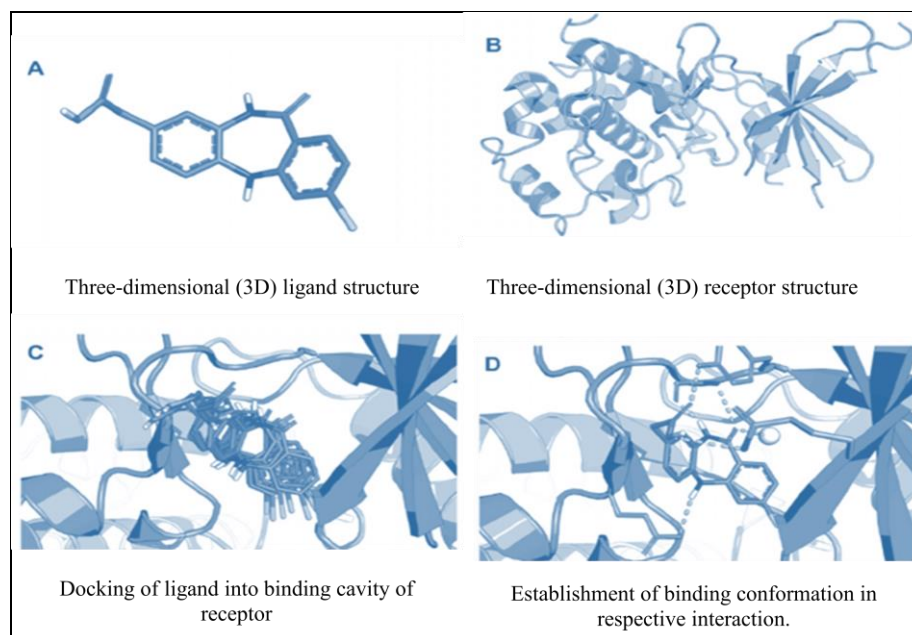


Figure 1. Molecular docking process in general

The software develops an algorithm, in which the conformation of the ligand is determined after performing docking analysis. The binding affinity resulted in a negative value of ΔG (in terms of units Kcal/mol). The binding energy shows a combination of Van der Waals as well as electrostatic energy, which concerning the interaction between ligand molecule and target molecule [14]. Also, in drug designing, the rigid system can be used, in which translational and rotational space in six dimensions can be identified for the fitting of ligand and particular binding structure. The research-based section represents a higher area of interest in molecular

modeling studies throughout recent decades. This is also true in the case of molecular modeling methods or computational methods for prediction [15].

The preliminary work in the area of molecular docking studies was initially performed using structural shape contacts and then Kuntz applied a shape matching strategy to identify potential conformations. After successful initiating work by Kuntz, various docking approaches were developed using Fourier transformations algorithms [16].

### Types of docking analysis

*Rigid body docking.* In this type of molecular docking both molecule and receptor assumed as rigid. The occurrence of modifications in structure possesses degrees of freedom. This approach represents an example of Zdock [14].

*Semi-flexible docking.* This is the method of docking in which their improvement in a rigid body is docking for identification of side chains and potential torsion angles. This method of docking is different from the Fourier transformation method. This new transformation was obtained by the HADDOCK protocol [15].

*Flexible docking.* This type of docking uses two logarithmic approaches: systematic incremental plotting and stochastic. The first approach is commonly used to develop binding conformations based on the ligand position and binding in all possible areas. These are for example: DOCK [16], Flex [17], Glide [18], Hammerhead [19], LUDI [20], Surflex [21]. In stochastic algorithms, there is improvement in computational methods. These are, for example, DARWIN [22], GOLD [23], AutoDock [24], Carlo [25].

### Experimental

*Data collection.* The structure of COVID-19 3CL pro or Mpro (Having PDB ID: 6LU7) were taken in PDB format from (https://www.rcsb.org/) [26]. Also, some part of this study was performed by the SwissDock web server [27, 28], which incorporates an automated in silico molecular docking procedure based on the EADock ESS docking algorithm [29]. The active binding sites of the protease enzyme were found by using the CASTp (http://sts.bioe.uic.edu/castp/index.html?3igg) [30].

Three-dimensional (3D) structures of the selected ligands were taken in SDF format from the https://pubchem.ncbi.nlm.nih.gov/ website [29]. A known anti-HIV drug Saquinavir was used as a positive control for comparative docking analysis.

*Molecular Docking.* The molecular docking studies analyze the mechanism of interaction between ligand and receptors. These mechanisms of interactions between ligand and receptor play a significant role in the case of drug discovery. In molecular modeling, docking analysis is a technique that is used to analyze stable complexes formed by the binding of two molecules and adaptation between them [31].

The protease file was prepared for COVID 19 6LU7 protease by using Autodock 4.2 [32]. Using A chain of protease, the macromolecule was produced by removal of a water molecule and addition of hydrogen bond. For further studies of analysis, the file was saved in PDBQT format. The calculation of binding affinity was done by using AutoDock–Vina [33]. The 3D structure of interaction between ligand and receptor was detected by using PyMOL [34].
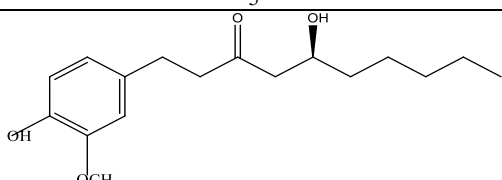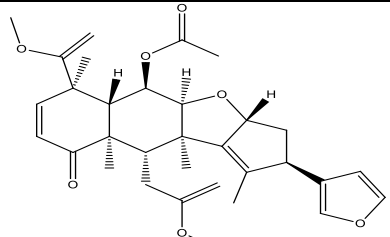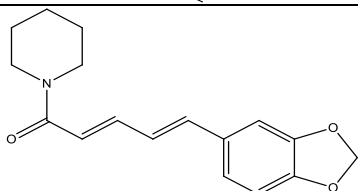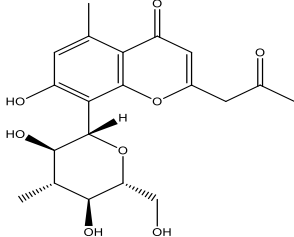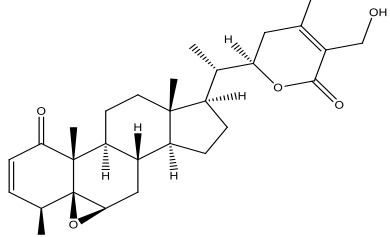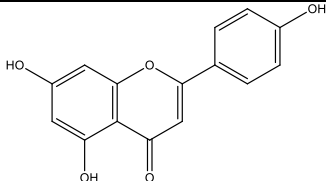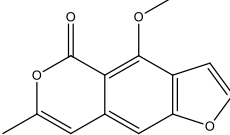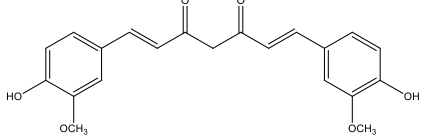
In this study we used flexible docking. Rigid-body docking, semi-flexible docking and flexible docking are three different types of docking procedures, but it was found that flexible-ligand docking shows significant results as compared to rigid body docking and semi-flexible docking

### Results and Discussion
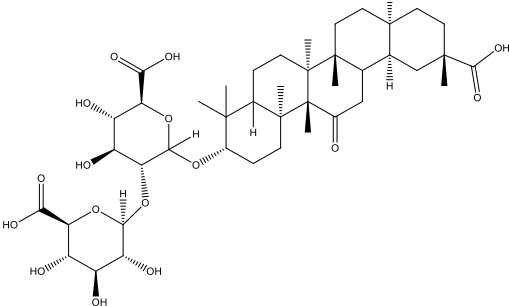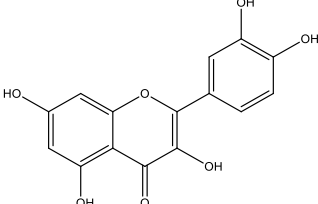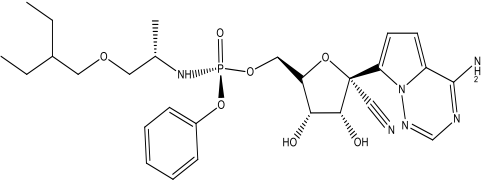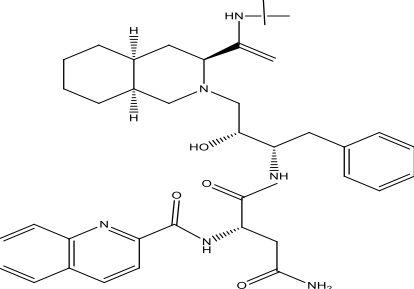
The present study is based on an analysis of ten selected bioactive compounds derived from Indian medicinal plants, and also there is a comparison of the herbal compound with known antiviral drugs based on binding affinity. The binding affinity of extracted bioactive compounds from plants with COVID-19 protease 6LU7 and their molecular structures are shown in Table [6, 35].

T a b l e

**Representation of docking results including binding affinities of natural products**

| Compound | Ligand source | Molecular formula | Binding affinity | Structure |
|---|---|---|---|---|
| 1 | 2 | 3 | 4 | 5 |
| Gingerol | Ginger (*Zingiber officinale*) | $C_{17}H_{26}O_4$ | −7.95 | |
| Nimbin | Neem (*Azadirachta indica*) | $C_{30}H_{36}O_9$ | −8.17 | |
| Piperin | Black and white pepper (*Piper nigrum, Piper longum and Piper officinarum*) | $C_{17}H_{19}NO_3$ | −6.98 | |
| Aloesin | Aloe vera (*Aloe Ferox, Aloe barbadensis*) | $C_{19}H_{22}O_9$ | −8.79 | |
| Withaferin A | Ashwagandha (*Acnistus arborescens, Withania somnifera, and Withania somnifera Dunal*) | $C_{28}H_{38}O_6$ | −8.05 | |
| Apigenin | Apple (*Malus domestica*), Red pepper (*Capsicum annuum*), Thyme (*Thymus vulgaris*), Garlic (*Allium sativum*). | $C_{15}H_{10}O_5$ | −7.8 | |
| Coriandrin | Coriander (*Coriandrum sativum*) | $C_{13}H_{10}O_4$ | −6.4 | |
| Curcumin | Turmeric (*Curcuma longa*) | $C_{21}H_{20}O_6$ | −7.0 | |

| 1 | 2 | 3 | 4 | 5 |
|---|---|---|---|---|
| Glycyrrhizin | Licorice (*Glycyrrhiza glabra*) | $C_{42}H_{62}O_{16}$ | −7.3 |  |
| Quercitin | Onion (*Allium cepa*), Buck-wheat (*Fagopyrum esculentum*), Green tea (*Camellia sinensis*). | $C_{15}H_{10}O_7$ | −7.3 |  |
| Remdesivir | Antiviral drug | $C_{27}H_{35}N_6O_8P$ | −8.32 |  |
| Saquinavir | Anti-HIV drug | $C_{38}H_{50}N_6O_5$ | −9.2 |  |

Most of the selected bioactive products have anti-malarial, anti-viral and other similar activities [29]. The binding affinities of selected natural products range between −6.4 Kcal/mol (Binding affinity of Coriandrin) and −8.79 Kcal/mol (Binding affinity of Aloesin), as shown in Figure 2 [6, 35].

Coriandrin is categorized as essential oil derived from *Coriandrum sativum*. It is found in seed, stem, and leaf of *Coriandrum sativum* [36]. Coriandrin [$C_{13}H_{10}O_4$] possesses many therapeutic activities such as antiviral, antifungal, antioxidant, anthelmintic as well as anxiolytic [37].

The main bioactive constituent Aloesin ($C_{19}H_{22}O_9$) is derived from fresh leaves of aloe (*Aloe Ferox, Aloe barbadensis*) and also has antioxidant, antibacterial, anti-inflammatory, and immunomodulatory effects [35]. Glycyrrhizin, as well as licorice, is found in *Glycyrrhiza glabra*, which is a potential immunomodulator and has other therapeutic effects such as hepato-protective, neuroprotective, anti-inflammatory, antineoplastic activities; it shows binding affinity of −7.3 Kcal/mol with COVID-19 protease [38, 39]. A steroidal bioactive constituent of Ashwagandha Withaferin A ($C_{28}H_{38}O_6$) has antiviral and antibacterial activities and is obtained from *Acnistus arborescens, Withania somnifera, and Withania somnifera Dunal* and shows −8.05 Kcal/mol binding affinity with COVID-19 protease [40]. Curcumin is a primary bioactive compound found in turmeric which consists of curcuminoids as secondary metabolites which are extracted from dried rhizomes of *Curcuma longa* from *the Zingiberacea*e family. Curcumin ($C_{21}H_{20}O_6$) exhibits known anti-inflammatory, antimicrobial and antioxidant properties has −7.0 Kcal/mol binding affinity with protease [41].

Nimbin is a triterpenoid compound extracted from neem (*Azadirachta indica)* and it shows the binding affinity of −8.17 Kcal/mol with protease. Nimbin ($C_{30}H_{36}O_9$), which is a bitter compound, shows many biological activities such as potential antibacterial, antiviral, antipyretic, fungicidal, and anti-inflammatory activities [42]. Gingerols are phenolic and the most abundant pungent compounds present in ginger, show −7.95 Kcal/mol binding affinity with COVID-19 proteases. Gingerol is the main bioactive compound found in

Ginger (*Zingiber officinale)*, which belongs to the Zingiberaceae family. Gingerol ($C_{17}H_{26}O_4$) has powerful antioxidant and anti-inflammatory effects [41].
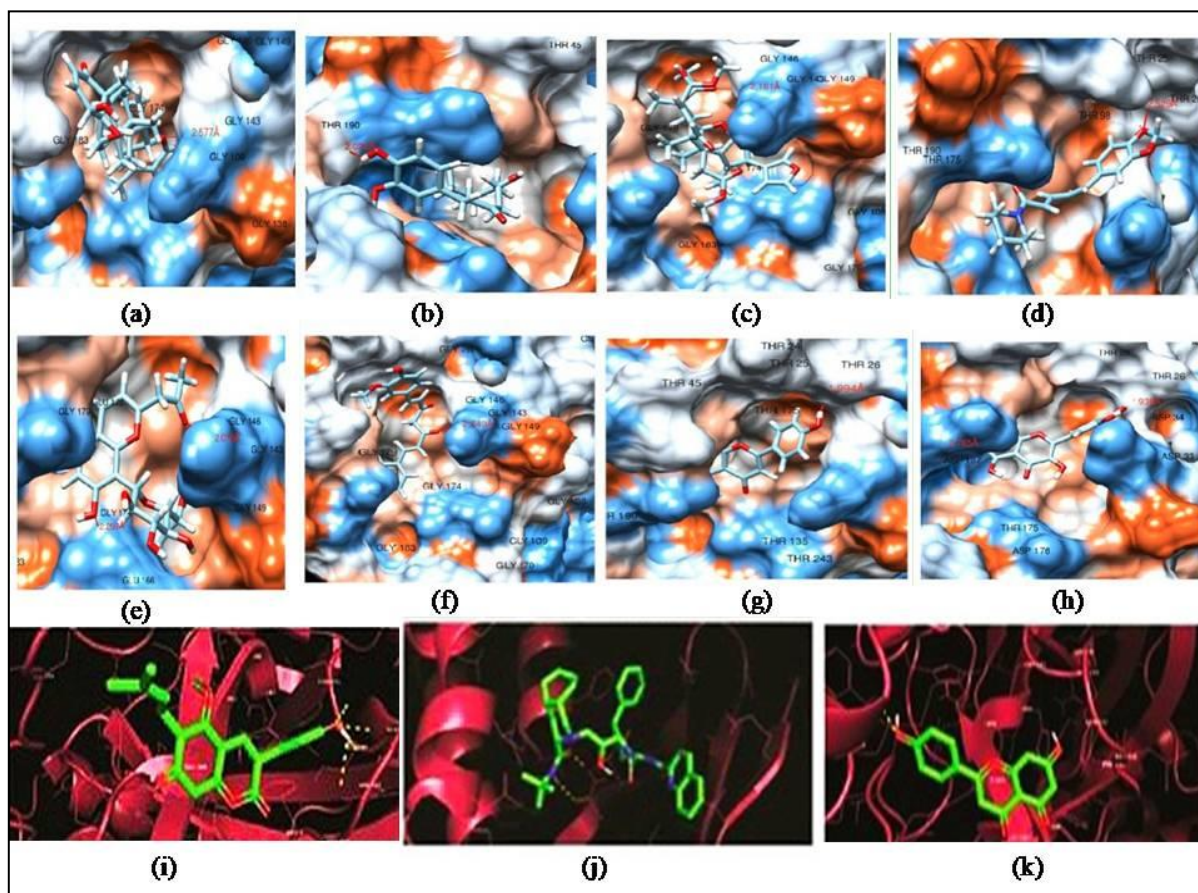


Figure 2. 3D visualization of docking analysis of 6LU7 protease binding with (*a*) Gingerol, (*b*) Nimbin, (*c*) Piperine, (*d*) Aloesin, (*e*) Withaferin, (*f*) Apigenin, (*g*) Curcumin, (*h*) Quercitin, (*i*) Coriandrin, (*j*) Glycyrrhizin, (*k*) Saquinavir

Apigenin is a flavonoid found in many plants Apple (*Malus Domestica*), Thyme (*Thymus vulgaris*), Chamomile (*Matricaria chamomilla*), Red pepper (*Capsicum annuum*), Garlic (*Allium sativum var. sativum*), etc [41]. It is a flavones class compound with a wide range of activities such as antiviral, antibacterial, antioxidant, and strong anti-inflammatory activities. Apigenin ($C_{15}H_{10}O_5$) shows –7.8 Kcal/mol binding affinity. Piperin is a pungent component found in black pepper and belongs to the vanilloid family of compounds [43]. Piperin is extracted from dried unripe fruit of black and white pepper (*Piper nigrum, Piper longum, and Piper officinarum*). Piperine ($C_{17}H_{19}NO_3$) has potent antioxidant, anti-inflammatory, and antitumor properties and shows greater (–6.98 Kcal/mol) binding affinity with COVID-19 protease [37], whereas quercitin has –7.3 Kcal/mol binding affinity with protease. Quercetin ($C_{15}H_{10}O_7$) is a flavonoid compound mainly found in onions, cherries, grapes, citrus fruits, which is obtained from various sources such as onion (*Allium cepa*), green tea (*Camellia sinensis*), apple (*Malus Domestica*), buckwheat (*Fagopyrum esculentum*) and possess antioxidant, antiviral, anticancer, cardiovascular, hepatoprotective and anti-inflammatory activities [41, 44].

Remdesivir is a known antiviral drug whereas saquinavir is an anti-HIV drug; both are subjected for analysis of binding affinity with COVID-19 protease by using a molecular docking approach. This study shows that Remdesivir ($C_{27}H_{35}N_6O_8P$) has –8.32 Kcal/mol and Saquinavir ($C_{38}H_{50}N_6O_5$) has –9.2 Kcal/mol binding affinity [45]. In summary, it shows that some of the selected natural products exhibit greater binding affinity with COVID-19 protease compared to known antiviral drugs, remdesivir and saquinavir [45, 46]. In this study we have conducted molecular docking studies used to identify the potential of herbal products which are isolated from plants. Substances taken for the study show inhibitory action of COVID-19 main protease [27]. We have studied 10 herbal drugs and their comparison with two reported antiviral drugs. Molecular docking analysis of these products helps to identify their binding potency with COVID-19 protease 6LU7 and their inhibition extent [6]. These docking studies show that some of the selected natural products show powerful inhibition

based on their binding affinities. Aloe vera shows a greater binding affinity among all selected herbal drugs. Also, other natural products such as glycyrrhizin, curcumin, coriandrin, and apigenin show potential inhibition of COVID-19 protease [47]. The plot of Binding affinity in comparison with natural compounds is shown in Figure 3.
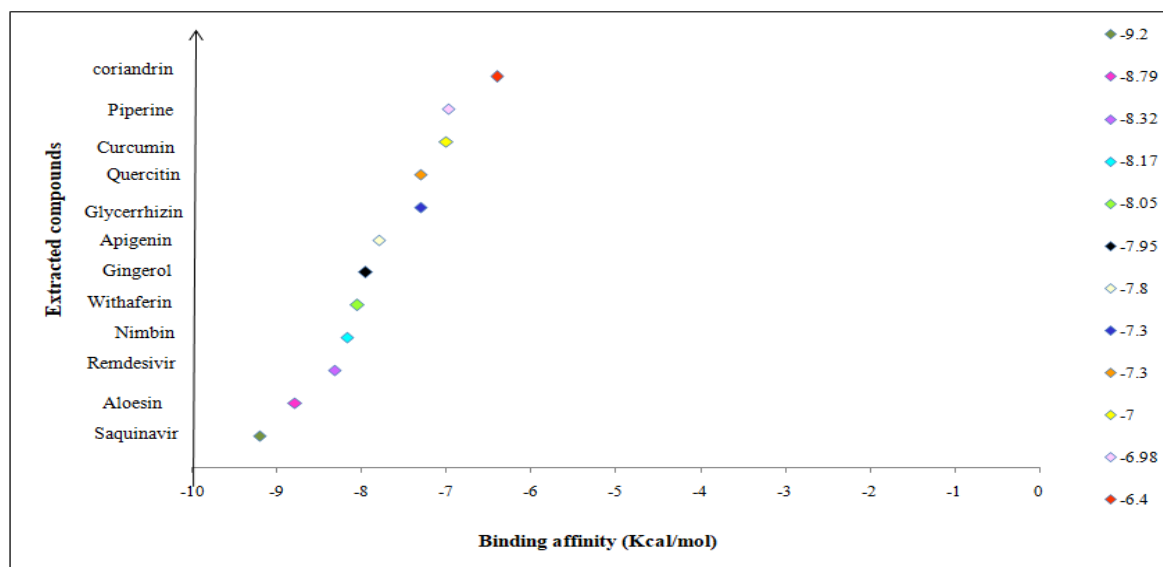


Figure 3. A plot of binding affinity extracted bioactive compounds from Indian herbal plants and a few drugs for comparison of inhibition potential against COVID-19 protease

### Conclusions

All of these natural bioactive compounds are biologically safe and have a high binding potential. Saquinavir is already reported as an anti-HIV drug for inhibition of replication of SARS-Cov-2 protease, also Remdesivir is known for inhibition of replication of protease but it has reported hepatotoxicity in some patients. Docking studies show that some of the selected natural extracts show greater COVID-19 protease inhibition potential compared to these known antiviral drugs. Some of the identified natural products show promising results in these studies and may require additional investigation. Because they are safer than synthetic drugs, these natural medicines can be used as important alternatives to synthetic treatments in the prevention of COVID-19 infection. These findings could become a significant starting point for drug development and provide great promise to develop potent therapeutics against COVID-19 infection.

### References

1   Adem, S., Eyupoglu, V., Sarfraz, I., Rasul, A., & Ali, M. (2020). Identification of Potent COVID-19 Main Protease (Mpro) Inhibitors from Natural Polyphenols: An in Silico Strategy Unveils a Hope against CORONA. *Preprints*. https://doi.org/10.20944/pre-prints202003.0333.v1

2   Narkhede, R.R., Pise, A.V., & Cheke, R.S. et al. (2020) Recognition of Natural Products as Potential Inhibitors of COVID-19 Main Protease (Mpro): In-Silico Evidences. *Nat. Prod. Bioprospect.,* 10, 297–306. https://doi.org/10.1007/s13659-020-00253-1

3   Rodríguez-Morales, A.J., MacGregor, K., Kanagarajah, S., Patel, D., & Schlagenhauf, P. (2020) Going global — Travel and the 2019 novel coronavirus. *Travel Med Infect. Dis*., 33, 101578. https://dx.doi.org/10.1016 %2Fj.tmaid.2020.101578

4   Medicinal plants and primary health care: part 2. (1991) Essent Drugs Monit, WHO (11):15–17.

5   Gideon A. Gyebi, Olalekan B. Ogunro, Adegbenro P. Adegunloye, Oludare M. Ogunyemi & Saheed O. Afolabi (2021). Potential inhibitors of coronavirus 3-chymotrypsin-like protease (3CL^pro): an *in silico* screening of alkaloids and terpenoids from African medicinal plants, *Journal of Biomolecular Structure and Dynamics*, 39:9, 3396–3408. https://doi.org/10.1080/07391102.2020.1764868

6   Sampangi-Ramaiah, M.H., Vishwakarma, R., & Shaanker, R.U. (2020) Molecular docking analysis of selected natural products from plants for inhibition of SARS-CoV-2 main protease. *Current Science*.; 118(7):1087-92.

7   Alejandra Hernández-Santoyo AYT-B, Altuzar V, Vivanco-Cid H, & Mendoza-Barrera C. (2013). Protein-protein and protein-ligand docking, protein engineering. In: Ogawa T, editor. *Technology and Application. IntechOpen*.

8   Ferreira, L.G., Dos Santos, R.N., Oliva, G., & Andricopulo, A.D. (2015). Molecular Docking and Structure-Based Drug Design Strategies. *Molecules, 20*, 13384–13421. https://doi.org/10.3390/molecules200713384

9  DesJarlais, R.L., Sheridan, R.P., Seibel, G.L., Dixon, J.S., Kuntz, I.D., & Venkataraghavan R. (1988). Using shape complementarity as an initial screen in designing ligands for a receptor binding site of known three-dimensional structure. *J. Med. Chem., 31,* 722–729. https://pubs.acs.org/doi/pdf/10.1021/jm00399a006

10  Kitchen, D.B., Decornez, H., Furr, J.R., & Bajorath, J. (2004). Docking and scoring in virtual screening for drug discovery: methods and applications. *Nature reviews Drug discovery, 3(11)*, 93549. https://doi.org/10.1038/nrd1549

11  Lavecchia A, & Di Giovanni C. (2013). Virtual screening strategies in drug discovery: A critical review. *Current Medicinal Chemistry, 20(23)*, 2839–2860.

12  Levinthal, C., Wodak, S.J., Kahn, P., & Dadivanian, A.K. (1975). Hemoglobin interaction in sickle cell fibers. I: Theoretical approaches to the molecular contacts. *Proceedings of the National Academy of Sciences of the United States of America, 72(4)*, 1330–1334 https://doi.org/10.1073/pnas.72.4.1330

13  Menchaca TM, Juárez-Portilla C, & Zepeda RC. (2020). Past, Present, and Future of Molecular Docking. *InDrug Discovery and Development-New Advances, IntechOpen.*

14  Dominguez, C., Boelens, R., & Bonvin, A.M. (2003). HADDOCK: A proteinprotein docking approach based on biochemical or biophysical information. *Journal of the American Chemical Society, 125(7)*, 1731–1737. https://doi.org/10.1021/ja026939x

15  Bohm, H.J. (1992). The computer program LUDI: A new method for the de novo design of enzyme inhibitors. *Journal of Computer-Aided Molecular Design, 6(1)*, 61–78. https://doi.org/10.1007/BF00124387

16  Kramer, B., Rarey, M., & Lengauer, T. (1999). Evaluation of the FLEXX incremental construction algorithm for protein–ligand docking. *Proteins: Structure, function. Bioinformatics, 37(2)*, 228-241. https://doi.org/10.1002/(SICI)10970134(19991101)

17  Welch, W., Ruppert, J., & Jain, A.N. (1996). Hammerhead: Fast, fully automated docking of flexible ligands to protein binding sites. *Chemistry & Biology, 3(6)*, 449–462.

18  Spitzer, R., & Jain, A.N. (2012). Surflexdock: Docking benchmarks and real-world application. *Journal of Computer-Aided Molecular Design, 26(6)*, 687–699. https://doi.org/10.1007/s10822-011-9533-y

19  Morris, G.M., Huey, R., Lindstrom, W., Sanner, M.F., Belew, R.K., & Goodsell, D.S., et al. (2009). AutoDock4 and AutoDockTools4: Automated docking with selective receptor flexibility. *Journal of Computational Chemistry, 30(16)*, 2785–2791. https://doi.org/10.1002/jcc.21256

20  Taylor, J.S., & Burnett, R.M. (2000). DARWIN: A program for docking flexible molecules. *Proteins, 41(2)*, 173–191. https://doi.org/10.1002/1097-0134(20001101

21  Liu, M., & Wang, S. (1999). MCDOCK: A Monte Carlo simulation approach to the molecular docking problem. *Journal of Computer-Aided Molecular Design, 13(5)*, 435–451. https://doi.org/10.1023/A:1008005918983

22  Jones, G., Willett, P., Glen, R.C., Leach, A.R., & Taylor, R. (1997). Development and validation of a genetic algorithm for flexible docking. *Journal of Molecular Biology,* 267(3), 727–748. https://doi.org/10.1006/jmbi.1996.0897

23  Oshiro, C.M., Kuntz, I.D., & Dixon, J.S. (1995). Flexible ligand docking using a genetic algorithm. *Journal of Computer-Aided Molecular Design, 9(2),* 113–130. https://doi.org/10.1007/BF00124402

24  Salomon-Ferrer, R., Case, D.A., Walker, R.C. (2013). An overview of the Amber biomolecular simulation package. *Wiley Interdisciplinary Reviews: Computational Molecular Science, 3(2)*, 198–210. https://doi.org/10.1002/wcms.1121

25  Liu, X., Zhang, B., Jin, Z., Yang, H. & Rao, Z. (2020). The crystal structure of 2019-NCoV main protease in complex with an inhibitor N3. *RCSB Protein Data Bank.*

26  Grosdidier, A., Zoete V., & Michielin, O. (2011). Fast docking using the CHARMM force field with EADock DSS. *Journal of computational chemistry, 30, 32(10)*, 2149–2159. https://doi.org/10.1002/jcc.21797

27  Tian, W., Chen, C., Lei, X., Zhao, J., & Liang, J. (2018). CASTp 3.0: computed atlas of surface topography of proteins. *Nucleic acids research, 46(W1),* W363–367.

28  Srivastava, A.K., Kumar, A., & Misra, N. (2020). On the Inhibition of COVID-19 Protease by Indian Herbal Plants: An In Silico Investigation. *arXiv preprint arXiv*: 2004.03411.

29  Lengauer, T., & Rarey, M. (1996). Methods for predicting molecular complexes involving proteins. *Curr. Opin. Struct. Biol., 5*, 402-6. https://doi.org/10.1002/0471721204

30  Grosdidier, A., Zoete, V., & Michielin, O. (2011). SwissDock, a protein-small molecule docking web service based on EADock DSS. *Nucleic acids research, 39(suppl_2),* W270-277. https://doi.org/10.1093/nar/gkr366

31  Morris, G.M., Goodsell, D.S., Huey, R., & Olson, A.J. (1996). Distributed automated docking of flexible ligands to proteins: parallel applications of AutoDock 2.4. *Journal of computer-aided molecular design, 10(4)*, 293–304. https://doi.org/10.1007/BF00124499

32  Trott, O., & Olson, A.J. (2010). AutoDock Vina: improving the speed and accuracy of docking with a new scoring function, efficient optimization, and multithreading. *Journal of computational chemistry, 31(2)*, 455-61. https://doi.org/10.1002/jcc.21334

33  DeLano, W.L. (2002) Pymol: An open-source molecular graphics tool. CCP4 *Newsletter on protein crystallography, 40(1)*, 82–92.

34  Sampangi-Ramaiah, M.H., Vishwakarma, R., & Shaanker, R.U. (2020). Molecular docking analysis of selected natural products from plants for inhibition of SARS-CoV-2 main protease. *Current Science, 118(7),* 1087–1092.

35  Ceska, O., Chaudhary, S.K., Warrington, P., Ashwood-Smith, M.J., Bushnell, G.W. & Poultont, G.A. (1988) Coriandrin, a novel highly photoactive compound isolated from Coriandrum sativum. *Phytochemistry, 27*, 2083–2087. https://doi.org/10.1016/0031-9422(88)80101-8

36  Gonzalez-Paz, L.A., Lossada, C.A., & Moncayo, L.S. et al. (2020). Theoretical Molecular Docking Study of the Structural Disruption of the Viral 3CL-Protease of COVID19 Induced by Binding of Capsaicin, Piperine and Curcumin Part 1: A Comparative Study with Chloroquine and Hydrochloroquine Two Antimalaric Drugs, 06 April, PREPRINT (Version 1) available at *Research Square* https://doi.org/10.21203/rs.3.rs-21206/v1

37  Zhang, Q., & Ye, M. (2009) Chemical analysis of the Chinese herbal medicine Gan-Cao (licorice). *Journal of Chromatography A, 1216(11),* 1954–1969. https://doi.org/10.1016/j.chroma.2008.07.072

38  Qiao, X., Song, W, Ji.S., Wang, Q., Guo, D.A., & Ye, M. (2015) Separation and characterization of phenolic compounds and triterpenoid saponins in licorice (*Glycyrrhiza uralensis*) using mobile phase-dependent reversed-phase× reversed-phase comprehensive two-dimensional liquid chromatography coupled with mass spectrometry. *Journal of Chromatography A, 1402,* 36–45. https://doi.org/10.1016/j.chroma.2015.05.006

39  Tripathi, M.K., Singh, P., Sharma, S., Singh, T.P., Ethayathulla, A.S., & Kaur, P. (2020). Identification of bioactive molecule from Withania somnifera (Ashwagandha) as SARS-CoV-2 main protease inhibitor. Jou*rnal of Biomolecular Structure and Dynamics,* 1–4. https://doi.org/10.1080/07391102.2020.1790425

40  Khaerunnisa, S., Kurniawan, H., Awaluddin, R., Suhartati, S. & Soetjipto, S. (2020). Potential inhibitor of COVID-19 main protease (Mpro) from several medicinal plant compounds by molecular docking study. *Preprints 2020*, 2020030226. https://doi.org/10.20944/preprints202003.0226.v1

41  Kumar A.HS. (2020). Molecular Docking of Natural Compounds from tulsi (Ocimum sanctum) and neem (Azadirachta indica) against SARS-CoV-2 Protein Targets. *BEMS Reports, 6(1),* 11–13. https://doi.org/10.5530/bems.6.1.4

42  Choudhary, P., Chakdar, H., Singh, D., Selvaraj, C., Singh, S.K., Kumar, S., & Saxena, A.K. (2020). Computational studies reveal piperine, the predominant oleoresin of black pepper (Piper nigrum) as a potential inhibitor of SARS-CoV-2 (COVID-19). *Current Science* (00113891);119(8). https://doi.org/10.18520/cs/v119/i8/1333-1342

43  Derosa, G., Maffioli, P., D'Angelo, A., & Di Pierro, F. (2020). A role for quercetin in coronavirus disease 2019 (COVID-19). *Phytotherapy Research.* https://doi.org/10.1002/ptr.6887

44  Elfiky, A.A. (2020). Ribavirin, Remdesivir, Sofosbuvir, Galidesivir, and Tenofovir against SARS-CoV-2 RNA dependent RNA polymerase (RdRp): A molecular docking study. *Life sciences;* 117592. https://doi.org/10.1016/j.lfs.2020.117592

45  Keretsu, S., Bhujbal, S.P., & Cho, S.J. (2020) Rational approach toward COVID-19 main protease inhibitors via molecular docking, molecular dynamics simulation and free energy calculation. *Scientific reports, 10(1),* 1–4. https://doi.org/10.1038/s41598-020-74468-0

46  Mpiana, P.T., Tshibangu, D.S., Kilembe, J.T., Gbolo, B.Z., Mwanangombo, D.T., Inkoto, C.L., Lengbiye, E.M., Mbadiko, C.M., Matondo, A., Bongo, G.N., & Tshilanda, D.D. (2020). Identification of potential inhibitors of SARS-CoV-2 main protease from Aloe vera compounds: a molecular docking study. *Chemical Physics Letters,* 754, 137751. https://doi.org/10.1016/j.cplett.2020.137751

47  Joshi, T., Joshi, T., Sharma, P., Mathpal, S., Pundir, H., Bhatt, V., & Chandra, S. (2020). In silico screening of natural compounds against COVID-19 by targeting Mpro and ACE2 using molecular docking. *Eur Rev Med Pharmacol Sci., 24(8),* 4529–4536.

48  Amin, S.A., Ghosh, K., Gayen, S., & Jha, T. (2020) Chemical-informatics approach to COVID-19 drug discovery: Monte Carlo based QSAR, virtual screening and molecular docking study of some in-house molecules as papain-like protease (PLpro) inhibitors. *Journal of Biomolecular Structure and Dynamics,* 1-0. https://doi.org/10.1080/07391102.2020.1780946

49  Mohammadi, N., & Shaghaghi, N. (2020). Inhibitory effect of eight Secondary Metabolites from conventional Medicinal Plants on COVID_19 Virus Protease by Molecular Docking Analysis. Preprint; 11987475: v1. https://doi. org/10.26434/chemrxiv

50  Alrasheid, A.A., Babiker, M.Y., & Awad, T.A. (2021). Evaluation of certain medicinal plants compounds as new potential inhibitors of novel corona virus (COVID-19) using molecular docking analysis. *In Silico Pharmacology, 9(1)*, 1–7. https://doi.org/10.1007/s40203-020-00073-8

51  Rameshkumar, M.R., Indu, P., Arunagirinathan, N., Venkatadri, B., El-Serehy, H.A, & Ahmad, A. (2021). Computational selection of flavonoid compounds as inhibitors against SARS-CoV-2 main protease, RNA-dependent RNA polymerase and spike proteins: A molecular docking study. *Saudi journal of biological sciences, 28(1),* 448–458, https://doi.org/10.1016/j.sjbs.2020.10.028

52  Llanes, A., Cruz, H., Nguyen, V.D., Larionov, O.V, & Fernández, P.L. (2021) A Computational Approach to Explore the Interaction of Semisynthetic Nitrogenous Heterocyclic Compounds with the SARS-CoV-2 Main Protease. *Biomolecules, 11(1)*, 18. https://doi.org/10.3390/biom11010018

53  Bharadwaj, S., Dubey, A., Yadava, U., Mishra, S.K., Kang, S.G., & Dwivedi, V.D. (2021). Exploration of natural compounds with anti-SARS-CoV-2 activity via inhibition of SARS-CoV-2 Mpro. *Briefings in Bioinformatics. J.* https://doi.org/10.1093/bib/bbaa382).

54  Su JT, Li XL, Huang YG, Lin HW, Luo H, & Luo LX. (2021). Network analysis and molecular docking of the mechanism of Shengmai decoction in treating patients with severe novel coronavirus pneumonia. *Tradit. Med. Res.*, *6(4)*, 33. https://doi.org/10.12032/TMR20201117207

55  Badavath, V.N., Kumar, A., Samanta, P.K., Maji, S., Das, A., Blum, G., Jha, A., & Sen, A. (2020) Determination of potential inhibitors based on isatin derivatives against SARS-CoV-2 main protease (mpro): a molecular docking, molecular dynamics and structure-activity relationship studies. *Journal of Biomolecular Structure and Dynamics,* 1–9, https://doi.org/10.1080/07391102.2020.1845800

56  Shah, A., Patel, V., & Parmar, B. (2020) Discovery of Some Antiviral Natural products to fight against Novel Corona Virus (SARS-CoV-2) using Insilico approach. *Combinatorial Chemistry & High Throughput Screening.* https://doi.org/10.2174/1386207323666200902135928

57  Yuan, S.I., Jiu, W.A., Liang, Z.H., Xue-wen, L.I., & Ying, L.I. (2020) Molecular docking prediction of three active components of Paris polyphylla against SARS-CoV-2. *Natural product research and development,* 32(7), 1. https://doi.org/10.16333/j.1001-6880.2020.7.002

С.С. Бхуджбал, М. Кале, Б. Чавале

## Молекулалық қондыру әдістерімен COVID-19 негізгі протеиназасының өсімдіктік ингибиторларын анықтау

Кейінгі айларда COVID-19 жағдайлары тез артып, қауіпті бола бастауда. Нәтижесінде бірнеше медициналық және ғылыми ұйымдар COVID-19 індетінің тиімді емін табуға тырысуда. Соңғы зерттеулерге сәйкес, көптеген табиғи өнімдердің COVID-19-ға қарсы белсенділігі жоғары. Мақаланың негізгі мақсаты — вирусқақарсы қасиеттері бар, табиғи түрде кездесетін биоактивті қосылыстарды анықтау. Луи және басқалар өз зерттеулерінде SARS-Cov-2 протеазасының негізгі емдік препаратқа нысана ретінде белгілі кристалды құрылымда болатынын хабарлады. Вирустық ақуыздардың репликациясын тоқтату үшін SARS-Cov-2 негізгі протеазасын тежеу маңызды. Бұл зерттеуде табиғи қосылыстар SARS-Cov-2 бөгейтін ықтимал биоактивті қосылыстарды зерттеу үшін молекулалық модельдеу әдістерінің көмегімен сыналды. Осы зерттеулердің нәтижесінде көптеген табиғи қосылыстардың вирустық ақуыздармен әрекеттесу және COVID-19 (Mpro) негізгі протеазасына қарсы ингибиторлық белсенділігі бар екендігі анықталды. Табиғи қосылыстар саквинавир мен ремдесивир сияқты белгілі вирусқақарсы препараттармен салыстырылды. Бұл потенциалды індетпен күресу үшін COVID-19-ға қарсы табиғи емдік агенттерге айналдырмас бұрын қосымша зерттеулер қажет екенін атап өтті.

*Кілт сөздер:* табиғи қосылыстар, SARS-Cov-2, тиімділігі, дәрілік нысана, молекулалық модельдеу, вирустық ақуыздар, Mpro, байланыстырушы аффинирлік.

С.С. Бхуджбал, М. Кале, Б. Чавале

## Идентификация растительных ингибиторов основной протеиназы COVID-19 методами молекулярного докинга

В последние месяцы количество случаев заражения COVID-19 быстро увеличивается и становится опасным. Как следствие, несколько медицинских и исследовательских организаций пытаются найти эффективное лекарство от вспышки COVID-19. Согласно недавним исследованиям, многие натуральные продукты обладают мощной активностью против COVID-19. Основная цель этой статьи — установить природные биологически активные соединения с подходящими противовирусными свойствами. Lui с соавторами сообщили в своем исследовании, что основная протеаза SARS-Cov-2 присутствует в кристаллической структуре, известной как мишень для нового терапевтического препарата. Важно ингибировать основную протеазу SARS-Cov-2, чтобы остановить репликацию вирусных белков. В этом исследовании природные соединения были проверены с использованием методов молекулярного моделирования для изучения возможных биоактивных соединений, которые блокируют SARS-Cov-2. В результате этих исследований было обнаружено, что многие природные соединения обладают способностью взаимодействовать с вирусными белками и проявляют ингибирующую активность в отношении основной протеазы COVID-19 (Mpro). Кроме того, эти природные соединения сравнивали с известными противовирусными препаратами, такими как Саквинавир и Ремдесивир. Отмечено, что необходимы дополнительные исследования, прежде чем эти потенциальные зацепки можно будет превратить в естественные терапевтические агенты против COVID-19 для борьбы с эпидемией.

*Ключевые слова*: природные соединения, SARS-Cov-2, эффективность, лекарственная мишень, молекулярное моделирование, вирусные белки, Mpro, аффинность связывания.

Information about authors:

**Santosh S. Bhujbal** (corresponding author) — Head of Department, Department of Pharmacognosy, Dr. D.Y. Patil Institute of Pharmaceutical Sciences and Research, Pimpri, Pune — 411018, Maharashtra, India; e-mail: santosh.bhujbal@dypvp.edu.in; https://orcid.org/0000-0002-2801-5955;

**Mayuri Kale** — 2nd year M Pharm student, Department of Pharmaceutical Quality Assurance, Dr. D.Y. Patil Institute of Pharmaceutical Sciences and Research, Pimpri, Pune — 411018, Maharashtra, India; e-mail: mayuri27kale@gmail.com; https://orcid.org/0000-0003-1051-6222;

**Bhushankumar Chawale** — 2nd year M Pharm student, Department of Pharmaceutical Quality Assurance, Dr. D.Y. Patil Institute of Pharmaceutical Sciences and Research, Pimpri, Pune — 411018, Maharashtra, India; e-mail: bhushankumarchawale@gmail.com; https://orcid.org/0000-0002-7309-9588

# M.Zh. Burkeyev[1], U.B. Tuleuov[1*], A.N. Bolatbay[1], D. Khavlichek[2], S.Zh. Davrenbekov[1], Ye.M. Tazhbayev[1], E.Zh. Zhakupbekova[1]

*[1]Karagandy University of the name of academician E.A. Buketov, Kazakhstan*
*[2]Charles University, Prague, Czech Republic*
*(\*Corresponding author`s e-mail: bekalols1@gmail.com)*

# Investigation of the destruction of copolymers of poly(ethylene glycol)fumarate with methacrylic acid using differential equations

In the article the thermal characteristics of a copolymer of poly(ethylene glycol)fumarate with methacrylic acid were studied in a dynamic mode in a nitrogen atmosphere for the first time. A kinetic analysis of the thermal destruction process was carried out using three different data processing methods (Freeman-Carroll, Sharp-Wentworth, Achar). Thermodynamic characteristics were also calculated, namely the change in the Gibbs energy ($\Delta G$), enthalpy ($\Delta H$) and entropy of activation ($\Delta S$). The curves of thermogravimetric and differential thermogravimetric analysis of the copolymer were studied in a nitrogen atmosphere at a heating rate of 10 °C/min. The main stage of the copolymer decomposition was found to occur in a narrow temperature range, which is confirmed by a peak in the differential curve. Changes in the reaction rate of the copolymer were shown due to the decrease in the sample mass. It was shown that the results of kinetic analysis depend on the molecular structure of the compounds under study. The activation energies found by the Freeman-Carroll method have lower values, while the Achar and Sharp-Wentworth methods give the same results.

*Keywords:* dynamic thermogravimetry, thermal destruction, copolymer of poly(ethylene glycol)fumarate with methacrylic acid, activation energy.

## *Introduction*

Currently the use of unsaturated polyester resins in industrial countries is promising and profitable, which in turn is due to the relative simplicity of the technology for their production and the low level of financial, material, energy, and labor costs. The presence of unsaturated double bonds in the molecule of unsaturated polyesters allows them to be used as a matrix for obtaining spatially crosslinked copolymers, the formation mechanism of which has been described in many works [1]. This is associated with the necessary stability of weak polyesters to hostile spheres, excellent energy and machine features [2].

Unsaturated polyesters are called hetero- or carbon-chain thermosetting oligomers and polymers containing ester groups and multiple carbon-carbon bonds [3–4]. They are usually obtained from acids and alcohols (or their derivatives) by field condensation or copolymerization of alkylene α-oxides with dicarboxylic acid anhydrides, and at least one reagent must be unsaturated.

Unsaturated polyester resins have a set of useful properties, in particular, they have a lower viscosity, and, they are easier to cure with vinyl monomers in comparison with epoxy resins, which indicates their greater reactivity [5]. The increase in the production of unsaturated polyesters required intensive research into the features of their synthesis, the possibility of copolymerization with other monomers and oligomers, the study of the structure and properties of the obtained copolymers, the search for the most effective methods of their processing and rational areas of application in a weatherometer and a fedeometer. After that, it was found that replacing styrene partially or completely with methyl acrylate improves the color stability of the material and the durability of the first layer to erosion and retains the shine.

Previously, the authors of [6, 7] synthesized polyester resins copolymers, which were used as moisture sorbents and metal-polymer complexes. The acquired knowledge indicates the interdependence of the degradation process on the components' ratio in the copolymer as well as the influence of the environment during the thermal analysis process. It was shown that the results of kinetic analysis depend on the molecular structure of the compounds under study [8].

In this work we investigated the thermal destruction of copolymers of poly(ethylene glycol)fumarate with methacrylic acid in a nitrogen atmosphere.

*Experimental part*

Poly(ethylene glycol)fumarate was obtained [9] by the polycondensation reaction of maleic anhydride and propylene glycol according to a standard procedure. The progress of the reaction was monitored by determining the acid number.

Copolymers of poly(ethylene glycol)fumarate (p-EGF) with methacrylic acid (MAA) were obtained [9] by copolymerization in a dioxane solution at a monomer mixture.

The study of the thermal properties of the p-EGF:MAA copolymer was carried out on a device for synchronous thermal analysis Labsys Evolution TG-DTA/DSC from Setaram in a dynamic mode in the temperature range of 30–700 °C when heated in an $Al_2O_3$ crucible at a rate of 10 °C/min in an inert nitrogen medium with a flow rate of 30 ml / min. The instrument for thermogravimetric studies and heat flux were calibrated using $CaCO_3$ and in standards, respectively. The experimental data was processed using Microsoft Excel and Processing programs.

A kinetic analysis was carried out in order to determine the kinetic parameters of the decomposition of poly(ethylene glycol)fumarate with methacrylic acid.

*Freeman and Carroll method* [10]. The order of the reaction $n$ and the activation energy of the reaction $E$ are calculated by the equation:

$$\frac{\left(\frac{E}{R}\right)\Delta\left(\frac{1}{T}\right)}{\Delta\log Wr} = -n + \frac{\Delta\log\left(\frac{dw}{dt}\right)}{\Delta\log Wr}, \tag{1}$$

where $w_r = w_c - w$, $w_c$ is the maximum weight loss; $w$ is the total weight loss by time $t$.

*Sharp and Wentworth method* [11].

$$\frac{\Delta\log\left(\frac{dc}{dt}\right)}{1-c} = \log\frac{A}{\beta} - \frac{E}{RT}, \tag{2}$$

where $c$ is the mass fraction of the sample that reacted during the time $t$; $\beta$ is a heating rate.

*Achar method* [12].

$$\log\left[\frac{1}{f(\alpha)}\frac{d\alpha}{dt}\right] = \log\frac{A}{\beta} + \frac{E}{RT}, \tag{3}$$

where $\alpha$ is the mass fraction of the sample that reacted during time $t$ and $\beta$ is a heating rate.

When linearizing the data the calculated points for all samples are placed on straight lines constructed using the least squares method, for which the slope corresponds to $-\frac{E}{R}$, the cut-off section on the ordinate corresponds to the effective order of the reaction.

*Thermodynamic characteristics change in Gibbs energy ($\Delta G$) and activation entropy ($\Delta S$).*

$$\Delta H = E - RT, \tag{4}$$

$$\Delta G = E - RT_{max}\ln\left(k_B\frac{T_{max}}{hA}\right), \tag{5}$$

$$\Delta S = \frac{\Delta H - \Delta G}{T_{max}}. \tag{6}$$

Here $k_B$ and $h$ are the Boltzmann and Plank's constants, respectively. $T_{max}$ is the temperature, at which the maximum mass loss of the sample occurs.

$$\alpha = \frac{m_i - m_t}{m_i - m_f}, \tag{7}$$

where $m_i$, $m_t$, and $m_f$ are the mass at the beginning, at time t, and at the end of the reaction.

## Results and discussion

One of the most important applied problems in the chemistry of macromolecular compounds is the creation of heat-resistant polymer and composite materials. Therefore, the most important issue is the possibility of determining the activation energy of thermal decomposition, which is used to characterize the mechanisms of thermal destruction and stability of polymers, including using methods of dynamic thermogravimetry. The

main kinetic parameters of the copolymer of poly(ethylene glycol)fumarate with methacrylic acid (p-EGF:MAA) using differential methods (Freeman-Carroll, Sharp-Wentworth, Achar) were determined in the course of the study. Copolymer of poly(ethylene glycol) fumarate with methacrylic acid was heated at 10 °C/min.

The resulting curves of thermogravimetric analysis and decomposition rates are shown in Figure 1.



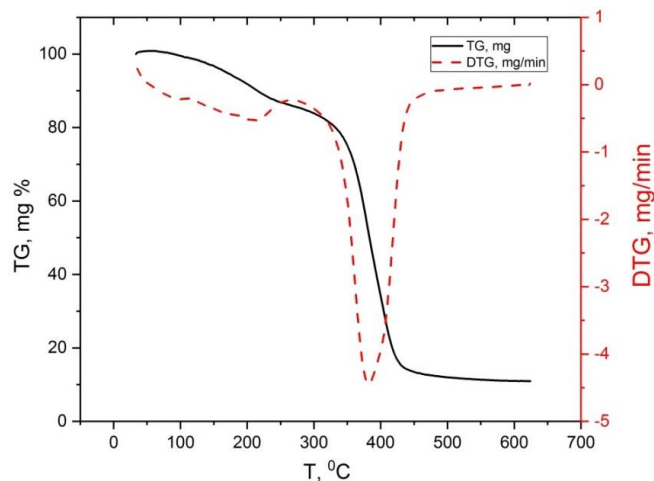Figure 1. Temperature dependences of weight change (TG curve), rate of weight change (DTG) for p-EGF: MAA copolymer at initial ratios $M_1:M_2$, wt% — 6.65:93.35 wt% (under nitrogen atmosphere)
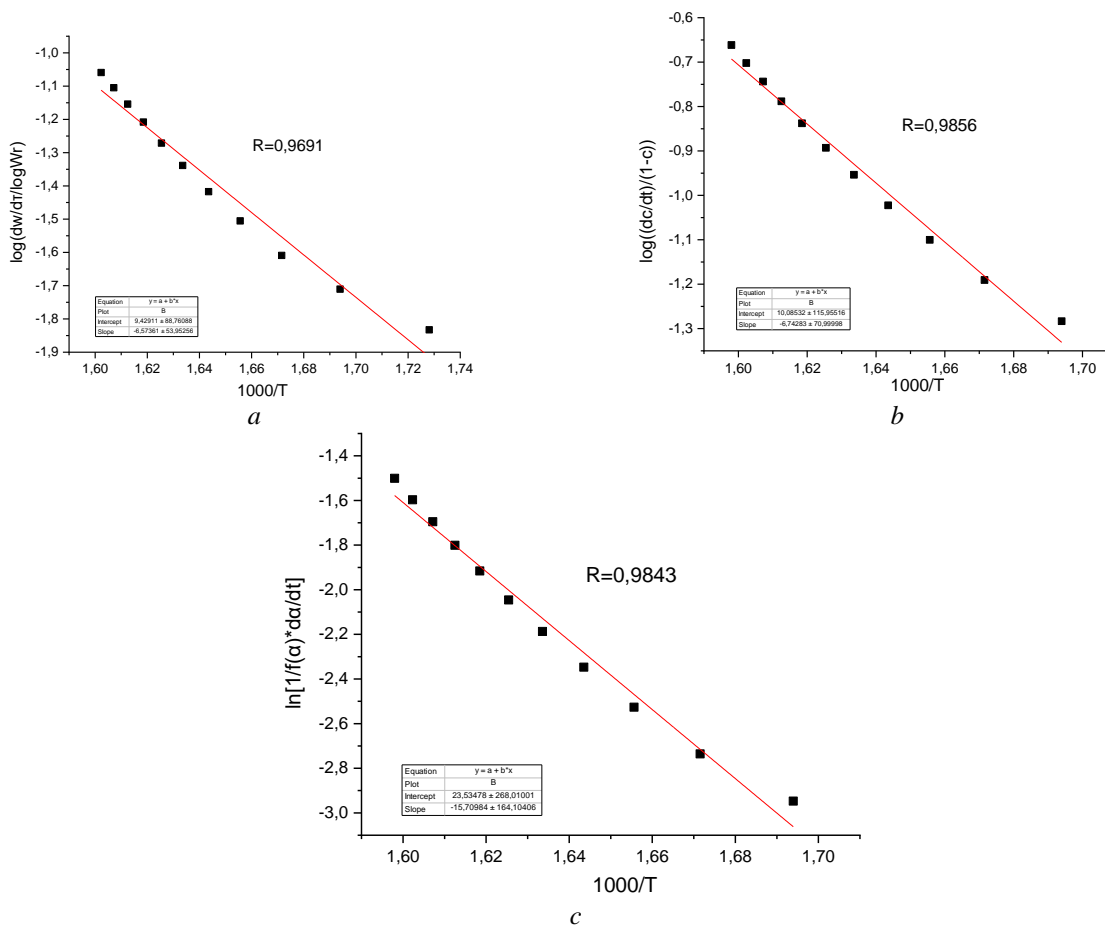


Figure 2. Graphical analysis results determined by the Freeman-Carroll (*a*), Sharp-Wentworth (*b*) and Achar (*c*) methods for the analyzed p-EGF:MAA samples at the M1:M2 ratios, wt.%: 6.65:93.35; with a heating rate of 10 deg/min

In Figure 1 a sample of a copolymer of poly(ethylene glycol) fumarate with methacrylic acid begins to decompose at 200 °C. Then, the beginning of the sample decomposition with the release of volatile substances is observed up to a temperature of about 300 °C. The main stage of the copolymer thermal decomposition occurs from a temperature of ~ 320 °C ~ 430 °C. Then the end of the thermal decomposition process can be observed. In this case, the total weight loss of the sample is ~ 74.42 % of the initial weight. A slight change in the rate of weight loss is observed on the DTG curve in the temperature range of 230–270 °C, followed by a sharp increase with a peak at 375 °C.

Based on the data obtained as a result of thermal analysis of the copolymer, the activation energy values were calculated using the Freeman-Carroll, Sharp-Wentworth and Achar methods. The effective values of the activation energy, preexponents and the order of the destruction reaction were established graphically (Fig. 2).

Comparing the graphs, we can conclude that the points have the greatest scatter for the Freeman-Carroll method (Fig. 2.), which leads to an inaccuracy in the estimation of the activation energy values. The straight line has a slope corresponding to the correlation coefficient $R = 0.9691$, which is slightly less than the values calculated by the Sharp-Wentworth and Achar methods (Fig. 2).

Table 1 shows the results of the activation energies calculated using three different methods.

Table 1

**Kinetic and thermodynamic parameters of the thermal destruction of the p-EGF-MAA copolymer**

| Methods | $E_a$, kJ/mol | $\Delta G$, kJ/mol | $\Delta H$, kJ/mol | $\Delta S$, kJ/mol | $R^2$ | n |
|---|---|---|---|---|---|---|
| Freeman-Carroll | 122.06 | 71.14 | 119.79 | –178.11 | 0.9691 | 0.32 |
| Sharp-Wentworth | 127.28 | 76.36 | 125.01 | –178.10 | 0.9856 | 0.29 |
| Achar | 128.57 | 77.65 | 126.29 | –178.09 | 0.9843 | 0.28 |

As one can see from the table, the data have excellent convergence with an error of less than 5 %. Using the obtained values of the activation energy, we calculated thermodynamic characteristics change in Gibbs energy ($\Delta G$) and activation entropy ($\Delta S$). We can also observe that the parameters calculated by the Freeman-Carroll method have lower values, while the Achar and Sharp-Wentworth methods give the same results. The positive value of the Gibbs energy $\Delta G$ indicates the impossibility of spontaneous implementation of the destruction process.

*Conclusion*

The kinetic characteristics and thermodynamic parameters of a copolymer of poly(ethylene glycol)fumarate with methacrylic acid have been determined for the first time. Analysis of TG and DTG curves showed sufficient thermal stability of these copolymers in a nitrogen atmosphere. It was found that the main stage of the decomposition of the copolymer occurs in a narrow temperature range, which is confirmed by a peak in the differential curve. The kinetic parameters of the decomposition reaction are calculated by the differential methods, namely Freeman-Carroll, Sharp-Wentworth and Achar methods. The activation energies obtained by these methods have satisfactory convergence. We can also notice that the parameters calculated by the Achar and Sharp-Wentworth methods give more accurate results. In this regard, we recommend application of exactly two of these methods.

References

1 Седов Л.Н. Ненасыщенные полиэфиры / Л.Н. Седов, З.В. Михайлова. — М.: Химия, 1977. — С. 7, 8.

2 Kandelbauer A. Handbook of Thermoset Plastics / A. Kandelbauer, G. Tondi, O.C. Zaske, S.H. Goodman. — Amsterdam: Elsevier Inc. Chapters, 2014. — P. 6–111.

3 Boenig H.V. Unsaturated Polyesters. Structure and Properties / H.V. Boenig. — Amsterdam: Elsevier Publishing Company, 1964.

4 Wu Y. Acrylated epoxidized soybean oil as a styrene replacement in a dicyclopentadiene-modified unsaturated polyester resin / Y. Wu, K. Li // Journal of Applied Polymer Science. — 2018. — Vol. 135, No. 19. — P. 46212. https://doi.org/10.1002/app.46212

5 Burkeev M.Zh. Thermal destruction of copolymers of polypropylene glycol maleate with acrylic acid / M.Zh. Burkeev, A.Zh. Sarsenbekova, E.M. Tazhbaev // Russian Journal of Physical Chemistry A. — 2015. — Vol. 89, No. 12. — P. 2183–2189. https://doi.org/10.1134/S0036024415120067

6 Burkeev M.Zh. New polyampholyte polymers based on polypropylene glycol fumarate with acrylic acid and dimethylaminoethyl methacrylate / M.Zh. Burkeev, G.K. Kudaibergen, G.K. Burkeeva et al. // Russian Journal of Applied Chemis-try. — 2018. — Vol. 91, No. 7. — P. 1145–1152. https://doi.org/10.1134/S1070427218070121

7 Burkeev M.Zh. Comparative analysis of the thermal decomposition kinetics of polyethylene glycol fumarate–acrylic acid copolymers / M.Zh. Burkeev, G.K. Kudaibergen et al. // Russian Journal of Physical Chemistry A. — 2019. — Vol. 93, No 7. —P. 1252–1257. https://doi.org/10.1134/S0036024419060281

8 Burkeev M.Zh. The use of differential calculation methods for the destruction of copolymers of poly(ethylene glycol)fumarate with the acrylic acid / M.Zh. Burkeev, A.Zh. Sarsenbekova, A.N. Bolatbay, E.M. Tazhbaev, S.Zh. Davrenbekov, E. Nasikhatuly, E.Zh. Zhakupbekova, A.A. Muratbekova // Bulletin of the Karaganda Univ. Chemistry Series. — 2020. — Vol. 3. — P. 4–11. https://doi.org/10.31489/2020Ch3/4-10

9 Burkeev, M.Zh. Synthesis and investigation of copolymer properties on the basis of poly(ethylene glycol)fumarate and methacrylic acid / M.Zh. Burkeev, G.K. Kudaibergen; Ye.M. Tazhbayev, J. Hranicek; G.K. Burkeyeva, A.Zh. Sarsenbekova // Bulletin of the Karaganda Univ. Chemistry Series. — 2019. — Vol. 93. — P. 32–38. https://doi.org/10.31489/2019Ch1/32-38

10 Freeman E.S. The application of thermoanalytical techniques to reaction kinetics: The thermogravimetric evaluation of the kinetics of the decomposition of calcium oxalate monohydrate / E.S. Freeman, B. Carroll // J. Phys. Chem. — 1958. — Vol. 62, No. 4. —P. 394–397.

11 Sharp J.H. Kinetic analysis of thermogravimetric data / J.H. Sharp, S.A. Wentworth // Anal. Chem. — 1969. — Vol. 41, No. 14. — P. 2060.

12 Achar B.N. Kinetics and mechanism of dehydroxylation processes, III, applications and limitations of dynamic methods / B.N. Achar, G.W. Brindley, J.H. Sharp // Proc. Int. Clay. Conf. — 1966. — P. 67–73.

М.Ж. Бүркеев, Ұ.Б. Төлеуов, А.Н. Болатбай, Д. Хавличек,
С.Ж. Дәуренбеков, Е.М. Тәжбаев, Э.Ж. Жақыпбекова

## Полиэтиленгликольфумараттың метакрил қышқылымен сополимерлерінің деструкциясын дифференциалдық теңдеулер қолдану арқылы зерттеу

Мақалада полиэтиленгликольфумараттың метакрил қышқылымен сополимерінің динамикалық режимдегі, азот атмосферасындағы термиялық сипаттамалары алғаш рет зерттелінген. Мәліметтерді өңдеудің үш әртүрлі әдістерін (Фримен-Кэррол, Шарп-Уэнтворт, Ахар) қолдана отырып, термиялық деструкция процесіне кинетикалық сараптау жүргізілді. Сонымен қатар, термодинамикалық сипаттамалар — Гиббс энергиясының өзгеруі ($\Delta G$) энтальпия ($\Delta H$) және активация энтропиясы ($\Delta S$) есептелінді. Сополимердің термогравиметриялық және дифференциалдық термогравиметриялық сараптама қисықтары азот атмосферасында қыздыру жылдамдығы 10°C/мин кезінде зерттелінді. Сополимердің температураның тар интервалында жүрген және дифференциалдық қисықтағы шыңмен дәлелденген ыдырауының негізгі кезеңі анықталды. Үлгінің массасының азаюымен байланысты сополимердің реакция жылдамдығының өзгеруі көрсетілді. Кинетикалық сараптау нәтижелерінің зерттелінген қосылыстардың молекулалық құрылымына байланыстылығы көрсетілген. Фримен-Кэррол әдісімен табылған активация энергиясының мәні төменірек шамаға ие, ал Ахар мен Шарп-Уэнтворт әдістері бірдей нәтижелер береді.

*Кілт сөздер*: динамикалық термогравиметрия, термиялық деструкция, полиэтиленгликольфумараттың метакрил қышқылымен сополимері, активация энергиясы.

М.Ж. Буркеев, У.Б. Толеуов, А.Н. Болатбай, Д. Хавличек,
С.Ж. Дауренбеков, Е.М. Тажбаев, Э.Ж. Жакупбекова

## Исследования деструкции сополимеров полиэтиленгликольфумарата с метакриловой кислотой с использованием дифференциальных уравнений

В статье впервые изучены термические характеристики сополимера полиэтиленгликольфумарата с метакриловой кислотой в динамическом режиме, в атмосфере азота. Проведен кинетический анализ процесса термической деструкции с использованием трех разных методов обработки данных (Фримена–Кэрролла, Шарпа–Уэнтворта, Ахара). Также были рассчитаны термодинамические характеристики — изменение энергии Гиббса ($\Delta G$), энтальпии ($\Delta H$) и энтропии активации ($\Delta S$). Кривые термогравиметрического и дифференциального термогравиметрического анализа сополимера были изучены в атмосфере азота при скорости нагревания 10ºC/мин. Были установлены основные этапы разложения сополимера, происходящие в узком интервале температур, который подтверждается пиком на дифференциальной кривой. Были показаны изменения скорости реакции сополимера в связи с убыванием массы образца. Показано, что результаты кинетического анализа зависят от молекулярной структуры исследуемых соединений. Значения энергии активации, найденные методом Фримена–Кэррола, имеют более низкие значения, а методы Ахара и Шарпа–Уэнтворта дают одинаковые результаты.

*Ключевые* слова: динамическая термогравиметрия, термическая деструкция, сополимер полиэтиленгликольфумарата с метакриловой кислотой, энергия активации.

## References

1 Sedov, L.N., & Mihailova, Z.V. (1977). Nenasyshchennye poliefiry [Unsaturated polyesters]. Moscow: Khimiia [in Russian].

2 Kandelbauer, A. (2014). Handbook of Thermoset Plastics. Amsterdam: Elsevier Inc. Chapters. 6, 111.

3 Boenig, H.V. (1964). Unsaturated Polyesters. Structure and Properties. Amsterdam: Elsevier Publishing Company.

4 Wu, Y., & Li, K. (2018). Acrylated epoxidized soybean oil as a styrene replacement in a dicyclopentadiene-modified unsaturated polyester resin. *Journal of Applied Polymer Science, 135(19)*, 46212. https://doi.org/10.1002/app.46212

5 Burkeev, M.Zh., Sarsenbekova, A.Zh., & Tazhbaev, E.M. (2015). Thermal destruction of copolymers of polypropylene glycol maleate with acrylic acid. *Russian Journal of Physical Chemistry A, 89(12)*, 2183–2189. https://doi.org/10.1134/S0036024415120067

6 Burkeev, M.Zh., Kudaibergen, G.K., & Burkeeva, G.K., et al. (2018). New polyampholyte polymers based on polypropylene glycol fumarate with acrylic acid and dimethylaminoethyl methacrylate. *Russian Journal of Applied Chemistry, 91(7)*, 1145–1152. https://doi.org/10.1134/S1070427218070121

7 Burkeev, M.Zh., Sarsenbekova, A.Zh., & Kudaibergen, G.K., et al. (2019). Comparative analysis of the thermal decomposition kinetics of polyethylene glycol fumarate–acrylic acid copolymers. *Russian Journal of Physical Chemistry A, 93(7)*, 1252–1257. https://doi.org/10.1134/S0036024419060281

8 Burkeev, M.Zh., Sarsenbekova, A.Zh., Bolatbay, A.N., Tazhbaev, E.M., Davrenbekov, S.Zh., & Nasikhatuly, E. et al. (2020). The use of differential calculation methods for the destruction of copolymers of poly(ethylene glycol)fumarate with the acrylic acid. *Bulletin of the Karaganda Univ. Chemistry Series. 99(3)*, 4-11. https://doi.org/10.31489/2020Ch3/4-10

9 Burkeev, M.Zh., Kudaibergen, G.K.; Tazhbayev, Ye.M., Hranicek, J., Burkeyeva, G.K., & Sarsenbekova, A.Zh. (2019). Synthesis and investigation of copolymer properties on the basis of poly(ethylene glycol)fumarate and methacrylic acid. *Bulletin of the Karaganda Univ. Chemistry Series, 93(1)*, 32-38. https://doi.org/10.31489/2019Ch1/32-38

10 Freeman, E.S., & Carroll, B. (1958). The Application of Thermoanalytical Techniques to Reaction Kinetics: The Thermogravimetric Evaluation of the Kinetics of the Decomposition of Calcium Oxalate Monohydrate. *Journal of Physical Chemistry, 62(4)*, 394–397.

11 Sharp, J.H., & Wentworth, S.A. (1969). Kinetic analysis of thermogravimetric data. *Anal. Chem., 41(14)*, 2060.

12 Achar, B.N., Brindley, G.W., & Sharp, J.H. (1966). Kinetics and mechanism of dehydroxylation processes, III, applicationsand limitations of dynamic methods. *Proc. Int. Clay. Conf.*, 67–73.

## Information about authors:

**Burkeyev Meyram Zhunusovich** — Full Professor, Doctor of Chemical Sciences, Karagandy University of the name of academician E.A. Buketov, Universitetskaya street, 28, 100024, Karaganda, Kazakhstan; e-mail: m_burkeev@mail.ru. https://orcid.org/0000-0001-8084-4825

**Tuleuov Ulygbek Borashevich** — 1st year PhD student, Karagandy University of the name of Academician E.A. Buketov, Kazakhstan, Karagandy, 100024, Universitetskaya str., 28. E-mail: beka-lols1@gmail.com, https://orcid.org/0000-0002-2664-6884

**Bolatbay Abylaikhan Nurmanovich** — 2nd year PhD student, Karagandy University of the name of Academician E.A. Buketov, Kazakhstan, Karagandy, 100024, Universitetskaya str., 28. E-mail: abylai_bolatbai@mail.ru, https://orcid.org/0000-0001-5047-3066

**Khavlichek David** — Associate Professor, RNDr., CSc. Charles University in Prague, Czech Republic, Prague, 400 96, Pasteurova 1. E-mail: David.havlicek@natur.cuni.cz

**Davrenbekov Santay Zhanabilovich** — Full Professor, Doctor of Chemical Sciences, Karagandy University of the name of academician E.A. Buketov, Universitetskaya street, 28, 100024, Karaganda, Kazakhstan; e-mail: sdavrenbekov@mail.ru, https://orcid.org/0000-0002-0218-7062

**Tazhbayev Yerkeblan Muratovich** — Full Professor, Doctor of Chemical Sciences, Karagandy University of the name of academician E.A. Buketov, Universitetskaya street, 28, 100024, Karaganda, Kazakhstan; e-mail: tazhbayev@mail.ru; https://orcid.org/0000-0003-4828-2521

**Zhakupbekova Elmira Zhumatayevna** — Candidate of Chemical Sciences, Assoc. Professor, Karagandy University of the name of academician E.A. Buketov, Universitetskaya street, 28, 100024, Karaganda, Kazakhstan; e-mail: elmira_zhakupbek@mail.ru; https://orcid.org/0000-0003-4384-9859

T.K. Jumadilov[1], Z.B. Malimbayeva[2*], Kh. Khimersen[1, 3],
I.S. Saparbekova[2], A.M. Imangazy[1], O.V. Suberlyak[4]

*[1]Bekturov Institute of Chemical Sciences, Almaty, Kazakhstan;*
*[2]Kazakh National Women's Teacher Training University, Almaty, Kazakhstan;*
*[3]Abai Kazakh National Pedagogical University, Almaty, Kazakhstan;*
*[4]Lviv Polytechnic National University, Lviv, Ukraine*
*(\*Corresponding author′s e-mail: malimbayeva.zamira@gmail.com)*

# Specific features of praseodymium extraction by intergel system based on polyacrylic acid and poly-4-vinylpyridine hydrogels

Some technological solutions contain valuable components and can become an additional source of rare-earth elements to satisfy the current production demands. This research provides the study on using a combination of polyacrylic acid hydrogel (hPAA) and hydrogel of poly-4-vinylpyridine (hP4VP) in different molar ratios for praseodymium ions sorption from its nitrate solution. The mutual activation of the hydrogels in an aqueous medium provides their transformation into a highly ionized state by the conformational and electrochemical changes in properties during their remote interaction. The electrochemical properties of solutions were studied by the methods of electrical conductivity, and pH measurements of the solutions. The research showed that the maximum activation of hydrogels was revealed within the molar ratio of hPAA:hP4VP equal to 1:5. Moreover, the total praseodymium ions sorption degree after 24 hours of sorption by individual hPAA and hP4VP was 54 % and 47 %, respectively, whereas the praseodymium ions sorption degree by the hPAA–hP4VP intergel system in the molar ratio 1:5 became 62 %. A slight increase in the sorption degree of praseodymium ions by the intergel system in comparison with individual hydrogels can be explained by the achievement of a higher ionization degree of hydrogels being activated in the hPAA–hP4VP interpolymer system by the remote interaction effect.

*Keywords:* intergel systems, polyacrylic acid hydrogel, poly-4-vinylpyridinehydrogel, remote interaction, sorption, praseodymium ions.

*Introduction*

Rare-earth metals have various applications in chemical industry, in nuclear engineering, in metallurgy, etc. For example, praseodymium being a rare-earth metal is commonly used to make high-power magnets that are known for their strength and endurance when combined with another rare-earth element neodymium [1, 2]. The recovery of praseodymium from technological solutions might provide an additional source of this valuable element.

Sorption and extraction techniques for the recovery of certain metals have been successfully used in hydrometallurgy [3]. Moreover, sorption techniques are presently favored over extraction methods owing to a variety of advantages: they are more environmentally friendly and have fewer technical cycles [4]. For the recovery of rare-earth metals from the solutions, adsorption processes using various materials such as polymers have recently sparked increased interest [5]. For instance, polymer hydrogels are generally considered smart materials with evolving progressive functions for sorption technology. A common method for praseodymium ions sorption from solutions can be the use of polymer hydrogels: polyacrylic acid hydrogel (hPAA) and poly-4-vinylpyridinehydrogel (hP4VP).

Our previous research [6] showed that the remote interaction effect provided the changes in the electrochemical and conformational properties which influenced on the increase in the sorption activity of hydrogels in their intergel system. For present study we decided to choose "hPAA–hP4VP" intergel system to test it in praseodymium ions sorption. Furthermore, the combination of hydrogels in the "hPAA–hP4VP" intergel system with different molar ratios X:Y (6:0, 5:1, 4:2, 3:3, 2:4, 1:5, and 0:6) can also be applied to investigate the remote interaction effect for improving the process of praseodymium ions sorption.

The goal of this research was to study the influence of the preliminary mutual activation of polyacrylic acid hydrogel (hPAA) and poly-4-vinylpyridine hydrogel (hP4VP) ("hPAA–hP4VP" intergel system) in praseodymium ions sorption from its nitrate solution.

*Experimental*

The following measurement instruments and equipment were used: conductometer MARK-603 (Vzor, Nizhny Novgorod, Russia) for the measurements of the specific electric conductivity of solutions, which is important for characterizing the equilibrium of polyelectrolytes dissociation. The hydrogen ions concentration was determined by a Metrohm 827 pH-meter pH-Lab (Switzerland). Measurements of pH were provided to study the acid–base properties of the solution. The mass of the samples was measured using an analytical balance SHIMADZU AY220 (Shimadzu Corporation, Kyoto, Japan). The optical density measurements for the subsequent calculation of the praseodymium (III) concentration in solution was determined by aJenway-6305 (Cole-Parmer, Jenway, York, UK) spectrophotometer. For the residual praseodymium ions detection from liquid samples, the Varian Atomic Absorption SpectrometerAA240. Measurement errors did not exceed 1 %.

*Materials*

The following reagents were used: praseodymium (III) nitrate hexahydrate (99.9 % trace metals basis, Sigma-Aldrich) as praseodymium ions source in solution, reagent arsenazo III (Sigma-Aldrich) in powder form as a color-forming reagent to determine cerium concentration, and perchloric acid ($HClO_4$) (Sigma-Aldrich, Darmstadt, Germany) for standard solution preparation. Poly-4-vinylpyridine hydrogel (hP4VP) (2 % cross-linked with divinylbenzene, Sigma-Aldrich) was used. Polyacrylic acid hydrogels were synthesized in the presence of the N,N-methylene-bis-acrylamide crosslinking agent and the $K_2S_2O_8$-$Na_2S_2O_3$ redox system in an aqueous medium in laboratory conditions.

*Electrochemical research*

The studies of the "hPAA–hP4VP" intergel system were carried out in the following order: each dry hydrogel was placed in separate polypropylene mesh, the pores of which were permeable to low molecular weight ions and molecules, but impermeable for dispersion of hydrogels. Then, the meshes with dry hydrogels were placed in a glass with distilled water for 48 hours for swelling. Upon reaching an equilibrium state in weight, the swollen hydrogels were taken, and according to molar ratios, the "hPAA–hP4VP" intergel system were composed for further mutual activation. The activation of the intergel system is required to transfer the hydrogels into a highly ionized state by changing their conformational and electrochemical properties by remote interaction [7]. For activation, the polypropylene meshes with swollen hydrogels inside (Fig. 1) were placed in a glass with distilled water at a distance of about 1–2 cm opposite each other, forming an interpolymer system "hPAA–hP4VP". After the activation, the meshes with swollen hydrogels were placed in glasses with praseodymium nitrate solutions and the electrical conductivity with pH measurements of the overgel liquid were determined. The experiments were carried out at room temperature.



Figure 1. Polypropylene meshes (left) and the illustration of the activation process of the intergel system (right)

The polymer chain binding degree of internode links of the polymer chain was calculated according to Eq. (1):

$$\theta = \frac{\vartheta_{sorbed}}{\vartheta_1 + \vartheta_2} \times 100\ \%,\tag{1}$$

where $\vartheta_{sorbed}$ is the amount of sorbed praseodymium ions (in mol), $\vartheta_1$ is the amount of hPAA (in mol), and $\vartheta_2$ is the amount of hP4VP(in mol).

The sorption degree was calculated using the following Eq. (2):

$$\eta = \frac{C_{initial} - C_{residual}}{C_{initial}} \times 100 \ \% \ , \qquad (2)$$

where $C_{initial}$ and $C_{residual}$ are the initial and residual concentration (in g/L) of praseodymium ions in the solution, respectively.

For the experiments 1000 mL of the praseodymium (III) nitrate hexahydrate solution (C = 100 mg/L) was prepared and poured into 7 glasses with 100 mL each. The hydrogels were put separately into 2 polypropylene meshes (1 common glass with solution) in accordance with their molar ratios X:Y (6:0, 5:1, 4:2, 3:3, 2:4, 1:5, and 0:6) to form the intergel system hPAA:hP4VP (X:Y). For spectrophotometer analysis, one aliquot (1 mL) was taken from each solution at the set time. Finally, 63 aliquots of solution were obtained.

*Results and Discussions*

The presence of the intergel system in an aqueous solution of praseodymium (III) nitrate hexahydrate leads to various processes that affect the electrochemical equilibrium in the solution. Fig. 2 shows the dependence of the electrical conductivity of $Pr(NO_3)_3 \cdot 6H_2O$ solutions on the molar ratios hPAA:hP4VP in time. Mostly all ratios, an increase in electrical conductivity values was observed, which might be explained by an increase in the $OH^-$ medium in solutions, released by the additional dissociation of the strongly basic P4VP hydrogel [8].
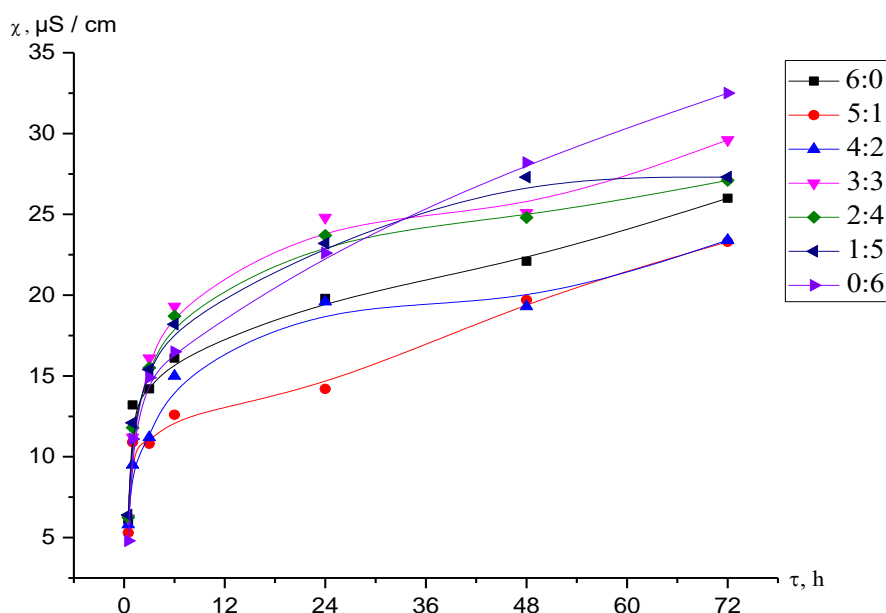


Figure 2. Dependence of specific electrical conductivity on the molar ratio of hydrogels on time

The conductivity of solutions increased with time for almost all ratios of hydrogels. However, the character of the parameter change was different for different ratios of hydrogels. As can be seen from Figure 2, there is an increase in electrical conductivity over time. This is due to the transition of the initial hydrogels of polyacrylic acid and poly-4-vinylpyridine to a highly ionized state due to mutual activation during their remote interaction.
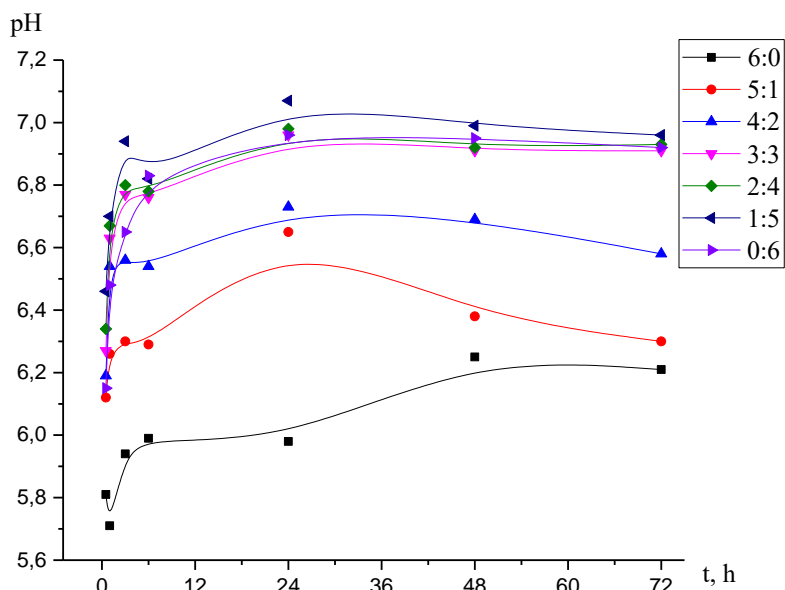
Figure 3. Dependence of pH on the molar ratio of hydrogels on time

The change in the pH of solutions is shown in Figure 3. As can be seen from the obtained results, an increase in pH values with the time of remote interaction was observed. The increase in pH may be explained due to the binding of the detached $H^+$ from the carboxyl group by poly-4-vinylpyridine, as a result, the process of protonation of the heteroatom in a ring occurred. This was evidenced by the maxima at the 1:5 ratio of hPAA–hP4VP, which correspond to the time of remote interaction after 24 and 48 hours. The minimum pH values were observed in the presence of only polyacid. This is due to the appearance of charged ions ($H^+$, $OH^-$) and groups ($-COO^-$). The maximum pH values indicated that the rate of dissociation of –COOH groups is lower than the rate of protonation of the poly-4-vinylpyridine heteroatom. This phenomenon indicates the process of ionization of the main polymer of the hydrogel. Consequently, both polymer hydrogels pass into a highly ionized state, undergoing mutual activation.

Figure 4 shows the change in the concentration of praseodymium ions during sorption by the intergel system hPAA–hP4VP.
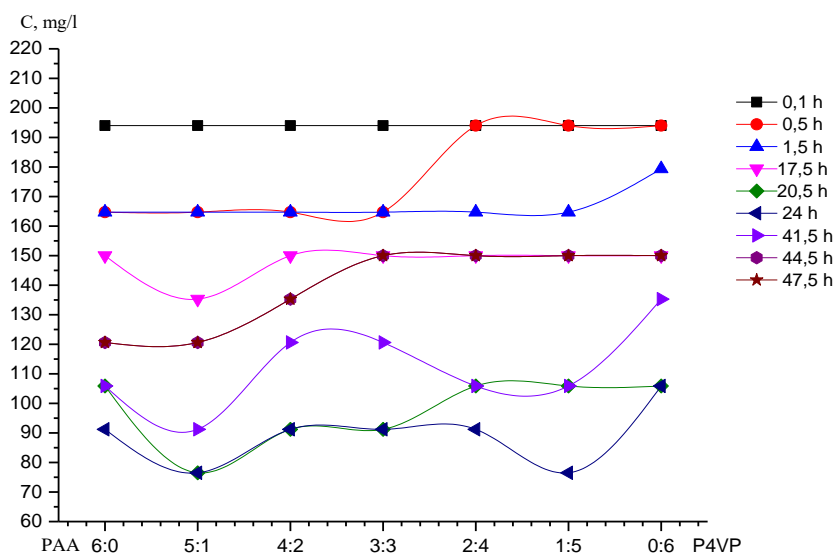


Figure 4. Dependence of the praseodymium ions concentration on the molar ratio of hydrogels
in the intergel system hPAA:hP4VP in praseodymium (III) nitrate hexahydrate medium

The data shows (Fig. 4) that the concentration of Pr$^{3+}$ ions in solution is much lower at molar ratios of hydrogels equal to 1:5 (that means the sorption is higher) after 24 hours of interaction. This may be explained that at a ratio 1:5, the hydrogels of polyacrylic acid and poly-4-vinylpyridine in intergel system reach the highly ionized state due to the mutual activation of hydrogels.

T a b l e  1

**Degree of praseodymium ionssorption, mol.%**

| Ratio | Time, h | | | | | | | | |
|---|---|---|---|---|---|---|---|---|---|
|  | 0.1 | 0.5 | 1.5 | 17.5 | 20.5 | 24 | 41.5 | 44.5 | 47.5 |
| 6:0 | 3.1 | 17.6 | 17.6 | 25 | 47.0 | 54.4 | 47.0 | 39.7 | 39.7 |
| 5:1 | 3.1 | 17.6 | 17.6 | 32.3 | 61.7 | 61.7 | 54.4 | 39.7 | 39.7 |
| 4:2 | 3.0 | 17.6 | 17.6 | 25.2 | 54.4 | 54.4 | 39.7 | 32.3 | 32.3 |
| 3:3 | 3.1 | 17.6 | 17.6 | 25.5 | 54.4 | 54.4 | 39.7 | 25.3 | 25.3 |
| 2:4 | 3.1 | 3.2 | 17.6 | 25.3 | 47.0 | 54.4 | 47.0 | 25.1 | 25.1 |
| 1:5 | 3.2 | 3.2 | 17.6 | 25.3 | 47.0 | 61.7 | 47.5 | 25.1 | 25.1 |
| 0:6 | 3.0 | 3.1 | 10.3 | 25 | 47.0 | 47.0 | 32.3 | 25.2 | 25.2 |

T a b l e  2

**Polymer chains binding degree, mol.%**

| Ratio | Time, h | | | | | | | | |
|---|---|---|---|---|---|---|---|---|---|
|  | 0.1 | 0.5 | 1.5 | 17.5 | 20.5 | 24 | 41.5 | 44.5 | 47.5 |
| 6:0 | 1.1 | 5.9 | 5.9 | 8.3 | 15.9 | 18.4 | 15.9 | 13.3 | 13.3 |
| 5:1 | 1.3 | 6.5 | 6.1 | 11.2 | 21 | 21 | 18.7 | 13.5 | 13.5 |
| 4:2 | 1.3 | 6.8 | 6.1 | 8.5 | 18.7 | 18.7 | 13.6 | 11.2 | 11.2 |
| 3:3 | 1.5 | 6.2 | 6.2 | 8.6 | 19.1 | 19.1 | 13.8 | 8.6 | 8.6 |
| 2:4 | 1.6 | 1.1 | 6.3 | 8.7 | 16.7 | 19.2 | 16.7 | 8.7 | 8.7 |
| 1:5 | 1.6 | 1.1 | 6.3 | 8.7 | 16.7 | 21.8 | 16.7 | 8.7 | 8.7 |
| 0:6 | 1.8 | 1.1 | 3.7 | 8.9 | 17 | 17 | 11.7 | 8.9 | 8.9 |

The polymer chain binding degree in relation to the praseodymium ions in the hPAA–hP4VP system is presented in Table 2. The obtained results indicated that the most intense polymer chain binding degree of praseodymium ions (21.8 %) by hPAA:hP4VP (1:5) intergel system occurred after 24 hours of sorption.

*Conclusions*

The obtained results demonstrate the potential of using intergel systems in rare-earth metal recovery. The activated hydrogels showed an increase in sorption activity in comparison with the individual hPAA (6:0) and hP4VP (0:6) hydrogels. This research showed that the maximum activation of hydrogels was revealed within the molar ratio of hPAA:hP4VP equal to 1:5. The total praseodymium ions sorption degree after 24 h. of sorption by individual hydrogels hPAA and hP4VP was 54 % and 47 %, respectively, whereas the praseodymium ions sorption degree by the intergel system of hPAA:hP4VP (1:5) was 62 %. An increase in the sorption degree of praseodymium ions by the intergel system of hPAA: hP4VP (1:5) in comparison with individual hydrogels can be explained by the achievement of a high ionization degree of the intergel system activated by the remote interaction effect, which opens up new opportunities for the development of innovative sorption technologies in Kazakhstan for the target rare-earth elements.

References

1   Gazulla, M.F. Praseodymium oxides. Complete characterization by determining oxygen content. /M.J. Ventura, C. Andreu, J. Gilabert, M. Orduña, & M. Rodrigo // Microchem. J. — 2019. — Vol. 148. — P. 291–298. https://doi.org/10.1016/j.microc.2019.05.013

2   Donia A.M. Selective Separation of Uranium (VI), Thorium (IV), and Lanthanum (III) from their aqueous solutions using a chelating resin containing amine functionality. /A.A. Atia, T.E. Amer, M.N. El-Hazek, M.H. Ismael // Journal of dispersion science and technology. — 2011. — Vol. 32. — P. 1673–1681.

3   Rombach E. Recycling of Rare Metals. / B. Friedrich // Handbook of Recycling. — 2014. — P. 125–150. https://doi.org/10.1016/b978-0-12-396459-5.00010-6

4   Miller D.D. Anion structural effects on interaction of rare earth element ions with Dowex 50W X8 cation exchange resin / R. Siriwardane, & D. Mcintyre // Journal of Rare Earths. — 2018. — No. 36(8). — P. 879–890. https://doi.org/10.1016/j.jre.2018.03.006

5   Noshin Mir. Self-separation of the adsorbent after recovery of rare-earth metals: Designing a novel non-wettable polymer / Carlos E. Castano, Jessika V. Rojas, NazgolNorouzi, Amir R. Esmaeili, Reza Mohammadi // Sep. Purif. Technol. — 2021. — P. 118-152. https://doi.org/10.1016/j.seppur.2020.118152

6   Jumadilov T.K. Phenomenon of remote interaction and sorption ability of rare cross–linked hydrogelsn of polymethacrylic acid and poly-4-vinylpyridine in relation to erbium ions / T.K. Jumadilov, R. Kondaurov, A. Imangazy, N. Myrzakhmetova, I. Saparbekova // Chem. Chem. Technol. — 2019. — Vol. 13, No. 4. — P. 451–458.

7   Jumadilov T. Effective Sorption of Europium Ions by Interpolymer System Based on Industrial Ion-Exchanger Resins Amberlite IR120 and AB-17-8 / K. Khimersen, Z. Malimbayeva, R. Kondaurov // Materials. — 2021. — Vol. 14, No. 14. — P. 3837. https://doi.org/10.3390/ma14143837

8   Petrukhin O.M. Workshop on Physical and Chemical Methods of Analysis / O.M. Petrukhin. — Moscow: Chemistry, 1987. — P. 77–80.

Т.Қ. Жұмаділов, З.Б. Малимбаева, Х. Химэрсэн,
И.С. Сапарбекова, А.М. Иманғазы, О.В. Суберляк

## Полиакрил қышқыл мен поли-4-винилпиридин интергельдік жүйесімен празеодимді бөлудің ерекшеліктері

Кейбір технологиялық ерітінділер құрамында құнды компоненттер бар және өндірістің әртүрлі қажеттіліктерін қанағаттандыру үшін сирек кездесетін элементтердің қосымша көзі бола алады. Мақала полиакрил қышқылы (гПАК) және поли-4-винилпиридин (гП4ВП) гидрогельдерінің қосындысын оның нитратты ерітіндісінен празеодим иондарының сорбциясы үшін әртүрлі мольдік қатынаста қолдануды зерттеуге бағытталған. Су ортасында гидрогельдердің өзара активтенуі олардың қашықтықтан өзара әрекеттесуі кезінде конформациялық және электрохимиялық қасиеттердің өзгеруіне байланысты гидрогельдердің жоғары ионалдаған күйге өтуін қамтамасыз етеді. Ерітінділердің электрохимиялық қасиеттері электр өткізгіштік және ерітінділердің PH өлшеу әдістерімен зерттелді. Зерттеу көрсеткендей, гидрогельдердің максималды активтенуі гПАК: гП4ВП-нің 1:5-ке тең моль қатынасында анықталды. Бұл ретте жеке гПАК және гП4ВП сорбциясынан кейін празеодим иондарының сорбция дәрежесі тиісінше 54 % және 47 %-ды құрады, ал празеодим иондарының гПАК-гП4ВП интергелдік жүйесімен сорбция дәрежесі 1:5 моль арақатынасында 62 %-ды құрады. Жеке гидрогельдермен салыстырғанда празеодим иондарының интергелдік жүйемен сорбция дәрежесінің біршама артуын қашықтықтан өзара әрекеттесу әсеріне байланысты гПАК–гП4ВП интергелдік жүйесінде белсендірілген гидрогельдердің ионалдауының жоғары дәрежесіне қол жеткізумен түсіндіруге болады.

*Кілт сөздер:* интергелдік жүйелер, полиакрил қышқылының гидрогелі, поли-4-винилпиридин гидрогелі, қашықтықтан әрекеттесу, сорбция, празеодим иондары.

Т.К. Джумадилов, З.Б. Малимбаева, Х. Химэрсэн,
И.С. Сапарбекова, А.М. Иманғазы, О.В. Суберляк

## Особенности извлечения празеодима интергелевой системой на основе гидрогелей полиакриловой кислоты и поли-4-винилпиридина

Некоторые технологические растворы содержат в своем составе ценные компоненты и могут стать дополнительным источником редкоземельных элементов для удовлетворения различных потребностей производства. Данная работа направлена на исследование применения комбинации гидрогелей полиакриловой кислоты (гПАК) и поли-4-винилпиридина (гП4ВП) в различных мольных соотношениях для сорбции ионов празеодима из его нитратного раствора. Взаимная активация гидрогелей в водной среде обеспечивает переход гидрогелей в высокоионизированное состояние за счет конформационных и электрохимических изменений свойств при их дистанционном взаимодействии. Электрохимические свойства растворов изучались методами электропроводности и измерения pH растворов. Исследование показало, что максимальная активация гидрогелей была выявлена при мольном соотношении гПАК:гП4ВП, равном 1:5. При этом степень сорбции ионов празеодима после 24 ч сорбции индивидуальными гПАК и гП4ВП составила 54 и 47 % соответственно, тогда как степень сорбции ионов

празеодима интергелевой системой гПАК–гП4ВП в мольном соотношении 1:5 составила 62 %. Некоторое увеличение степени сорбции ионов празеодима интергелевой системой по сравнению с индивидуальными гидрогелями можно объяснить достижением более высокой степени ионизации гидрогелей, активированных в интергелевой системе гПАК–гП4ВП за счет эффекта дистанционного взаимодействия.

*Ключевые слова:* интергелевые системы, гидрогель полиакриловой кислоты, гидрогель поли-4-винилпиридина, дистанционное взаимодействие, сорбция, ионы празеодима.

# References

1 Gazulla, M.F., Ventura, M.J., Andreu, C., Gilabert, J., Orduña, M., & Rodrigo, M. (2019). Praseodymium oxides. Complete characterization by determining oxygen content. *Microchem. J, 148*, 291–298. https://doi.org/10.1016/j.microc.2019.05.013

2 Donia, A.M. (2011). Selective Separation of Uranium (VI), Thorium (IV), and Lanthanum (III) from their aqueous solutions using a chelating resin containing amine. *Journal of dispersion science and technolog*, 1673–1681.

3 Rombach, E., & Friedrich, B. (2014). Recycling of Rare Metals. Handbook of Recycling, 125–150. https://doi.org/10.1016/b978-0-12-396459-5.00010-6

4 Miller, D.D., Siriwardane, R., & Mcintyre, D. (2018). Anion structural effects on interaction of rare earth element ions with Dowex 50W X8 cation exchange resin. *Journal of Rare Earths, 36(8)*, 879–890. https://doi.org/10.1016/j.jre.2018.03.006

5 Noshin Mir, Carlos E. Castano, Jessika V. Rojas, NazgolNorouzi, Amir R. Esmaeili, & Reza Mohammadi (2021). Self-separation of the adsorbent after recovery of rare-earth metals: Designing a novel non-wettable polymer, *Sep. Purif. Technol.*, 118-152. https://doi.org/10.1016/j.seppur.2020.118152.

6 Jumadilov, T.K., Kondaurov, R., Imangazy, A., Myrzakhmetova, N., & Saparbekova, I. (2019). Phenomenon of remote interaction and sorption ability of rare cross–linked hydrogelsn of polymethacrylic acid and poly-4-vinylpyridine in relation to erbium ions, *Chem. Chem. Technol., 13(4)*, 451–458.

7 Jumadilov, T, Khimersen, K, Malimbayeva, Z, & Kondaurov, R. (2021). Effective Sorption of Europium Ions by Interpolymer System Based on Industrial Ion-Exchanger Resins Amberlite IR120 and AB-17-8. *Materials*, *14(14),* 3837. https://doi.org/10.3390/ma14143837

8 Petrukhin, O.M. (1987). Workshop on Physical and Chemical Methods of Analysis. Moscow: Chemistry.

# Information about authors:

**Jumadilov Talkybek Kozhataevich** — Doctor of Chemical Sciences, Professor, Chief Researcher at Bekturov Institute of Chemical Sciences, Academician of the Russian Academy of Natural History,106 Valikhanov str., 050013, Almaty, Kazakhstan; e-mail: jumadilov@mail.ru; https://orcid.org/0000-0001-9505-3719

**Malimbayeva Zamira Bakytzhankyzy** (corresponding author) — Master of Science, PhD candidate at the Kazakh National Women's Teacher Training University, 99 Ayteke bi street, 050000, Almaty, Kazakhstan; e-mail: malimbayeva.zamira@gmail.com; https://orcid.org/0000-0003-0029-0522;

**Khimersen Khuangul** — Master of Science, PhD student at Abai Kazakh National Pedagogical University, 13 Dostyk avenue, 050013, Almaty, Kazakhstan; e-mail: huana88@mail.ru; https://orcid.org/0000-0002-5138-5997;

**Saparbekova Indira** — Candidate of Chemical Sciences, Kazakh National Women's Teacher Training University, 99 Ayteke bi street, 050000, Almaty, Kazakhstan; e-mail: indiaru74@gmail.com; https://orcid.org/0000-0003-3551-9526;

**Aldan Imangazy** — Master of Science, PhD candidate, Scientific Researcher at Bekturov Institute of Chemical Sciences, 106 Valikhanov street, 050013, Almaty, Kazakhstan; e-mail: imangazy.aldan@mail.ru; https://orcid.org/0000-0001-7834-1022

**Oleg Suberlyak** — Doctor of Chemistry, Professor, Head of the Department of Chemical Technology of Plastics Processing, Institute of Chemistry and Chemical Technology, Lviv Polytechnic National University, Academician of the Technological Academy of Ukraine, Lviv Polytechnic National University, 12Bandera street, 79013, Lviv, Ukraine; e-mail:suberlak@polynet.lviv.ua; https://orcid.org/0000-0002-6046-5972

# INORGANIC CHEMISTRY

## Sh.B. Kasenova[1], Zh.I. Sagintaeva[1], B.K. Kasenov[1*], M.O. Turtubaeva[2], A. Nukhuly[3], Ye.Ye. Kuanyshbekov[1], M.A. Isabaeva[2]

*[1]Abishev Chemical-Metallurgical Institute, Karaganda, Kazakhstan;*
*[2]Toraigyrov University, Pavlodar, Kazakhstan;*
*[3]Pavlodar Pedagogical University, Kazakhstan*
*(\*Corresponding author's e-mail: kasenov1946@mail.ru)*

# New nanostructured manganites of LaMe$^{II}$CuZnMnO$_6$ (Me$^{II}$ — Mg, Ca, Sr, Ba)

The copper-zinc manganites of LaMe$^{II}$CuZnMnO$_6$ (Me$^{II}$ — Mg, Ca, Sr, Ba) have been synthesized with the high-temperature interaction of alkaline earth metals carbonates with oxides of lanthanum (III), copper (II), zinc (II) and manganese (III). The synthesized polycrystalline copper-zinc manganites have been grinded on the Retsch vibration mill MM301 (Germany). As a result their nanostructured particles have been obtained. Their sizes have been determined using an electron microscope Mira3 LMU, Tescan. Methods of radiography determined that all synthesized nanostructured copper-zinc manganites crystallize in the cubic syngony with the following parameters of a lattice: LaMgCuZnMnO$_6$ — a = 13.53±0.02 Å, V° = 2476.81±0.06 Å$^3$, Z = 4, V°$_{elect.cell}$ = 619.20±0.02 Å$^3$, $\rho_{roent}$ = 4.52; $\rho_{pick}$ = 4.50±0.01 g/cm$^3$; LaCaCuZnMnO$_6$ — a = 13.69±0.02 Å, V° = 2565.73±0.06 Å$^3$, Z = 4, V°$_{elect.cell.}$ = 641.43±0.02 Å$^3$, $\rho_{roent}$ = 4.43; $\rho_{pick}$ = 4.41±0.01 g/cm$^3$; LaSrCuZnMnO$_6$ — a = 13.91±0.02 Å, V° = 2691.42±0.06 Å$^3$, Z = 4, V°$_{elect.cell}$ = 672.85±0.02 Å$^3$, $\rho_{roent}$ = 4.99; $\rho_{pick.}$ = 4.96±0.01 g/cm$^3$; LaBaCuZnMnO$_6$ — a = 14.55±0.02 Å, V° = 3080.27±0.06 Å$^3$, Z = 4, V°$_{elect.cell}$ = 770.07±0.02 Å$^3$, $\rho_{roent}$ = 4.95; $\rho_{pick}$ = 4.94±0.01 g/cm$^3$. The X-ray investigations demonstrated that the values of lattice parameters of the studied copper-zinc manganites have been increased from Mg to Ba. As a result of the investigations, these compounds can be included in Pm3m spatial group.

*Keywords:* synthesis, copper-zinc manganite, lanthanum, alkaline-earth metals, nanostructured particles, electron microscopy, radiography.

## Introduction

Cuprates, manganites, zincates of the rare-earth elements, which partially substituted by oxides of alkaline-earth metals, have the unique physical and physicochemical properties [1–10]. Abishev Chemical-Metallurgical Institute has been conducting the systematic and targeted investigation in this direction for many years. Thus their results have been summarized in monographs [11–14]. This paper presents the results of synthesis and the radiousgraphic studies of the new nanostructured copper-zinc manganites of lanthanum and the alkaline earth metals. Zincates, cuprates and manganites have been combined into a single phase as the copper-zinc manganites.

## Experimental

In order to obtain the copper-zinc manganites of lanthanum and the alkaline earth metals of LaMe$^{II}$CuZnMnO$_6$ (Me$^{II}$ — Mg, Ca, Sr, Ba) the stoichiometric ratios of La$_2$O$_3$ (especially pure), ZnO (analytically pure), CuO (analytically pure), Mn$_2$O$_3$ (analytically pure) and MgCO$_3$, CaCO$_3$, SrCO$_3$ and BaCO$_3$ (analytically pure) have been intensively mixed, milled in an agate mortar. Then the mixtures have been placed in the alundum crucibles and placed in a muffle furnace SNOL. The annealing has been performed at 600 ºC for 10 h, 800 ºC for 10 h, 1000 ºC for 10 h, 1200 ºC for 10 h and at 1100 ºC for 20 h. After each annealing at these temperatures, the mixtures have been cooled to a room temperature and intensively milled and mixed. The low temperature

annealing of the mixtures have been performed at 400 °C for 10 h to obtain the stable and equilibrium phases at low temperatures.

Then, the received polycrystalline samples of the copper-zinc manganites have been mixed under the special conditions to the nanostructured particles on the Retsch vibration mill (Germany). Their sizes have been determined on an electron microscope Mira3 LMU, Tescan (Fig.).

The X-ray phase analysis of the synthesized nanostructured copper-zinc manganite particles have been performed on DRON-2.0. The operating conditions: $CuK_\delta$-radiation, $U = 30$ kV, $J = mA$, rotation speed is 100 pps, time constant $\tau = 5$ s, an angle interval $2\theta$ from 10 to 90°. The intensity of the diffraction maxima has been estimated on a100-point scale. The indexing of radiographs has been performed with the analytical method [15]. The pycnometric density has been determined with a procedure described in [16]. Toluene has been used as an indifferent liquid.

### Results and discussion

It has been found that the nanoparticle sizes of the synthesized copper-zinc manganites exceed 100 nm.

Referring to [17], if a nanoparticle has a complex shape and structure, as a result the size of its structural element is studied to be characteristic. Such particles are generally referred to as the nanostructured particles, and their linear sizes can be significantly exceeded 100 nm [17].
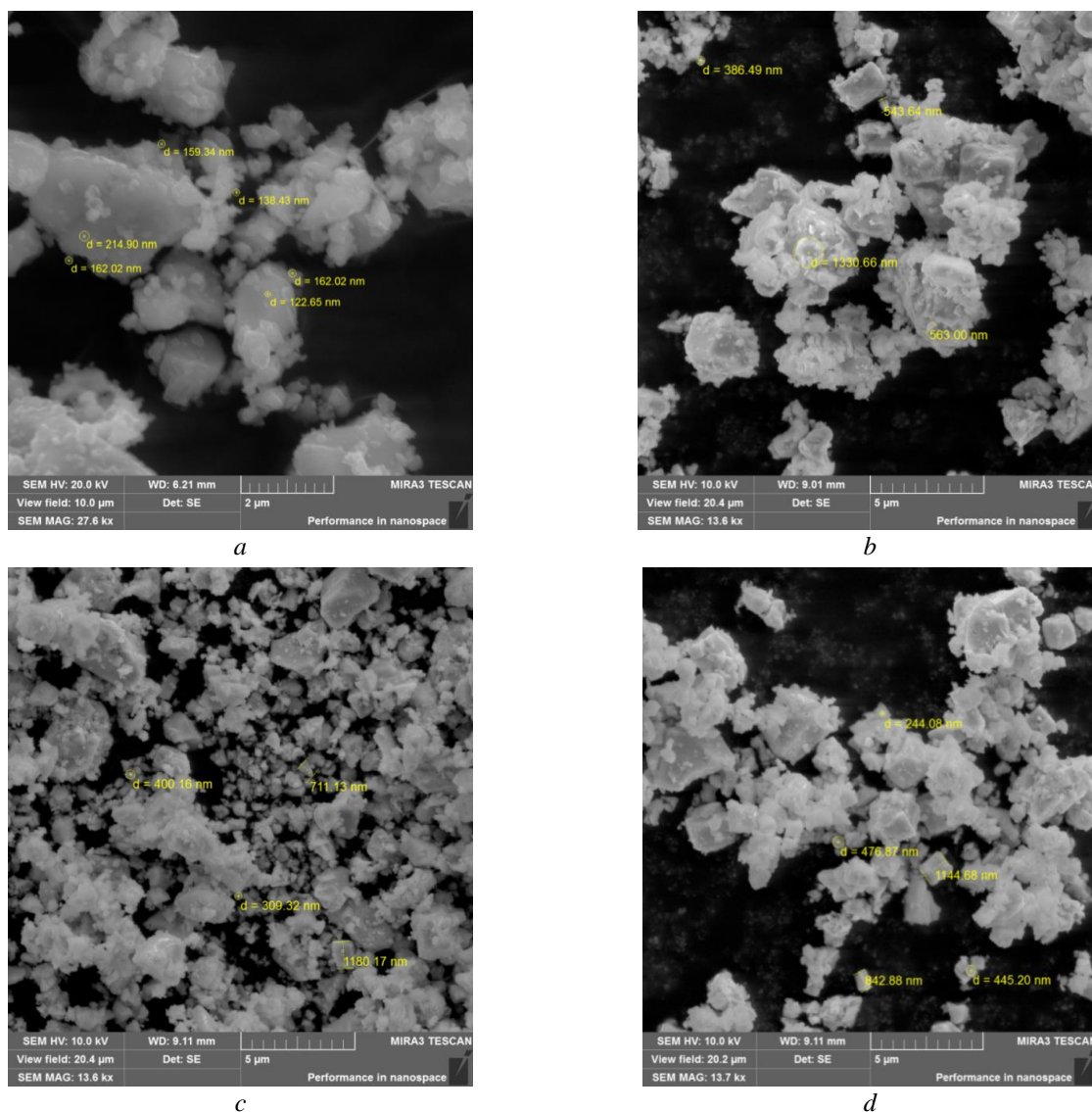


$a$ — LaMgCuZnMnO_6; $b$ — LaCaCuZnMnO_6; $c$ — LaSrCuZnMnO_6; $d$ — LaBaCuZnMnO_6

Figure. The electron microscopy of samples

It should also be pointed out that this compound can be referred to nanostructured clusters.

Referring to [18], the nanoclusters formed in the solid-phase reactions are measured from one to hundreds of nanometers.

These above mentioned arguments demonstrate that copper-zinc manganites of lanthanum and alkaline earth metals can be studied as the nanostructured nanoclusters.

The Figure illustrates that the $LaMgCuZnMnO_6$ has particles within 122.6; 138.4; 159.3: 162.0: 214.9 nm; $LaCaCuZnMnO_6$ — 386.5; 543.6; 563.0; 1330.7 nm; $LaSrMgCuZnMnO_6$ — 309.3; 400.2; 711.1 and 1180.2 nm; $LaBaCuZnMnO_6$ — 244.1; 445.2; 476.9 and 842.9 nm.

The Table demonstrates results on the indexing of radiographs of $LaMe^{II}CuZnMnO_6$ ($Me^{II}$ — Mg, Ca, Sr, Ba).

T a b l e  1

**The indexing of radiographs of $LaMe^{II}CuZnMnO_6$ ($Me^{II}$ — Mg, Ca, Sr, Ba)**

| $I/I^0$ | d, Å | $10^4/d^2$exp. | hkl | $10^4/d^2$calcul. |
|---|---|---|---|---|
| 1 | 2 | 3 | 4 | 5 |
| $LaMgCuZnMnO_6$ | | | | |
| 17 | 3.905 | 655.8 | 422 | 656.0 |
| 100 | 2.763 | 1310 | 444 | 1312 |
| 15 | 2.509 | 1588 | 730 | 1585 |
| 13 | 2.458 | 1655 | 650 | 1667 |
| 25 | 2.245 | 1984 | 661 | 1995 |
| 9 | 2.126 | 2212 | 900 | 2213 |
| 4 | 1.989 | 2528 | 8.5.3 | 2541 |
| 32 | 1.948 | 2635 | 9.4.0 | 2651 |
| 7 | 1.746 | 3280 | 10.4.2 | 3279 |
| 33 | 1.586 | 3975 | 11.5.0 | 3990 |
| 8 | 1.499 | 4450 | 991 | 4454 |
| 12 | 1.379 | 5259 | 12.7.0 | 5274 |
| 14 | 1.230 | 6610 | 15.4.1 | 6613 |
| $LaCaCuZnMnO_6$ | | | | |
| 10 | 3.862 | 670.4 | 500 | 670.0 |
| 100 | 2.738 | 1334 | 1341 | 1341 |
| 8 | 2.642 | 1433 | 1421 | 1421 |
| 13 | 2.480 | 1626 | 1636 | 1636 |
| 7 | 2.339 | 1828 | 1823 | 1823 |
| 15 | 2.233 | 2005 | 2011 | 2011 |
| 4 | 2.006 | 2485 | 2494 | 2494 |
| 35 | 1.928 | 2690 | 2682 | 2682 |
| 5 | 1.727 | 3353 | 3352 | 3352 |
| 7 | 1.626 | 3782 | 3781 | 3781 |
| 32 | 1.599 | 3911 | 3915 | 3915 |
| 15 | 1.365 | 5367 | 5363 | 5363 |
| 11 | 1.220 | 6719 | 6704 | 6704 |
| $LaSrCuZnMnO_6$ | | | | |
| 9 | 3.877 | 665.3 | 511 | 665.0 |
| 5 | 3.370 | 880.5 | 600 | 887.1 |
| 32 | 2.850 | 1231 | 550 | 1232 |
| 100 | 2.735 | 1337 | 552 | 1331 |
| 13 | 2.475 | 1632 | 741 | 1626 |
| 4 | 2.319 | 1859 | 555 | 1848 |
| 13 | 2.222 | 2025 | 910 | 2021 |
| 6 | 2.118 | 2229 | 931 | 2242 |
| 8 | 2.017 | 2458 | 10.0.0 | 2464 |
| 42 | 1.925 | 2699 | 952 | 2710 |
| 8 | 1.638 | 3727 | 12.2.2 | 3745 |
| 28 | 1.576 | 4026 | 10.8.0 | 4041 |
| 6 | 1.469 | 4634 | 13.4.2 | 4657 |

| I/I$^0$ | d, Å | 10$^4$/d$^2$exp. | hkl | 10$^4$/d$^2$calcul. |
|---|---|---|---|---|
| 1 | 2 | 3 | 4 | 5 |
| 15 | 1.363 | 5383 | 13.7.0 | 5372 |
| 12 | 1.216 | 6730 | 16.4.1 | 6727 |
| LaBaCuZnMnO$_6$ | | | | |
| 1 | 2 | 3 | 4 | 5 |
| 12 | 3.905 | 655.8 | 520 | 656.0 |
| 13 | 3.247 | 948.5 | 541 | 949.8 |
| 12 | 2.890 | 1197 | 720 | 1199 |
| 100 | 2.763 | 1310 | 730 | 1312 |
| 5 | 2.598 | 1481 | 811 | 1493 |
| 10 | 2.475 | 1632 | 822 | 1628 |
| 16 | 2.249 | 1977 | 664 | 1990 |
| 35 | 1.948 | 2635 | 10.4.1 | 2646 |
| 8 | 1.737 | 3314 | 11.5.1 | 3324 |
| 17 | 1.375 | 5289 | 12.9.3 | 5292 |
| 4 | 1.258 | 6319 | 12.10.6 | 6332 |
| 13 | 1.231 | 6599 | 17.0.0 | 6581 |

Correctness and assurance of results on the indexing have been confirmed with the experimental and calculated values of 10$^4$/d$^2$, the X-ray and pycnometric densities (Table).

Based on the indexing of radiographs of the nanostructured LaMe$^{II}$CuZnMnO$_6$ (Me$^{II}$ — Mg, Ca, Sr, Ba), it has been found that all synthesized copper-zinc manganites are crystallized in the cubic syngony with the following parameters of the lattice: LaMgCuZnMnO$_6$ — a = 13.53±0.02 Å, V$^o$ = 2476.81±0.06 Å$^3$, Z = 4, V$^o_{unit\ cell.}$ = 619.20±0.02 Å$^3$, $\rho_{x\text{-}ray.}$ = 4.52; $\rho_{pick}$ = 4.50±0.01 g/cm$^3$; LaCaCuZnMnO$_6$ — a = 13.69±0.02 Å, V$^o$ = 2565.73±0.06 Å$^3$, Z = 4, V$^o_{unit\ cell.}$ = 641.43±0.02 Å$^3$, $\rho_{x\text{-}ray}$ = 4.43; $\rho_{pick}$ = 4.41±0.01 g/cm$^3$; LaSrCuZnMnO$_6$ — a = 13.91±0.02 Å, V$^o$ = 2691.42±0.06 Å$^3$, Z = 4, V$^o_{unit\ cell}$ = 672.85±0.02 Å$^3$, $\rho_{x\text{-}ray}$ = 4.99; $\rho_{pick.}$ = 4.96±0.01 g/cm$^3$; LaBaCuZnMnO$_6$ — a = 14.55±0.02 Å, V$^o$ = 3080.27±0.06 Å$^3$, Z = 4, V$^o_{unit\ cell}$ = 770.07 ± 0.02 Å$^3$, $\rho_{x\text{-}ray}$ = 4.95; $\rho_{pick}$ = 4.94±0.01 g/cm$^3$.

Referring to [19], the obtained LaMe$^{II}$CuZnMnO$_6$ can be included in Pm3m spatial group.

In a row from Mg to Ba, the values of "a" parameters and cell volumes have been increased.

*Conclusions*

The polycrystalline copper-zinc manganites of LaMe$^{II}$CuZnMnO$_6$ have been first synthesized with a solid-phase method. Their nanostructured particles have been obtained with further milling.

Their parameters of lattices have been determined with the radiographic methods.

The results of investigations make a certain contribution to the nanochemistry, radiography of the new inorganic oxide compounds. They are a basis for further thermodynamic and electrophysical studies of the obtained nanostructured particles.

References

1   Третьяков Ю.Д. Новые поколения неорганических функциональных материалов / Ю.Д. Третьяков, О.А. Брылёв // Журн. Рос. хим. общ-ва им. Д.И. Менделеева. — 2000. — Т. 45, № 4. — С. 10–16.

2   Грюнберг П.А. От спиновых волн к гигантскому магнитосопротивлению и далее / П.А. Грюнберг // Успехи физ. наук. — 2008. — Т. 178, № 12. — С. 1349–1358.

3   Померанцев Е.А. Синтез и свойства твердого раствора CaCu$_x$Mn$_{7-x}$O$_{12}$ с колоссальным магнетосопротивлением / Е.А. Померанцев, Д.М. Иткис, Е.А. Гудилин и др. // Докл. Академии наук. — 2003. — Т. 388, № 3. — С. 344–348.

4   Чупахина Т.И. Синтез и магнитные свойства сложного оксида La$_{1,5}$Sr$_{1,5}$CuMnO$_{6,67}$ / Т.И. Чупахина, Г.В. Базуев, Е.В. Заболоцкая, М.А. Мелкозерова // Журн. неорг. хим. — 2011. — Т. 56, № 8. — С. 1248–1252.

5 Выборнов Н.А. Субмикрокристаллическое состояние и магниторезистивный эффект в горячепрессованных перовскитоподобных манганитах / Н.А. Выборнов, В.К. Карнасюк, А.М. Смирнов и др. // Перспективные материалы. — 2008. — № 4. — С. 58–63.

6 Troyanchuk I.O. Spin crossover and magnetic properties of Ba-substituted cobaltites/ I.O. Troyanchuk, M.V. Bushinsky, V.V. Sikolenko, ect. // Journal of Experimental and Theoretical Physics. — 2019. — Vol. 128, No. 1. — P. 98–104. https://doi.org/10.1134/S1063776119010047

7 Gudin S.A. Colossal magnetoresistance of layered manganite La$_{1.2}$Sr$_{1.8}$Mn$_{2(1-z)}$O$_7$ and its description by a "Spin-Polaron" conduction mechanism / S.A. Gudin, N.I. Solin, N.N. Gapontseva // Physics of the Solid State. — 2018. — Vol. 60, No. 6. — P. 1078–1081. https://doi.org/10.1134/S1063783418060112

8 Troyanchuk I.O. Causes of the metamagnetism in a disordered EuCo$_{0.5}$Mn$_{0.5}$O$_3$ perovskite / I.O. Troyanchuk, M.V. Bushinsky, N.V. Tereshko, etc. // Journal of Experimental and Theoretical Physics. — 2018. — Vol. 126, No. 6. — P. 811–815. https://doi.org/10.1134/S1063776118050072

9 Solin N.I. Exchange bias training effect in GdBaCo$_2$O$_{5.5}$ cobaltite / N.I. Solin, S.V. Naumov, S.V. Telegin // Journal of Experimental and Theoretical Physics. — 2019. — Vol. 128, No. 2. — P. 281–289. https://doi.org/10.1134/S1063776119010035

10 Giraldo-Gallo, P. Scale-invariant magnetoresistance in a cuprate superconductor / P. Giraldo-Gallo, J.A. Galvis, Z. Stegen, etc. // Science. — 2018. — Vol. 361. — P. 479-481. https://doi.org/10.1126/science.aan3178

11 Касенов Б.К. Двойные и тройные манганиты, ферриты и хромиты щелочных, щелочноземельных и редкоземельных металлов / Б.К. Касенов, Ш.Б. Касенова, Ж.И. Сагинтаева, Б.Т. Ермагамбет, Н.С. Бектурганов, И.М. Оскембеков. — М.: Научный мир, 2017. — 416 с.

12 Касенов Б.К. Новые материалы на основе оксидов s-, d- и f-элементов / Б.К. Касенов, Ш.Б. Касенова, Ж.И. Сагинтаева, Е.Е. Куанышбеков. — Караганда: ТОО «Litera», 2017. — 117 с.

13 Kasenov B.K. Physical properties of manganites / B.K. Kasenov, Sh.B.Kasenova, Zh.I.Sagintaeva, M.O. Turtubayeva, E.E. Kuanyshbekov. — Karaganda: LPP «Litera», 2017. — 123 р.

14 Касенов Б.К. Новые замещенные поликристаллические и наноразмерные манганиты / Б.К. Касенов, Ш.Б. Касенова, Ж.И. Сагинтаева, Б.Т. Ермагамбет, Е.Е. Куанышбеков, М.О. Туртубаева, А.Ж. Бектурганова. — Караганда: Экожан, 2019. — 108 с.

15 Ковба Л.М. Рентгенофазовый анализ / Л.М. Ковба, В.К. Трунов. — М.: Изд-во МГУ, 1969. — 232 с.

16 Кивилис С.С. Техника измерений плотности жидкостей и твердых тел / С.С. Кивилис. — М.: Стандартгиз, 1959. — 191 с.

17 Третьяков Ю.Д. Проблема развития нанотехнологии в России и за рубежом / Ю.Д. Третьяков, О.А. Брылёв // Вестн. РАН. — 2007. — Т. 77, № 1. — С. 3–10.

18 Сергеев П.И. Нанокластеры и нанокластерные системы. Организация, взаимодействие, свойства / П.И. Сергеев, П.И. Суздалев // Успехи химии. — 2001. — Т.70, № 3. — С. 203–240.

19 Вест А. Химия твердого топлива / А. Вест. — М.: Мир, 1988. — 588 с.

Ш.Б. Қасенова, Ж.И. Сағынтаева, Б.Қ. Қасенов, М.О. Түртібаева, А. Нұхұлы, Е.Е. Қуанышбеков, М.А. Исабаева

# LaMe$^{II}$CuZnMnO$_6$ (Me$^{II}$ — Mg, Ca, Sr, Ba) жаңа наноқұрылымды манганиттері

Сілтіліжер металдар карбонаттары мен лантана (III), мыс (II), мырыш (II) және марганец (III) тотықтарының жоғарытемпературалық әрекеттесуі арқылы LaMe$^{II}$CuZnMnO$_6$ (Me$^{II}$ — Mg, Ca, Sr, Ba) құрамды мыс-мырышты-манганиттері синтезделініп алынды. «ММ301» маркалы «Retsch» (Германия) вибрациялық диірменінде синтезделініп алынған поликристалдық мыс-мырышты-манганиттерді үгіту арқылы олардың наноқұрылымдыбөлшектері алынып, Mira3 LMU, Tescan электрондық микроскоп көмегімен олардың өлшемдері анықталды. Рентгенография әдісімен синтезделінген наноқұрылымды мыс-мырышты-манганиттердің кубтық сингонияда келесідей тор көрсеткіштермен кристалданатыны анықталды: LaMgCuZnMnO$_6$ — a = 13,53±0,02 Å, V° = 2476,81±0,06 Å$^3$, Z = 4, V°$_{эл.ұя.}$ = 619,20±0,02 Å$^3$, ρ$_{рент.}$ = 4,52; ρ$_{пикн.}$ = 4,50±0,01 г/см$^3$; LaCaCuZnMnO$_6$ — a = 13,69±0,02 Å, V° = 2565,73±0,06 Å$^3$, Z = 4, V°$_{эл.ұя.}$ = 641,43±0,02 Å$^3$, ρ$_{рент.}$ = 4,43; ρ$_{пикн.}$ = 4,41±0,01 г/см$^3$; LaSrCuZnMnO$_6$ — a = 13,91±0,02 Å, V° = 2691,42±0,06 Å$^3$, Z = 4, V°$_{эл.ұя.}$ = 672,85±0,02 Å$^3$, ρ$_{рент.}$ = 4,99; ρ$_{пикн.}$ = 4,96±0,01 г/см$^3$; LaBaCuZnMnO$_6$ — a = 14,55±0,02 Å, V° = 3080,27±0,06 Å$^3$, Z = 4, V°$_{эл.ұя.}$ = 770,07±0,02 Å$^3$, ρ$_{рент.}$ = 4,95; ρ$_{пикн.}$ = 4,94±0,01 г/см$^3$. Рентгендік зерттеулер негізінде, яғни иондық радиустардың өсуімен Mg-ден Ва-ге зерттеліп отырған мыс-мырышты-манганиттердің тор көрсеткіштер шамасы ұлғаяды. Жасалған зерттеулерді ескере отырып, бұл қосылыстарды Pm3m кеңістіктік топқа жатқызуға болады.

*Кілт сөздер:* синтез, мыс-мырышты манганит, лантан, сілтіліжер металдар, наноқұрылымды бөлшектер, электронды микроскопия, рентгенография.

Ш.Б. Касенова, Ж.И. Сагинтаева, Б.К. Касенов, М.О. Туртубаева,
А. Нухулы, Е.Е. Куанышбеков, М.А. Исабаева

# Новые наноструктурированные манганиты LaMeᴵᴵCuZnMnO₆ (Meᴵᴵ — Mg, Ca, Sr, Ba)

Высокотемпературным взаимодействием карбонатов щелочноземельных металлов с оксидами лантана (III), меди (II), цинка (II) и марганца (III) синтезированы медно-цинковые манганиты состава $LaMe^{II}CuZnMnO_6$ ($Me^{II}$ — Mg, Ca, Sr, Ba). Измельчением синтезированных поликристаллических медно-цинковых манганитов на вибрационной мельнице «Retsch» (Германия) марки «ММ301» получены их наноструктурированные частицы, размеры которых определены с помощью электронного микроскопа Mira3 LMU, Tescan. Методами рентгенографии установлено, что все синтезированные наноструктурированные медно-цинковые манганиты кристаллизуются в кубической сингонии со следующими параметрами решетки: $LaMgCuZnMnO_6$ — $a = 13{,}53 \pm 0{,}02$ Å, $V^o = 2476{,}81 \pm 0{,}06$ Å³, $Z = 4$, $V^o_{эл.яч.} = 619{,}20 \pm 0{,}02$ Å³, $\rho_{рент.} = 4{,}52$; $\rho_{пикн.} = 4{,}50 \pm 0{,}01$ г/см³; $LaCaCuZnMnO_6$ — $a = 13{,}69 \pm 0{,}02$ Å, $V^o = 2565{,}73 \pm 0{,}06$ Å³, $Z = 4$, $V^o_{эл.яч.} = 641{,}43 \pm 0{,}02$ Å³, $\rho_{рент.} = 4{,}43$; $\rho_{пикн.} = 4{,}41 \pm 0{,}01$ г/см³; $LaSrCuZnMnO_6$ — $a = 13{,}91 \pm 0{,}02$ Å, $V^o = 2691{,}42 \pm 0{,}06$ Å³, $Z = 4$, $V^o_{эл.яч.} = 672{,}85 \pm 0{,}02$ Å³, $\rho_{рент.} = 4{,}99$; $\rho_{пикн.} = 4{,}96 \pm 0{,}01$ г/см³; $LaBaCuZnMnO_6$ — $a = 14{,}55 \pm 0{,}02$ Å, $V^o = 3080{,}27 \pm 0{,}06$ Å³, $Z = 4$, $V^o_{эл.яч.} = 770{,}07 \pm 0{,}02$ Å³, $\rho_{рент.} = 4{,}95$; $\rho_{пикн.} = 4{,}94 \pm 0{,}01$ г/см³. На основании рентгенографических исследований установлено, что с повышением ионных радиусов от Mg к Ba увеличиваются величины параметров решетки исследуемых медно-цинковых манганитов. С учетом проведенных исследований можно отнести эти соединения к пространственной группе Pm3m.

*Ключевые слова:* синтез, медно-цинковый манганит, лантан, щелочноземельные металлы, наноструктурированные частицы, электронная микроскопия, рентгенография.

## References

1   Tretyakov, Yu.D., & Brylyov, O.A. (2000). Novye pokoleniia neorganicheskikh funktsionalnykh materialov [New generations of inorganic functional materials]. *Zhurnal Rossiiskogo khimicheskogo obshchestva im. D.I. Mendeleeva — Journal of the Russian Chemical Society named after D.I. Mendeleev, 44, 4*, 10–16 [in Russian].

2   Grunberg, P.A. (2008). Ot spinovykh voln k gigantskomu magnitosoprotivleniiu i dalee [From spin waves to giant magnetoresistance and further]. *Uspekhi fizicheskikh nauk — Physics-Uspekhi, 178, 12*, 1349–1358 [in Russian].

3   Pomerantsev, Ye.A. (2003). Sintez i svoistva tverdogo rastvora $CaCu_xMn_{7-x}O_{12}$ s kolossalnym magnetosoprotivleniem [Synthesis and properties of solid solution of $CaCu_xMn_{7-x}O_{12}$ with colossal magnet resistance]. *Doklady Akademii nauk — Reports of the Academy of Sciences, 388, 3*, 344–348 [in Russian].

4   Chupakhina, T.I. (2011). Sintez i magnitnye svoistva slozhnogo oksida $La_{1,5}Sr_{1,5}CuMnO_{6,67}$ [Synthesis and magnetic properties of complex oxide of $La_{1,5}Sr_{1,5}CuMnO_{6,67}$]. *Zhurnal neorganicheskoi khimii — Journal of inorganic chemistry, 56, 8*, 1248–1252 [in Russian].

5   Vybornov, N.A. (2008). Submikrokristallicheskoe sostoianie i magnitorezistivnyi effekt v goriache pressovannykh perovskito podobnykh manganitakh [Submicrocrystalline state and magnetoresistive effect in hot pressed perovskite manganites]. *Perspektivnye materialy — Promising materials, 4*, 58–63 [in Russian].

6   Troyanchuk, I.O. (2019). Spin crossover and magnetic properties of Ba-substituted cobaltites. *Journal of Experimental and Theoretical Physics, 128, 1*, 98–104. https://doi.org/10.1134/S1063776119010047

7   Gudin, S.A. (2018). Colossal magnetoresistance of layered manganite $La_{1,2}Sr_{1,8}Mn_{2(1-z)}O_7$ and its description by a "Spin-Polaron" conduction mechanism. *Physics of the Solid State, 60, 6*, 1078–1081. https://doi.org/10.1134/S1063783418060112

8   Troyanchuk, I.O. (2018). Causes of the metamagnetism in a disordered $EuCo_{0,5}Mn_{0,5}O_3$ perovskite. *Journal of Experimental and Theoretical Physics, 126, 6*, 811–815. https://doi.org/10.1134/S1063776118050072

9   Solin, N.I. (2019). Exchange bias training effect in $GdBaCo_2O_{5,5}$ cobaltite. *Journal of Experimental and Theoretical Physics, 128, 2*, 281–289. https://doi.org/10.1134/S1063776119010035

10   Giraldo-Gallo, P. (2018). Scale-invariant magnetoresistance in a cuprate superconductor. *Science, 361*, 479–481. https://doi.org/10.1126/science.aan3178

11   Kasenov, B.K., Kasenova, Sh.B., Sagintaeva, Zh.I., Ermagambet, B.T., Bekturganov, N.S., & Oskembekov, I.M. (2017). *Dvoinye i troinye manganity, ferrity i khromity shchelochnykh, shchelochnozemelnykh i redkozemelnykh metallov [Double and triple manganites, ferrites and chromites of alkali, alkaline earth and rare earth metals]*. Moscow: Nauchnyi mir [in Russian].

12   Kasenov, B.K., Kasenova, Sh.B., Sagintaeva, Zh.I., & Kuanyshbekov, E.E. (2017). *Novye materialy na osnove oksidov s-, d- i f-elementov [New materials based on oxides of s-, d- and f-elements]*. Karaganda: LPP "Litera" [in Russian].

13   Kasenov, B.K., Kasenova, Sh.B., Sagintaeva, Zh.I., Turtubaeva M.O., & Kuanyshbekov, E.E. (2017). *Physical properties of manganites*. Karaganda: LPP "Litera".

14   Kasenov, B.K., Kasenova, Sh.B., Sagintaeva, Zh.I., Yermagambet, B.T., Kuanyshbekov, E.E., Turtubaeva, M.O., & Bekturganova, A.Zh. (2019). *Novye zameshchennye polikristallicheskie i nanorazmernye manganity [New substituted polycrystalline and nanodimensional manganites]*. Karaganda: Ekozhan [in Russian].

15  Kovba, L.M., & Trunov, V.K. (1976). *Rentgenofazovyi analiz [X-ray phase analysis]*. Moscow: Moscow State Univ. Publ. [in Russian].

16  Kivilis, S.S. (1959). *Tekhnika izmerenii plotnosti zhidkostei i tverdykh tel [Technique of measuring of the density of liquids and solids]*. Moscow: Standartgiz [in Russian].

17  Tretyakov, Yu.D. (2007). Problema razvitiia nanotekhnologii v Rossii i za rubezhom [Problem of development of nanotechnology in Russia and abroad]. *Vestnik Rossiiskoi akademii nauk — Bulletin of the Russian Academy of Sciences, 77, 1*, 3–10 [in Russian].

18  Sergeev, P.I. (2001). Nanoklastery i nanoklasternye sistemy. Organizatsiia, vzaimodeistvie, svoistva [Nanoclusters and nanocluster Iscates. Organization, interaction, properties]. *Uspekhi khimii — Successes of chemistry, 70, 3*, 203–240 [in Russian].

19  Vest, A. (1988). *Khimiia tverdogo tela [Chemistry of solid state]*. Moscow: Mir [in Russian].

## Information about authors:

**Kasenova Shuga Bulatovna** — Doctor of chemical sciences, professor, chief researcher of the laboratory of thermochemical processes of Abishev Chemical-Metallurgical Institute, Karaganda, Kazakhstan; e-mail: kasenovashuga@mail.ru, ORCID: 0000-0001-9755-7478

**Sagintaeva Zhenisgul Imangalievna** — candidate of chemical sciences, associate professor, leading researcher of the laboratory of thermochemical processes of Abishev Chemical-Metallurgical Institute, Karaganda, Kazakhstan; e-mail: kai_sagintaeva@mail.ru, ORCID: 0000-0001-8655-356

**Kasenov Bulat Kunurovich** (corresponding author) — Doctor of chemical sciences, professor, head of the laboratory of thermochemical processes of Abishev Chemical-Metallurgical Institute, Karaganda, Kazakhstan; e-mail: kasenov1946@mail.ru, ORCID: 0000-0001-9394-0592

**Turtubaeva Meruert Orazgalievna** — PhD, docent of the Department of Chemistry and Chemical Technology of Toraigyrov University, Pavlodar, Kazakhstan, e-mail: azat-2000@bk.ru, ORCID: 0000-0001-7932-5075

**Kuanyshbekov Erbolat Ermekovich** — Master of engineering, researcher at the laboratory of thermochemical processes of Abishev Chemical-Metallurgical Institute, Karaganda, Kazakhstan; e-mail: mr.ero1986@mail.ru, ORCID: 0000-0001-9172-9566

**Nukhuly Altynbek** — Doctor of Chemical Sciences, Professor of Pavlodar Pedagogical University, Pavlodar, Kazakhstan; e-mail: nukhuly@mail.ru, ORCID: 0000-0001-5006-879x

**Isabaeva Manara Amangeldievna** — Candidate of Chemical Sciences, Professor of the Department of Chemistry and Chemical Technology of Toraigyrov University, Pavlodar, Kazakhstan, e-mail: isabaeva.manar@mail.ru, ORCID: 0000-0002-8119-3865

## A.A. Toibek[1], K.T. Rustembekov[1*], D.A. Kaikenov[1], M. Stoev[2]

*[1]Karagandy University of the name of academician E.A. Buketov, Kazakhstan;*
*[2]South-West University "Neofit Rilski", Blagoevgrad, Bulgaria*
*(\*Corresponding author's e-mail: rustembekov_kt@mail.ru)*

# Synthesis and properties of double gadolinium tellurites

For the first time, double gadolinium tellurites of the composition $GdM^{II}TeO_{4.5}$ ($M^{II}$ — Sr, Ba) were synthesized by the solid-phase method. The solid-phase synthesis of samples was carried out from decrepitated gadolinium (III) and tellurium (IV) oxides, strontium, and barium carbonates according to the standard ceramic technology. The synthesis was carried out in the temperature range of 800-1100 °C. The samples obtained were confirmed by X-ray phase analysis. X-ray phase analysis was carried out on an Empyrean instrument in the XRDML Pananalitical format. The intensity of the diffraction maxima was estimated on a 100-point scale. X-ray diffraction patterns indexing of the powder of gadolinium tellurites — alkaline earth metals studied were carried out by the homology method. The reliability and correctness of the results of indexing the X-ray diffraction patterns are confirmed by the good agreement between the experimental and calculated values of the interplanar distances (*d*) and the agreement between the values of the X-ray and pycnometric densities. It was found that compounds $GdSrTeO_{4.5}$ and $GdBaTeO_{4.5}$ crystallize in the monoclinic system and have the unit cell parameters, namely $GdSrTeO_{4.5}$ — $a = 12.7610$, $b = 10.4289$, $c = 8.6235$ Å, $V° = 1141.83$ Å$^3$, $\beta = 95.77°$, $Z = 5$, $\rho_{rent.} = 3.22$, $\rho_{pikn.} = (3.10\pm0.09)$ g/cm$^3$; $GdBaTeO_{4.5}$ — $a = 15.7272$, $b = 15.8351$, $c = 7.1393$ Å, $V° = 1769.72$ Å$^3$, $\beta = 95.53°$, $Z = 8$, $\rho_{rent} = 3.71$, $\rho_{pick} = (3.61\pm0.10)$ g/cm$^3$. Using the Landiya method, the standard heat capacities of the compounds were estimated from the calculated values of the standard entropies, and the temperature dependences of the heat capacities of the gadolinium tellurites synthesized were determined in the temperature range of 298–850 K.

*Keywords:* double gadolinium tellurites, X-ray phase analysis, crystal system, lattice parameters, heat capacity.

## Introduction

It is known that tellurium compounds with metals have semiconducting properties and superconductivity, such as transition and non-transition metals tellurites. On the other hand, chalcogen compounds containing three or more elements tend to polymerize, especially if in addition to tellurium there is an oxygen atom in the composition. These kinds of compounds are used in the non-organic synthesis of composite materials with organic substances.

Tellurium derivatives are characterized by high chemical activity, which determines the prospects of synthetic transformations aimed at obtaining new semiconductor, ferroelectric, and radioluminescent materials of a wide range of implementations. Recently, the attention of scientists has been especially attracted by compounds based on rare earth, alkaline earth oxides, and transition metals in connection with their properties in microelectronics [1]. The investigation of complex oxides of 3d- and 4f- elements with a perovskite structure has great importance for non-organic materials science [2, 3]. In this regard, the purpose of this work was to synthesize and study the properties of new phases — double tellurites of gadolinium with composition $GdM^{II}TeO_{4.5}$ ($M^{II}$ — Sr, Ba).

## Experimental

The solid-phase synthesis of samples was carried out according to the standard ceramic technology from decrepitated gadolinium (III) and tellurium (IV) oxides, strontium, and barium carbonates. The stoichiometric amounts of the original materials were thoroughly mixed and ground in an agate mortar. Then they were annealed in alundum crucibles in a SNOL furnace. The following heat treatment mode was used, namely, Stage I for 15 hours at 400 °C, Stage II 20 hours at 800 °C, Stage III 20 hours at 1100 °C, then annealing was carried out at 400 °C for 20 hours in order to obtain stable compounds at low temperatures. After each stage, the mixtures were cooled, mixed, and thoroughly ground.

An X-ray study of the equilibrium compositions of the tellurites synthesized was carried out on an Empyrean device. Empyrean is the only platform that offers many benefits and high data accuracy for all sample types. This instrument is designed for a wide range of applications that include X-ray diffraction and X-ray scattering, as well as X-ray imaging. The Empyrean is designed to operate at 60 kV, which is optimal for X-ray

tubes with an anode of Mo and Ag. The intensity of the diffraction maxima was evaluated on a 100-point scale. The X-ray diffraction patterns of the obtained compounds were indexed by the homology method [4].

The pycnometric density of tellurites was determined by the method [5]. Toluene served as an indifferent liquid. The density of each tellurite was measured 3–5 times and the data was averaged.

Using the Landiya method [6], the standard heat capacities of the compounds were estimated from the calculated values of the standard entropies, and the temperature dependences of the heat capacities of the gadolinium tellurites synthesized were determined in the temperature range of 298–850 K.

### Results and Discussion

X-ray phase analysis consists in identifying crystalline phases based on their inherent interplanar distances $d_{(hkl)}$ and the corresponding line intensities $I_{(hkl)}$ of the X-ray spectrum. The individuality and distribution of atoms determine the intensity of the diffracted rays. A powder diffraction pattern is an individual characteristic of a crystalline substance [7].

Figure 1 shows X-ray diffraction patterns of double gadolinium tellurites synthesized.
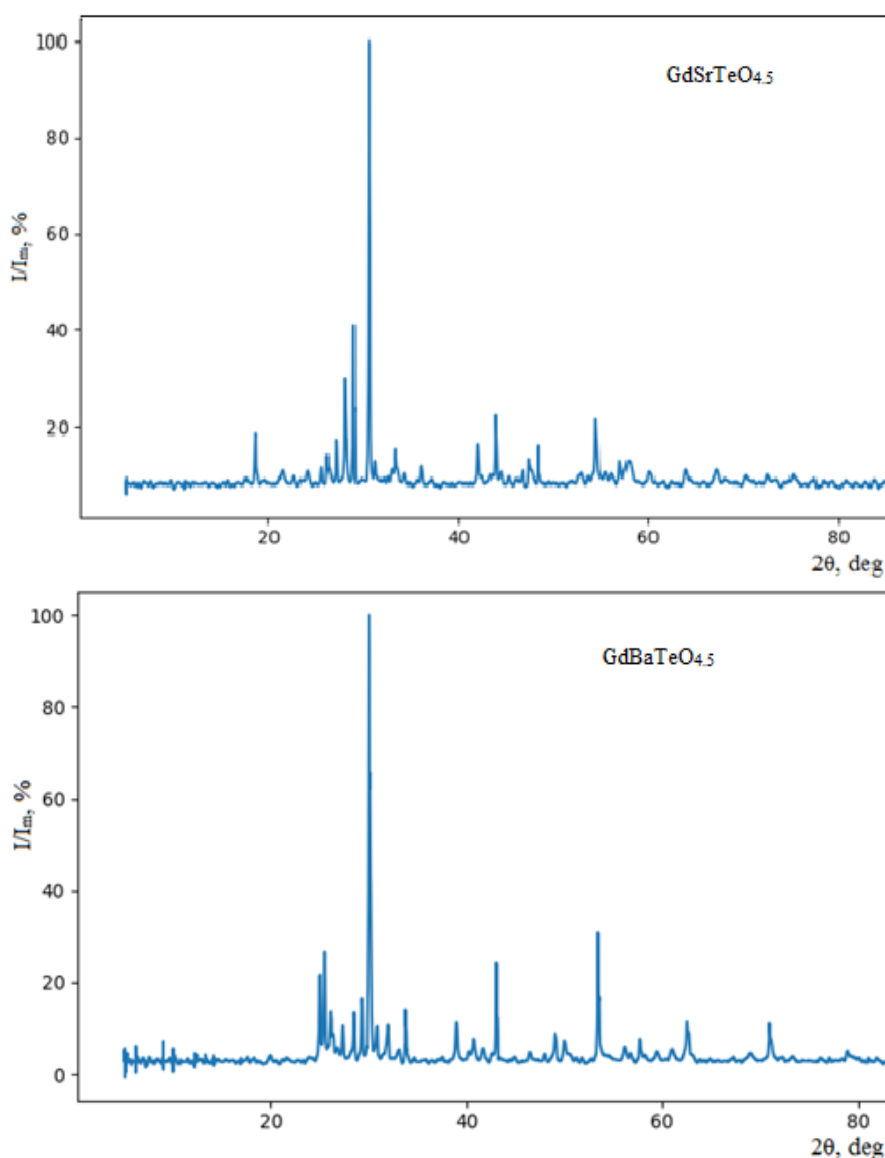


Figure 1. X-ray diffraction of the double-tellurite synthesized

The results of indexing the X-ray diffraction patterns of gadolinium tellurites synthesized are presented in Table 1.

**Radiographs indexing of tellurite GdM$^{II}$TeO$_{4,5}$(M$^{II}$ — Sr, Ba) synthesized**

| h | k | l | d$_{obs.}$, Å | d$_{calc.}$, Å | 2 th$_{obs}$, deg | 2 th$_{calc}$, deg | I/I$_{max}$ (%) |
|---|---|---|---|---|---|---|---|
| | | | | GdSrTeO$_{4.5}$ | | | |
| 2 | 1 | -1 | 4.76531 | 4.76827 | 18.605 | 18.593 | 11.56 |
| 1 | 2 | 1 | 4.13362 | 4.13439 | 21.480 | 21.476 | 3.44 |
| 3 | 1 | 0 | 3.92007 | 3.91936 | 22.665 | 22.669 | 1.86 |
| 3 | 1 | -1 | 3.69242 | 3.69683 | 24.083 | 24.053 | 2.64 |
| 0 | 3 | 0 | 3.47500 | 3.47408 | 25.614 | 25.621 | 4.03 |
| 2 | 0 | 2 | 3.39862 | 3.39690 | 26.200 | 26.213 | 6.06 |
| 3 | 2 | 0 | 3.28648 | 3.28438 | 27.111 | 27.128 | 9.63 |
| 3 | 0 | -2 | 3.17599 | 3.17418 | 28.073 | 28.089 | 18.58 |
| 4 | 0 | 0 | 3.17599 | 3.17278 | 28.073 | 28.102 | 18.58 |
| 4 | 0 | -1 | 3.07721 | 3.07777 | 28.993 | 28.988 | 35.75 |
| 2 | 3 | -1 | 2.91623 | 2.91613 | 30.632 | 30.633 | 100.00 |
| 0 | 0 | 3 | 2.85710 | 2.85733 | 31.282 | 31.279 | 4.29 |
| 2 | 0 | -3 | 2.70951 | 2.70922 | 33.033 | 33.037 | 1.64 |
| 3 | 2 | -2 | 2.70951 | 2.71110 | 33.033 | 33.013 | 1.64 |
| 4 | 2 | 0 | 2.70951 | 2.71023 | 33.033 | 33.024 | 1.64 |
| 3 | 3 | 0 | 2.68234 | 2.68506 | 33.378 | 33.343 | 5.52 |
| 4 | 0 | -2 | 2.68234 | 2.68220 | 33.378 | 33.380 | 5.52 |
| 0 | 4 | 0 | 2.60492 | 2.60591 | 34.400 | 34.387 | 2.28 |
| 1 | 3 | 2 | 2.60492 | 2.60676 | 34.400 | 34.375 | 2.28 |
| 3 | 0 | -3 | 2.48651 | 2.48655 | 36.093 | 36.093 | 4.16 |
| 1 | 3 | 3 | 2.14720 | 2.14661 | 42.046 | 42.059 | 8.35 |
| 6 | 1 | -1 | 2.06222 | 2.06207 | 43.867 | 43.870 | 14.88 |
| 2 | 3 | 3 | 2.03531 | 2.03632 | 44.478 | 44.454 | 2.24 |
| 5 | 3 | -1 | 2.03111 | 2.03126 | 44.575 | 44.571 | 1.72 |
| 5 | 0 | -3 | 2.00034 | 2.00021 | 45.298 | 45.301 | 1.78 |
| | | | | GdBaTeO$_{4.5}$ | | | |
| 0 | 0 | 2 | 3.55333 | 3.55306 | 25.040 | 25.042 | 16.47 |
| 4 | 1 | -1 | 3.49081 | 3.48785 | 25.496 | 25.518 | 21.87 |
| 1 | 4 | -1 | 3.40853 | 3.41004 | 26.122 | 26.111 | 9.03 |
| 4 | 2 | -1 | 3.25760 | 3.25868 | 27.356 | 27.346 | 7.19 |
| 5 | 0 | 0 | 3.13071 | 3.13077 | 28.487 | 28.487 | 9.72 |
| 4 | 2 | 1 | 3.04373 | 3.04372 | 29.319 | 29.319 | 12.82 |
| 5 | 0 | -1 | 2.97033 | 2.97194 | 30.061 | 30.044 | 100.00 |
| 0 | 5 | 1 | 2.89253 | 2.89227 | 30.889 | 30.892 | 6.74 |
| 4 | 3 | 1 | 2.79599 | 2.79629 | 31.984 | 31.980 | 7.69 |
| 3 | 5 | 0 | 2.70704 | 2.70698 | 33.064 | 33.065 | 7.69 |
| 3 | 2 | 2 | 2.65330 | 2.65161 | 33.754 | 33.776 | 10.43 |
| 4 | 4 | -1 | 2.55330 | 2.65330 | 33.754 | 33.754 | 10.43 |
| 1 | 0 | 3 | 2.30952 | 2.30958 | 38.967 | 38.966 | 8.29 |
| 7 | 1 | 0 | 2.21459 | 2.21429 | 40.709 | 40.715 | 3.84 |
| 1 | 3 | -3 | 2.16622 | 2.16651 | 41.660 | 41.654 | 21.48 |
| 5 | 5 | -1 | 2.16622 | 2.16697 | 41.660 | 41.645 | 21.48 |
| 6 | 3 | 1 | 2.16622 | 2.16702 | 41.660 | 41.644 | 21.48 |
| 4 | 1 | -3 | 2.09957 | 2.09956 | 43.047 | 43.047 | 3.78 |
| 2 | 7 | -1 | 2.09470 | 2.09348 | 43.152 | 43.179 | 3.78 |
| 5 | 4 | -2 | 2.09470 | 2.09495 | 43.152 | 43.147 | 3.78 |
| 5 | 3 | -3 | 1.85549 | 1.85589 | 49.057 | 49.046 | 5.75 |
| 6 | 6 | 0 | 1.85549 | 1.85524 | 49.057 | 49.064 | 5.75 |
| 3 | 7 | -2 | 1.82256 | 1.82241 | 50.004 | 50.008 | 3.70 |

*Notes*. hkl — Miller indices; d$_{obs.}$ — experimental interplanar distances; d$_{cal.}$ — calculated interplanar distances; 2th$_{obs.}$ — experimental double angle of Bragg reflection; 2th$_{calc.}$ — calculated double angle of Bragg reflection; I/I$_{max.}$ — is the relative intensity of the X-ray patterns.

As can be seen from the data in Table 1, the experimental and calculated values of (d) and the X-ray and pycnometric densities values (Table 2) are in satisfactory agreement with each other, which shows the reliability and correctness of indexing results.

Based on indexing radiographs of tellurites investigated, it was found that the compounds GdSrTeO$_{4.5}$ and GdBaTeO$_{4.5}$ crystallize in the monoclinic system and have the unit cell parameters presented in Table 2.

T a b l e  2

**Type of syngonies and tellurites unit cell parameters**

| Compound | Syngony type | The lattice parameters, Å | | | V$^0$, Å$^3$ | β, deg. | Z | Density, g/cm$^3$ | |
|---|---|---|---|---|---|---|---|---|---|
| | | a | b | c | | | | Radiog. | Pycnom. |
| GdSrTeO$_{4.5}$ | monoclinic | 12.7610 | 10.4289 | 8.6235 | 1141.83 | 95.77 | 5 | 3.22 | 3.10±0.09 |
| GdBaTeO$_{4.5}$ | monoclinic | 15.7272 | 15.8351 | 7.1393 | 1769.72 | 95.53 | 8 | 3.71 | 3.61±0.10 |

According to ASTM card files reference databases [8], tellurites synthesized X-ray diffraction patterns have been compared with X-ray indices [I/I$_0$, d] of original materials and with possible tellurites of this system. It was revealed that the diffractograms of new tellurites had no analogues. This data additionally confirms that synthesized tellurites are new compounds.

X-ray diffraction data shows that synthesized tellurites crystallize in the structural types of distorted perovskite P$_m$3$_m$. It allows supposing that these compounds can have unique electrophysical properties [9–12].

To calculate the temperature dependence of the heat capacities of the gadolinium tellurites synthesized, we chose the Landiya method [6], which is the most reliable of those available in the literature. The standard entropies were calculated using the Kumok ion increment method [13]. Using the Landiya method, the standard heat capacities of tellurites were estimated from the calculated values of the standard entropies, and the temperature dependences of the heat capacity were calculated using the Mayer-Kelly equation. The calculation results are shown in Table 3.

T a b l e 3

**Calculated heats capacity of double gadolinium tellurites in the range of 298-831 K**

| T, K | C$_p^0$, J/(mol·K) | | T, K | C$_p^0$, J/(mol·K) | |
|---|---|---|---|---|---|
| | GdSrTeO$_{4.5}$ | GdBaTeO$_{4.5}$ | | GdSrTeO$_{4.5}$ | GdBaTeO$_{4.5}$ |
| 298.15 | 152.84 | 154.42 | 575 | 181.69 | 177.19 |
| 300 | 153.20 | 154.37 | 600 | 183.47 | 180.38 |
| 325 | 157.31 | 154.36 | 625 | 185.19 | 183.65 |
| 350 | 160.86 | 155.12 | 650 | 186.87 | 186.97 |
| 375 | 163.98 | 156.46 | 675 | 188.52 | 190.34 |
| 400 | 166.78 | 158.25 | 700 | 190.14 | 193.75 |
| 425 | 169.33 | 160.37 | 725 | 191.73 | 197.20 |
| 450 | 171.69 | 162.76 | 750 | 193.30 | 200.68 |
| 475 | 173.90 | 165.36 | 775 | 194.85 | 204.18 |
| 500 | 175.98 | 168.13 | 780 | 195.15 | 204.89 |
| 525 | 177.96 | 171.04 | 800 | 196.38 | |
| 550 | 179.86 | 174.07 | 831 | 198.26 | |

Figure 2 below depicts graphically the temperature dependences of the heat capacity of the tellurites investigated.
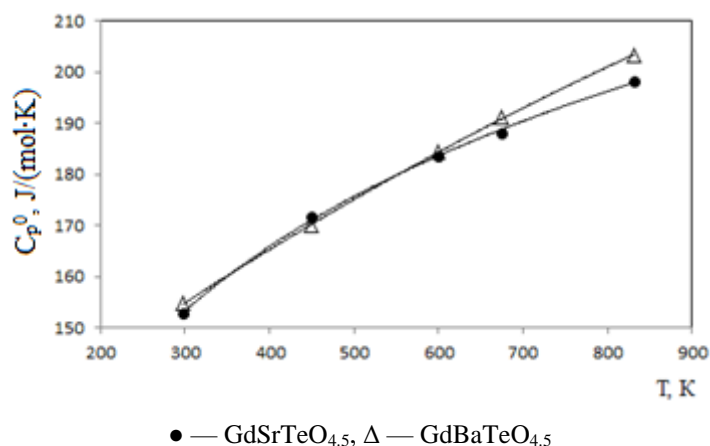
● — GdSrTeO$_{4.5}$, Δ — GdBaTeO$_{4.5}$

Figure 2. The temperature dependence of tellurites heat capacity

Thus, based on the calculated values of S°(298.15) by the Landiya method, for the first time, the estimated values of the standard heat capacity of double gadolinium tellurites are given and their equations for the temperature dependence of the heat capacities are derived. The obtained values of the standard heat capacities of tellurites are equal for GdSrTeO$_{4.5}$ (152.84±9.23) and GdBaTeO$_{4.5}$ (154.42±10.22) J/(mol·K). Equations of the temperature dependence of the heat capacity are as follows:

for GdSrTeO$_{4.5}$ $\qquad$ $C_p^0 = 37.16 + 13 \cdot 10^{-3} T - 4.0 \cdot 10^5 \cdot T^{-2}$ (298–831 K),

for GdBaTeO$_{4.5}$ $\qquad$ $C_p^0 = 19.98 + 36 \cdot 10^{-3} T + 5.5 \cdot 10^5 \cdot T^{-2}$ (298–780 K).

## Conclusions

New double gadolinium-strontium GdSrTeO$_{4.5}$ and gadolinium-barium GdBaTeO$_{4.5}$ tellurites were synthesized by the method of ceramic technology. The formation of equilibrium compositions in the compounds synthesized was controlled by X-ray phase analysis. The XRF method was used to determine the system types, unit cell parameters, X-ray, and pycnometric densities. Tellurites crystallize in the structural types of distorted perovskite P$_m$3$_m$. It allows supposing that these compounds can have unique electrophysical properties.

Using the Landiya method, the compounds standard heat capacities were estimated from the standard entropies calculated values, and the heat capacities temperature dependence of the tellurites synthesized in the temperature range of 298–850 K was presented. The data obtained is of certain interest for chemistry and non-organic materials science of rare earth elements and chalcogenes complex oxide compounds.

## References

1 Ерин Ю. Найдено вещество с гигантским значением диэлектрической проницаемости / Ю. Ерин // Химия и химики. — 2009. — № 1. — С. 16–22. http://chemistryandchemists.narod.ru.

2 Третьяков Ю.Д. Новые поколения неорганических функциональных материалов / Ю.Д. Третьяков, О.А. Брылев // Журн. Рос. хим. об-ва им. Д.И. Менделеева. — 2000. — Т. 45, № 4. — С. 10.

3 Рустембеков К.Т. Оксоселениты, селенаты и теллуриты ряда s-, d- и f-элементов: моногр. / К.Т. Рустембеков. — Караганда: Гласир, 2018. — 252 с.

4 Ковба Л.М. Рентгенофазовый анализ / Л.М. Ковба, В.К. Трунов. — М.: Изд-во МГУ, 1976. — 256 с.

5 Кивилис С.С. Техника измерений плотности жидкостей и твердых тел / С.С. Кивилис. — М.: Стандартгиз, 1959. — 191 с.

6 Ландия Н.А. Расчет высокотемпературных теплоемкостей твердых неорганических веществ по стандартной энтропии / Н.А. Ландия. — Тбилиси: Изд-во АН ГрузССР, 1962. — 221 с.

7 Кузнецова Г.А. Качественный рентгенофазовый анализ: метод. указ. / Г.А. Кузнецова. — Иркутск, 2005. — С. 28.

8 [Электронный ресурс]. Режим доступа: http://docs.cntd.ru/search/internationalstandards/astm/offset/1000

9 Шрайвер Д. Неорганическая химия / Д. Шрайвер, П. Эткинс. — М.: Мир, 2004. — Т. 1. — С. 83.

10 Rustembekov K.T. Tellurites of some s-f-elements: synthesis, X-Ray diffraction, and electrophysical properties / K.T. Rustembekov, A.T. Dyusekeeva // Russian Journal of General Chemistry. — 2012. — Vol.82, No. 8. — P. 1357–1360. https://doi.org/10.1134/S1070363212080051.

11 Rustembekov K.T. Lanthanum – magnesium – nicel tellurite: thermodynamic and electrophysical characteristic / K.T. Rustembekov, M.S. Kasymova, Ye.V. Minayeva, A. Zh. Bekturganova // Bulletin of the Karaganda University. Chemistry series. — 2019. — No. 2(94). — P. 69–75. https://doi.org/10.31489/2019Ch2/69-75.

12 Rustembekov K.T. Thermodynamic and Electrophysical Properties of La₂SrNiTeO₇ / K.T. Rustembekov, B.K. Kasenov, A. Zh. Bekturganova, M.S. Kasymova // Russian Journal of Physical chemistry A. — 2019. — Vol. 9. — P. 1657–1661. https://doi.org/10.1134 / S003602441909020.

13 Кумок В.Н. Прямые и обратные задачи химической термодинамики / В.Н. Кумок. — Новосибирск: Наука, 1987. — С. 108.

А.А. Тойбек, К.Т. Рустембеков, Д.А. Кайкенов, М.Стоев

## Гадолиний қос теллуриттерінің синтезі және қасиеттері

Алғаш рет қатты фазалық әдіспен GdM$^{II}$TeO$_{4,5}$ (M$^{II}$ — Sr, Ba) құрамды гадолинийдің қос теллуриттері синтезделді. Үлгілердің қатты фазалық синтезі алдын-ала күйдірілген гадолиний (III) және теллур (IV) оксидтері, стронций және барий карбонаттарынан стандартты керамикалық технология бойынша іске асырылды. Синтез 800–1100 °C температура аралығында жүргізілді. Алынған үлгілер рентгенфазалық анализ әдісімен зерттелді. Рентгенфазалық анализ Empyrean қондырғысында жүргізілді. Дифракциялық максимумдардың қарқындылығы жүз балдық шкаламен бағаланды. Зерттелетін гадолиний — жерсілтілік металдары теллуриттерінің ұнтақтарының рентгенограммаларын индицирлеу гомология әдісімен жүргізілді. Рентгенограммаларды индицирлеу нәтижелерінің дұрыстығын және дәлдігін жазықтықаралық қашықтықтың (d) тәжірибелік және есептелген мәндері мен рентгендік және пикнометрлік тығыздықтарының мәндерінің сәйкестігі дәлелдейді. GdSrTeO$_{4,5}$ және GdBaTeO$_{4,5}$ қосылыстары моноклинді сингонияда кристалданатыны және келесідей элементарлық ұяшық параметрлері табылды: GdSrTeO$_{4,5}$ — a = 12,7610, b = 10,4289, c = 8,6235 Å, V° = 1141,83 Å³, β = 95,77°, Z = 5, ρ$_{рент.}$ = 3,22, ρ$_{пикн}$ = (3,10±0,09) г/см³; GdBaTeO$_{4,5}$ — a = 15,7272, b = 15,8351, c = 7,1393 Å, V° = 1769,72 Å³, β = 95,53°, Z = 8, ρ$_{рент.}$ = 3,71, ρ$_{пикн.}$ = (3,61±10) г/см³. Ландия әдісімен есептелген стандартты энтропия мәндерінен қосылыстардың стандартты жылу сыйымдылықтары табылды және 298-850 К температура аралығында синтезделген гадолиний теллуриттерінің жылу сыйымдылықтарының температуралық тәуелділіктері анықталды.

*Кілт сөздер:* гадолиний қос теллуриттері, рентгенфазалық анализ, сингония, тор параметрлері, жылу сыйымдылық.

А.А. Тойбек, К.Т. Рустембеков, Д.А. Кайкенов, М. Стоев

## Синтез и свойства двойных теллуритов гадолиния

Твердофазным методом впервые синтезированы двойные теллуриты гадолиния состава GdM$^{II}$TeO$_{4,5}$ (M$^{II}$ — Sr, Ba). Твердофазный синтез образцов был осуществлен по стандартной керамической технологии из предварительно прокаленных оксидов гадолиния (III) и теллура (IV), карбонатов стронция и бария. Синтез проводился в температурном интервале 800–1100 °C. Полученные образцы были аттестованы методом рентгенофазового анализа. Рентгенофазовый анализ проведен на приборе *Empyrean*. Интенсивность дифракционных максимумов оценивалась по стобалльной шкале. Индицирование рентгенограмм порошка исследуемых теллуритов гадолиния — щелочноземельных металлов проводили методом гомологии. Достоверность и корректность результатов индицирования рентгенограмм подтверждаются хорошим соответствием экспериментальных и расчетных значений межплоскостных расстояний (d) и согласованностью величин рентгеновской и пикнометрической плотностей. Установлено, что соединения GdSrTeO$_{4,5}$ и GdBaTeO$_{4,5}$ кристаллизуются в моноклинной сингонии и имеют параметры элементарных ячеек: GdSrTeO$_{4,5}$ — a = 12,7610, b = 10,4289, c = 8,6235 Å, V° = 1141,83 Å³, β = 95,77°, Z = 5, ρ$_{пикн.}$ = 3,22, ρ$_{пикн.}$ = (3,10±0,09) г/см³; GdBaTeO$_{4,5}$ — a = 15,7272, b = 15,8351, c = 7,1393 Å, V° = 1769,72 Å³, β = 95,53°, Z = 8, ρ$_{рент.}$ = 3,71, ρ$_{пикн.}$ = (3,61±0,10) г/см³. Методом Ландия из вычисленных значений стандартных энтропий рассчитаны стандартные теплоемкости соединений, определены температурные зависимости теплоемкостей синтезированных теллуритов гадолиния в интервале температур 298–850 К.

*Ключевые слова:* двойные теллуриты гадолиния, рентгенофазовый анализ, сингония, параметры решетки, теплоемкость.

## References

1 Yerin, Y. (2009). Naideno veshchestvo s gigantskim znacheniem dielektricheskoi pronitsaemosti [Found a substance with a giant value of the dielectric constant]. *Khimiia i khimiki — Chemistry and chemists, 1*, 16–22. http://chemistryandchemists.narod.ru [in Russian].

2    Tretyakov, Yu.D., & Brylev, O.A. (2000). *Novye pokoleniia neorganicheskikh funktsionalnykh materialov [New generations of inorganic functional materials] Zhurnal Rossiiskogo khimicheskogo obshchestva im. D.I. Mendeleeva — Journal of the Russian Chemical Society D.I. Mendeleev, 45, 4,* 10 [in Russian].

3    Rustembekov, K.T. (2018). *Oksoselenity, selenaty i tellurity riada s-, d- i f-elementov [Oxoselenites, selenates and tellurites of a series of s-, d- and f-elements].* Karaganda: Glasir [in Russian].

4    Covba, L.M., & Trunov, V.K. (1976). *Rentgenofazovyi analiz [X-ray phase analysis].* Moscow: Publishing house of Moscow State University [in Russian].

5    Kivilis, S.S. *Tekhnika izmerenii plotnosti zhidkostei i tverdykh tel [Technique for measuring the density of liquids and solids].* Moscow: Standartgiz [in Russian].

6    Landia, N.A. (1962). *Raschet vysokotemperaturnykh teploemkostei tverdykh neorganicheskikh veshchestv po standartnoi entropii [Calculation of high-temperature heat capacities of solid inorganic substances by standard entropy].* Tbilisi: Publishing House of the Academy of Sciences of the Georgian SSR [in Russian].

7    Kuznetsova, G.A. (2005). *Kachestvennyi rentgenofazovyi analiz [Qualitative X-ray phase analysis].* Irkutsk [in Russian].

8    Retrieved from http://docs.cntd.ru/search/internationalstandards/astm/offset/1000 [in Russian].

9    Shriver, D., & Atkins, P. (2004). *Neorganicheskaia khimiia [Inorganic chemistry].* Moscow: Mir [in Russian].

10   Rustembekov, K.T., & Dyusekeeva, A.T. (2012). Tellurites of some s-f-elements: synthesis, X-ray diffraction, and electrophysical properties. *Russian Journal of General Chemistry, 82, 8,* 1357–1360. https://doi.org/10.1134/S1070363212080051

11   Rustembekov, K.T., Kasymova, M.S., Minayeva, Ye.V., & Bekturganova, A. Zh. (2019). Lanthanum – magnesium – nicel tellurite: thermodynamic and electrophysical characteristic. *Bulletin of the University of Karaganda — Chemistry, 94–2,* 69–75. https://doi.org/10.31489/2019Ch2/69-75

12   Rustembekov, K.T., Kasenov, B.K., Bekturganova, A. Zh., & Kasymova, M.S. (2019). Thermodynamic and Electrophysical Properties of $La_2SrNiTeO_7$. *Russian Journal of Physical chemistry A. 9,* 1657–1661. https://doi.org/10.1134 / S003602441909020

13   Kumok, V.N. (1987). *Priamye i obratnye zadachi khimicheskoi termodinamiki [Direct and Inverse Problems of Chemical Thermodynamics].* Novosibirsk: Nauka [in Russian].

## Information about authors:

**Toibek Aitolkyn Ablaikyzy** — PhD student Faculty of Chemistry Karagandy University of the name of academician E.A. Buketov, Universitetskaya str., 28, 100024, Karaganda, Kazakhstan; e-mail: aitoka_95@mail.ru; https://orcid.org/0000-0002-8616-5257;

**Rustembekov Kenzhebek Tusupovich** — Academician of Kazakhstan National Academy of Natural Sciences (KazNaNs), Doctor of chemical sciences, Professor, Karagandy University of the name of academician E.A. Buketov, Universitetskaya str., 28, 100024, Karaganda, Kazakhstan; e-mail: rustembekov_kt@mail.ru; https://orcid.org/0000-0003-0853-523X;

**Kaikenov Dauletkhan Asanovich** — Leading researcher of the laboratory of engineering profile "Physical and chemical methods of research", Karagandy University of the name of academician E.A. Buketov, Universitetskaya str., 28, 100024, Karaganda, Kazakhstan; e-mail: krg.daykai@mail.ru;

**Stoev Mitko** — PhD, Associate Professor, South-West University "Neofit Rilski", Blagoevgrad, Bulgaria.

# CHEMICAL TECHNOLOGY

M.I. Baikenov[1,2], D.E. Aitbekova[1*], N.Zh. Balpanova[1], A. Tusipkhan[1], G.G. Baikenova[2, 3], Y.A. Aubakirov[4], A.R. Brodskiy[5], Fengyun Ma[6], D.K. Makenov[1]

[1]*Karagandy University of the name of academician E.A. Buketov, Kazakhstan;*
[2]*South Ural State University, Chelyabinsk, Russia;*
[3]*Karagandy Economic University of Kazpotrebsoyuz, Kazakhstan;*
[4]*Al-Farabi Kazakh National University, Almaty, Kazakhstan;*
[5]*D.V. Sokolskiy Institute of Fuel, Catalysis and Electrochemistry, Almaty, Kazakhstan;*
[6]*Xinjiang University, Xinjiang Uyghur Autonomous Region, People's Republic of China*
*(\*Corresponding author's e-mail: darzhan91@mail.ru)*

## Hydrogenation of polyaromatic compounds over NiCo/chrysotile catalyst

The activity and selectivity of the bimetallic NiCo/chrysotile catalyst during the hydrogenation of model objects (anthracene and phenanthrene) for 1 hour at an initial hydrogen pressure of 3 MPa and a temperature of 400 °C were studied. The chrysotile mineral used as a substrate for active centers of nickel and cobalt is a waste product of asbestos production at Kostanay Minerals JSC (the Republic of Kazakhstan). The catalyst was characterized by a complex of methods of physical and chemical analysis. The chrysotile mineral consists of nanotubes with an inner diameter of about 10 nm and an outer diameter of about 60 nm. The amount of hydrogenation products is 61.91 %, destruction — 15.08 % and isomerization — 8.37 % during the hydrogenation of anthracene. The amount of hydrogenation products is 26.09 %, and that of destruction is 2.51 % during the hydrogenation of phenanthrene. It was found that the catalyst selectively accelerates the hydrogenation reaction and allows increasing the yields of hydrogenation products. The schemes of the hydrogenation reaction of model objects were drawn up according to the results of gas chromatography-mass spectrometric analysis of hydrogenates.

*Keywords*: polyaromatic hydrocarbons, anthracene, phenanthrene, nanocatalyst, hydrogenation, chrysotile, nickel, cobalt.

### Introduction

Research on the processing of heavy and solid hydrocarbon raw materials has been a topical theme in recent years. Increasing the depth of processing of heavy oil residues, primary coal tar and improving the quality of the obtained low-boiling low-molecular compounds are one of the key areas of coal and oil refining [1, 2]. Heavy oil residue and primary coal tar usually contain a large amount of undesirable aromatic compounds and are much more difficult to convert into a pure transport fuel. In this regard, the hydrotreating process is introduced into the structure of coal and oil refining, which makes it possible to obtain a wide range of products of high demand [3, 4].

Therefore it is highly desirable to improve the efficiency of aromatic hydrogenation. This can be achieved by optimizing the process and improving the catalysts, which in turn requires a deeper understanding of the aromatic hydrogenation process.

Comparison with previous studies has shown that the nature of the catalyst strongly affects the relative reactivity of aromatic compounds [5]. Currently there is a wide range of catalysts for the hydroconversion of heavy hydrocarbon feedstock, which are due to their various purposes. As is known, metals of the VIII group of the periodic system (nickel, cobalt, iron) are usually used as the hydrogenating component [6, 7], as well as oxides and sulfides of the metals of the VIII group [6, 8]. It is known from literary sources [8, 9] that a combination of nickel and tungsten has a greater hydrogenating activity.

Model combinations, such as anthracene, phenanthrene, pyrene, naphthalene, etc., are often used to determine the mechanisms of activity and selectivity of the selected catalysts in the hydrogenation process, which make it possible to establish a more detailed mechanism for heavy hydrocarbons concentration and scientifically based methods for predicting their control [10].

Sahle-Demessie et al. [11] and Liu et al. [12] show the results of catalytic hydrogenation, where anthracene is hydrogenated to di-, tetra- and octa-hydroanthracene, depending on the conditions. Phenanthrene, in comparison with the linear isomer — anthracene, undergoes hydrogenation more difficultly [13, 14]. A completely hydrogenated molecular form — perhydrophenanthrene was obtained along with di-, tetra- and octa-hydroderivatives under more severe conditions and in a larger amount of catalyst [15].

The aim of this work is to evaluate the activity and selectivity of the NiCo/chrysotile catalyst during the hydrogenation of polyaromatic model objects, such as anthracene and phenanthrene.

## Experimental

### Obtaining and physicochemical studies of the catalyst

Preliminary leaching with a 20 % hydrochloric acid solution was carried out to remove magnesium and calcium salts in the original chrysotile. The preparation of a binary catalyst was carried out by first dissolving nickel nitrate (20 %) in water with heating, followed by the addition of leached chrysotile to the resulting solution. The resulting mixture was stirred and dried at room temperature, and then dried in an oven at 105 °C until constant weight. Then, cobalt nitrate was dissolved in water and the process was repeated with the already obtained dry mass of chrysotile with a nickel salt. Further, the heat treatment of nickel and cobalt salts deposited on chrysotile was carried out in a muffle furnace at 500 °C for 2 hours. The mass fraction of nickel and cobalt in the total mass of the obtained NiCo/chrysotile catalyst is 5 % each.

A Dron-4-07 X-ray diffractometer was used (a tube with a cobalt anode, tube parameters: 30 kV, 20 mA) to determine the phase composition of the catalyst obtained.

The surface morphology of the leached chrysotile and the NiCo/chrysotile catalyst were obtained using a MIRA3 TESCAN scanning electron microscope and a Jeol JEM-1400Plus transmission electron microscope.

Using a NanoS90 laser particle sizer and Zetasizer Nano (DTS) software, the particle size and distribution of the catalyst were determined, and water was used as the dispersant.

### Process of catalytic hydrogenation of model objects

Hydrogenation of polyaromatic hydrocarbons (anthracene (Interchem, Russia) and phenanthrene (Merck, Russia)) was carried out in an autoclave (manufactured in the People's Republic of China) with an internal stirrer with a capacity of 0.05 L. Hydrogenation of anthracene and phenanthrene lasts 60 minutes at an initial hydrogen pressure of 3.0 MPa, a temperature of 400 °C. The working pressure was ~6.0 MPa. The mass of the polyaromatic hydrocarbon of 1 g and the mass of the catalyst of 0.01 g were premixed. Then the prepared mass was loaded into the autoclave. The reactor was purged with hydrogen, and required gas pressure was supplied. The reactor was held for a specified time after reaching the temperature required. The reaction mixture was dissolved in benzene when it was cooled to room temperature.

The gas chromatography-mass spectrometry analysis of anthracene and phenanthrene hydrogenation products was performed on an Agilent Technologies 7890A gas chromatograph with a 5975C mass-spectrometric detector. The column temperature was gradually varied from 60 to 300 °C with time; a flow rate of helium was 8 mL/s. The test sample with a volume of 1 μL was introduced into the column using a 7683B autosampler. The test sample entered the ionization chamber of the mass spectrometer after separation in the column. The incoming molecules underwent fragmentation by electron impact with energy of 70 eV at a temperature of 250 °C in the chamber. After extracting from the ionization chamber by an electrostatic field the fragments arrived at a quadrupole capacitor. The mass spectra of test sample components were obtained with the use of the quadrupole capacitor. The chromatograms and mass spectra were processed using the MSD ChemStation E02.00.493 software. The NIST-8 database of mass spectra was used to identify compounds.

## Results and Discussion

### Parameters of NiCo/chrysotile catalyst

The chrysotile mineral used as a substrate for active centers of nickel and cobalt is a waste product of asbestos production at Kostanay Minerals JSC (the Republic of Kazakhstan), which is a serpentine raw material $3MgO \cdot 2SiO_2 \cdot H_2O$. Man-made waste contains a significant amount of magnesium oxide, on average 38–42 % by weight, and derivatives of silicon dioxide as main accompanying components [16]. Chrysotile

fibers consist of 12–20 twisted planes. It was found that the twist of the fibers decreases after leaching of chrysotile using a hydrochloric acid solution due to the removal of magnesium oxide. Thus, the acidity of chrysotile increases due to an increase in the concentration of $SiO_2$.

The natural mineral chrysotile is of great interest because its macroscopic matrix consists of nanotubes, the inner diameter of which is about 10 nm, and the outer diameter is about 60 nm. These nanotubes can be about 1 cm long, and they are arranged in a close-to-hexagonal packing. Chrysotile has been successfully used for the formation of semiconductor, ferroelectric, and metal nanowires [17]. When a catalyst is prepared by wet mixing, chrysotile nanotubes can be filled with nickel and cobalt ions from the corresponding salts solutions. Figure 1 shows the diffraction pattern of the catalyst obtained.
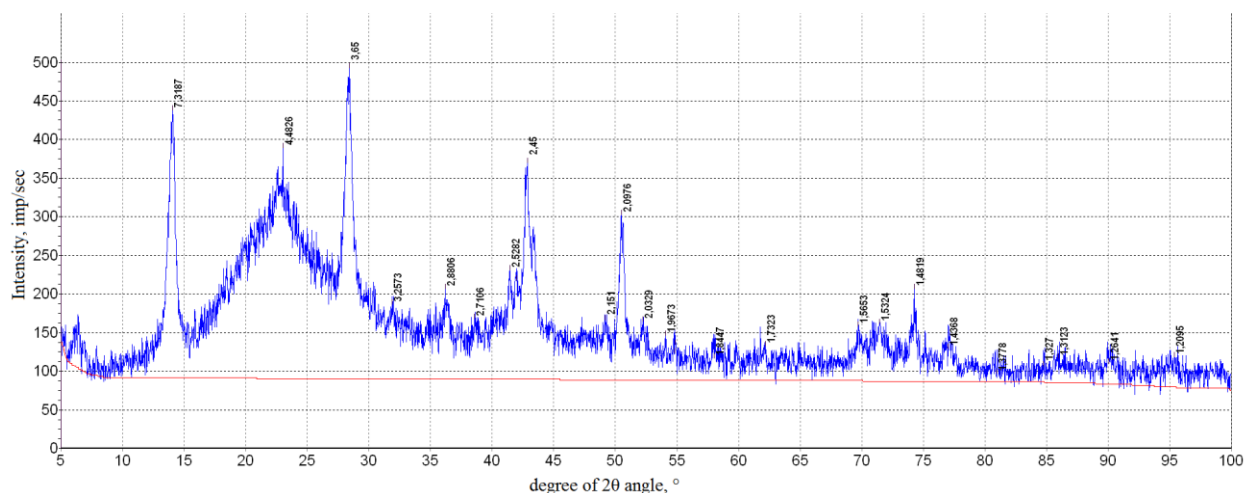


Figure 1. X-ray diffractograms of NiCo/chrysotile

According to the diffraction pattern, the reflections are 7.31; 4.48; 3.65; 2.52; 2.09; 1.53 Å correspond to the crystal structures of chrysotile $Mg_3[OH]_4\{Si_2O_5\}$, reflections 2.88; 2.45; 2.03; 1.56; 1.43 Å — cobalt oxide $CoCo_2O_4$, reflections 2.42; 2.09; 1.48; 1.26; 1.20 Å — nickel oxide NiO.

Figure 2 shows photomicrographs of leached chrysotile and catalyst NiCo/chrysotile.
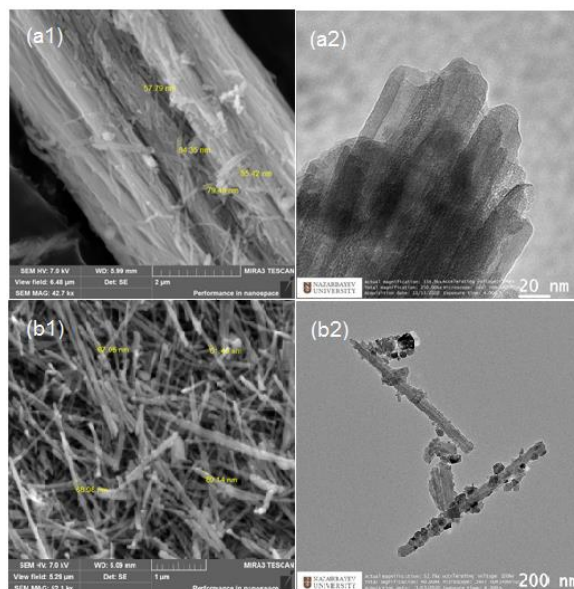


Figure 2. SEM (1) and TEM (2) micrographs of chrysotile (a) and NiCo/chrysotile (b)

The micrographs (a1 and a2) show that the chrysotile tubes are tightly packed in the short order. However, in the long range order, chrysotile can be described as "amorphously" packed. The mineral consists of

nanotubes with an inner diameter of about 10 nm and an outer diameter of about 60 nm. Oxides of nickel and cobalt with a diameter of ~50 nm deposited on the surface of chrysotile tubes are visible (micrographs b1 and b2).

The particle size and distribution of the catalytic additive particles, determined using a laser particle sizing device, are shown in Figure 3.
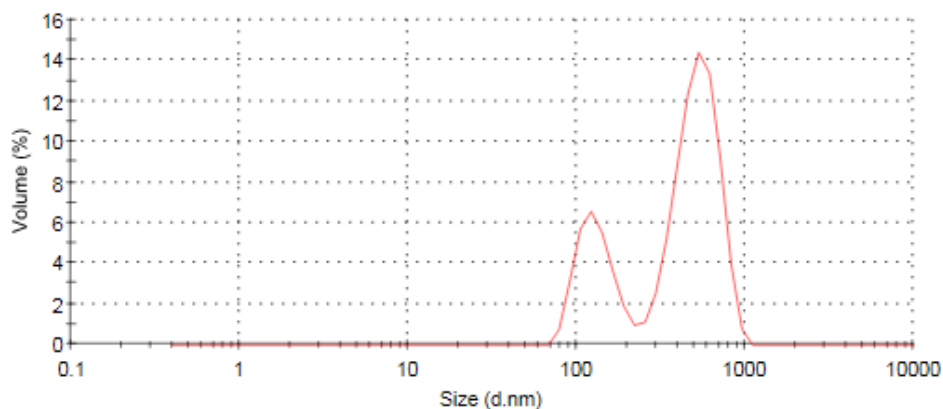


Figure 3. Size and distribution of particles in an aqueous suspension of NiCo/chrysotile

According to the laser determiner, the average particle size of the catalyst is 546.5 nm.

*Influence of the catalyst on hydrogenation of model objects*

Table 1 shows the results of the hydrogenation of anthracene and phenanthrene in the presence of NiCo/chrysotile catalyst.

T a b l e  1

**The yield of products of anthracene and phenanthrene hydrogenation process in the presence of NiCo/chrysotile**

| No. | Individual chemical composition | The yield of products, % | |
|---|---|---|---|
| | | Anthracene | Phenanthrene |
| 1 | 1-Methyl-2-(phenylmethyl)-benzene | 3.51 | 0.20 |
| 2 | 2-Ethyl-naphthalene | 1.38 | 1.10 |
| 3 | 2-Butyl-naphthalene | 2.20 | 0.25 |
| 4 | Biphenyl | – | 0.40 |
| 5 | 2-Methyl-1,1'-biphenyl | 1.04 | – |
| 6 | 2-Ethyl-1,1'-biphenyl | 6.95 | 0.37 |
| 7 | Fluorene | – | 2.75 |
| 8 | 9-Methyl-9H-fluorene | – | 0.90 |
| 9 | 9,10-Dihydro-anthracene | 24.83 | 2.82 |
| 10 | 1,2,3,4-Tetrahydro-anthracene | 34.92 | 1.68 |
| 11 | 1,2,3,4,5,6,7,8-Octahydro-anthracene | 2.16 | – |
| 12 | 9,10-Dihydro-phenanthrene | – | 13.45 |
| 13 | 1,2,3,4-Tetrahydro-phenanthrene | – | 4.09 |
| 14 | Anthracene | 14.65 | – |
| 15 | Phenanthrene | 8.37 | 74.70 |
| 16 | Undetermined | – | 0.57 |
| | **Conversion** | 76.99 | 28.60 |

It was noted that phenanthrene is hydrogenated less selective than anthracene, although the order of the shortened bond in it is greater than in anthracene. Obviously, the number of shortened bonds should also be taken into account: in phenanthrene, one with an order of 1.775, in anthracene — four, although with an order of 1.738. Thus, an important tendency determining the rate of hydrogenation of aromatic hydrocarbons is its dependence on the presence of shortened bonds and their number if the process is not complicated by the peculiarities of the catalysts effect [18].

Diagrams have been presented in Figures 4 and 5 according to the results of the hydrogenation of anthracene and phenanthrene in the presence of NiCo/chrysotile catalyst at an initial hydrogen pressure of 3 MPa and a temperature of 400 °C.



Figure 4. Scheme of anthracene hydrogenation reactions according to hydrogenated product composition

During the hydrogenation of anthracene the amount of hydrogenation products is 61.91 %, destruction — 15.08 % and isomerization — 8.37 %. It is known that the first reaction in anthracene hydrocracking is stepwise hydrogenation to di-, tetra- and octahydro-anthracenes, alternately [11, 12]. The cyclohexane ring of the tetrahydroanthracene is then cracked to naphthalenes. The conversion of anthracene to 1-methyl-2-(phenylmethyl)-benzene occurs stepwise through the formation of dihydro-anthracene.

A general pattern of naphthenic rings opening along with α-bonds has been observed according to the results of model objects hydrogenation. The preferential cleavage of this bond under conditions simulating coal liquefaction, i.e., under the hydrogen pressure is explained by the ipso-attack of atomic hydrogen, formed by the interaction of molecular hydrogen with radicals [18]. The formation of 1-methyl-2-(phenylmethyl)-benzene from dihydroanthracene (1) and 2-butyl-naphthalene from tetrahydroanthracene (2) occurs by cleavage of α-bonds initiated by ipso-attack H• (Fig. 5).



Figure 5. Scheme of 1-methyl-2-(phenylmethyl)-benzene formation from dihydroanthracene (1) and 2-butyl-naphthalene from tetrahydroanthracene (2)

The amount of hydrogenation products is 26.09 %, and that of destruction is 2.51 % during the phenanthrene hydrogenation.
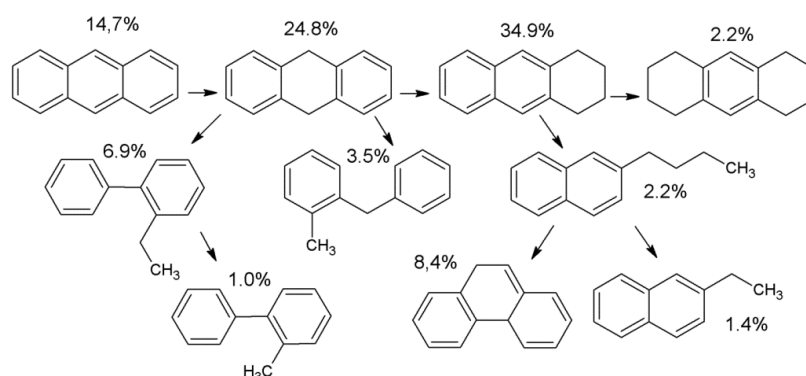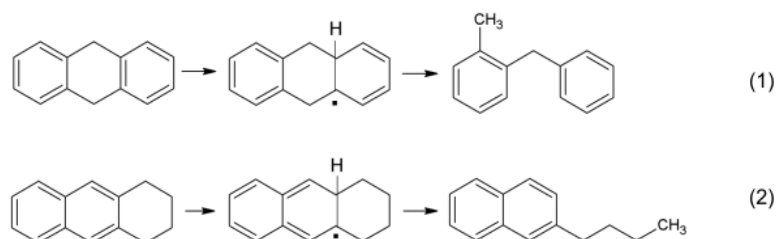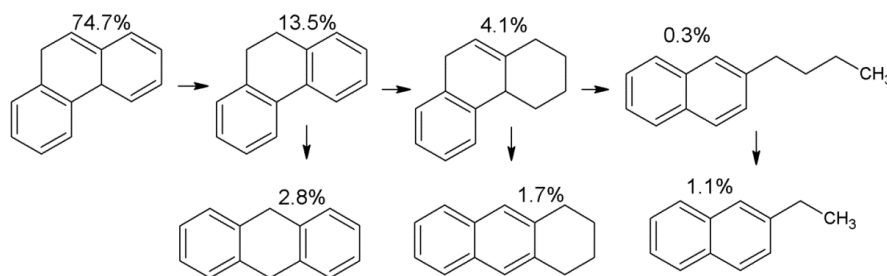


Figure 6. Scheme of phenanthrene hydrogenation reactions according to hydrogenated product composition

Successive hydrogenation and cracking reactions prevail in the process of phenanthrene hydrogenation. Apparently, 9,10-dihydrophenanthrene and 1,2,3,4-tetrahydrophenanthrene formed as a result of phenanthrene hydrogenation are isomerized to 9,10-dihydroanthracene and 1,2,3,4-tetrahydroanthracene, respectively [19]. The formation of 2-butyl-naphthalene from tetrahydrophenanthrene also occurs by cleavage of the α-bond initiated by ipsoattack H• (Fig. 7).
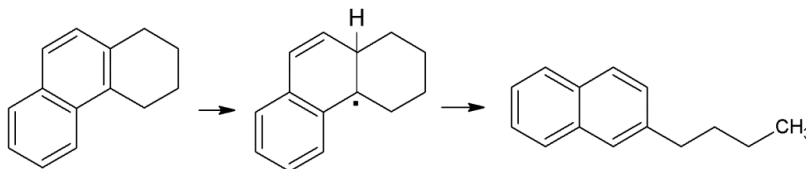


Figure 7. Scheme of 2-butyl-naphthalene formation from tetrahydrophenanthrene

9-methyl-9H-fluorene formed during the hydrogenation of phenanthrene is a Fluorene product present in the starting phenanthrene (3.7 %). Also, most likely, 1-methyl-2-(phenylmethyl)-benzene, 2-ethyl-1,1'-biphenyl, biphenyl are the degradation products of dibenzothiophene present in the starting phenanthrene (2.1 %).

Earlier, we found that during the hydrogenation of a mixture of anthracene and phenanthrene with a ratio of 1:1 in the presence of a catalytic additive CoO/microsphere, at an initial hydrogen pressure of 3 MPa and a temperature of 420 °C, the conversion of the mixture is 92.5 %, where the amounts of unreacted anthracene and phenanthrene accounted for 1.3 % and 6.2 %, respectively [20]. The high conversion of the mixture can be explained by the fact that the products of anthracene hydrogenation (di-, tetrahydroanthracene) act as a hydrogen donor. 9,10-Dihydroanthracene and 1,2,3,4-tetrahydroanthracene formed during the phenanthrene hydrogenation in the presence of a NiCo/chrysotile catalyst can also be hydrogen donors.

## Conclusions

Thus, when studying the effect of the NiCo/chrysotile catalyst on the hydrogenation of anthracene and phenanthrene for 1 hour at an initial hydrogen pressure of 3 MPa and a temperature of 400 °C, it was found that the catalyst selectively accelerates the hydrogenation reaction and allows increasing the yields of hydrogenation products and is ~62 % and ~26 %, respectively. The yields of the degradation products of anthracene and phenanthrene are ~15 % and ~2.5 %, respectively. Anthracene conversion is ~77 % and phenanthrene conversion is ~29 %.

## References

1  Hu F. Technical progress and industrialization status of coal to fuel oil in China / F. Hu, B. Yan, G. Wang, X. Gu, Q. Chang // Clean Coal Technology. — 2019. — No. 25. — P. 57–63. http://m.jjmjs.com.cn/artdetail-449.html

2  Hui D. Role of Hydrogen Pressure in Slurry-Phase Hydrocracking of Venezuela Heavy Oil / D. Hui, L. Dong, L. Hua, G. Peng, L. Renqing, L. Ming, L. Bin, Y. Yuanxi // Energy & Fuels. — 2015. — Vol. 29, No. 4. — P. 2104–2110. https://pubs.acs.org/doi/10.1021/ef502457p

3  Kuznetsov P.N. Thermal dissolution of different-ranked coals in tetralin and the anthracene fraction of coking tar / P.N. Kuznetsov, N.V. Perminov, L.I. Kuznetsova, S.M. Kolesnikova, E.S. Kamenskii, N.I. Pavlenko, F.A. Buryukin // Solid Fuel Chemistry. — 2020. — Vol. 54, No. 29. — P. 61–68. https://link.springer.com/article/10.3103 %2FS036152192002007X

4  Dmitriev D.E. Transformations of resins and asphaltenes during the thermal treatment of heavy oils / D.E. Dmitriev, A.K. Golovko // Petroleum Chemistry. — 2010. — Vol. 50, No. 2. — P. 106–113. https://doi.org/10.1134/S0965544110020040

5  Beltramone A.R. Simultaneous Hydrogenation of Multiring Aromatic Compounds over NiMo Catalyst / A.R. Beltramone, D.E. Resasco, W.E. Alvarez, T.V. Choudhary // Ind. Eng. Chem. Res. — 2008. — No. 47. P. 7161–7166. https://doi.org/10.1021/ie8004258

6  Bricker M. Hydrocracking in Petroleum Processing / M. Bricker, V. Thakkar, J. Petri // Handbook of Petroleum Processing: 2nd ed. / A.T. Steven, R.P. Peter, S.J. David. — Switzerland: Springer International Publishing, 2015. — P. 317–359.

7  Dik P.P. Hydroprocessing of Hydrocracker Bottom on Pd Containing Bifunctional Catalysts / P.P. Dik, O.V. Klimov, I.G. Danilova, K.A. Leonova, V.Yu. Pereyma, S.V. Budukva, D.D. Uvarkina, M.O. Kazakov, A.S. Noskov // Catalysis Today. — 2016. — No. 271. — P. 154–162. https://doi.org/10.1016/j.cattod.2015.09.050

8  Gonzalez-Cortes S.L. Comparing the hydrodesulfurization reaction of thiophene on γ-Al₂O₃ supported CoMo, NiMo and NiW sulfide catalysts / S.L. Gonzalez-Cortes // Reaction Kinetics and Catalysis Letters. — 2009. — No. 97. — P. 131–139. https://doi.org/10.1007/s11144-009-0008-2

9   Yasuda H. Hydrogenation of tetralin over sulfided nickel-tungstate/alumina and nickel-molybdate/alumina catalysts / H. Yasuda, M. Higo, S. Yoshitomi, T. Sato, M. Imamura, H. Matsubayashi, H. Shimada, A. Nishijima, Y. Yoshimura // Catalysis Today. — 1997. — No. 39. — P. 77–87. https://doi.org/10.1016/S0920-5861(97)00090-4

10   Baikenov M.I. Influence of catalytic systems on process of model object hydrogenation. / M.I. Baikenov, G.G. Baikenova, B.S. Sarsembayev, A.T. Baimagambetova, A. Tusipkhan, A.Z. Matayeva // International Journal of Coal Science and Technology. — 2014. — Vol. 1, No. 1. — P. 88–92. https://doi.org/10.1007/s40789-014-0012-7

11   Sahle-Demessie E. Hydrogenation of Anthracene in Supercritical Carbon Dioxide Solvent Using Ni Supported on Hβ-Zeolite Catalyst / E. Sahle-Demessie, V.G. Devulapelli, A.A. Hassan // Catalysts. — 2012. — No. 2. — P. 85–100. https://doi.org/10.3390/catal2010085

12   Liu H. The Catalytic Performance of Metalloporphyrins during Hydrogenation of Anthracene / H. Liu, S.F. Ji, Z.X. Wang, A.J. Guo, K. Chen // Energy Technology. — 2015. — No. 3. — P. 145–154. https://doi.org/10.1002/ente.201402124

13   Schachtl E. Understanding Ni Promotion of $MoS_2$/g-$Al_2O_3$ and its Implications for the Hydrogenation of Phenanthrene / E. Schachtl, L. Zhong, E. Kondratieva, J. Hein, O.Y. Gutierrez, A. Jentys, J.A. Lercher // ChemCatChem. — 2015. — No. 7. — P. 4118–4130. https://doi.org/10.1002/cctc.201500706

14   Yang H.B. Kinetics of Phenanthrene Hydrogenation System over CoMo/Al2O3 Catalyst / H.B. Yang, Y.C. Wang, H.B. Jiang, H.X. Weng, F. Liu, F. Li // Industrial and Engineering Chemistry Research. — 2014. — No. 53. — P. 12264–12269. https://dx.doi.org/10.1021/ie501397n

15   Nuzzi M. Hydrogenation of phenanthrene in the presence of Ni catalyst. Thermal dehydrogenation of hydrophenanthrenes and role of individual species in hydrogen transfers for coal liquefaction / M. Nuzzi, B. Marcandalli // Fuel Processing Technology. — 2002. — No. 80. — P. 35-45. http://dx.doi.org/10.1016/S0378-3820(02)00189-3

16   Джафаров Н.Н. Хризотил-асбест Казахстана: моногр. / Н.Н. Джафаров. — Алматы: РИО ВАК РК, 2000. — 180 с.

17   Belotitskii V.I. Optical properties of metal nanoparticles in chrysotile channels / V.I. Belotitskii, Y.A. Kumzerov, A.E. Kalmykov, D.A. Kirilenko, U. Peschel, S.G. Romanov, L.M. Sorokin, A.A. Sysoeva, O. Zhuromskyy // Technical Physics Letters. — 2016. — No. 42. — P. 656–658. https://doi.org/10.1134/S1063785016060183

18   Калечиц И.В. Моделирование ожижения угля / И.В. Калечиц. — М.: ИВТАН, 1999. — 229 с.

19   Meiramov M.G. Angular-linear isomerization on the hydrogenation of phenanthrene in the presence of iron-containing catalysts / M.G. Meiramov // Solid Fuel Chemistry. — 2017. — No. 51. — P. 107–110. https://doi.org/10.3103/S0361521917020070

20   Aitbekova D.E. Catalytic Hydrogenation of a Model Mixture of Anthracene and Phenanthrene / D.E. Aitbekova, F.Y. Ma, M.G. Meiramov, G.G. Baikenova, F.E. Kumakov, A. Tusipkhan, S.K. Mukhametzhanova, M.I. Baikenov // Solid Fuel Chemistry. — 2019. — No. 53. — P. 230–238. https://doi.org/10.3103/S0361521919040025

М.И. Байкенов, Д.Е. Айтбекова, Н.Ж. Балпанова, А. Түсіпхан, Г.Г. Байкенова,
Е.А. Аубакиров, А.Р. Бродский, Фен Юн Ма, Д.К. Макенов

## Полиароматты қосылыстардың NiCo/хризотил катализаторында гидрогенизациялау

Модельдік объектілерді (антрацен мен фенантрен) 1 сағат бойы сутегінің бастапқы қысымы 3 МПа және 400 °C температурада гидрогенизациялаған кезде биметалдық NiCo/хризотилді катализатордың белсенділігі мен селективтілігі зерттелді. Никель мен кобальттың белсенді орталықтары үшін субстрат ретінде пайдаланылған хризотил минералы «Қостанай минералдары» АҚ (Қазақстан Республикасы) асбест өндірісінің қалдығы болып табылады. Катализатор физика-химиялық талдау әдістерінің кешенімен сипатталды. Хризотил минералы ішкі диаметрі шамамен 10 нм және сыртқы диаметрі шамамен 60 нм болатын нанотүтіктерден тұрады. Антраценді гидрогенизациялау кезінде гидрлеу өнімдерінің мөлшері 61,91 %, деструкция өнімдері 15,08 % және изомеризация өнімдері 8,37 % құрады. Фенантренді гидрогенизациялау кезінде гидрлеу өнімдерінің мөлшері 26,09 %, ал деструкция өнімдері 2,51 % болды. Катализатор гидрлеу реакциясын селективті түрде жылдамдататыны және гидрлеу өнімдерінің шығымын арттыруға мүмкіндік беретіні анықталды. Гидрогенизаттарды хромато-масс-спектрометрлік талдау нәтижелері бойынша модельдік объектілерді гидрогенизациялау реакциясының схемалары жасалды.

*Кілт сөздер*: полиароматты көмірсутектер, антрацен, фенантрен, нанокатализатор, гидрогенизация, хризотил, никель, кобальт.

М.И. Байкенов, Д.Е. Айтбекова, Н.Ж. Балпанова, А. Тусипхан, Г.Г. Байкенова,
Е.А. Аубакиров, А.Р. Бродский, Фен Юн Ма, Д.К. Макенов

## Гидрогенизация полиароматических соединений на катализаторе NiCo/хризотил

Исследованы активность и селективность биметаллического катализатора NiCo/хризотил при гидрогенизации модельных объектов (антрацена и фенантрена) в течение 1 ч при исходном давлении водорода 3 МПа и температуре 400 °C. Минерал хризотил, использованный в качестве подложки для активных

центров никеля и кобальта, является отходом асбестового производства АО «Костанайские минералы» (Республика Казахстан). Катализатор охарактеризован комплексом методов физико-химического анализа. Минерал хризотил состоит из нанотрубок с внутренним диаметром около 10 нм и внешним диаметром около 60 нм. При гидрогенизации антрацена количество продуктов гидрирования составляет 61,91 %, деструкции — 15,08 % и изомеризации — 8,37 %. При гидрогенизации фенантрена количество продуктов гидрирования составляет 26,09 %, а деструкции — 2,51 %. Установлено, что катализатор селективно ускоряет реакцию гидрирования и позволяет увеличить выход продуктов гидрирования. По результатам хромато-масс-спектрометрического анализа гидрогенизатов были составлены схемы реакции гидрогенизации модельных объектов.

*Ключевые слова*: полиароматические углеводороды, антрацен, фенантрен, нанокатализатор, гидрогенизация, хризотил, никель, кобальт.

# References

1   Hu, F., Yan, B., Wang, G., Gu, X., & Chang, Q. (2019). Technical progress and industrialization status of coal to fuel oil in China. *Clean Coal Technology, 25*, 57–63. http://m.jjmjs.com.cn/artdetail-449.html

2   Hui, D., Dong, L., Hua, L., Peng, G., Renqing, L., & Ming, L., et al. (2015). Role of Hydrogen Pressure in Slurry-Phase Hydrocracking of Venezuela Heavy Oil. *Energy & Fuels, 29, 4*, 2104–2110. https://pubs.acs.org/doi/10.1021/ef502457p

3   Kuznetsov, P.N., Perminov, N.V., Kuznetsova, L.I., Kolesnikova, S.M., Kamenskii, E.S., & Pavlenko, N.I., et al. (2020). Thermal dissolution of different-ranked coals in tetralin and the anthracene fraction of coking tar. *Solid Fuel Chemistry, 54, 2*, 61–68. https://link.springer.com/article/10.3103 %2FS036152192002007X

4   Dmitriev, D.E., & Golovko, A.K. (2010). Transformations of resins and asphaltenes during the thermal treatment of heavy oils. *Petroleum Chemistry, 50, 2*, 106–113. https://doi.org/10.1134/S0965544110020040

5   Beltramone, A.R., Resasco, D.E., Alvarez, W.E., & Choudhary, T.V. (2008). Simultaneous Hydrogenation of Multiring Aromatic Compounds over NiMo Catalyst. *Ind. Eng. Chem. Res., 47*, 7161–7166. https://doi.org/10.1021/ie8004258

6   Bricker, M., Thakkar, V., & Petri, J. (2015). Hydrocracking in Petroleum Processing. Handbook of Petroleum Processing. A.T. Steven, R.P. Peter, S.J. David (2nd ed.). Switzerland: Springer International Publishing.

7   Dik, P.P., Klimov, O.V., Danilova, I.G., Leonova, K.A., Pereyma, V.Yu., & Budukva, et al. (2016). Hydroprocessing of Hydrocracker Bottom on Pd Containing Bifunctional Catalysts. *Catalysis Today, 271*, 154–162. https://doi.org/10.1016/j.cattod.2015.09.050

8   Gonzalez-Cortes, S.L. (2009). Comparing the hydrodesulfurization reaction of thiophene on $\gamma$-Al$_2$O$_3$ supported CoMo, NiMo and NiW sulfide catalysts. *Reaction Kinetics and Catalysis Letters, 97*, 131–139. https://doi.org/10.1007/s11144-009-0008-2

9   Yasuda, H., Higo, M., Yoshitomi, S., Sato, T., Imamura, M., & Matsubayashi, H., et al. (1997). Hydrogenation of tetralin over sulfided nickel-tungstate/alumina and nickel-molybdate/alumina catalysts. *Catalysis Today, 39*, 77–87. https://doi.org/10.1016/S0920-5861(97)00090-4

10   Baikenov, M.I., Baikenova, G.G., Sarsembayev, B.S., Baimagambetova, A.T., Tusipkhan, A., & Matayeva, A.Z. (2014). Influence of catalytic systems on process of model object hydrogenation. *International Journal of Coal Science and Technology, 1, 1*, 88–92. https://doi.org/10.1007/s40789-014-0012-7

11   Sahle-Demessie, E., Devulapelli, V.G., & Hassan, A.A. (2012). Hydrogenation of Anthracene in Supercritical Carbon Dioxide Solvent Using Ni Supported on H$\beta$-Zeolite Catalyst. *Catalysts, 2*, 85–100. https://doi.org/10.3390/catal2010085

12   Liu, H., Ji, S.F., Wang, Z.X., Guo, A.J., & Chen, K. (2015). The Catalytic Performance of Metalloporphyrins during Hydrogenation of Anthracene. *Energy Technology, 3*, 145–154. https://doi.org/10.1002/ente.201402124

13   Schachtl, E., Zhong, L., Kondratieva, E., Hein, J., Gutierrez, O.Y., Jentys, A., & et al. (2015). Understanding Ni Promotion of MoS$_2$/g-Al$_2$O$_3$ and its Implications for the Hydrogenation of Phenanthrene. *ChemCatChem, 7*, 4118–4130. https://doi.org/10.1002/cctc.201500706

14   Yang, H.B., Wang, Y.C., Jiang, H.B., Weng, H.X., Liu, F., & Li, F. (2014). Kinetics of Phenanthrene Hydrogenation System over CoMo/Al$_2$O$_3$ Catalyst. *Industrial and Engineering Chemistry Research, 53*, 12264–12269. https://dx.doi.org/10.1021/ie501397n

15   Nuzzi, M., & Marcandalli, B. (2002). Hydrogenation of phenanthrene in the presence of Ni catalyst. Thermal dehydrogenation of hydrophenanthrenes and role of individual species in hydrogen transfers for coal liquefaction. *Fuel Processing Technology, 80*, 35–45. http://dx.doi.org/10.1016/S0378-3820(02)00189-3

16   Jafarov, N.N. (2000). *Khrizotil-asbest Kazakhstana [Chrysotile-asbestos of Kazakhstan]*. Almaty: RIO VAK RK [in Russian].

17   Belotitskii, V.I., Kumzerov, Y.A., Kalmykov, A.E., Kirilenko, D.A., Peschel, U., & Romanov, S.G., et al. (2016). Optical properties of metal nanoparticles in chrysotile channels. *Technical Physics Letters, 42*, 656–658. https://doi.org/10.1134/S1063785016060183

18   Kalechits, I.V. (1999). *Modelirovanie ozhizheniia uglia [Modeling of Coal Liquefaction]*. Moscow: IHTAS [in Russian].

19   Meiramov, M.G. (2017). Angular-linear isomerization on the hydrogenation of phenanthrene in the presence of iron-containing catalysts. *Solid Fuel Chemistry, 51*, 107–110. https://doi.org/10.3103/S0361521917020070

20   Aitbekova, D.E., Ma, F.Y., Meiramov, M.G., Baikenova, G.G., Kumakov, F.E., & Tusipkhan. A., et al. (2019). Catalytic Hydrogenation of a Model Mixture of Anthracene and Phenanthrene. *Solid Fuel Chemistry, 53*, 230–238. https://doi.org/10.3103/S0361521919040025

Information about authors:

**Baikenov Murzabek Ispolovich** — Doctor of Chemical Sciences, Professor, Karagandy University of the name of academician E.A. Buketov, Universitetskaya street, 28, 100024, Karagandy, Kazakhstan; e-mail: murzabek_b@mail.ru; https://orcid.org/0000-0002-8703-0397;

**Aitbekova Darzhan Ergalievna** (corresponding author) — Doctoral student, Karagandy University of the name of academician E.A. Buketov, Universitetskaya street, 28, 100024, Karagandy, Kazakhstan; e-mail: darzhan91@mail.ru; https://orcid.org/0000-0002-6839-9711;

**Balpanova Nazerke Zhumagalievna** — Doctoral student, Karagandy University of the name of academician E.A. Buketov, Universitetskaya street, 28, 100024, Karagandy, Kazakhstan; e-mail: nazerke_90@mail.ru; https://orcid.org/0000-0003-3089-1871;

**Tusipkhan Almas** — PhD, senior lecturer, Karagandy University of the name of academician E.A. Buketov, Universitetskaya street, 28, 100024, Karagandy, Kazakhstan; e-mail: almas_kz_22@mail.ru; https://orcid.org/0000-0002-6452-4925;

**Baikenova Gulzhan Gausilevna** — Doctor of Chemical Sciences, Professor, Karaganda Economic University of Kazpotrebsoyuz, Karaganda, Kazakhstan; South Ural State University, Chelyabinsk, Russia; e-mail: murzabek_b@mail.ru; https://orcid.org/0000-0002-2816-3341;

**Aubakirov Yermek Aiktazynovich** — Doctor of Chemical Sciences, Professor, Al-Farabi Kazakh National University, Al-Farabi, 71, 050040, Almaty, Kazakhstan; e-mail: miral.64@mail.ru; https://orcid.org/0000-0001-5405-4125;

**Brodskiy Alexandr Rafaelevich** — Candidate of Chemical Sciences, Associate Professor, D.V. Sokolskiy Institute of Fuel, Catalysis and Electrochemistry, D. Kunayev, 142, 050010, Almaty, Kazakhstan; e-mail: albrod@list.ru; https://orcid.org/0000-0001-6216-4738;

**Ma Fengyun** — PhD, Professor, Xinjiang University, Urumqi, People's Republic of China, ma_fy@126.com;

**Makenov Daulet Kairzhanovich** — Doctoral student, Karagandy University of the name of academician E.A. Buketov, Universitetskaya street, 28, 100024, Karagandy, Kazakhstan; e-mail: mckenov.daulet@gmail.com; https://orcid.org/0000-0002-1011-7662

# V.V. Glukhikh[*], A.E. Shkuro, P.S. Krivonogov

*Ural State Forest Engineering University, Yekaterinburg, Russia*
*(\*Corresponding author's e-mail: gluhihvv@m.usfeu.ru)*

# The effect of chemical composition on the biodegradation rate and physical and mechanical properties of polymer composites with lignocellulose fillers

The results of TPLC scientific research, practical experience of their preparation, and application as of 2016 are presented in eight volumes of the "Handbook of Composites from Renewable Materials" (2017, John Wiley & Sons, Inc.). This article provides an analysis of books and articles with open access to the Science Direct (Elsevier) database for the period 2017–2020 to assess the biodegradation rate and physical and mechanical properties of polymer composites with lignocellulosic fillers. The production and use of polymer composites with a thermoplastic polymer matrix and lignocellulosic fillers (TPLC) have significant ecological and economic prospects since waste biomass from forests, agriculture, and polymers obtained from petroleum raw materials can be used for their production. However, depending on the TPLC application area, there are opposite requirements for the biodegradation rate. For the use in construction and medicine materials and products must have a minimum biodegradation rate. Materials and products for single-use packaging must have the necessary biodegradability potential and have an adjusted biodegradation rate in soil, water, compost environment. Research results show that the properties of TPLC can be significantly influenced not only by the physical but also by the chemical structure of all components of these composites. The chemical properties of polymers, fillers, additives for various purposes can affect their industrial production efficiency.

*Keywords:* composite, chemical structure, thermoplastic polymer, filler, cellulose, lignin, biodegradation, properties.

## *Introduction*

To date there is no conventional terminology in the scientific literature to designate composites based on rapidly renewable raw materials. These composites are ordinarily termed "biocomposites", "green composites", "bioplastics". Composite materials obtained from recycled synthetic polymers with plant-based fillers began to be called "eco-composites" [1].

Lignocellulosic-filled composites are an enormous group of materials that include composites with an organic and inorganic binder phase. CMLC with binders based on thermoplastic polymers finds a wide and varied practical application. Composites with a thermoplastic polymer phase and lignocellulose fillers (TPLC) are used in significant volumes in the automotive industry, furniture, and construction materials. The results of the TPLC scientific research, practical experience and application as of 2016 are presented in eight volumes of "Handbook of Composites from Renewable Materials" (2017, John Wiley & Sons, Inc.).

According to scientific materials published in journals and books in 2017–2020 and the first half of 2021 [2–4], an increase in commercial interest in the production of TPLC and their use in medicine, water treatment, heat power engineering, packaging, aerospace industry, automotive structural parts, building materials, furniture, and driveways is predicted. At the same time there is also an environmental interest, as waste thermoplastic polymers (polyethylene, polypropylene) may be used to produce TPLC. TPLC products may be recycled after use as well. The chemical sciences play an essential role in the processing of various wastes, including not only polymeric materials [5] but also the residues of forest biomass [6] and agriculture [7] due to their use for the production of popular marketable products from TPLC.

Until now, the priority goal of scientific TPLC research is to study the influence of their components' morphological, physical, and chemical parameters on the physicomechanical and functional properties. However, the studies of the TPLC component's chemical composition influence their biodegradation rate have not been systemic and are difficult to meta-analysis since a great variety of methods for its assessment.

Depending on the area of application of TPLC there are opposite requirements for the rate of their biodegradation. For example, construction materials and products that directly contact soil, water, microorganisms, and solar radiation must have a minimum biodegradation rate. The medical industry also needs bioresistant products. On the other hand, materials and products for single-use packaging must have the necessary biodegradability potential and have a given biodegradation rate in soil, water, and compost environment.

  

Currently, in connection with the tightening of requirements for the environmental safety of consumer waste in several countries, there is a need for TPLC products with a given biodegradation rate and the change dynamics of physical and mechanical properties.

Many countries enacted laws prohibiting the production of non-biodegradable plastics for reducing plastic waste. Thanks to this, scientific research of biodegradable TPLC is actively developing. The activity in conducting scientific research on the production and study of biostable TPLC is low. There is an erroneous opinion [2, 3] that TPLC with a synthetic polymer matrix has a very high biostability. Rapid laboratory test results often form this opinion. A.A. Klyosov [8] noted that ASTM standard microbial resistance tests generally showed that TPLCs have excellent microbial resistance properties. However, in his opinion, laboratory results and environmental impacts do not always correlate.

Recent studies [9–12] have confirmed the biodegradability of TPLC materials. Biodegradation of TPLC occurred primarily due to the action on lignocellulose fillers (LCP) in the composite of various rotting and mold fungi, algae, and termites.

In the study [10] an express assessment of the biodegradation potential in active soil of various TPLC products obtained by multiple methods was carried out. The authors assessed biodegradation by the dynamics of changes in their morphological and visual characteristics. They used five types of soil substrates with different compositions of microbiocenosis. The maximum exposure time of the samples in soil substrates was at least nine months. At the same time, to analyze the potential phytotoxicity of TPLC biodegradation products, a test with growing annual plants in soil substrates was carried out. The research results showed that all tested TPLC products have a higher biodegradability potential in soil than polyethylene, polypropylene, and polyethylene terephthalate. In addition, the breakdown of the lignocellulosic filler gave the polymer composites a characteristic spongy appearance by "emptying" the polymer matrix (Fig. 1).
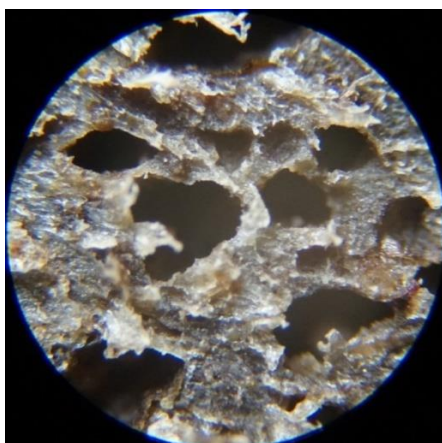


Figure 1. A sample of a strand obtained by extrusion from a mixture of polyethylene
and wheat husk after holding in an active soil for nine months (×160 magnification)

A.A. Klyosov gave the factors influencing the TPLC biodegradation rate in the book [8]. According to him and the results of many recent studies [11, 12], moisture content (absorption) is one of the critical parameters for the growth of microorganisms in TPLC materials. However, there is a strong correlation between the total moisture content of the TPLC and its susceptibility to microbial degradation.

As noted by the authors of many recent studies, in addition to the moisture content the following physicochemical parameters of the composites also significantly affect the physical and mechanical properties and the TPLC biodegradation rate under the influence of various microorganisms:

 − Physicochemical structure and composition of the polymer phase;
 − Content and chemical structure of lignin and cellulose in fillers;
 − Content and chemical structure of special additives (biocides, plasticizers, and others).

*Influence of the polymer phase physicochemical structure and composition
on the TPLC properties and biodegradation rate*

Until now the names of polymers used in publications have often not matched with their chemical structure. For example, a polymer synthesized by polymerization reactions of ethylene obtained by a

microbiological method is called "bio polyethylene" and belongs to the group of biopolymers. The name "microbiological cellulose" appears similarly. In this article we use polymers' words corresponding to their chemical composition rather than the origin of the monomers for their synthesis. Natural polymers are obtained from natural raw materials, and synthetic polymers are obtained by industrial synthesis from monomers. The term "bio-polymers" combines natural polymers and synthetic polymers of a similar chemical composition obtained from monomers of natural origin.

Based on many research results in the review [13], the authors proposed to divide biodegradable polymers into three groups: unmodified biopolymers, structurally modified biopolymers, and chemically modified biopolymers. Review authors concluded that the structural modification has practically no effect on its biodegradation in soil, and chemically modified biopolymers can be subjected to different biodegradation mechanisms and, consequently, have different rates of biodegradation. In many cases, biodegradable plastics made from biopolymers retained the regularities of biodegradation in soil, characteristic of biopolymers. These conclusions followed the example of thermoplastic starch, cellulose acetate, and lignin. When the chemical structure of the polymer changes, as in the case of cellulose acetate, various microorganisms and enzymes were involved in biodegradation. Based on the biodegradation process of cellulose acetate, the authors of the review proposed a conceptual model that can be used as a starting point for predicting biodegradation, the rate of decomposition of other chemically modified biopolymers used as bioplastics. This review noted that cellulose, like starch, is a glucose polysaccharide, but cellulose is more resistant to biodegradation because it contains prepotent β-glycosidic bonds. The degree of cellulose crystallinity affected the rate of biodegradation in soil. The biodegradation of amorphous cellulose was faster than the biodegradation of crystalline cellulose. Acetylation of cellulose slowed down its biodegradation rate, i.e., the acetyl groups protected against microbial attack. The degradation rate depended on the degree of cellulose acetylation, the distribution of acetyl groups along the cellulose chain, and its molecular weight. The results of studies that have established a negative nonlinear dependence of the rate of enzymatic decomposition of films based on cellulose on the degree of its acetylation are cited.

The review [14] drawn attention to the industrial production of composites with a polymer matrix from two or more polymers mixtures, and due to this, proposed a viable alternative for reducing the cost of industrial products. These blends in various combinations have been used to produce traditional and biodegradable plastics to improve some of their mechanical properties, regulate product life cycles and reduce manufacturing costs.

Currently, the most prominent polymer matrix for producing biodegradable composites is polylactide (PLA). Its availability has significantly increased in the past decade, and its prices have dropped. That was making polylactide a competitive material. The polylactide biodegradation process has been well studied not only in tests but also in practical terms. The fundamental limitations that prevent the use of pure PLA are its fragility and toughness. However, this problem can be solved by mixing PLA with other bio-based polymers, including thermoplastic starch (TPS), polyhydroxybutyrate valerate (PHBV), which allows the use of composites with a polymer matrix from these mixtures in almost any conditions. The example of PLA, which is increasingly used in commercial solutions, demonstrates the necessity to continue large-scale research on the use of its mixtures with other polymers, for example, polyhydroxyalkanoates (PHB) polybutylene succinate (PBS), modified starch, modified polyethylene terephthalate (PET). The biodegradation of composites with such mixtures under practical terms has not been sufficiently studied. Synthetic polymers containing fragments that accelerate the biodegradability process can be used to make composites biodegradable. These can be polyesters and polyesteramides, copolyesters based on aliphatic diols, and organic dicarboxylic acids. Unfortunately, this work does not provide a comparative assessment of the effect of the type and amount of functional groups introduced into the structure of synthetic polymers on the rate of TPLC biodegradation. The method of producing biodegradable polymeric materials consists in obtaining composites based on natural polymers: starch, cellulose, chitosan, proteins. However, a comparative assessment of various factors' effect on the biodegradation rate is given only for polymers. Data on the performance properties of composites during their biodegradation are not provided.

Considering the possible prospects for the industrial production of TPLC products, scientific research continues to study the properties of composites with synthetic biodegradable polymer matrices, mixtures of biopolymers with synthetic biodegradable polymers with chemical modification of these polymers and additives.

The review [12] presented a detailed analysis of the effect of the physicochemical structure and composition of the polymer phase consisting of some synthetic polyolefins and their mixtures (polyethylene,

polypropylene and their mixtures, propylene-ethylene copolymers, ethylene-vinyl acetate, ethylene-octene, and their combinations), on the biodegradation of TPLC. In these composites, cellulose and wood flour were used as fillers with a content of 0 to 30 %. This work analyzed the influence of the following factors on the composites biodegradable properties:

– chemical structure and conformation of monomeric units and branching of the macromolecular chain;
– chemical composition of copolymers of ethylene with propylene, ethylene with vinyl acetate, ethylene with octene;
– regularity of distribution of ethylene units in copolymers with propylene;
– supramolecular structure of polymers, including the degree of crystallinity and orientation effect;
– phase structure of polymer blends of polyolefins. The authors made conclusions about the influence of these factors on the processes of rupture of polymer macromolecules, water absorption of composites, and their assimilation by microorganisms by the following mechanisms:
– chemical structure of polymer monomer units;
– the presence of hydrolyzable functional groups in the polymer backbone;
– conformation and branching of the main macromolecular chain;
– type of distribution of monomer units in the copolymer.

This work did not provide information on the effect of the polymer physicochemical structure on the properties of the composites during biodegradation.

Biodegradation studies of composites with synthetic and natural polymers associated with assessing their functional properties are ongoing. At the same time, methods are being developed for obtaining new composites not only with above mentioned synthetic, natural polymers and their mixtures but also with others. However, based on the results of these studies, it is impossible to draw general conclusions about the effect of the polymer phase physicochemical structure and composition on the TPLC biodegradation rate since the studied composites did not have an accurate same chemical composition.

*Influence of the content and chemical structure of lignin and cellulose in fillers on the TPLC properties and biodegradation rate*

The origin of the natural lignocellulosic filler usually determines its chemical composition and structure. However, these fillers contain cellulose, lignin, hemicelluloses, extracts, and other substances regardless of genesis. There are no doubts about the conclusions based on the results of the studies performed on a higher rate of TPLC biodegradation with a decrease in the lignin content in the cell walls of lignocellulose fillers. Therefore, in many studies, the content of cellulose and lignin in LCPs is controlled. In addition, new data have appeared on the effect of the fiber content in the filler on the TPLC properties [1], which, in addition to cellulose and lignin, may contain other chemical substances.

The review [2] presented a comprehensive analysis of the components and their features and many other factors that influence the mechanical properties and prospects for the composites with a biopolymer matrix. The physicochemical structure of the polymer matrix, fillers, plasticizers, and other biocomposites components significantly affected the properties of such composites. A significant aspect for obtaining composites with desired properties was searching for optimal parameters for their preparation: homogeneous distribution of components in the polymer matrix, the optimal amount of filler, and the optimal interfacial connection of elements. Biocomposite's mechanical properties could be adjusted by choosing an appropriate biopolymer. Adaptation of functional groups to potent compounds due to their physical and chemical modifications improved interfacial bonding. The work [15] provided data on all-cellulosic composites (ACC) properties with a cellulosic polymer matrix and cellulosic fillers. Films made of these composites had high physical and mechanical properties, as well as light transmission. In terms of their mechanical properties, these materials were superior to most commercial composites with nano cellulosic fillers and other polymer matrices due to the ideal bonding of the cellulosic filler to the cellulosic matrix because of their identical chemical composition. Furthermore, experiments on the burial of composites in soil have shown that ACC biodegradability is better than other biodegradable polymers such as polylactic acid. In this case, the biodegradation of ACC occurred mainly in the matrix phase.

The authors of the review [14] classed lignin as an amorphous polyester heteropolymer with aromatic alcohol groups. Lignin is a more rot-resistant polymer than starch and cellulose due to its complex chemical structure. Therefore, the lignin biodegradation rate in the composition of lignocellulose complexes was lower than that of free lignin obtained in the pulp and paper industry. Consequently, many physical and mechanical

properties of composites with a polymer matrix of lignin and starch were inferior to those of composites with a cellulose matrix.

Recently, studies of the effect of various fillers, including cellulose and lignin, isolated from plant materials, various plant wastes, and products of their chemical modification on the biodegradability and other TPLC properties have intensified [1, 14, 16-21].

The review [16] analyzed the studies of composites with a polyurethane polymer phase and fillers obtained by functionalizing lignin with various chemical compounds. The use of lignin chemical modification products significantly improved the mechanical properties of polyurethane composites compared to unmodified lignin. Therefore, the review authors believe that its use as a filler for thermoplastic polyurethanes has an industrial perspective.

The review [17] analyzed the studies of lignin nanoparticles and products of their chemical modification as fillers for various thermoplastic polymers. During the chemical modification of nano lignin by different reactions new functional groups are formed (functionalization) on the surface of lignin nanoparticles. According to the conclusions of the review authors, functionalized nano lignin in composites with different polymer phases retained the antimicrobial properties inherent in ordinary lignin. Improvement of the performance properties of composites with varying phases of a polymer depends on the type and content of functional groups in nano lignin, depending on the chemical structure of the polymer. According to the reviewers, nano lignin is an ideal material with a promising future in nanocomposites.

The authors of the article [18], based on the results of their research on composites with a polymeric phase of polylactic acid and a filler based on cellulose waste fibers, noted that chemical modification of the filler with lactic acid improves the biodegradability of the composite and some of its mechanical properties.

The authors of [19] described the chemical interaction of two silanes with surface functional groups of lignocellulose particles and the chemical bond between them. The authors suggested that functionalization of the lignocellulose surface leads to stronger bonds in the composite between the LCP and the polymer matrix of the ethylene-norbornene copolymer. Furthermore, the modification of lignocellulose by silanes increased the thermal stability of these composites, and the effect on the elastic modulus of the composites is the opposite: N-(2-aminoethyl)-3-aminopropyltrimethoxysilane decreases this index, while vinyltrimethoxysilane increases. Thus, in future studies the authors hoped to obtain epy evidence of an increase in the hydrophobic properties of composites with lignocellulosic fillers with a silane-modified surface.

The authors of the article [20] investigated the preliminary treatment of bagasse powder with choline acetate to improve the properties of polypropylene composites. The results showed a positive effect of filler functionalization on the tensile strength of the composite and a decrease in its porosity by increasing the compatibility of the polypropylene phase with the filler treated with choline acetate.

In [21] the influence of aspen sawdust treatment with a water-soluble polyelectrolyte complex (LPEC), consisting of hardwood soda lignin and polyethyleneimine on the properties of a wood-polymer composite (WPC) with recycled polypropylene were established. The treatment of sawdust with LPEC nanoparticles increased the content of fixed nitrogen in them and led to a slight improvement in the mechanical properties of WPC and a decrease in their wettability. Furthermore, the authors explained the revealed effect of a reduction in the ability of WPC to be wetted with water because of the imine and amide bonds formed between the free amino groups of LPEC and the carbonyl and carboxyl groups of the lignocellulose matrix of the modified topics.

In general, it can be considered that the results of recent studies confirmed not only a significant effect on the TPLC properties of cellulose and lignin content in fillers but also the prospects of regulating this effect using a chemical modification of lignocellulosic fillers by various methods. However, systematic studies of the impact on TPLC properties of the content of hemicelluloses and extractives in lignocellulosic fillers were not carried out.

*Influence of content and chemical structure of special additives*
*on TPLC properties and biodegradation rate*

For the production of TPLC products various chemicals are used as special purpose additives. For example, biocides (antiseptics) are added to the TPLC to increase biostability. In addition, depending on the manufacturing technology of TPLC products, the composite contains plasticizers, compatibilizers, lubricants, and other additives [8]. There is no doubt that some of these additives can affect the chemical structure of the surfaces of the polymer and filler phases in TPLC, the processes of physicochemical interactions between phases, and change the structure and properties of composites.

With the wide variety of environmental parameters leading to TPLC biodegradation, to decrease the rate of composites biodegradation (increase their biostability) modern scientific research continues mainly to find effective biocides for specific operating conditions of products made from these composite materials. At the same time, the search for biocides is carried out among inorganic compounds of various metals, organic compounds of different chemical structures, and the origins of their mixtures. Therefore, nanobiocides are of great interest to scientists [2].

Many factors, including the chemical structure of TPLC components, affect the effectiveness of biocides. For example, the article [9] reported that for composites with a polyethylene matrix and lignocellulosic fillers (flour from wood and bamboo), the composition and chemical structure of the extractive substances of the fillers affect the effectiveness of biocides. The biocides used were 4,5-dichloro-2-octithiazolone, zinc pyrithione, and carbendazim. The extractive matters of the fillers in the presence of biocides had a positive or negative effect on the resistance to algal and fungal degradation of TPLC.

Chinese scientists continued their studies [22] to assess the effect on the properties of TPLC of organomontmorillonite (OMMT) additives synthesized in situ by the exchange of montmorillonite sodium cations for dodecyl dimethyl ammonium chloride. Composites were prepared by hot pressing from mixtures of polypropylene (PP), lignocellulose flour, and OMMT obtained in a twin-screw extruder. The mass ratio of lignocellulose flour/PP was 1:1. Three types of lignocellulose flour were used: poplar flour (WF), cellulose flour (CF), and lignin flour (LF). Studies results showed that the OMMT conferred on TPLC with a polypropylene matrix and lignocellulose flour against fungi of brown (Gloeophyllum trabeum) and white (Coriolus Versicolor) rot. The TPLC mass loss after exposure to rot-fungi for 12 weeks ranged from 0 to 6 %, in contrast to solid pine and poplar wood (over 45 %). The TPLC resistance to brown and white rot varied and depended on the type of lignocellulosic filler.

The review [22] assessed the state and prospects of obtaining antimicrobial composite materials for active packaging of food products, which contain antibacterial nanoparticles (metals, metal oxides, mesoporous silica, and graphene-based nanomaterials) with biodegradable polymers (gelatin, alginate, cellulose, and chitosan).

The state and prospects of using oxo-biodegradable additives to obtain TPLC based on synthetic polymers with increased resistance to UV radiation and microorganisms are reviewed [23].

The general regularities of the influence of special additives chemical structure on TPLC biodegradation rate have not been revealed. TPLC production forecasts, considering their environmental friendliness and economic feasibility, are presented in reviews [1, 24, 25].

*Conclusions*

The production and use of composites with a thermoplastic polymer matrix and lignocellulosic fillers (TPLC) have environmental and economic prospects since waste biomass from forests, agriculture, and plastics is obtained from raw petroleum materials be used for their production. The results of recent studies have confirmed and, in some cases, established the influence of the chemical composition of the polymer phase and lignocellulosic fillers of composites on the performance properties of products obtained from TPLC. This influence on TPLC's physical and mechanical properties and, to a lesser extent, on the rate of their biodegradation in various media has been studied in more detail. Furthermore, TPLC's biodegradability rate is associated with various microorganisms and bacteria used in research and their composition and technological modes of preparation.

The overall conclusion of recent studies is experimental confirmation of a significant effect of TPLC's ability to absorb water and its vapor on their biodegradation rate. The authors of several studies [26–30] predicted the biodegradation rate based on water absorption or sorption by the composites. Another conclusion is that the TPLC biodegradation rate rises with increasing lignocellulose content while its chemical composition remains constant.

The influence of thermoplastic synthetic polymers' physicochemical structure on the TPLC biodegradation rate is explained by the presence of functional groups in the polymer phase that affect its degree of crystallinity, interaction with functional groups of the lignocellulosic filler, uniform distribution of filler particles, and their agglomeration in the composite. However, assessing the effect of the natural polymers' physicochemical structure and the presence and amount of functional groups in the polymer phase on TPLC biodegradation rate is still uncertain.

There is no doubt only the previously established regularity of decrease in TPLC biodegradation rate with an increase in the polymer phase composites deacetylation degree based on cellulose acetate [31].

The modern assessment of TPLC biodegradation rate from the physicochemical structure of lignocellulosic fillers requires simultaneous consideration of their particle size and morphology, which significantly affect the water absorption of composites. Recent studies have confirmed a significant impact on the TPLC biodegradation rate of cellulose and lignin content in fillers and the promise of regulating this effect using a chemical modification of lignocellulose fillers. However, one should consider that the range of plant fillers in which the content of not cellulose and lignin, but other compounds predominates is expanding.

Research on reducing the TPLC biodegradation rate due to the introduction of biocides into their composition continues, but unfortunately, in modern research the environmental hazard of degradation products in soil and water is not assessed.

## References

1    Nassar M.M.A. Progress and challenges in sustainability, compatibility, and production of eco-composites: A state-of-art review / M.M.A. Nassar, K.I. Alzebdeh, T. Pervez, N. Al-Hinai, A. Munam // J. Appl. Polym. Sci. — 2021. — P. 51284. https://doi.org/10.1002/app.51284.

2    Vinod A. Review. Renewable and sustainable biobased materials: An assessment on biofibers, biofilms, biopolymers and biocomposites / A. Vinod, M.R. Sanjay, S. Suchart, P. Jyotishkumar // Journal of Cleaner Production. — 2020. — Vol. 258. — P. 1–27. https://doi.org/10.1016/j.jclepro.2020.120978.

3    Rodriguez L.J. A literature review on life cycle tools fostering holistic sustainability assessment: An application in biocomposite materials / L.J. Rodriguez, P. Peças, H. Carvalho, C.E. Orrego // Journal of Environmental Management. — 2020. — Vol. 262. — P. 110308. https://doi.org/10.1016/j.jenvman.2020.110308.

4    Feng J. Effects of fungal decay on properties of mechanical, chemical, and water absorption of wood plastic composites / J. Feng, S. Li, R. Peng, T. Sun, X. Xie, Q. Shi // J. Appl. Polym. Sci. — 2020. — P. 50022. https://doi.org/10.1002/app.50022.

5    Matlin S.A. Material circularity and the role of the chemical sciences as a key enabler of a sustainable post-trash age / S.A. Matlin, G. Mehta, H. Hopf, A. Krief, L. Keßlerf, K. Kümmerer // Sustainable Chemistry and Pharmacy. — 2020. — Vol. 17. — P. 100312. https://doi.org/10.1016/j.scp.2020.100312.

6    Braghiroli F.L. Valorization of Biomass Residues from Forest Operations and Wood Manufacturing Presents a Wide Range of Sustainable and Innovative Possibilities / F.L. Braghiroli, L. Passarini // Current Forestry Reports. — 2020. — Vol. 6. — P. 172–183. https://doi.org/10.1007/s40725-020-00112-9.

7    Tajeddin B. The effect of wheat straw bleaching on some mechanical properties of wheat straw/LDPE biocomposites / B. Tajeddin, R.F. Momen // Journal of Food and Bioprocess Engineering. — 2020. — Vol. 3, No. 1 — P. 23–28. https://doi.org/10.0.86.43/JFABE.2020.75620.

8    Клёсов А.А. Древесно-полимерные композиты / А.А. Клёсов. — СПб.: Научные основы и технологии, 2010. — С. 461–512.

9    Feng J. Effects of biocide treatments on durability of wood and bamboo/high density polyethylene composites against algal and fungal decay / J. Feng, J. Chen, M. Chen, X. Su, Q. Shi // J. Appl. Polym. Sci. — 2017. — P. 45148. DOI: 10.1002/APP.45148.

10   Glukhikh V.V. Plastics: physical-and-mechanical properties and biodegradable potential / V.V. Glukhikh, V.G. Buryndin, A.V. Artemov, A.V. Savinovskih, P.S. Krivonogov, A.S. Krivonogova // Foods and Raw Material. — 2020. — Vol. 8, No 1. — P. 149–154. https://doi.org/10.21603/2308-4057-2020-1-149-154.

11   Candelier K. Termite and decay resistance of bioplast-spruce green wood-plastic composites / K. Candelier, A. Atli, J. Alteyrac // European Journal of Wood and Wood Products. — 2019. — Vol. 77. — P. 157–169. https://doi.org/10.1007/s00107-018-1368-y.

12   Попов А.А. Биоразлагаемые композиционные материалы. (Обзор) / А.А. Попов, А.К. Зыкова, Е.Е. Масталыгина // Химическая физика. — 2020. — Т. 39, № 6. — С. 71–80.

13   Polman E.M.N. Comparison of the aerobic biodegradation of biopolymers and the corresponding bio-plastics: A review / E.M.N. Polman, G.-J.M. Gruter, J.R. Parsons, A. Tietema // Science of the Total Environment. — 2021. — Vol. 753. — P. 141953. https://doi.org/10.1016/j.scitotenv.2020.141953 0048-9697.

14   Marczak D. Characteristics of biodegradable textiles used in environmental engineering: A comprehensive review / D. Marczak, K. Lejcus, J. Misiewicz // Journal of Cleaner Production. — 2020. — Vol. 268. — P. 122129. https://doi.org/10.1016/j.jclepro.2020.122129.

15   Fujisawa S. All-Cellulose (Cellulose–Cellulose) Green Composites / S. Fujisawa, T. Saito, and A. Isogai // Advanced Green Composites. — 2018. — P. 111–134. https://doi.org/10.1002/9781119323327.

16   Li H. Conversion of biomass lignin to high-value polyurethane: A review / H. Li, Y. Lianga, P. Li, C. He // Journal of Bioresources and Bioproducts. — 2020. — Vol. 5, No 3. — P. 163–179.

17   Parvathy, G. Lignin based nano-composites: Synthesis and applications / G. Parvathy, S. AS, J. S Jayan, A. Raman, A. Saritha // Process Safety and Environmental Protection. — 2021. — Vol. 145. — P. 395–410. https://doi.org/10.1016/j.psep.2020.11.017 0957-5820.

18   Gama N. New poly(lactic acid) composites produced from coffee beverage wastes // N. Gama, A. Ferreira, D.V. Evtuguin // J. Appl. Polym. Sci. — 2021. — Vol. 138, No. 35. — P. 51434. https://doi.org/10.1002/app.51434.

19   Wolski K. Surface hydrophobisation of lignocellulosic waste for the preparation of biothermoelastoplastic composites / K. Wolski, S. Cichosz, A. Masek // European Polymer Journal. — 2019. — Vol. 118. — P. 481–491.

20   Ninomiya K. Ionic liquid pretreatment of bagasse improves mechanical property of bagasse/polypropylene composites / K. Ninomiya, M. Abe, T. Tsukegi, K. Kuroda, M. Omichi, K. Takada, et al. // Industrial Crops & Products — 2017. — Vol. 109. — P. 158–162. http://dx.doi.Org/10.1016/j.indcrop.2017.08.019.

V.V. Glukhikh[*], A.E. Shkuro, P.S. Krivonogov

21 Shulga G. Lignin-containing Adhesion Enhancer for Wood-plastic Composites / G. Shulga, B. Neiberte, J. Jaunslavietis, A. Verovkins, S. Vitolina, V. Shakels, et al. // BioResources. — 2021. — Vol. 16, No. 2. — P. 2804–2823. https://doi.org/10.15376/biores.16.2.2804-2823.

22 Liu R. Fungi Resistance of Organo-Montmorillonite Modified Lignocellulosic Flour/Polypropylene Composites // R. Liu, M. Liu, J. Cao, E. Ma, A. Huang // POLYMER COMPOSITES-2017. — 2017. https://doi.org/10.1002/pc.24413.

23 Луканина Ю.К. Оксо-биодеградируемые полимерные материалы. (Обзор) / Ю.К. Луканина, А.А. Попов // Все материалы. Энцикл. справ. — 2021 — № 3. — С. 9–15. https://doi.org/10.31044/1994-6260-2021-0-3-9-15.

24 Vikhareva I.N. An Overview of the Main Trends in the Creation of Biodegradable Polymer Materials /I.N. Vikhareva, E.A. Buylova, G.U. Yarmuhametova, G.K. Aminova, A.K. Mazitova // Journal of Chemistry. — Vol. 2021. https://doi.org/10.1155/2021/5099705.

25 Pellis A. Renewable polymers and plastics: Performance beyond the green / A. Pellis, M. Malinconico, A. Guarneri, L. Gardossi // New Biotechnology — 2021. — Vol. 60. — P. 146–158.

26 Kaboorani A. Tailoring the low-density polyethylene — thermoplastic starch composites using cellulose nanocrystals and compatibilizer / A. Kaboorani, N. Gray, Y. Hamzeh, A. Abdulkhani // Polymer Testing. — 2021. — Vol. 93. — P. 107007. https://doi.org/10.1016/j.polymertesting.2020.107007.

27 Kocaman S. Chemical and plasma surface modification of lignocellulose coconut waste for the preparation of advanced biobased composite materials / S. Kocaman, M. Karaman, M. Gursoy, G. Ahmetli // Carbohydrate Polymers. — 2017. — Vol. 159. — P. 48–57. http://dx.doi.org/doi:10.1016/j.carbpol.2016.12.016.

28 Gerbin E. Tuning the functional properties of lignocellulosic films by controlling the molecular and supramolecular structure of lignin / E. Gerbin, G.N. Rivière, L. Foulon, Y.M. Frapart, B. Cottyn, M. Pernes, et al. // International Journal of Biological Macromolecules. — 2021. — Vol. 181. — P. 136–149. https://doi.org/10.1016/j.ijbiomac.2021.03.081.

29 Gaudio I. Water sorption and diffusion in cellulose acetate: The effect of plasticisers / I. Gaudio, E. Hunter-Sellars, I.P. Parkin, D. Williams, S.D. Ros, K. Curran // Carbohydrate Polymers. — 2021. — Vol. 267. — P. 118185. https://doi.org/10.1016/j.carbpol.2021.118185.

30 Bazunova M. The Surface Structure Of Polymer Composites Based On Recycled Polypropylene And Natural Components Of Vegetable Origin In The Process Of Biodegradation / M. Bazunova, R. Salikhov, A. Sadritdinov, V. Chernova, V. Zakharov // J. Pharm. Sci. & Res. — 2018. — Vol. 10, No. 2. — P. 288–292.

31 Yadav N. Degradable or not? Cellulose acetate as a model for complicated interplay between structure, environment and degradation / N. Yadav, M. Hakkarainen // Chemosphere. — 2021. — Vol. 265. — P. 128731. https://doi.org/10.1016/j.chemosphere.2020.128731.

В.В. Глухих, А.Е. Шкуро, П.С. Кривоногов

# Лигноцеллюлозалық толтырғыштары бар полимерлі композиттердің биодеградация жылдамдығына және физикалық-механикалық қасиеттеріне компоненттердің химиялық құрамының әсерін қарастыру

Термопластикалық полимер фазасы мен лигноцеллюлозалық толтырғыштармен (TPLC) композитті ғылыми зерттеулердің нәтижелері, оларды дайындау мен қолданудың практикалық тәжірибесі 2016 ж. «Жаңартылатын материалдардан жасалған композиттердің анықтамасының» (2017, John Wiley & Sons, Inc.) сегіз томдығында ұсынылған. Мақалада лигноцеллюлоза толтырғыштары бар полимерлі композиттердің биоыдырау жылдамдығын және физикалық-механикалық қасиеттерін бағалау үшін 2017–2020 жылдар мен 2021 жылдың бірінші жартыжылдығына арналған кітаптар мен мақалаларға талдау жасалған. TPLC алу мен қолданудың экологиялық және экономикалық болашағы зор, өйткені оларды өндіру үшін ормандардың, ауыл шаруашылық және мұнай шикізатынан алынған полимерлердің қалдықтары пайдаланылуы мүмкін. TPLC қолдану аймағына байланысты олардың биодеградация жылдамдығына қарама-қарсы талаптар бар. Құрылыста және медицинада қолдану үшін материалдар мен бұйымдардың биологиялық ыдырауының минималды жылдамдығы болуы керек. Бір рет қолданылатын қаптамаға арналған материалдар мен бұйымдар биологиялық ыдырауға бейімді болуы және топырақта, суда, компост ортасында белгілі жылдамдықта биологиялық ыдырауға ұшырай алуы қажет. Зерттеу нәтижелері TPLC қасиеттеріне физикалық ғана емес, сонымен қатар осы композиттердің барлық компоненттерінің химиялық құрылымы да қатты әсер ететінін көрсетеді. Полимерлердің, толтырғыштардың, әртүрлі мақсаттағы қоспалардың химиялық қасиеттері олардың өнеркәсіптік өндірісінің тиімділігіне әсер етуі мүмкін.

*Кілт сөздер*: композит, химиялық құрылымы, термопластикалық полимер, толтырғыш, целлюлоза, лигнин.

В.В. Глухих, А.Е. Шкуро, П.С. Кривоногов

# Обзор влияния химического состава компонентов на скорость биоразложения и физико-механические свойства полимерных композитов с лигноцеллюлозными наполнителями

Результаты научных исследований композитов с термопластичной полимерной фазой и лигноцеллюлозными наполнителями (TPLC), практический опыт их получения и применения по состоянию на 2016 г. представлены в восьми томах «Handbook of Composites from Renewable Materials» (2017, John Wiley & Sons, Inc.). В статье приведён обзор книг и статей за период 2017–2020 годы и первую половину 2021 г. по оценке скорости биоразложения и физико-механических свойств полимерных композитов с лигноцеллюлозными наполнителями. Получение и применение TPLC имеют большие экологические и экономические перспективы, так как для их производства могут быть использованы отходы биомассы леса, сельского хозяйства и полимеров, получаемых из нефтяного сырья. В зависимости от области применения TPLC, существуют противоположные требования к скорости их биоразложения. Для применения в строительстве и медицине материалы и изделия должны иметь минимальную скорость биоразложения. Материалы и изделия для одноразовой упаковки должны обладать необходимым потенциалом биоразложения и иметь заданную скорость биоразложения в грунте, воде, компостной среде. Результаты исследований показывают, что на свойства TPLC большое влияние может оказывать, не только физическое, но и химическое строение всех компонентов этих композитов. Химические свойства полимеров, наполнителей, добавок различного назначения могут повлиять на экономичность их промышленного производства.

*Ключевые слова*: композит, химическая структура, термопластичный полимер, наполнитель, целлюлоза, лигнин.

## References

1    Nassar, M.M.A., Alzebdeh, K.I., Perve,z T., Al-Hinai, N., & Munam, A. (2021). Progress and challenges in sustainability, compatibility, and production of eco-composites: A state-of-art review. *J Appl. Polym. Sci.*, 51284. https://doi.org/10.1002/app.51284.

2    Vinod, A., Sanjay, M.R., Suchart, S., Jyotishkumar, P. (2020). Review. Renewable and sustainable biobased materials: An assessment on biofibers, biofilms, biopolymers and biocomposites. *Journal of Cleaner Production, 258*, 1-27. https://doi.org/10.1016/j.jclepro.2020.120978.

3    Rodriguez, L.J., Peças, P., Carvalho, H., & Orrego, C.E. (2020). A literature review on life cycle tools fostering holistic sustainability assessment: An application in biocomposite materials. *Journal of Environmental Management, 262*, 110308. https://doi.org/10.1016/j.jenvman.2020.110308.

4    Feng, J., Li, S., Peng, R., Sun, T., Xie, X., & Shi, Q. (2020). Effects of fungal decay on properties of mechanical, chemical, and water absorption of wood plastic composites. *J. Appl. Polym. Sci.*, 50022. https://doi.org/10.1002/app.50022.

5    Matlin, S.A., Mehta, G., Hopf, H., Krief, A., Keßlerf, L., & Kümmerer, K. (2020). Material circularity and the role of the chemical sciences as a key enabler of a sustainable post-trash age Sustainable. *Chemistry and Pharmacy, 17*, 100312. https://doi.org/10.1016/j.scp.2020.100312.

6    Braghiroli, F.L., Passarini, L. (2020). Valorization of Biomass Residues from Forest Operations and Wood Manufacturing Presents a Wide Range of Sustainable and Innovative Possibilities. *Current Forestry Reports, 6*, 172–183. https://doi.org/10.1007/s40725-020-00112-9.

7    Tajeddin, B., & Momen, R.F. (2020). The effect of wheat straw bleaching on some mechanical properties of wheat straw/LDPE biocomposites. *Journal of Food and Bioprocess Engineering, 3, 1*, 23–28. https://doi.org/10.22059/JFABE.2020.75620.

8    Klyosov, A.A. (2010). *Drevesno-polimernye kompozity [Wood-plastic composites]*. Saint Petersburg: Scientific foundations and technologies [in Russian].

9    Feng, J., Chen, J., Chen, M., Su, X., & Shi, Q. (2017). Effects of biocide treatments on durability of wood and bamboo/high density polyethylene composites against algal and fungal decay. *J. Appl. Polym. Sci.*, 45148. https://doi.org/10.1002/APP.45148.

10   Glukhikh, V.V., Buryndin, V.G., Artemov, A.V., Savinovskih, A.V., Krivonogov, P.S., & Krivonogova, A.S. (2020). Plastics: physical-and-mechanical properties and biode-gradable potential. *Foods and Raw Material, 8, 1*, 149–154. https://doi.org/10.21603/2308-4057-2020-1-149-154.

11   Candelier, K., Atli, A., Alteyrac, J. (2019). Termite and decay resistance of bioplast-spruce green wood-plastic composites. *European Journal of Wood and Wood Products, 77*, 157–169. https://doi.org/10.1007/s00107-018-1368-y.

12   Popov, A.A., Zykova, A.K., & Mastalygina, A.K. (2020). Biorazlagaemye kompozitsionnye materialy. (Obzor) [Biodegradable composite materials (Review)]. *Khimicheskaia fizika — Chemical Physics, 39, 6*, 71–80 [in Russian].

13   Polman, E.M.N., Gruter, G.-J.M., Parsons, J.R., & Tietema, A. (2021). Comparison of the aerobic biodegradation of biopolymers and the corresponding bio-plastics: A review. *Science of the Total Environment, 753*, 141953. https://doi.org/10.1016/j.scitotenv.2020.141953 0048-9697.

14   Marczak, D., Lejcus, K., & Misiewicz, J. (2020). Characteristics of biodegradable textiles used in environmental engineering: A comprehensive review. *Journal of Cleaner Production, 268*, 122129. https://doi.org/10.1016/j.jclepro.2020.122129.

15 Fujisawa, S., Saito, T., & Isogai, A. (2018). All-Cellulose (Cellulose–Cellulose) Green Composites. *Advanced Green Composites*, 111–134. https://doi.org/10.1002/9781119323327.

16 Li, H., Lianga, Y., Li, P., & He, C. (2020). Conversion of biomass lignin to high-value polyurethane: A review. *Journal of Bioresources and Bioproducts, 5, 3*, 163–179.

17 Parvathy, G., AS, S., Jayan, J.S., Raman, A., & Saritha, A. (2021). Lignin based nano-composites: Synthesis and applications. *Process Safety and Environmental Protection, 145*, 395–410. https://doi.org/10.1016/j.psep.2020.11.017 0957-5820.

18 Gama, N., Ferreira, A., & Evtuguin, D.V. (2021). New poly(lactic acid) composites produced from coffee beverage wastes. *J. Appl. Polym. Sci., 138, 35*, 51434. https://doi.org/10.1002/app.51434.

19 Wolski, K., Cichosz, S., & Masek, A. (2019). Surface hydrophobisation of lignocellulosic waste for the preparation of biothermoelastoplastic composites. *European Polymer Journal, 118*, 481–491.

20 Ninomiya, K., Abe, M., Tsukegi, T., Kuroda, K., Omichi, M., & Takada, K., et al. (2017). Ionic liquid pretreatment of bagasse improves mechanical property of bagasse/polypropylene composites. *Industrial Crops & Products, 109*, 158–162. https://dx.doi.Org/10.1016/j.indcrop.2017.08.019.

21 Shulga, G., Neiberte, B., Jaunslavietis, J., Verovkins, A., Vitolina, S., & Shakels V., et al. (2021). Lignin-containing Adhesion Enhancer for Wood-plastic Composites. *BioResources, 16, 2*, 2804–2823. https://10.15376/biores.16.2.2804-2823.

22 Liu, R., Liu, M., Cao, J., Ma, E., Huang, A. (2017). Fungi Resistance of Organo-Montmorillonite Modified Lignocellulosic Flour/Polypropylene Composites. *POLYMER COMPOSITES-2017*. https://doi.org/10.1002/pc.24413.

23 Lukanina, Y.K. & Popov, A.A. (2021). Okso-biodegradiruemye polimernye materialy. (Obzor) [Oxo-biodegradable polymer materials (Review)]. *All materials. An encyclopedic reference book, 6*, 9–15 [in Russian].

24 Vikhareva, I.N., Buylova, E.A., Yarmuhametova, G.U., Aminova, G.K., & Mazitova, A.K. (2021). An Overview of the Main Trends in the Creation of Biodegradable Polymer Materials. *Journal of Chemistry*, 2021. https://doi.org/10.1155/2021/5099705.

25 Pellis, A., Malinconico, M., Guarneri, A., Gardossi, L. (2021). Renewable polymers and plastics: Performance beyond the green. *New Biotechnology, 60*, 146–158.

26 Kaboorani, A., Gray, N., Hamzeh, Y., & Abdulkhani, A. (2021). Tailoring the low-density polyethylene — thermoplastic starch composites using cellulose nanocrystals and compatibilizer. *Polymer Testing, 93*, 107007. https://doi.org/10.1016/j.polymertesting.2020.107007.

27 Kocaman, S., Karaman, M., Gursoy, M., & Ahmetli, G. (2017). Chemical and plasma surface modification of lignocellulose coconut waste for the preparation of advanced biobased composite materials. *Carbohydrate Polymers, 159*, 48–57. http://dx.doi.org/doi:10.1016/j.carbpol.2016.12.016.

28 Gerbin, E., Rivière, G.N., Foulon, L., Frapart, Y.M., Cottyn B., & Pernes, M. et al. (2021). Tuning the functional properties of lignocellulosic films by controlling the molecular and supramolecular structure of lignin. *International Journal of Biological Macromolecules, 181*, 136–149. https://doi.org/10.1016/j.ijbiomac.2021.03.081.

29 Gaudio, I., Hunter-Sellars, E., Parkin, I.P., Williams, D., Ros, S.D., & Curran, K. (2021). Water sorption and diffusion in cellulose acetate: The effect of plasticisers. *Carbohydrate Polymers, 267*, 118185. https://doi.org/10.1016/j.carbpol.2021.118185.

30 Bazunova, M., Salikhov, R., Sadritdinov, A., Chernova, V., & Zakharov, V. (2018). The Surface Structure Of Polymer Composites Based On Recycled Polypropylene And Natural Components Of Vegetable Origin In The Process Of Biodegradation. *J. Pharm. Sci. & Res., 10, 2*, 288–292.

31 Yadav, N., & Hakkarainen, M. (2021). Degradable or not? Cellulose acetate as a model for complicated interplay between structure, environment and degradation. *Chemosphere, 265*, 128731. https://doi.org/10.1016/j.chemosphere.2020.128731.

Information about authors:

**Glukhikh Victor Vladimirovich** (corresponding author) — Doctor of technical sciences, Professor, Ural State Forest Engineering University, Siberian tract, 37, 620100, Yekaterinburg, Sverdlovsk region, Russia; e-mail: gluhihvv@m.usfeu.ru; https://orcid.org/0000-0001-6120-1867;

**Shkyro Alekseiy Yevgenyevich** — Candidate of technical sciences, Docent, Ural State Forest Engineering University, Siberian tract, 37, 620100, Yekaterinburg, Sverdlovsk region, Russia; e-mail: shkuroae@m.usfeu.ru; https://orcid.org/0000-0002-0469-2601;

**Krivonogov Pavel Sergeevich** — Candidate of technical sciences, Docent, Ural State Forest Engineering University, Siberian tract, 37, 620100, Yekaterinburg, Sverdlovsk region, Russia; e-mail: krivonogovps@m.usfeu.ru; https://orcid.org/0000-0001-5171-4482.

# M.D. Plotnikova, A.B. Shein, M.G. Shcherban`*, A.D. Solovyev

*Perm State National Research University, Perm, Russia*
*(\*Corresponding author's e-mail: ma-sher74@mail.ru)*

# The study of thiadiazole derivatives as potential corrosion inhibitors of low-carbon steel in hydrochloric acid

The inhibition effect of series of thiadiazole derivatives against the corrosion of mild steel in 15 % HCl was studied by weight-loss method and electrochemical measurements. The experiments were performed on steel St3 at 293 K, the exposure time of the samples in solution for weight-loss measurements was 24 h. Potentiodynamic polarization curves were obtained in a typical three electrode cell with the help of electrochemical measuring complex SOLARTRON 1280 C. A scan rate was 1 mV·s$^{-1}$ and a measurement point was taken every 0.2 s. 2-aminothiazole, 5-amino-1,3,4-thiadiazole-2-thiol, 2-amino-1,3,4-thiadiazole, 2-amino-5-(furan-2-yl)-1,3,4-thiadiazole, 1,3,4-thiadiazole-2-ylamide of acetic acid were studied as potential inhibitors. The maximal inhibition efficiency was obtained at concentration 0.10-0.20 g·L$^{-1}$. The best result was demonstrated by 5-amino-1,3,4-thiadiazole-2-thiol (inhibition effect was more than 90 %). The minimal inhibition effect had 1,3,4-thiadiazole-2-ylamide acetic acid. The corrosion inhibition effect calculated from data of the corrosion current density and from the weight-loss measurements were in sufficiently good agreement. The effective activation energy of the corrosion of St3 increased significantly due the presence of the inhibitors (from 3.3 to 94.8 kJ·mol$^{-1}$). The results point to promising of investigating of series of thiadiazole derivatives and inhibitory compositions based on thiadiazole as potential acid corrosion inhibitors.

*Keywords*: low-carbon steel, corrosion, inhibitors, thiadiazole, thiazole, weight-loss method, impedance spectroscopy, adsorbtion.

## Introduction

Corrosion of metals and alloys is a big problem for the oil and gas industry. The use of acidic media leads to the failure of well equipment, oil collection and distillation units, and pipelines [1–3]. Inhibitors are specially selected compounds that are used to prevent the destruction of metals and alloys from corrosion [4, 5]. They are added into the corrosion system in a low concentration and reduce the rate of corrosion without significantly changing the composition of the system. At the present time, the development of new environmentally friendly corrosion inhibitors that do not contain toxic metals and inorganic phosphates is of great importance [6–9].

Many organic compounds containing heteroatoms are able to slow down metal corrosion in acidic media. The most widespread are inhibitors based on nitrogen-containing compounds [10]. However, compounds containing sulfur atom in the molecule are also of great interest today. Such compounds include thiols, thiosulfonic acids, thiophenes, and sulfur-containing triazoles [11, 12].

Thus, the purpose of this work was the research of some thiadiazole derivatives as corrosion inhibitors for mild steel in a 15 % solution of hydrochloric acid.
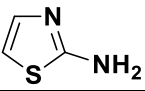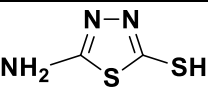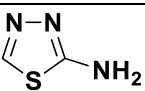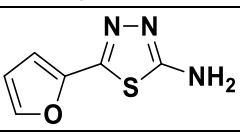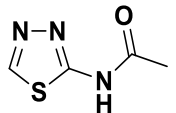
## Experimental

The material for the study were the samples made of low-carbon steel St3 of composition, wt%, Fe, 98.36; C, 0.2; Mn, 0.5; Si, 0.15; P, 0.04; S, 0.05; Cr, 0.3; Ni, 0.2; Cu, 0.2. All measurements were conducted in unstirred 15 % HCl solutions prepared on the basis of distilled water and HCl of the chemically pure grade. Products of organic synthesis, thiadiazole derivatives, were used as corrosion inhibitors (Table 1).

All the data presented in the work was obtained by averaging the results of three parallel measurements. MS Excel software was used to calculate the average results and standard deviations of direct and indirect measurements.

The main parameters of steel corrosion were estimated according to generally accepted methods [13]. Rectangular samples made of St3 steel with a size of 25×20×2 mm were used for weight-loss analysis. The working surface area was 1180 mm$^2$.

**Chemical compounds studied in the work as corrosion inhibitors**

| Cipher | Formula | Name by nomenclature |
|--------|---------|----------------------|
| AK-9 | | 2-aminothiazole |
| AK-10 | | 5-amino-1,3,4-thiadiazole-2-thiol |
| AK-23 | | 2-amino-1,3,4-thiadiazole |
| AK-44 | | 2-amino-5-(furan-2-yl)-1,3,4-thiadiazole |
| AK-69 | | 1,3,4-thiadiazole-2-yl acetic acid amide |

The corrosion rates ($K$), the inhibition factor ($\gamma$) and the degree of protection ($Z_{gr}$) were calculated using equations:

$$K = \frac{m_0 - m}{S \cdot \tau} \; ;$$

$$\gamma = \frac{K_0}{K} \; ;$$

$$Z_{gr} = \frac{K_0 - K}{K_0} \cdot 100 \; \% \; ,$$

where $m_0$ is the mass of the initial sample, g; $m$ is the mass of the sample after corrosion testing and removal of corrosion products, g; $S$ is the surface area of the sample, m$^2$; $\tau$ is the immersion time, h; $K_0$ and $K$ are the corrosion rates of steel in pure solution and with the addition of an inhibitor, g·m$^{-2}$·hour$^{-1}$, respectively.

Electrochemical measurements were performed in a three-electrode cell with cathode and anode compartments separated by a porous glass diaphragm using a potentiostat-galvanostat with a built-in SOLARTRON 1280C frequency analyzer (Solartron Analytical). Polarization curves were obtained by potentiodynamic polarization from the cathode region to the anode region with scan rate of 1 mV·s$^{-1}$. All values of potential are presented in the standard hydrogen electrode scale.

Polarization measurements were carried out in the temperature range from 293 to 353 K. The cell was connected to an LT 100 thermostat with external circulation to set the required temperature.

Thanks to this method, it is also possible to determine the Tafel sections of the polarization curves and calculate the degree of protection from electrochemical data:

$$Z_{el/ch} = \frac{i_0 - i_{inh}}{i_0} \cdot 100 \; \% \; ,$$

where $i_0$ and $i_{inh}$ are the current densities of steel corrosion in pure solution and with the addition of an inhibitor, A·m$^{-2}$, respectively.

Based on the electrochemical results the activation energy of the corrosion process was calculated. The calculations were performed according to the temperature-kinetic method. The effect of temperature on the current density when concentration polarization or delayed discharge stage is described by an equation similar to the Arrhenius equation:

$$\ln i = -E_{ef} / RT \; ,$$

where $i$ is the corrosion current density, A·m$^{-2}$; $E_{ef}$ is the effective activation energy of corrosion process, J·mol$^{-1}$; $T$ is the temperature, K.

A straight line in the coordinates $\lg(i) = f(1/T)$ allows to calculate $E_{ef}/R$ as the tangent of the angle of inclination.

Measurements of the impedance spectra were carried out at a temperature of ~293 K. The range of frequencies used in impedance measurements was $f$ from 20 kHz to 0.01 Hz, and the amplitude of the alternating signal was 5–10 mV. The electrodes were immersed into the solution for an hour to establish the corrosion potential.

Parameter $\chi^2$ (calculated in ZView2) was used as an evaluation criterion for equivalent electrical circuits for their suitability for simulation of experimental impedance spectra. The equivalent circuit was considered satisfactory at $\chi^2 < 10^{-3}$ (using weight coefficients calculated by the experimental values of the impedance module) [14].

The surface coverage ($\theta$) of C1018-electrode by corrosion inhibitor was determined from equation:

$$\theta = \frac{C_o - C}{C_o - C_1},$$

where $C_o$, $C$ and $C_1$ are the capacity of the double electric layer in a pure acid solution, in a solution with a given concentration of the inhibitors and in a solution where $\theta = 1$, respectively.

The value of $C_1$ was determined by extrapolating the curve in coordinates

$$C = f\left(\frac{1}{C_{inh}}\right) \text{ to } \left(\frac{1}{inh}\right) = 0,$$

where $C_{inh}$ is the concentration of the inhibitor in solution, $g \cdot L^{-1}$.

### Results and Discussion

At the first stage of the study, the corrosion rate of the St3 steel in 15 % HCl solution was studied by the weight-loss method. Then the corrosion rate of mild steel in the presence of some thiadiazole derivatives was measured. In the course of the work, it was found that some of the testing samples are not-well soluble in 15 % HCl solution. As the result the following concentrations were used: 0.05–0.2 $g \cdot L^{-1}$.

The results are presented in Table 2.

Table 2

**The main parameters of the St3 corrosion in 15 % HCl solution and in the presence of inhibitors**

| Cipher | $C_{inh}$, $g \cdot L^{-1}$ | $K$, $g \cdot m^{-2} \cdot hour^{-1}$ | $Z_{gr}$, % | $\gamma$ |
|---|---|---|---|---|
| – | – | 15.2±0.8 | – | – |
| AK-9 | 0.20 | 6.9±0.4 | 54±3 | 2.19±0.11 |
| | 0.10 | 8.0±0.4 | 48±2 | 1.91±0.04 |
| | 0.05 | 9.4±0.3 | 38±2 | 1.62±0.03 |
| AK-10 | 0.20 | 1.5±0.1 | 90±3 | 10.22±0.32 |
| | 0.10 | 2.6±0.1 | 83±3 | 5.91±0.13 |
| | 0.05 | 4.0±0.2 | 74±3 | 3.83±0.11 |
| AK-23 | 0.20 | 6.1±0.2 | 67±2 | 2.51±0.09 |
| | 0.10 | 10.0±0.5 | 46±2 | 1.53±0.04 |
| | 0.05 | 15.7±0.7 | 16±1 | 0.96±0.01 |
| AK-44 | 0.20 | 5.5±0.2 | 92±4 | 12.30±0.43 |
| | 0.10 | 1.2±0.1 | 64±3 | 2.77±0.04 |
| AK-69 | 0.20 | 11.6±0.6 | 40±2 | 1.67±0.03 |
| | 0.10 | 9.5±0.4 | 37±1 | 1.60±0.03 |
| | 0.05 | 9.1±0.4 | 24±1 | 1.32±0.02 |

According to the results of weight loss measurements presented in Table 2, the nature of the substituent in the thiadiazole molecule has a significant influence on the values of the inhibition effect. The corrosion rate of St3 increases in the presence of potential inhibitors with increasing in the acid concentration. From weight-loss measurements (Table 2) and the results of solubility of substances we can conclude that the optimal inhibition effect has been shown by AK-9, AK-10, AK-23. Then, a number of electrochemical studies for estimation of the mechanism of the action of inhibitors were made.

The polarization curves were obtained in 15 % HCl solution without and with addition of 0.1 gL$^{-1}$ of thiadiazoles. The temperature range varied from 293 to 353 K. The polarization curves are given in Figure 1, and the electrochemical parameters of the processes are presented in Table 3.
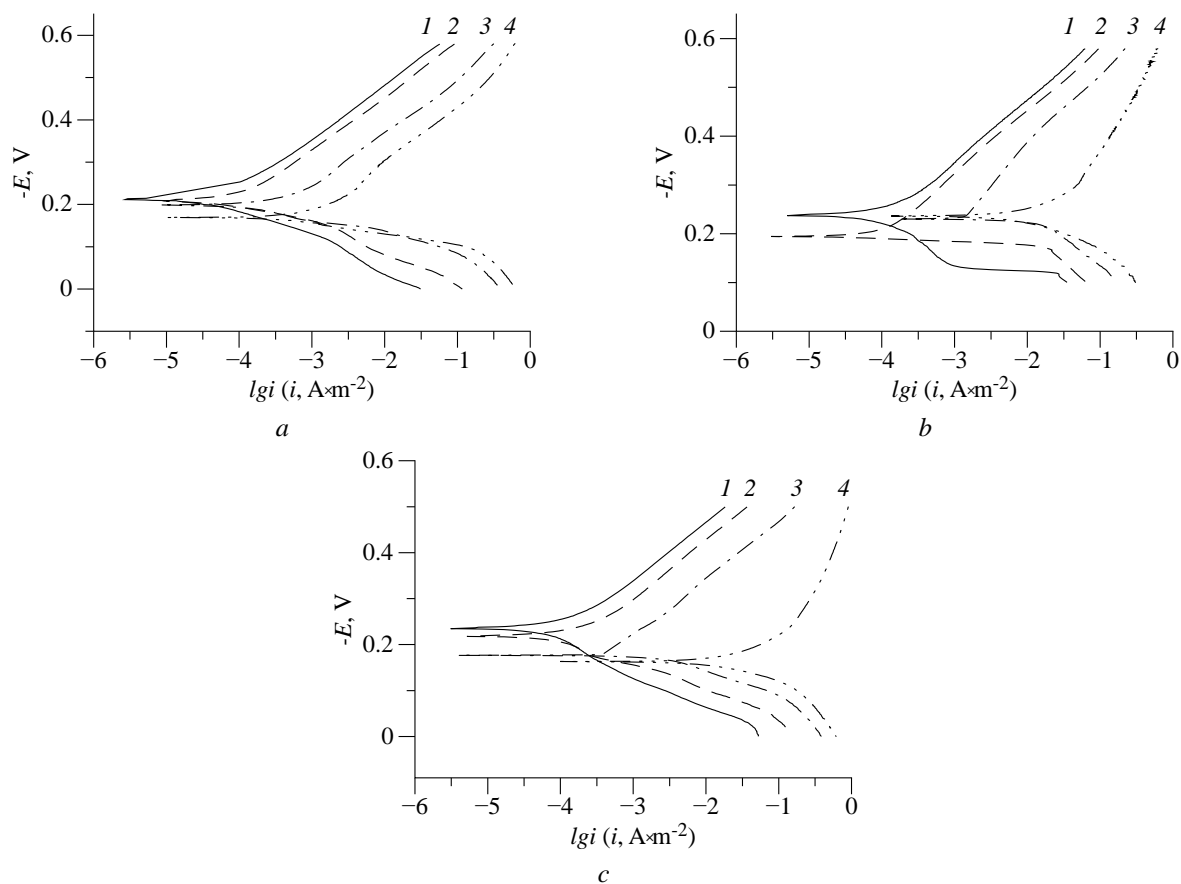


Figure 1. Polarization curves of St3 in solution of 15 % HCl in the presence of 0.10 gL$^{-1}$ inhibitor AK-9 (*a*), AK-10 (*b*), AK-23 (*c*) at temperatures of: *1* — 293 K; *2* — 313 K; *3* — 333 K; *4* — 353 K

In the solutions of 15 % HCl containing 0.10 g·L$^{-1}$ of inhibitors, the corrosion potential of the St3 is shifted to the cathodic region.

The currents in the system are reduced in both the cathodic and anodic processes for each inhibitor. Therefore, testing substances can be classified as inhibitors possessing relatively mixed effect (anodic/cathodic inhibition) in acidic solutions. From the results of Table 3, it follows that the values of the Tafel coefficients $b_c$ decrease in comparison with the pure solution of 15 % HCl. This result indicates that hydrogen can be removed from the steel surface in two ways — by electrochemical desorption and recombination.

As can be seen from these polarization results, all inhibitors have significant effect on the $b_a$ values in the temperature range of 293–333 K. A sharp increase in $b_c$ is observed for AK-10 and AK-23 inhibitors at a temperature of 353 eK. The Tafel coefficients obtained in the presence of AK-9 are less affected by temperature.

This result indicates that the AK-9 protects St3 from corrosion effectively with increasing temperature, while in the case of the AK-10 and AK-23 protective effect significantly decreases with increasing temperature. It can be assumed that AK-10 and AK-23 slow down the corrosion process due to physical adsorption on the steel surface and they desorb from the electrode surface into the solution with temperature. In contrast, in the case of AK-9, a chemisorption process is likely.

The temperature dependence of the St3 steel dissolution in deaerated 15 % HCl and in the presence of thiadiazoles is ploted in Arrhenius coordinates ln $i – 1/T$ (where $i$ is the corrosion current density). The calculated values of the apparent activation corrosion energy in the absence and presence of AK-23, AK-10 and AK-9 are 23.3, 120.7, 60.8 and 35.3 kJ·mol$^{-1}$, respectively.

The presence of the inhibitor increases the energy barrier for the dissolution process of St3 and this leads to a decreasing of the corrosion rate.

**Polarization parameters and the corresponding inhibition efficiency for the corrosion of the St3 in solution of 15 % HCl containing 0.10 g·L$^{-1}$ of inhibitors in the temperature range 293–353 K**

| Cipher | $T$, K | $b_a$, mV | $b_c$, mV | $i_{corr} \cdot 10^3$, A·m$^{-2}$ | $-E_{corr}$, V | $Z_{el/ch}$, % |
|---|---|---|---|---|---|---|
| – | 293 | 93±2 | 140±2 | 1.58±0.04 | 0.200±0.002 | - |
| AK-9 | | 47±1 | 133±2 | 0.06±0.01 | 0.192±0.001 | 96±2 |
| AK-10 | | 133±3 | 125±2 | 0.10±0.01 | 0.235±0.003 | 94±3 |
| AK-23 | | 65±1 | 154±3 | 0.06±0.01 | 0.208±0.001 | 96±2 |
| – | 303 | 74±2 | 148±2 | 2.01±0.03 | 0.197±0.001 | – |
| AK-9 | | 43±1 | 140±2 | 0.06±0.01 | 0.197±0.001 | 97±2 |
| AK-10 | | 138±3 | 123±2 | 0.45±0.01 | 0.250±0.003 | 78±2 |
| AK-23 | | 59±1 | 154±3 | 0.22±0.01 | 0.209±0.002 | 89±2 |
| – | 313 | 62±1 | 154±4 | 3.16±0.03 | 0.190±0.001 | – |
| AK-9 | | 40±1 | 143±3 | 0.08±0.01 | 0.201±0.002 | 97±2 |
| AK-10 | | 144±4 | 120±2 | 1.20±0.02 | 0.258±0.002 | 62±1 |
| AK-23 | | 54±1 | 154±5 | 0.40±0.01 | 0.208±0.001 | 87±3 |
| – | 333 | 55±1 | 167±5 | 5.01±0.02 | 0.180±0.001 | – |
| AK-9 | | 36±1 | 143±2 | 0.32±0.01 | 0.183±0.001 | 94±3 |
| AK-10 | | 160±3 | 167±4 | 2.0±0.02 | 0.191±0.001 | 60±2 |
| AK-23 | | 44±1 | 154±3 | 1.00±0.01 | 0.177±0.001 | 20±2 |
| – | 353 | 20±1 | 182±5 | 199.50±9.98 | 0.120±0.002 | – |
| AK-9 | | 31±2 | 151±2 | 0.71±0.01 | 0.167±0.001 | 99±1 |
| AK-10 | | 174±4 | 200±3 | 79.43±4.32 | 0.177±0.001 | 60±4 |
| AK-23 | | 28±1 | 250±4 | 158.50±6.98 | 0.168±0.002 | 20±3 |

In the case of AK-23 and AK-10 the corrosion process proceeds with kinetic control, but in the case of an uninhibited solution and AK-9 with a mixed one. One can notice definite contradiction between high inhibition effect and low values of activation energy of corrosion for AK-9 as compared to AK-23 and AK-10. This fact be explained possibly by the film formation in chemisorption process, which creates an additional diffusion barrier [15].
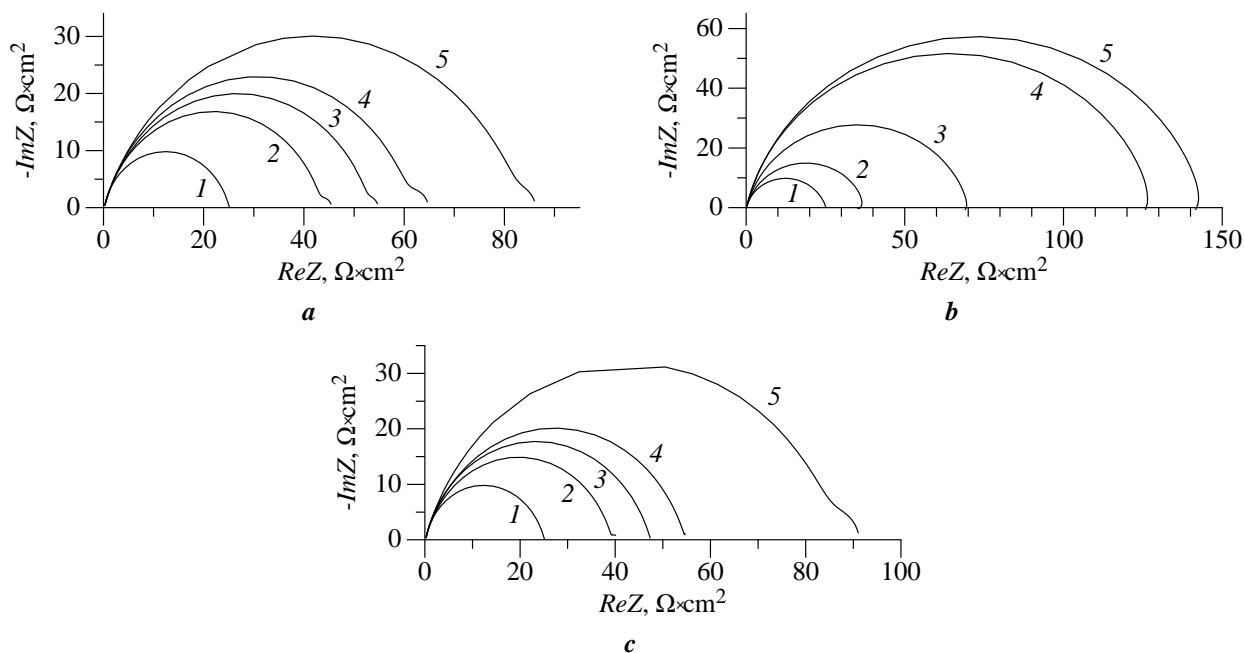


Figure 2. Nyquist diagrams of the St3 electrode in 15 % HCl solution at E$_{cor}$ (*1*) in presence of the compounds: (*a*) — AK-9, (*b*) — AK-10, (*c*) — AK-23 with concentration: *2* — 0.01 g·L$^{-1}$; *3* — 0.05 g·L$^{-1}$; *4* — 0.10 g·L$^{-1}$; *5* — 0.20 g·L$^{-1}$

The impedance spectra of St3 in 15 % HCl solution at corrosion potential $E_{corr}$ were in the form of combination of one semicircle in the high-frequency range and one inductive or capacity arc in the low-frequency range. In Figure 2 $ReZ$ is the real component of impedance and $ImZ$ is the imaginary e component of impedance.

The diameter of the capacitive semicircle increased the in the high frequency region in the solutions containing inhibitors. This growth is stronger at high concentrations of the inhibitor. This fact can be explained probably by the difficulties of realization of the electrode reactions.

To simulate the corrosion-electrochemical behavior of the St3 electrode in 15 % HCl solutions in the presence of AK-10 inhibitor the equivalent electrical circuit is proposed as shown in Figure 3a. In the presence of AK-9 and AK-23 inhibitors, the behavior of the St3 electrode in 15 % HCl solutions is acceptably described by the equivalent scheme in Figure 3b.

The values of the parameter $\chi^2$ for the schemes calculated in ZView2 were in the range of $(2–6)\cdot10^{-4}$, which indicates a good correlation with experimental data. The values of the parameters of the equivalent schemes are given in Table 4.
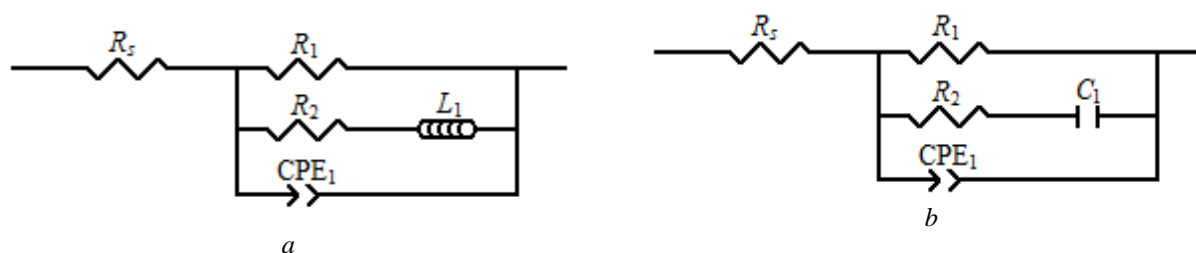


Figure 3. Equivalent electrical circuits for the St3 electrode in 15 % HCl solutions at $E_{cor}$

T a b l e  4

**Numerical values of parameters of equivalent circuits**
**for St3 electrode in 15 % HCl solution without and in the presence of inhibitors**

| $C_{inh}$, g·L$^{-1}$ | $R_{ct}$, Ω·cm$^2$ | $R$, Ω·cm$^2$ | CPE$_{dl}$, μF·cm$^{-2}$·s$^{(p-1)}$ | | $C/L$, F·cm$^{-2}$/H·cm$^2$ | θ |
|---|---|---|---|---|---|---|
| | | | $Q$ | $p$ | | |
| Without inhibitor | | | | | | |
| - | 31.97±0.12 | 389.4±5.3 | 1.92±0.10 | 0.83±0.02 | 0.000195±0.000010 | – |
| AK-9 | | | | | | |
| 0.01 | 41.42±0.13 | 829.0±10.2 | 1.48±0.10 | 0.84±0.02 | 0.000225±0.000010 | 0.21±0.01 |
| 0.05 | 54.18±0.12 | 977.7±11.0 | 1.26±0.10 | 0.84±0.03 | 0.000378±0.000012 | 0.44±0.01 |
| 0.10 | 64.77±0.14 | 1156±15.4 | 1.22±0.10 | 0.82±0.02 | 0.000211±0.000010 | 0.66±0.01 |
| 0.20 | 77.56±0.16 | 2573±21.1 | 1.10±0.10 | 0.80±0.02 | 0.000070±0.000013 | 0.86±0.01 |
| AK-10 | | | | | | |
| 0.01 | 37.79±0.11 | 393.9±3.2 | 0.95±0.10 | 0.86±0.02 | 11.7±0.6 | 0.56±0.01 |
| 0.05 | 54.34±0.13 | 556.0±5.4 | 0.83±0.10 | 0.87±0.02 | 85.5±3.2 | 0.77±0.01 |
| 0.10 | 113.6±0.32 | 757.3±8.9 | 0.78±0.10 | 0.89±0.03 | 482.5±28.0 | 0.91±0.01 |
| 0.20 | 128.6±0.22 | 1263.0±9.3 | 0.82±0.10 | 0.86±0.02 | 786.5±35.1 | 0.93±0.01 |
| AK-23 | | | | | | |
| 0.01 | 29.46±0.11 | 711.0±11.2 | 1.38±0.10 | 0.86±0.02 | 0.000175±0.000019 | 0.15±0.01 |
| 0.05 | 33.28±0.12 | 1429.0±16.7 | 1.45±0.10 | 0.84±0.02 | 0.000140±0.000015 | 0.31±0.01 |
| 0.10 | 39.41±0.13 | 1508.0±12.9 | 1.31±0.10 | 0.84±0.01 | 0.000203±0.000010 | 0.64±0.01 |
| 0.20 | 91.38±0.15 | 1906.0±19.4 | 1.14±0.10 | 0.80±0.01 | 0.000125±0.000010 | 0.84±0.01 |

There is a regular increase in resistances $R_1$ and $R_2$ and a decrease in parameter $Q_1$ of constant phase element CPE$_1$ (with comparable p$_1$) with the increase of the concentration of AK compounds (it follows from Table 4). The latter increase indicates the inhibition of electrode processes (mainly the cathodic process) in the presence of the studied compounds and their adsorption on the electrode surface. The parameters $R_2$ and $C_1$ can also be associated with the kinetics of the adsorption of AK compounds on the electrode surface (the Frumkin–Melik-Gaikazyan impedance without diffusion impedance).

The capacity of the double-electric layer and the degree of the surface coverage by inhibitors were calculated (Table 4) from the obtained values of the parameters of the equivalent circuit (Fig. 5). These results were processed in the coordinates of the Langmuir and Freundlich equations (Fig. 4, Table 5).
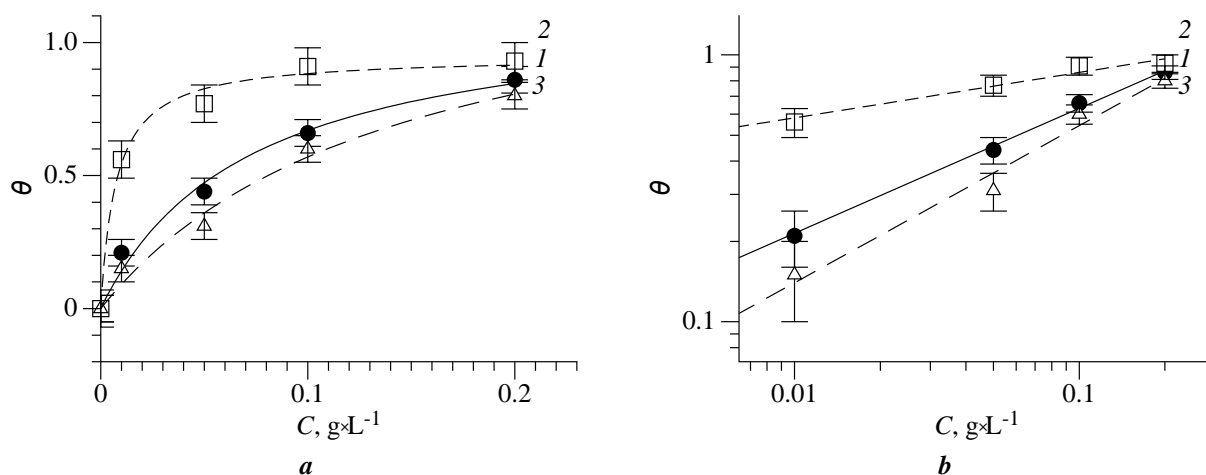


Figure 4. Langmuir (*a*) and Freundlich (*b*) isotherms of adsorption of AK-9 (curve *1*), AK-10 (curve *2*) and AK-23 (curve *3*) on the surface of St3 in 15 % HCl solutions

Table 5

**Parameters of Langmuir and Freundlich isotherms for the adsorption of AK-9, AK-10, and AK-23 on the surface of St3 in 15 % HCl solutions**

| Inhibitor | Langmuir | | | Freundlich | | |
|---|---|---|---|---|---|---|
| | $K$, dm$^3$·g$^{-1}$ | $Q$, μmol·m$^{-2}$ | $R^2$ | $K$ | $n$ | $R^2$ |
| AK-9 | 13.99 | 1.15 | 0.9870 | 1.85 | 0.47 | 0.9972 |
| AK-10 | 133.80 | 0.95 | 0.9927 | 1.27 | 0.17 | 0.9925 |
| AK-23 | 7.06 | 1.38 | 0.9838 | 2.11 | 0.59 | 0.9854 |

The calculated values of the correlation coefficients indicate that the process of the surface coverage by inhibitor molecules to a greater extent follows the Freundlich isotherm. It describes adsorption on an energetically inhomogeneous surface [16].

*Conclusions*

Thiadiazole derivatives act as effective inhibitors of acid corrosion for the mild steel St3. They possess a mixed effect, reducing the rates of partial cathodic and anodic reactions. The mechanism of action of thiadiazoles changes with increasing temperature, that is expressed in a sharp increase in the coefficients $b_k$ of the Tafel equation. At the same time, the free corrosion potential shifts to the cathodic region. The analysis of the polarization curves correlates with the results that have been obtained by the impedance spectroscopy and they confirm mostly the cathodic mechanism of inhibitors action.

The degree of the surface coverage by inhibitor with growing of its concentration causes an increase in the protective effect. It was established from the analysis of the impedance spectra. The coverage of the St3 surface is described by the Freundlich isotherm for an energetically inhomogeneous surface. The activation energy values have been calculated and they indicate that the corrosion process is slowed down due to the physical adsorption on the surface of St3 in the case of AK-10 and AK-23. But the chemisorption process is more likely for AK-9. The values of the inhibiting effect calculated from the results of weight-loss and electrochemical measurements are qualitatively correlated. The differences in the results of the experimental methods used in this work are related to the peculiarities of the rate of the adsorption equilibrium establishing.

## References

1    Brylee D.B.T. Polymeric corrosion inhibitors for the oil and gas industry: Design principles and mechanism / D.B.T. Brylee, C.A. Rigoberto // Reactive and Functional Polymers. — 2015. — Vol. 95. — P. 25–45.

2    Alamri A.H. Localized corrosion and mitigation approach of steel materials used in oil and gas pipelines — An overview / A.H. Alamri // Engineering Failure Analysis. — 2020. — Vol. 116.

3    Chauhan D.S. Ansari Chitosan-cinnamaldehyde Schiff base: A bioinspired macromolecule as corrosion inhibitor for oil and gas industry / D.S. Chauhan, M.A. Jafar Mazumder, M.A. Quraishi, K.R. Ansari // International Journal of Biological Macromolecules. — 2020. — Vol. 158. — P. 127–138.

4    Serpil Ş. Schiff bases as corrosion inhibitor for aluminium in HCl solution / Ş. Serpil, D. Berrin, Y. Aysel, T. Gülşen // Corrosion Science. — 2012. — Vol. 54. — P. 251–259.

5    Heakal F.E. Gemini surfactants as corrosion inhibitors for carbon steel / F.E. Heakal, A.E. Elkholy // Journal of Molecular Liquids. — 2017. — Vol. 230. — P. 395–407.

6    Murat F. A new corrosion inhibitor for protection of low carbon steel in HCl solution / F. Murat, K. Hülya, K. Mustafa // Corrosion Science. — 2015. — Vol. 98. — P. 223–232.

7    El-Haddad M.N. Chitosan as a green inhibitor for copper corrosion in acidic medium / M.N. El-Haddad // International Journal of Biological Macromolecules. — 2013. — Vol. 55. — P. 142–149.

8    El-Haddad M.N. Hydroxyethylcellulose used as an eco-friendly inhibitor for 1018 c-steel corrosion in 3.5 % NaCl solution / M.N. El-Haddad // Carbohydrate Polymers. — 2014. — Vol. 112. — P. 595–602.

9    Dehghani A. Potential role of a novel green eco-friendly inhibitor in corrosion inhibition of mild steel in HCl solution: Detailed macro/micro-scale experimental and computational explorations / A. Dehghani, G. Bahlakeh, B. Ramezanzadeh, M. Ramezanzadeh // Construction and Building Materials. — 2020. — Vol. 245.

10    Singh P. Novel quinoline derivatives as green corrosion inhibitors for mild steel in acidic medium: Electrochemical, SEM, AFM, and XPS studies / P. Singh, V. Srivastava, M.A. Quraishi // Journal of Molecular Liquids. — 2016. — Vol. 216. — P. 164–173.

11    Varvara S. Evaluation of some non-toxic thiadiazole derivatives as bronze corrosion inhibitors in aqueous solution / S. Varvara, L.M. Muresan, K.Rahmouni, H.Takenouti // Corrosion Science. — 2008. — Vol. 50. — P. 2596–2604.

12    Lalitha A. Surface protection of copper in acid medium by azoles and surfactants / A. Lalitha, S. Ramesh, S. Rajeswari // Electrochimica Acta. — 2005. — Vol. 51. — P. 47–55.

13    Negm N.A. Gravimetric and electrochemical evaluation of environmentally friendly nonionic corrosion inhibitors for carbon steel in 1M HCl / N.A. Negm, N.G. Kandile, E.A. Badr, M.A. Mohammed // Corrosion Science. — 2012. — Vol. 65. — P. 94–103.

14    Шеин А.Б. Защитные свойства ряда производных тиадиазола в растворах серной кислоты / А.Б. Шеин, М.Д. Плотникова, А.Е. Рубцов // Изв. вузов. Химия и химическая технология. — 2019. — Т. 62, № 7. — С. 123–129.

15    Kovačević N. Chemistry of the interaction between azole type corrosion inhibitor molecules and metal surfaces / N. Kovačević, A. Kokalj // Materials Chemistry and Physics. — 2012. — Vol. 137. — P. 331–339.

16    Batueva T.D. Mesoporous silicamaterials and their sorption capacity for tungsten (VI) and molybdenum (VI) ions / T.D. Batueva, M.G. Shcherban', N.B. Kondrashova // Inorganic Materials. — 2019. — Vol. 55. — P. 1146–1150.

М.Д. Плотникова, А.Б. Шеин, М.Г. Щербань, А.Д. Соловьев

## Тиадиазол туындыларын тұз қышқылындағы азкөміртекті болаттың коррозияға қарсы ингибиторлары ретінде зерттеу

Мақалада бірқатар тиадиазол туындыларын 15 % тұз қышқылы ерітінділеріндегі азкөміртекті болаттың коррозия ингибиторлары ретінде зерттеу нәтижелері келтірілген. Гравиметриялық сынақтар және электрохимиялық зерттеулер St3 аз көміртекті болатта 293 К температурада жүргізілді, сынамалардың әсер ету уақыты 24 сағ. Поляризация қисықтары катодты аймақтан үш электродты жасушада потенциодинамикалық режимде SOLARTRON 1280 С электрохимиялық өлшеу кешенін қолдана отырып тіркелді. 2-аминотиазол, 5-амино-1,3,4-тиадиазол-2-тиол, 2-амино-1,3,4-тиадиазол, 2-амино-5-(фуран-2-ил)-1,3,4-тиадиазол, сірке қышқылының 1,3,4-тиадиазол-2-иламидтері зерттелді. Зерттелген қосылыстар 0,10–0,20 г·л$^{-1}$ концентрациясында барынша жақсы қорғаныс әсерін көрсететіні анықталды. 90 %-дан жоғары қорғаныш қасиетке ие болған қосылысқа 5-амин-1,3,4-тиадиазол-2-тиол жататыны анықталды. Ең аз қорғаныс қасиетке (60 %-дан аз) ие болған қосылысқа сірке қышқылының 1,3,4-тиадиазол-2-иламиді. Электрохимиялық зерттеулердің нәтижесі қарастырылған қосылыстардың аралас (катодты-анодтық) типті ингибиторлар болып келетінін көрсетті. Ингибиторлардың қорғау әсерін ток тығыздығының өзгерісі бойынша есептеу гравиметриялық сынақтардың нәтижелерімен сәйкес келетін нәтижелер береді. Ингибиторларды коррозиялық ортаға енгізу St3-тің еру процесінің тиімді активтендіру энергиясын 3,3-тен 94,8 кДж / мольға дейін едәуір арттырады. Жұмыстың нәтижелерін қышқылды коррозияның потенциалды тежегіштерін тиадиазол туындылары арасында іздеу және олардың негізінде ингибирлеуші композицияларды дамыту перспективалы екендігін көрсетеді.

*Кілт сөздер*: жұмсақ болат, қышқылды коррозия, ингибиторлар, тиадиазол, тиазол, гравиметрия, импеданс, адсорбция.

М.Д. Плотникова, А.Б. Шеин, М.Г. Щербань, А.Д. Соловьев

# Исследование производных тиадиазола в качестве потенциальных ингибиторов коррозии малоуглеродистой стали в соляной кислоте

В статье приведены результаты исследования ряда производных тиадиазола в качестве ингибиторов коррозии малоуглеродистой стали в 15-процентных растворах соляной кислоты. Гравиметрические испытания и электрохимические исследования выполнены на малоуглеродистой стали Ст3 при температуре 293 K, время экспозиции образцов составило 24 ч. Поляризационные кривые снимали в потенциодинамическом режиме в трехэлектродной ячейке из катодной области в анодную со скоростью развертки потенциала 1 мВ·с$^{-1}$, используя электрохимический измерительный комплекс SOLARTRON 1280 C. Исследованы 2-аминотиазол, 5-амино-1,3,4-тиадиазол-2-тиол, 2-амино-1,3,4-тиадиазол, 2-амино-5-(фуран-2-ил)-1,3,4-тиадиазол, 1,3,4-тиадиазол-2-иламид уксусной кислоты. Установлено, что исследованные соединения в концентрациях 0.10–0.20 г·л$^{-1}$ проявляют достаточно хорошее защитное действие. Наилучший результат дает 5-амино-1,3,4-тиадиазол-2-тиол с защитным действием более 90 %. Наименьшим защитным действием (менее 60 %) обладает 1,3,4-тиадиазол-2-иламид уксусной кислоты. Электрохимическими исследованиями установлено, что данные соединения являются ингибиторами смешанного (катодно-анодного) типа. Расчет защитного действия ингибиторов по изменению величин плотности тока коррозии показал результаты, качественно совпадающие с результатами гравиметрических испытаний. Введение ингибиторов в коррозионную среду значительно повышает эффективную энергию активации коррозионного процесса растворения Ст3 с 3,3 до 94,8 кДж·моль$^{-1}$. Результаты работы указывают на перспективность поиска потенциальных ингибиторов кислотной коррозии в ряду производных тиадиазола и разработки ингибирующих композиций на их основе.

*Ключевые слова*: малоуглеродистая сталь, кислотная коррозия, ингибиторы, тиадиазол, тиазол, гравиметрия, импеданс, адсорбция.

## References

1    Brylee, D.B.T. & Rigoberto, C.A. (2015). Polymeric corrosion inhibitors for the oil and gas industry: Design principles and mechanism. *Reactive and Functional Polymers, 95*, 25–45. https://doi.org/10.1016/j.reactfunctpolym.2015.08.006

2    Alamri, A.H. (2020). Localized corrosion and mitigation approach of steel materials used in oil and gas pipelines. *Engineering Failure Analysis*, 116. https://doi.org/10.1016/j.engfailanal.2020.104735

3    Chauhan, D.S., Jafar Mazumder, M.A., Quraishi, M.A. & Ansari, K.R. (2020). Chitosan-cinnamaldehyde Schiff base: A bio-inspired macromolecule as corrosion inhibitor for oil and gas industry. *International Journal of Biological Macromolecules, 158*, 127–138. https://doi.org/10.1016/j.ijbiomac.2020.04.200

4    Serpil, Ş., Berrin, D., Aysel, Y. & Gülşen, T. (2012). Schiff bases as corrosion inhibitor for aluminium in HCl solution. *Corrosion Science, 54*, 251–259. https://doi.org/10.1016/j.corsci.2011.09.026

5    Heakal, F.E. & Elkholy, A.E. (2017). Gemini surfactants as corrosion inhibitors for carbon steel. *Journal of Molecular Liquids, 230*, 395–407. https://doi.org/10.1016/j.molliq.2017.01.047

6    Murat, F., Hülya, K. & Mustafa, K. (2015). A new corrosion inhibitor for protection of low carbon steel in HCl solution. *Corrosion Science, 98*, 223–232. https://doi.org/10.1016/j.corsci.2015.05.036

7    El-Haddad, M.N. (2013). Chitosan as a green inhibitor for copper corrosion in acidic medium. *International Journal of Biological Macromolecules, 55*, 142–149. https://doi.org/10.1016/j.ijbiomac.2012.12.044.

8    El-Haddad, M.N. (2014). Hydroxyethylcellulose used as an eco-friendly inhibitor for 1018 c-steel corrosion in 3.5 % NaCl solution. *Carbohydrate Polymers, 112*, 595–602. https://doi.org/10.1016/j.carbpol.2014.06.032

9    Dehghani, A., Bahlakeh, G., Ramezanzadeh, B., & Ramezanzadeh, M. (2020). Potential role of a novel green eco-friendly inhibitor in corrosion inhibition of mild steel in HCl solution: Detailed macro/micro-scale experimental and computational explorations. *Construction and Building Materials*, 245. https://doi.org/10.1016/j.conbuildmat.2020.118464

10    Singh, P., Srivastava, V. & Quraishi, M.A. (2016). Novel quinoline derivatives as green corrosion inhibitors for mild steel in acidic medium: Electrochemical, SEM, AFM, and XPS studies. *Journal of Molecular Liquids, 216*, 164–173. https://doi.org/10.1016/j.molliq.2015.12.086

11    Varvara, S., Muresan, L.M., Rahmouni, K. & Takenouti, H. (2008). Evaluation of some non-toxic thiadiazole derivatives as bronze corrosion inhibitors in aqueous solution. *Corrosion Science, 50*, 2596–2604. https://doi.org/10.1016/j.corsci.2008.06.046

12    Lalitha, A., Ramesh, S., & Rajeswari, S. (2005). Surface protection of copper in acid medium by azoles and surfactants. *Electrochimica Acta, 51*, 47–55. https://doi.org/10.1016/j.electacta.2005.04.003

13    Negm, N.A., Kandile, N.G., Badr, E.A., & Mohammed, M.A. (2012). Gravimetric and electrochemical evaluation of environmentally friendly nonionic corrosion inhibitors for carbon steel in 1M HCl. *Corrosion Science, 65*, 94–103. https://doi.org/10.1016/j.corsci.2012.08.002

14    Shein, A.B., Plotnikova, M.D., & Rubtsov, A.E. (2019). Zashchitnye svoistva riada proizvodnykh tiadiazola v rastvorakh sernoi kisloty [Protective properties of some thiadiazole derivatives in sulfuric acid solutions]. *Izvestiia vuzov. Khimiia i khimicheskaia tekhnologiia — Proceedings of universities. Chemistry and chemical technology, 62*, 123–129 [in Russian]. https://doi.org/10.6060/ivkkt.20196207.5968

15 Kovačević, N., & Kokalj, A. (2012). Chemistry of the interaction between azole type corrosion inhibitor molecules and metal surfaces. *Materials Chemistry and Physics, 137*, 331–339. https://doi.org/10.1016/j.matchemphys.2012.09.030

16 Batueva, T.D., Shcherban', M.G., & Kondrashova, N.B. (2019). Mesoporous silica materials and their sorption capacity for tungsten (VI) and molybdenum (VI) ions. *Inorganic Materials, 55*, 1146–1150. https://doi.org/10.1134/S0020168519110013

Information about authors:

**Plotnikova Maria Dmitrievna** — Candidate of chemical sciences, Assistant professor of Physical Chemistry Department, Perm State National Research University, Bukireva street, 614990, Perm, Russia; e-mail: plotnikova-md@mail.ru; https://orcid.org/0000-0002-4050-5682;

**Shein Anatoly Borisovich** — Doctor of Chemical sciences, Professor of Physical Chemistry Department, Perm State National Research University, Bukireva street, 614990, Perm, Russia; e-mail: ashein@psu.ru; https://orcid.org/0000-0002- 2102-0436;

**Shcherban' Marina Grigoryevna** (corresponding author) — Candidate of chemical sciences, Assistant professor of Physical Chemistry Department, Perm State National Research University, Bukireva street, 614990, Perm, Russia; e-mail: ma-sher74@mail.ru; https://orcid.org/0000-0002-6905-6622;

**Solovyev Aleksandr Dmitriyevich** — 3rd year student (undergraduate studies), Perm State National Research University, Bukireva street, 614990, Perm, Russia; e-mail: solovev_s92@mail.ru; https://orcid.org/0000-0002-7852-3683

# METHODS OF TEACHING CHEMISTRY

## T. Sadykov[1*], H. Ctrnactova[2], G.T. Kokibasova[1]

*[1]Karagandy University of the name of academician E.A. Buketov, Kazakhstan;*
*[2]Charles University, Prague, Czech Republic*
*(\*Corresponding author's e-mail: sadastayer@mail.ru)*

## Students' opinions toward interactive apps used for teaching chemistry

The solution of the problem of effective use of apps is not only in the analysis of learning outcomes, but also in consideration of the students' opinions toward learning chemistry with the help of these applications. Good results can undoubtedly be achieved in teaching chemistry if traditional and interactive teaching methods are intelligently combined. Mobile interactive apps allow educators to teach regardless of place and time, they provide the opportunity to learn both in the classroom and outside, and this is their big advantage. It also gives the teacher opportunity to interact with students on a more personal level with the help of mobile digital devices that the learners use regularly. This article, presents the results of a study of students' opinions about the use of mobile interactive applications in chemistry lessons. The approbation was carried out at a specialized school of information technologies in Karaganda (Kazakhstan), at the school Chýně, and at the first private language gymnasium Hradec Králové (Czech Republic). The results showed that more than 60 % of the students enjoy interactive apps, which positively affects their opinions towards the subject.

*Keywords:* chemistry, interactive apps, interactive teaching, information and communication technologies, smart devices, bring your own device (BYOD), secondary school, students' opinions, students' engagements.

### Introduction

In the past two decades, despite the boom in information and communication technologies (ICT) for education, the dominant paradigm of the educational system around the world has not changed. It is still largely based on the transfer of knowledge to passive learners, where teachers impose content and methods on students. According to Falcao et al. [1], technologies were simply aggregated into this outdated structure, despite the radical changes they brought in people's lives. Schools are at the core of education systems. At the same time, the ratio of computers to school size has been identified as a potential factor that influences student academic achievement [2].

According to OECD (Organisation for Economic Co-operation and Development) [3] statistics, the average percentage of households with internet access at home increased from 74 % in 2012 to 88 % in 2017 among its member countries. Moreover, 96 percent of 15-year-old students have a computer, smartphone, or tablet at home across the OECD countries [4]. The growing use of smartphones and tablets by the population, in general, increases opportunities to support learning and motivation in the educational domain. Students' access to ICT at schools and homes has also been improved by increased national investment in ICTs and lower prices for ICT tools [5]. Integration of mobile digital devices with learning has been validated as a promising way to improve the educational achievements, motivations, and interests of students [6], to engage learners [7], improve academic performance through sharing learning with social networks [8]. Ally and Prieto-Blázquez [9] emphasized that smart devices are crucial for both teachers and students, as learning can be available in different time zones and locations. However, Moos and Marroquin [10] research have shown that the effects of participation in technological activities on students' academic interests are often short-lived because the technology novelty wears out quickly.

Interactive apps can be used not only as software applications but also for communication and entertainment [11, 12]. From an educational community perspective, interactive apps can be viewed as communication channels used for information sharing, social and learning support, as well as for problem solving [13]. Students can quickly find information online, but finding out which sources are credible and useful is difficult for them [14]. Weimer [15] and McCombs [16] suggest that successful implementation of educational apps requires changes in content function instructor's role, learning responsibility, personalization of learning, processes and purposes of assessment. This often means establishing positive interpersonal relationships, facilitating the learning process adapting to the individual, social and class learning needs, and encouraging students to take responsibility and personal challenges. In another study, I-Chun et al. [17] have created some of the steps to introduce digital lesson applications. First, the teacher starts with a brief introduction and expresses motivation regarding the learning content at the beginning of the lessons. Then, the prompting activity: the student is asked a question, and the learner has some time for reflection before answering. After that, within the framework of activity students should complete a small exercise or a simple simulation related to a learning concept. During the period of performing, the embodied experience becomes learning clues to assist the students' mental processing for knowledge construction. Through this example, student gains knowledge regarding what and how the concept can be applied when the character provides further analysis and explanation. After the exemplifying process the student can better understand the learning concept by speaking out the summary of the example or ideal case in a concise sentence. Finally, the student can ask as many times as he/she wants to clearly understand the learning concept, which would be obscure to him/her.

The aim of the paper was to study the students' opinions based on interactive apps application in chemistry teaching. This article also covers 10 popular and mostly free apps in 5 areas of activity that can be used to learn chemistry.

*1. Chemical molecular viewers.* This type of apps can simulate models of molecular systems, and users can manipulate the model to visualize it under different conditions (Fig. 1). Moreover, students can visualize abstract concepts as well as explore and test scientific modelling to promote deep learning and conceptual understanding in science [11].
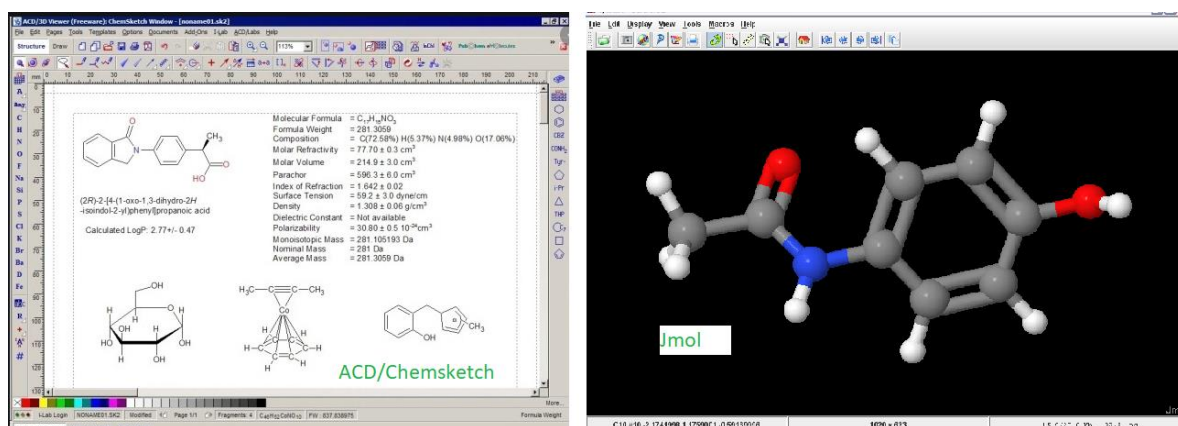


Figure 1. Chemical molecular viewer

Some students tend to prefer to learn from animations compared to other forms of representation. For these reasons, animation is an attractive option for educators. Examples of molecular viewer apps for lower-secondary schools:

• Chem Tutor provides visual representations of atoms: Lewis structures, energy diagrams, and orbital diagrams. Students receive an introduction to the representations and worked on two problem sets, in which they used representations to learn about atomic structure. Moreover, Chem Tutor provides error-specific feedback [18].

• ACD/Chemsketch is designed specifically to support the teaching of chemistry, so it contains many graphical options to facilitate the creation and editing of various chemical structures. Students can drag and rotate 3D models, zoom in and out, record frames, and manipulate the view in many ways [19].

• Jmol is a computer app for molecular modelling chemical structures in 3 dimensions. It can be integrated into web pages to display molecules in a variety of ways (ball-and-stick models, space-filling models, ribbon diagrams) [20].

*2. Periodic Table and databases apps.* Several apps address the need for portable devices as study guides or easy chemistry helpers [21]. Although the web browsers on mobile devices can access modern Periodic Table and online databases for browsing, there is also an increasing shift to lightweight apps dedicated to the platform (Fig. 2).
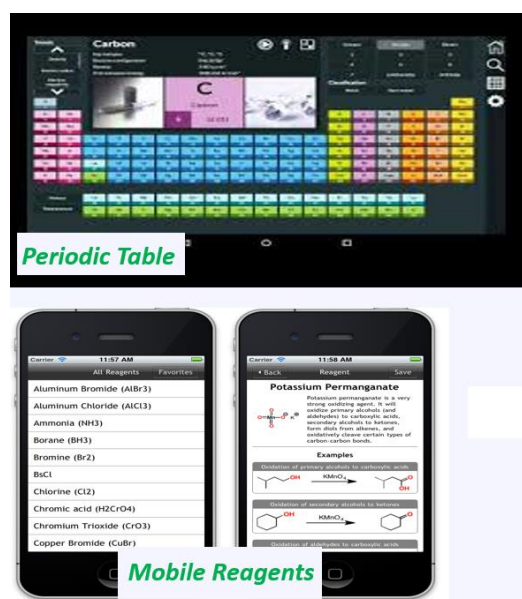


Figure 2. Periodic Table and databases apps

These apps can also be integrated to search chemical names or other identifiers of chemical structures in chemistry lesson [22]:

• Periodic Table is a digital application that is more geared towards learning general or inorganic chemistry and reinforcing various aspects of the periodicity of elements.

• iElements provides a good Periodic Table with a lot of information for each element such as its name, symbol, atomic number, phase, density, melting point, boiling point, heats of fusion and vaporization, specific heat, oxidation states, electronegativity.

• Mobile Reagents provides access to an 11 million reagent database and can be searched by exact or partial name and formula, or by using the camera to take a photograph of a chemical structure and automatically convert it to a structure search query.

*3. Chemical calculation and reaction apps.* In addition to chemical compounds and related chemical reactions, their balancing, common calculations, search and associated details are certainly of interest to chemists (Fig. 3).
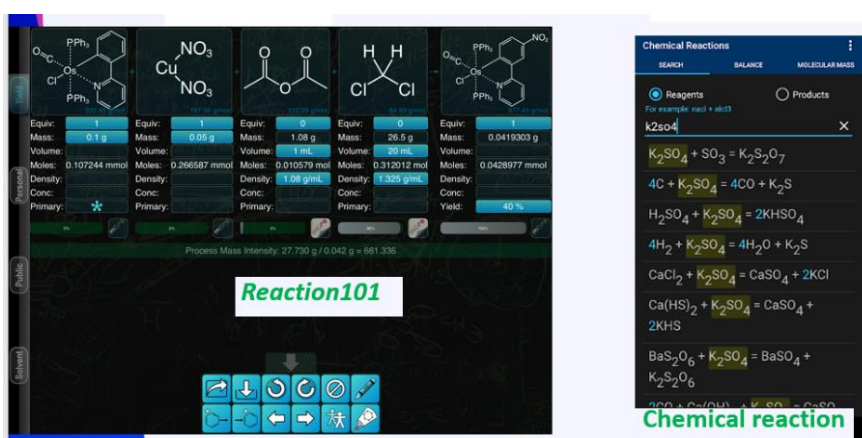


Figure 3. Chemical calculation and reaction apps

These applications are intended to aid routine calculations in the field of chemistry [21–22]:

• MolWeight is a tool that allows calculation of the molecular weight and other key properties of the compound. Moreover, a calculator is provided to determine the molecular weight of any substance by its chemical formula.

• Chemical reaction and Reaction101 are used as a chemical reaction editor with features for reaction balancing. The individual reaction components can be easily found by name, formula, structure or structure similarity methods. These apps use molecular weight (calculated from structures) and stoichiometry to derive any of the missing quantities, saving laborious calculations and manual checking.

*4. Virtual chemical laboratory apps* (Fig. 4). In traditional laboratory work students usually spend a lot of time in data collection while doing only simple manipulation and analysis of data. However, this tactile experience of learning might produce naive and mistaken explanation by students. Such experience would not be enough to prepare future scientist [23]. As a consequence, virtual application labs are still considered the most effective approach, as students can instantly run a high-quality lab [24], save time in data collection and processing, and change the system configuration that often cannot be changed in a real laboratory [25]. The main advantage of a virtual lab is the safety that it offers for handling dangerous equipment and reagents [26].
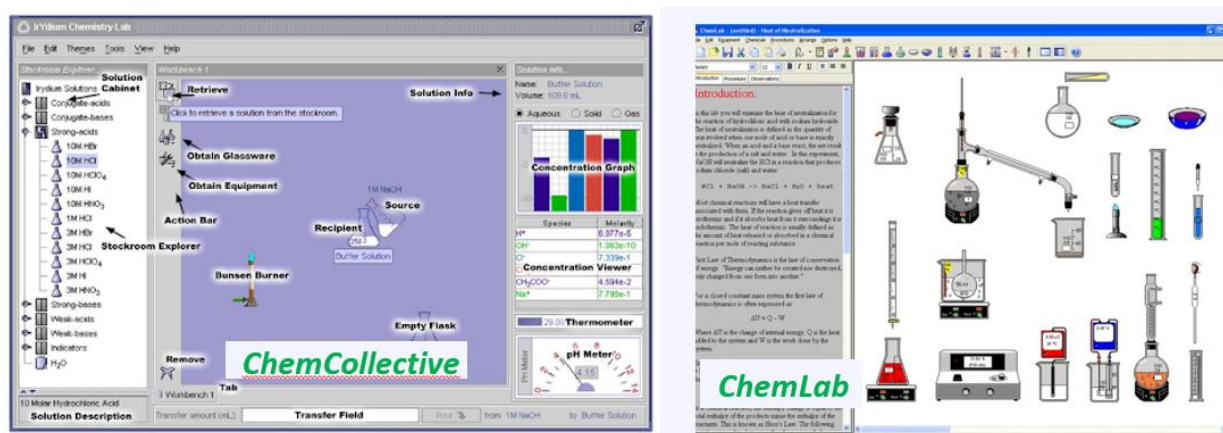


Figure 4. Virtual chemical laboratory apps

Here are examples of virtual chemical laboratory apps for lower-secondary schools:

• Chem Collective offers several virtual chemistry experiments and includes tools such as scenario-based-learning activities, tutorials and tests [27];

• ChemLab is the interactive chemistry lab simulation that is necessary to create your own virtual laboratory experiment. The database contains a large selection of chemicals and commonly used laboratory equipment [28].

*5. Game-based learning apps*. In game-based learning self-explanation can help students to generate more explicit representations of their knowledge, and, in turn, can positively affect accessibility, recall and transfer of knowledge [29]. Sadykov and Ctrnactova [30] stated in their research that students enjoy working with interactive tasks, and this has a positive effect on their attitude towards the subject. In addition, gamification involves the use of features such as scores, badges, rankings, and rewards, making immediate feedback possible. It encourages students to participate in the learning environment and allows them to complete tasks (Fig. 5). During gamification it is possible to monitor and assess successful learning and provide feedback on the assessment to students for formative purposes [31].

Here are some examples of game-based learning apps for lower-secondary schools:

• Learningapps.org is an interactive game-based app that allows the teacher to create personal interactive tasks and exercises. These programs also allow students to use their mobile devices for learning, and the teacher, respectively, can see the results of students on their own device. This model of organization of educational interaction is called Bring Your Own Device (BYOD) or Bring Your Own Technology (BYOT). The ability to provide immediate feedback to all participants increases the interactivity and adaptability of learning [30].

Figure 5. Game-based learning apps

• Kahoot is game-based learning and platform used in classrooms. It can be used with any subject, any age, and any device equipped with either cell signal or internet, and players do not even need to register to sign up for an account. This game also provides a tool for creating quizzes including adding pictures and videos to the questions. It also makes it possible to publish and share your own quizzes, as well as edit quizzes made by others [32].

*Experimental*

We have developed our questionnaire to study the students' opinions based on application interactive lessons with mobile apps during ten interactive lessons. The questionnaire used in this research consisted of ten closed-ended questions. A three-level rating scale from 1 to 3 (1 — Agree, 2 — Neutral, 3 — Disagree) was chosen as the most appropriate for measuring participants' opinions.

In the introductory part the students were briefed on the purpose of the questionnaire. The first part of the questionnaire collected factual data concerning, in addition to age and gender, the type of school and the level of students in chemistry for the last year. The second part of the questionnaire concerned the attitude of lower-secondary school students towards interactive forms of learning.

Questions 1, 2, 7, 9 were aimed at determining the interest and motivation of the students in the interactive lesson conducted using interactive apps compared to traditional lessons. Questions 3 and 4 determined how interactive lesson is understandable and does not pose any significant difficulties. In questions 5, 6, 8, 10 we were interested in whether students find this method interesting or useful and would they like to learn this way more often.

The survey participants were asked the following questions:

1. Do you like interactive lessons with the use of mobile apps?
2. Do you think that interactive lessons are more interesting than traditional?
3. Was the explanation in the interactive lesson with the use of mobile apps clear enough to understand the topic well?
4. Do you think that the interactive lessons had too much information, diagrams, and images, so you found it difficult?
5. Was knowledge gained in an interactive chemistry lesson with the use of mobile apps applied in real life?
6. Would you like if an interactive lesson with the use of mobile apps like these could be carried out more often?
7. Were you interested in using the mobile apps with a mobile phone or tablet?
8. Do you like the Kahoot and Learningapps.org apps? Is it quick and interesting and does it help you to check your knowledge?
9. Do you think that solving tasks with interactive apps more interesting than traditional ways?
10. Would you like if interactive apps like these could be used more often?

*Results and Discussion*

**Part 1**. The verification of interactive materials was carried out in two groups of students: 8-KZ (15 male and 11 female adolescents) from specialized school-board information technologies in Karaganda (Kazakhstan); 8-CZ (8 male and 10 female adolescents) from first private language gymnasium Hradec Králové (Czech Republic). Interactive materials were tested on the topics: "*Chemical reaction, Factors affecting the rate of chemical reaction, and Classification of chemical reactions*" (Fig. 6–7). Among the respondents there were

52 % male and 47 % female adolescents. The average age of students was 13.5 years. According to the types of schools, we used *Chemical reaction, Reaction101, Kahoot* apps in our interactive lessons.
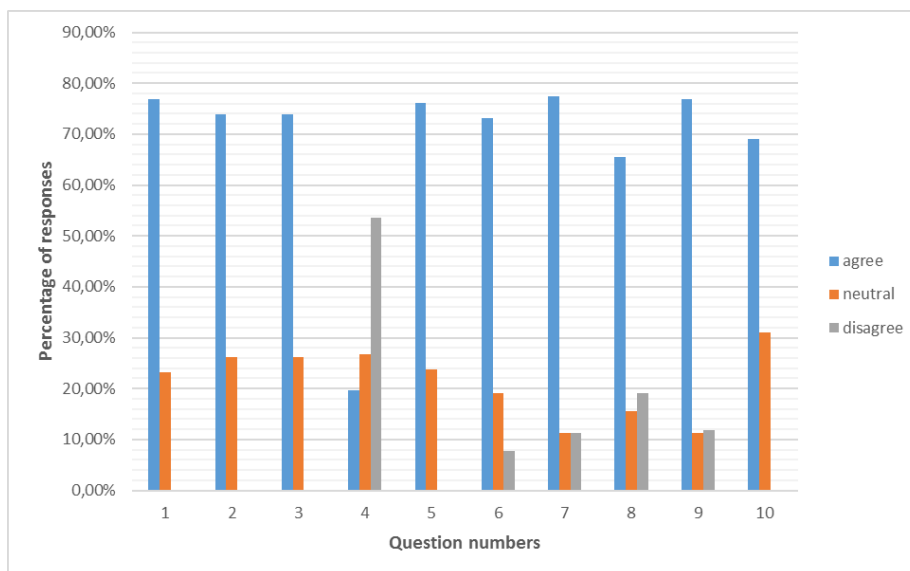


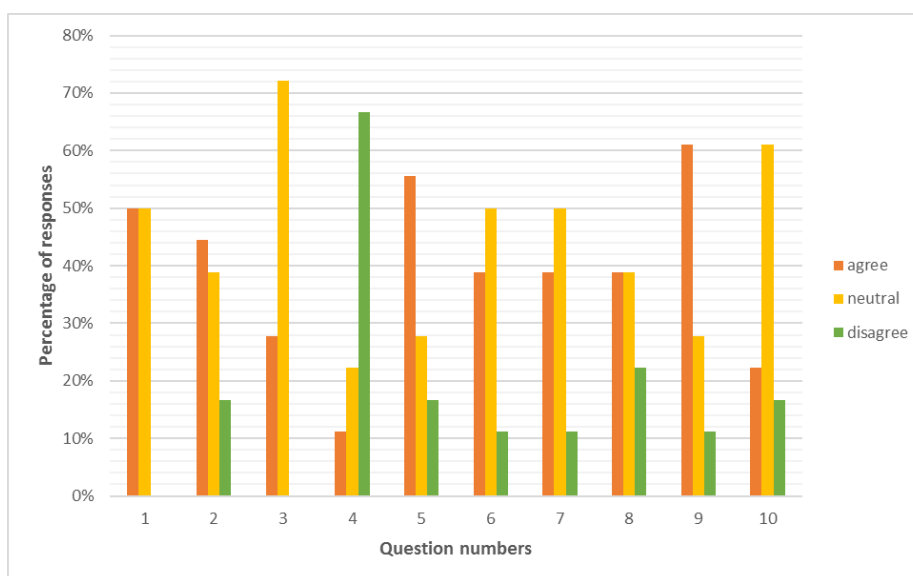Figure 6. The results of the survey. Part 1 for 8-KZ group students



Figure 7. The results of the survey. Part 1 for 8-CZ group students

As can be seen in Figure 8, the majority of respondents (64 %) rated interactive lessons with using mobile apps positively, and more than 60 % of respondents think that interactive lessons are more interesting than the traditional (questions 1-2). 62 % of respondents would like to an interactive lesson more often, about 30 % of respondents rated their attitude to this form of learning with the answers "neutral", and only 5–8 % of respondents expressed a completely negative attitude to this form of learning (question 6).

Most of the students (64 %) believe that interactive lessons with the mobile apps were illustrative and did not contain too much information, diagrams, and pictures, 30 % of the surveyed students answered "neutral", 16 % of students find it too difficult (question 4). About 70 % of students believe that the knowledge that was obtained in an interactive chemistry lesson can be applied in real life, only 5 % of students consider this chemistry lesson to be of little use for real life (question 5).
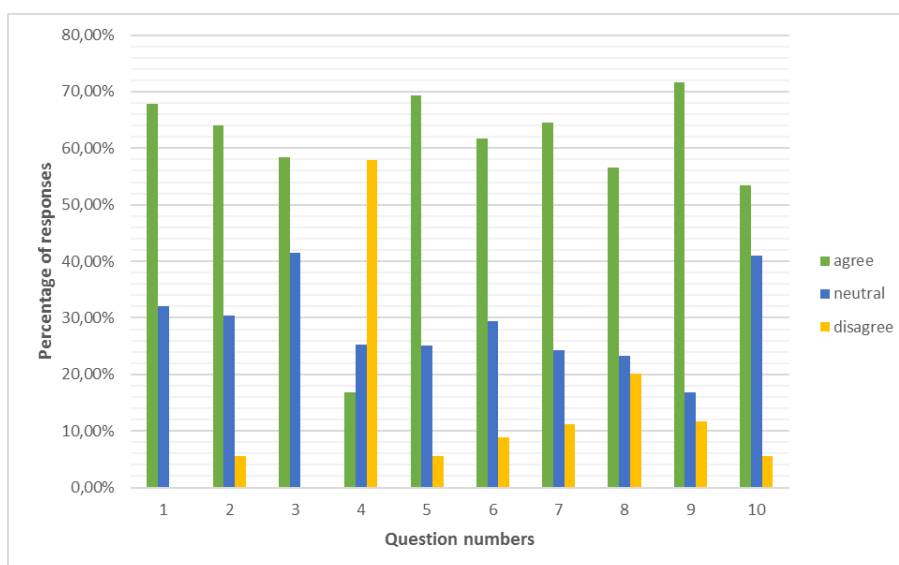
Figure 8. Total results of the survey. Part 1

More than two-thirds of respondents were interested in using interactive apps on a mobile phone or tablet, only 15 % of respondents were not interested in this form of learning (question 7). More than 70 % of respondents rated solving tasks using interactive apps more interesting than the traditional way, and 53 % of respondents would like to be engaged in this way of learning more often (question 9–10).

There was a significant difference between the two group's grades from Kazakhstan and the Czech Republic regarding answers. It can be seen from Figures 6-7 that group 8-KZ rated the interactive materials more positively than group 8-CZ, which had a significantly higher "neutral" response rate.

**Part 2.** The verification of interactive materials was carried out in two groups of students: 8-KZ (15 male and 10 female adolescents) from specialized school-board information technologies in Karaganda (Kazakhstan); 8-CZ (8 male and 10 female adolescents) from school in Chýně (Czech Republic). Interactive materials were tested on the topics: "Periodic table, Chemical bond" (Fig. 9–10). Among the respondents there were 48 % male and 52 % female adolescents. The average age of students was 13.5 years. In this part 2 we used various applications such as *Learningapps.org*, *Periodic table* and *Database apps*.
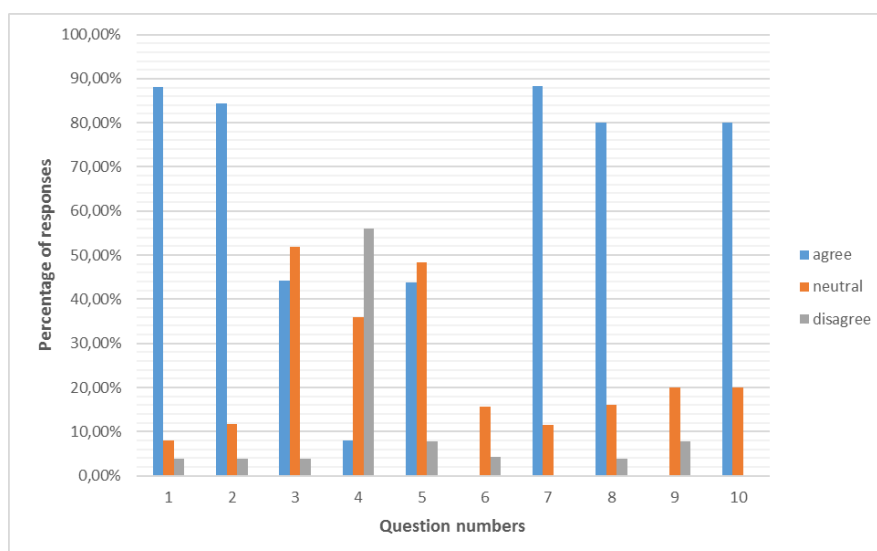


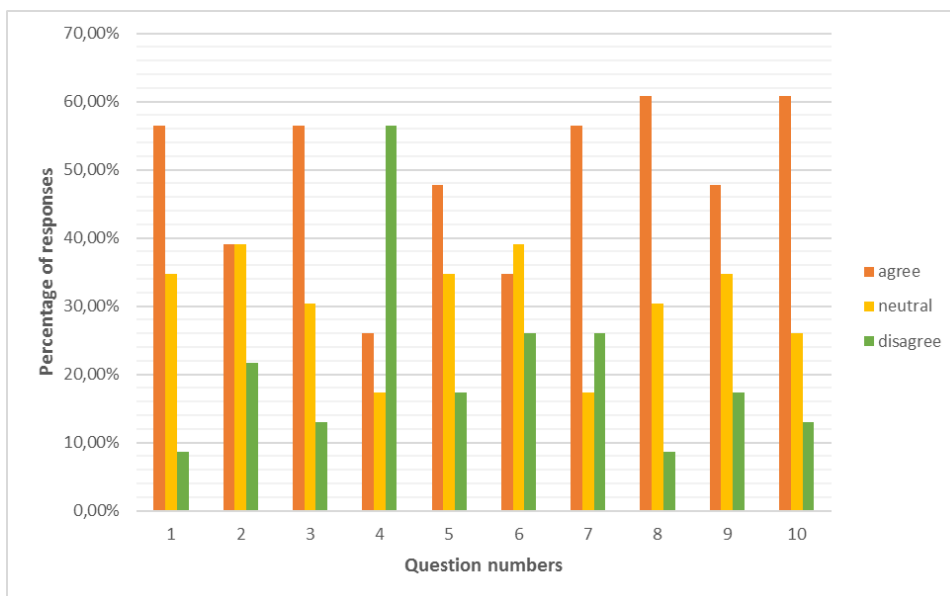Figure 9. The results of the survey. Part 2 for 8-KZ group students

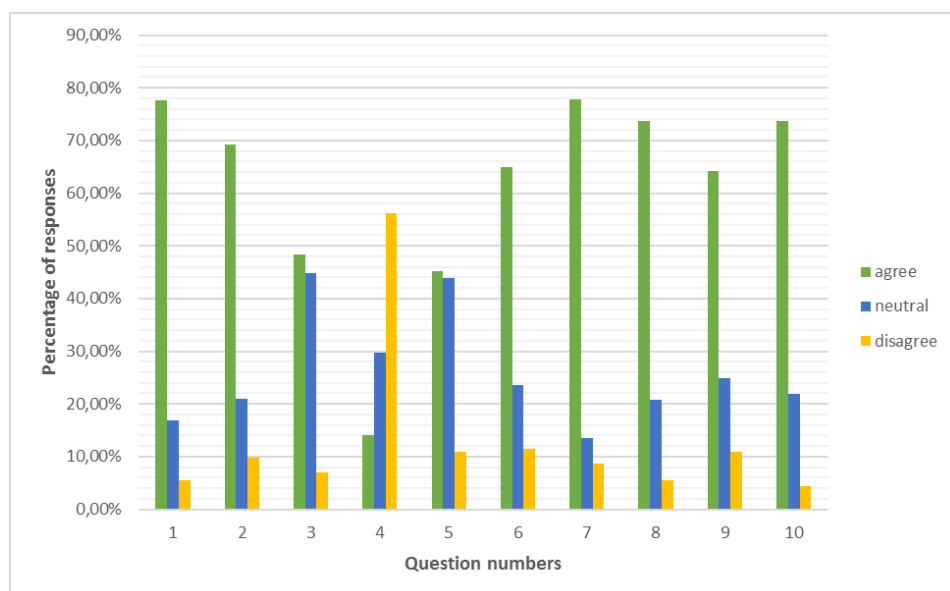Figure 10. The results of the survey. Part 2 for 8-CZ group students



Figure 11. Total results of the survey. Part 2

As can be seen in Figure 11, the majority of respondents (70 %) rated interactive lessons with using mobile apps positively and think that interactive lessons are more interesting than the traditional, only 9 % prefer the traditional form of the lessons (questions 1–2). Further question 4 showed that 56 % of respondents believe that interactive lessons with the mobile apps were illustrative and did not contain too much information, diagrams and pictures, 16 % of students find it too difficult.

45 % of students answered "agree", 43 % — "neutral" and 12 % — "disagree" at the question 5 "Do you think that the knowledge that was obtained in an interactive chemistry lesson can be applied in real life?". Questions 7 and 8 were asked to find out whether students like to use mobile apps on a mobile phone and tablet. The respondents rated this method of learning mostly positively (70 %), only 8 % of respondents believe that it is not suitable for learning.

In questions 6 and 9 respondents were asked if they would like an interactive lesson and solving tasks with mobile apps carried out more often, 65 % of respondents answered positively.

There was a significant difference between two group's grades from Kazakhstan and the Czech Republic regarding answers. It can be seen from Figures 9-10 that group 8-KZ rated the interactive materials more positively than group 8-CZ, which had a significantly higher "neutral" response rate.

Figures 12–13 showed a significant difference in some responses to the questionnaire in Kazakhstan and Czech Republic. The differences are particularly evident in questions 2, 6, 7, and 9. In our opinion, this difference is due to the fact that verification of interactive lessons with mobile apps carried out in one school and two groups in Kazakhstan, and two schools and two groups of students taught by two different teachers in the Czech Republic. Another factor may be the generally lower interest in learning using ICTs, due to the widespread and frequent use of this technique only for entertainment purposes in the Czech Republic.
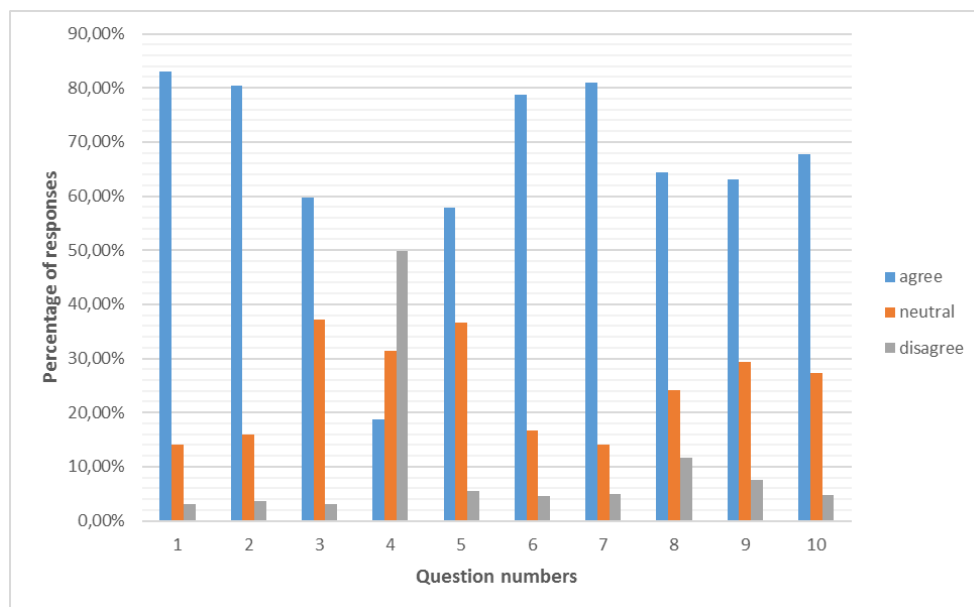


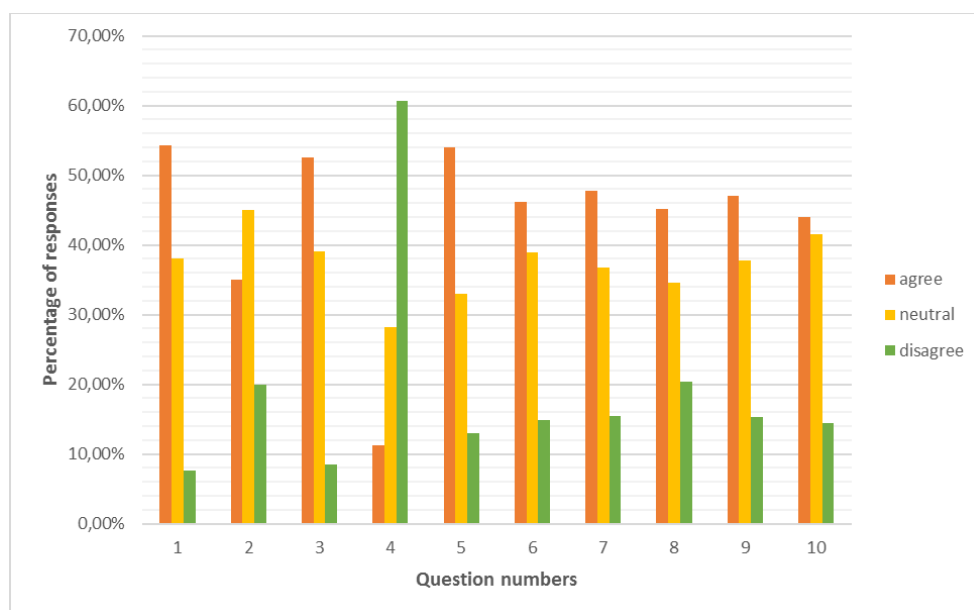Figure 12. Total results in Kazakhstan



Figure 13. Total results in Czech Republic

*Conclusions*

A literature review of previous studies has shown that mobile apps used for lower-secondary school improve achievement and engagement. It is clear that students with mobile digital devices can access virtual information equivalent to a large research library.

During the verification of interactive materials we are faced with the willingness of teachers to use tablets and mobile phones, but also with the lack of scientific training and understanding of current science and

technology issues on the application market. There was no statistically significant difference between the use of different types of mobile apps during ten interactive lessons. One of the possible alternative explanations for this result is the small amount of methodological literature for the use of interactive applications for tablets and mobile phones in teaching chemistry.

Special chemical software can help students to generate more explicit representations of their knowledge, positively affect accessibility, recall and transfer of the knowledge to chemists. In this study we have defined and described the interactive apps supporting an increase in the activity of students, and the effectiveness of the learning process for lower secondary schools. This study was limited by a relatively small sample size; however, the findings have important implications for teacher professional development and educational app design.

This result suggests that interactive apps support learning and increase student enjoyment, and this positively affects their attitude towards the subject. We think that one way to solve this problem is to involve teachers in the app's development process. Moreover, we believe that the combination of mobile phones and tablets allows multiple students to perform the activities at the same time, and this encouraged them to interact with each other. Therefore, in the next research we will focus on verification of the use of interactive apps as well as identifying the most effective apps for teaching chemistry in other schools in both Kazakhstan and the Czech Republic.

# References

1    Falcao, T.P, Mendes, F., de Andrade, P., de Morais, D.C., & da Silva Oliveira L. (2018). Participatory methodologies to promote student engagement in the development of educational digital games. *Computers & Education, 116*, 161–175. https://doi.org/10.1016/j.compedu.2017.09.006

2    Eickelmann, B., Gerick, J., & Koop, C. (2017). ICT use in mathematics lessons and the mathematics achievement of secondary school students by international comparison: Which role do school level factors play? *Education and Information Technologies, 22(4)*, 1527–1551. https://doi.org/10.1007/s10639-016-9498-5

3    OECD. Stat (2018). *Student-teacher ratio and average class size*. Retrieved from: https://stats.oecd.org/Index.aspx? DataSet-Code=EAG_PERS_RATIO#

4    OECD. (2015). *Students, computers and learning. Making the connection*. PISA: OECD Publishing.

5    Istance, D., & Kools, M. (2013). OECD work on technology and education: Innovative learning environments as an integrating framework. *European Journal of Education, 48(1)*, 43–57. https://doi.org/10.1111/ejed.12017

6    Hwang, G.J., & Wu, P.H. (2014). Applications, impacts and trends of mobile technology-enhanced learning: A review of 2008–2012 publications in selected SSCI journals. *International Journal of Mobile Learning and Organisation, 8(2)*, 83–95.

7    Evans, C. (2014). Twitter for teaching: Can social media be used to enhance the process of learning? *British Journal of Educational Technology, 45(4)*, 902–915. https://doi.org/10.1504/ijmlo.2014.062346

8    Sobaih, A.E.E., Moustafa, M.A., Ghandforoush, P., & Khan, M. (2016). To use or not to use? Social media in higher education in developing countries. *Computers and the Humanities, 58*, 296–305. https://doi.org/10.1016/j.chb.2016.01.002

9    Ally, M., & Prieto-Blázquez, J. (2014). What is the future of mobile learning in education? *International Journal of Educational Technology in Higher Education, 11(1)*, 142–151.

10    Moos, D.C., & Marroquin, E. (2010). Multimedia, hypermedia, and hypertext: motivation considered and reconsidered. *Computers in Human behaviour, 26(3)*, 265–276. http://doi.org/10.1016/j.chb.2009.11.004

11    Zhang, L., Gupta, D., & Mohapatra, P. (2012). How expensive are free smartphone apps? *ACM SIGMOBILE Mobile Computing and Communications Review, 16(3)*, 21–32. https://doi.org/10.1145/2412096.2412100

12    Karch, M. (2016). *What are apps? Definitions and examples. Livewire*. Retrieved from https://www.lifewire

13    Aghaee, N. (2015). Finding potential problems in the thesis process in higher education: analysis of e-mails to develop a support system. *Education and Information Technologies, 20(1)*, 21–36. https://doi.org/10.1007/s10639-013-9262-z

14    Seemiller, C., & Grace, M. (2015). *Generation Z goes to college*. San Francisco, CA: Jossey-Bass.

15    Weimer, M. (2002). *Learner-centred teaching*. San Francisco: Jossey-Bass.

16    McCombs, B. (2015). Learner-centred online instruction. *New Directions for Teaching and Learning, 144*, 57–71. http://dx.doi.org/10.1002/tl.20163

17    I-Chun, H., Kinshukc, Nian-Shing, C. (2018). Embodied interactive video lectures for improving learning comprehension and retention. *Computers & Education, 117*, 116–131. https://doi.org/10.1016/j.compedu.2017.10.005

18    Karch, M. (2016). *What are apps? Definitions and examples. Livewire*. Retrieved from https://www.lifewire

19    Aghaee, N. (2015). Finding potential problems in the thesis process in higher education: analysis of e-mails to develop a support system. *Education and Information Technologies, 20(1)*, 21–36. https://doi.org/10.1007/s10639-013-9262-z

20    Seemiller, C., & Grace, M. (2015). *Generation Z goes to college*. San Francisco, CA: Jossey-Bass.

21    Khan, S. (2011). New pedagogies on teaching science with computer simulations. *Journal of Science Education and Technology, 20(3)*, 215–232. https://doi.org/10.1007/s10956-010-9247-2

22 Rau, M. A., Michaelis, J. E., & Fay, N. (2015). Connection making between multiple graphical representations: A multi-methods approach for domain-specific grounding of an intelligent tutoring system for chemistry. *Computers and Education, 82*, 460–485. https://doi.org/10.1016/j.compedu.2014.12.009

23 *ACD/Chemsketch*. (2017). Retrieved from https://www.acdlabs.com/resources/freeware/chemsketch/

24 Jmol: an open-source Java viewer for chemical structures in 3D (2017). Retrieved from http://jmol.sourceforge.net/

25 Libman, D. & Huang, L. (2013). Chemistry on the Go: Review of Chemistry Apps on Smartphones. *Journal of Chemical Education, 90(3)*, 320–325. https://doi.org/10.1021/ed300329e

26 Williams, A.J., Ekins, S., Clark, A.M., Jack, J.J., & Apodaca, R.L. (2011). Mobile apps for chemistry in the world of drug discovery. *Drug Discovery Today, 16 (21–22)*, 928–939. https://doi.org/10.1016/j.drudis.2011.09.002

27 Chen, S., Chang, W.H., Lai, C.H., & Tsai, C.Y. (2014). A comparison of students' approaches to inquiry, conceptual learning, and attitudes in simulation-based and microcomputer-based laboratories. *Science Education, 98(5)*, 905–935. https://doi.org/10.1002/sce.21126

28 Pierri, E., Karatrantou, A., & Panagiotakopoulos, C. (2008). Exploring the phenomenon of "change of phase" of pure substances using the microcomputer based laboratory (MBL) system. *Chemistry Education Research and Practice, 9*, 234–239. https://doi.org/10.1039/b812412b

29 Srisawasdi, N. (2012). Student teachers' perceptions of computerized laboratory practice for science teaching: A comparative analysis. *Procedia — Social and Behavioural Sciences, 46*, 4031–4038. https://doi.org/10.1016/j.sbspro.2012.06.192

30 Sadykov T., & Čtrnáctová., H. (2019). ICT-supported Interactive Tasks in Chemistry teaching at the ISCED 2 Level as a Method of Active Teaching. In Rusek M., Vojíř K., *Project-Based Education and Other Activating Strategies in Science Education XVI (PBE 2018).* Praha: UniverzitaKarlova v Praze, pp. 8–17. ISBN 978-80-7603-066-4

31 ChemCollective (2019). Retrieved from: http://chemcollective.org/about_us/introduction

32 Model ChemLab (2013). Retrieved from: https://www.modelscience.com/products.html

Т. Садыков, Г. Чтрнацтова, Г.Т. Кокибасова

## Химияны оқытуда интерактивті қосымшалар пайдалану бойынша оқушылардың пікірлері

Интерактивті қосымшаларды тиімді пайдалану мәселесін шешу тек бағалау арқылы оқу нәтижелерін талдау ғана емес, сонымен қатар оқушылардың осы қосымшалар арқылы химияны оқытуға деген пікірлерін ескеру болып табылады. Сөзсіз, оқытудың дәстүрлі және интерактивті әдістерін ұтымды үйлестіре отырып, химияны оқытуда жоғары нәтижелерге қол жеткізуге болады. Мобильді интерактивті қосымшалардың үлкен артықшылығы олар оқытушыларға орны мен уақытына қарамастан сабақ беруге, сыныпта да, одан тыс жерлерде де оқуға мүмкіндік береді. Сондай-ақ, бұл мұғалімге оқушылар мен жүйелі түрде қолданатын мобильді сандық құрылғылардың көмегімен оқушылар мен жеке деңгейде қарым-қатынас жасауға мүмкіндік туғызады. Мақалада химия сабақтарында мобильді интерактивті қосымшаларды қолдану туралы оқушылардың пікірлерін зерттеу нәтижелері келтірілген. Апробация Қарағандыдағы (Қазақстан) мамандандырылған ақпараттық технологиялар мектебінде, Хыня мектебінде (Чехия) және Градец Краловтың (Чехия) бірінші жеке тілдік гимназиясында жүргізілді. Нәтижесінде оқушылардың 60 %-дан астамы интерактивті қосымшалар мен жұмыс істеуді ұнататынын көрсетті, бұл олардың химия пәніне деген көзқарасына оң әсер етеді.

*Кілт сөздер*: химия, интерактивті қосымшалар, интерактивті оқыту, ақпараттық-коммуникациялық технологиялар, интеллектуалды құрылғылар, жеке құрылғыңызды алып келіңіз (BYOD, негізгі мектеп, оқушылардың пікірлері, оқушылардың қызығушылығы.

Т. Садыков, Г. Чтрнацтова, Г.Т. Кокибасова

## Мнения учащихся об интерактивных приложениях, применяемых для обучения химии

Решение проблемы эффективного использования интерактивных приложений заключается не только в анализе результатов обучения с помощью оценок, но и в учете мнений учащихся на обучение химии с помощью этих приложений. Бесспорно, разумно сочетая традиционные и интерактивные методы обучения, можно добиться высоких результатов в обучении химии. Большим плюсом мобильных интерактивных приложений является и то, что они позволяют преподавателям обучать вне зависимости от места и времени, дают возможность учиться как в классе, так и за его пределами. Это также возможность взаимодействовать с учащимися на более личностном уровне с помощью мобильных цифровых устройств, которые учащиеся используют на регулярной основе. В данной статье авторами приведены результаты исследования мнения учащихся об использовании мобильных интерактивных приложений на уроках химии. Апробация проводилась в Специализированной школе информационных технологий

в Караганде (Казахстан), в школе Хыне (Чехия) и в первой Частной языковой гимназии Градец Кралове (Чехия). Результаты показали, что более 60 % учащихся получают удовольствие от работы с интерактивными приложениями, что положительно влияет на их отношение к предмету.

*Ключевые слова:* химия, интерактивные приложения, интерактивное обучение, информационно-коммуникационные технологии, интеллектуальные устройства, принеси свое собственное устройство (BYOD), основная школа, мнения учащихся, вовлеченность учащихся.

## Information about authors:

**Sadykov Timur Meiramovich** (corresponding author) — Ph.D. in Didactics of Chemistry, Assistant Professor, Academician E.A. Buketov Karaganda University, Karaganda, Universitetskaya 28 street, 100028, Kazakhstan; e-mail: sadastayer@mail.ru; https://orcid.org/0000-0002-0678-4585;

**Ctrnactova Hana** — Candidate of Chemical Sciences, Prof. RNDr., guarantors of DPS chemistry, department of teaching and didactics of chemistry, Charles University in Prague, Albertov 3, 128 43 Praha 2; e-mail: hana.ctrnactova@natur.cuni.cz; https://orcid.org/0000-0003-2975-4386;

**Kokibasova Gulmira Tolepbergenovna** — Candidate of Chemical Sciences, Associate Professor, Academician E.A. Buketov Karaganda University, Karaganda, Universitetskaya 28 street, 100028, Kazakhstan; e-mail: kokibasova@mail.ru; https://orcid.org/0000-0002-3418-7315.